SOFT MAGNETIC MATERIALS FOR TELECOMMUNICATIONS

Conference on Soft Magnetic Materials

SOFT MAGNETIC MATERIALS FOR TELECOMMUNICATIONS

A SYMPOSIUM HELD AT THE POST OFFICE ENGINEERING RESEARCH STATION IN APRIL 1952

EDITED BY

C. E. RICHARDS and A. C. LYNCH
Post Office Engineering Research Station

INTERSCIENCE PUBLISHERS INC. · NEW YORK
PERGAMON PRESS LTD · LONDON
1953

Published in Great Britain by Pergamon Press Ltd.
242 *Marylebone Road, London, N.W.*1
U.S.A. edition published by Interscience Publishers Inc.,
250 *Fifth Avenue, New York,* 1, *N.Y.*
Printed in Great Britain by The Thanet Press, Margate, Kent

CONTENTS

EDITORS' NOTE

THE origin of this book was an informal conference held at the Post Office Engineering Research Station in April 1952. The subject was defined as "Soft magnetic materials whose properties are of use or significance for telecommunications". Originally a discussion group of about twenty people was intended; invitations were sent to those known to be interested, both in England and abroad, but inevitably many who would have liked to come were overlooked. Even so, the number attending grew to seventy. The meetings filled two days and overflowed into a further half-day of discussion.

The chairmen at the four main sessions were Brigadier L. H. Harris (Controller of Research, Post Office Engineering Department), Professor, W. Sucksmith, Professor L. F. Bates, and Professor E. B. Moullin ; and the editors of this book, who were also the organizers of the meetings, would like to record their thanks to these Chairmen for their friendly but efficient control of the discussions.

The Papers, of which slightly shortened versions appear in this book, were taken as read and were followed by informal discussion which there has been no attempt to reproduce here. Those who took part were, however, invited to send in their written comments if they so wished; and these comments, with replies by the authors of the Papers, form the Discussions which now appear.

The Papers from France and Germany were submitted in their respective languages and translated in England (the German by Dr. V. G. Welsby and the French by Mr. D. A. Nye). The translations were then checked by the authors.

The editors have modified some of the symbols which have been used, and the following are used in all (or nearly all) of the Papers, whether or not they were used originally by the authors :—

μ_0 : permeability of free space.

μ_a : initial permeability.

μ', μ'' : real and imaginary parts of permeability.

h : hysteresis coefficient (Legg, 1936), identical with Legg's a.

The units in all the Papers are C.G.S. electromagnetic, except in Prof. Feldtkeller's Papers which use a rationalized C.G.S. system in which field is measured in mA/cm and the permeability of free space is $4\pi \cdot 10^{-9}$ H/cm.

The editors' work has been greatly lightened by the willing co-operation of the various authors and of the staff of the Pergamon Press.

FOREWORD

It is always a pleasure to express one's appreciation of a successful new departure in the world of physics, and appreciation is precisely what one who was fortunate enough to take part feels concerning the excellent Conference on Soft Magnetic Materials held at the Post Office Research Station, Dollis Hill, at the beginning of April this year. The Papers presented at this Conference, together with some of the discussions which they evoked, are now to be before us in the form of a convenient book of reference printed, one may add, because of the general interest which the communications aroused and because of the clearly expressed desire of many electrical engineers and physicists to have them all in the form of a permanent record. Invitations to the Conference were necessarily restricted, partly because of space and partly because it is well known that when a meeting designed for intimate discussion becomes too big there is a tendency for it also to become too diffuse and impersonal.

There were perforce very many scientists who did not have an opportunity of first reading and later listening to the many interesting contributions and of following the discussions which were so often helpful and stimulating. But, although they may have missed much in this way, they should welcome the volume now available, for it brings before them a very up-to-date account of the many important facets of magnetic experiment and theory. The theories concerning high initial permeability and low coercivity, hysteresis losses, magnetic viscosity, the properties of ferromagnetic powders, the production and properties of ferrites—all these find their places in this book, which will for some time to come be an authoritative guide.

We are indeed indebted to the many contributors for the care with which they have presented their work, and to Mr. C. E. Richards and Mr. A. C. Lynch, who have acted as editors with such obvious success. And, finally, our warm thanks are due to Brigadier L. H. Harris and many others of the Post Office Research Station for the careful arrangements and planning which gave such excellent results, and so much pleasure to the distinguished body of men from Britain and other European countries who met at Dollis Hill.

L. F. Bates.

August 1952

THEORETICAL REMARKS ON THE INFLUENCE OF SLIGHT HETEROGENEOUS IMPURITIES ON THE INITIAL PERMEABILITY OF NICKEL-IRON ALLOYS

Martin Kersten

(Vacuumschmelze A-G., Hanau)

Abstract: The initial permeability (μ_a) of pure iron is reduced to a greater extent by slight heterogeneous impurities than μ_a for equally pure nickel-iron alloys under equivalent conditions. Based on a much simplified model derived from the inclusion theory, an approximate formula for the μ_a with and without very small heterogeneous inclusions ($d < \delta$) can be obtained. The satisfactory agreement, in order of magnitude, with known experimental results suggests that a more fundamental theoretical and experimental investigation, along the lines suggested here, would be worth while.

1. INTRODUCTION

The initial permeability, μ_a, of technically pure iron, normally heat-treated, is about 300 to 1000. Cioffi (1934) was able to raise it to over 10 000, however, by the use of extreme purification in hydrogen at temperatures just below the melting-point. The μ_a of iron after this special treatment is not less than the highest permeability of technically pure binary nickel-iron alloys with about 78% nickel (78-Permalloy). An important difference, which is of particular interest here, is that this abnormally high μ_a for iron can only be obtained with Cioffi's very expensive and complicated purification process, whereas with Permalloy it can be obtained with a simple heat-treatment. Also other experimental results show that slight impurities lower the μ_a of iron far more than they would that of the practically-important homogeneous nickel-iron alloys with 35% to 100% nickel.

The question now arises as to whether this greater sensitivity of the μ_a of iron to heterogeneous impurities can be explained by known theoretical work. In this paper it will be shown to what extent this can be done qualitatively and also quantitatively in the form of a rough approximation. This question has recently been dealt with in greater detail elsewhere (Kersten, 1951).

2. GENERAL CONSIDERATIONS

The initial permeability of binary homogeneous nickel-iron alloys of practical purity, after suitable heat treatment, lies between about 300 for nickel alone and 10 000 for 78-Permalloy (Figure 1). We know now that in polycrystalline material the μ_a is mainly determined by two different effects:

(*a*) the randomly-distributed internal stresses (σ_i) ;

(*b*) the elastic binding of the domain boundaries to coarse ($d > \delta$) or fine ($d < \delta$) heterogeneous inclusions.

δ has the usual meaning of domain-wall thickness.

We shall not consider here the case of very great internal stresses σ_i following plastic deformation, and shall also neglect other influences which in many normal cases are apparently less important and have not yet been sufficiently investigated, for example unavoidable defects in the crystal structure, the crystal grain-boundaries and the average size of the individual crystallites.

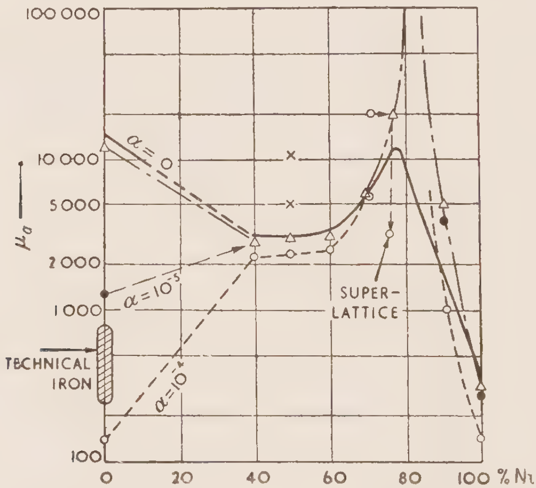

Figure 1. Variation of initial permeability with nickel content in nickel-iron alloys (neglecting the range 0 to 40% nickel). Maximum limits : — measured ; - - - theoretical, from equation 1 ; × new measurement by Williams (Bozorth, 1951, p. 123).
● $\alpha = 10^{-5}$, o $\alpha = 10^{-4}$;
for $h = 10^{-3}$ cm, $s = 10^{-4}$ cm.

In so far as the two above influences (*a*) and (*b*) are decisive, it should be possible to raise μ_a indefinitely if the internal stresses and heterogeneous inclusions could be reduced sufficiently. In fact, however, in the last twenty years or so, it has only been possible to raise the practical values of μ_a, given in Figure 1, by the use of particularly complicated Cioffi purification methods and, even with that degree of purification, limits have been reached which apparently cannot be greatly exceeded. For iron, this purification has given a particularly great improvement, μ_a having been raised from the usual value of 500 to between 10 000 and 20 000. Only recently a relatively small increase of this type in μ_a for alloys in the region of 50% nickel wa

reported, in which 5000 to 11000 was reached (Bozorth, 1951, pp. 61 and 114).

The cause of the upper limit to μ_a has, for a long time, been considered to be the stresses $\sigma_i \doteqdot \lambda_s . E$ which arise, as a result of magnetostriction, from the spontaneous distortion of adjacent domains when the material is cooled below the Curie point. λ_s is the saturation magnetostriction and E is the modulus of elasticity. Based on this assumption, earlier work by Becker led to the approximate formula

$$(\mu_a)_{max} - 1 = (\kappa_a)_{max} \doteqdot 2M_s^2/9\lambda_s^2 E \qquad \ldots(1)$$

for the maximum obtainable μ_a in the absence of appreciable amounts of heterogeneous impurities (Kersten, 1931). A few numerical values, calculated with equation (1) from the appropriate measured values of M_s, λ_s and E, are shown in Figure 1 (cf. Bozorth, 1951, Figures 13-42).

It should be pointed out, however, that the simple model, from the assumption of which equation (1) was obtained (Kersten, 1931 ; Becker, 1932 ; Becker and Döring, 1939, p. 156), must today be regarded as superseded. Néel (1946) and Döring (1949), particularly, have shown that in the quantitative theory of initial permeability, the magnetic stray fields, connected with the internal stresses, must be taken into account. Equation (1), however, still appears to apply within certain limits, although it has been found necessary to produce a new and improved model to explain them. We are thus justified in using equation (1) as a very approximate formula, since this relationship has at least proved itself for the nickel-iron alloys, provided no over-exact significance is attributed to it. The formula naturally fails, in this simplest form, for materials with no magnetostriction or, to put it better, with such small magnetostriction that the initial permeability is determined by effects other than magnetostrictive stresses.

Equation (1) does not take into account the additional effect of heterogeneous inclusions, mentioned under (*b*) above. The inclusion theory, introduced in my earlier papers, which were open to some criticism (Kersten, 1943a), has been greatly developed, particularly by Néel (1946). According to this theory, the domain walls in the initial unmagnetized condition are elastically bound to heterogeneous inclusions so that the shift of the walls in a weak external field H is approximately proportional to the field strength. The surface energy γ of the wall is an important factor in determining the binding force. When heterogeneous inclusions have a marked effect ($d < \delta$) the initial permeability thus becomes smaller as the surface energy becomes larger. The more extreme case of large included particles ($d > \delta$) will not be considered at present.

The wall energy γ is proportional to the product of the crystal anisotropy K and wall thickness δ. K denotes the difference between the reversible work done in magnetizing a single crystal in the directions of easiest and most

difficult magnetization, respectively. The meaning of the anisotropy constants K_1 and K_2 of the cubic crystal will be assumed here to be known (see, for example, Bozorth, 1951, p. 563).

The constant K is about ten times greater for iron than for the technically important nickel-iron alloys. For the same arrangement of heterogeneous inclusions, in particular for equivalent size distribution throughout the material, it is thus to be expected that iron will have a higher sensitivity of the initial permeability to impurities. This result is in agreement with experience.

In this connection it should be pointed out that the highest value of initial permeability of the nickel-iron alloys lies roughly halfway between 82% nickel where the magnetostriction λ_s changes sign and 76% nickel where the anisotropy constant K_1 for random atom distribution passes through zero. The sum of the two boundary-wall restrictions mentioned under (*a*) and (*b*) above appears to reach a minimum for this mean alloy constitution (78% nickel). It should be noted that, even for small amounts of impurities, effect (*b*) can be more marked than effect (*a*) in cases such as this, where the magnetostriction is very small.

3. NUMERICAL ESTIMATE

There is still no perfect quantitative theory of initial permeability which satisfactorily takes into account all present known and assumed elementary effects. Such a theory has so far failed as a result of incomplete knowledge of the condition of the lattice in a true crystal and in polycrystalline materials having grain boundaries. Promising new advances in this direction will perhaps provide, in the foreseeable future, sufficient knowledge of these properties. The difficulties attending a theory of initial permeability are fundamentally greater than for a theory of coercive force because the absolute dimensions of the Weiss domains in general have a more important effect on the initial permeability. In spite of this we are already in a position to make a rough estimate by limiting ourselves to a simple schematic model. For this purpose it is assumed that only very finely-dispersed heterogeneous inclusions are present, whose dimensions d, in any direction, are less than the thickness δ of the boundary wall. In this case, which often arises for small amounts of impurities, there are none of the "spikes", mentioned by Néel (1946) and Williams (1947), which affect the initial permeability when d is greater than δ. Furthermore, as shown in Figure 2, we assume a regular space distribution of non-magnetic or weakly magnetic particles with the mutual separation s as the lattice constant of a simple cubic lattice of this particle distribution. The individual particles of this simple model are roughly spherical and all have the same diameter d.

This extremely simplified model naturally differs greatly from the true conditions. Probably the mosaic structure of the true crystal often justifies

a fairly regular distribution of the inclusions with separations of the known lengths of the mosaic edges ($s = 10^{-4}$ to 10^{-5} cm). However, in obtaining a future improved theory the possibility of taking into account a random statistical distribution of inclusions must not be entirely ruled out. Néel has already shown that, for a statistical distribution of inclusions the values of initial permeability and coercive force would not be expected to be vastly different from those for our simplified model. This is known to result from the additional effect, referred to above, of the internal fields caused by the distorted domain walls as they try to adjust themselves to the inclusions.

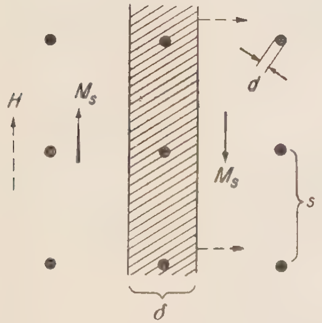

Figure 2. The model for the material : $d < \delta$.

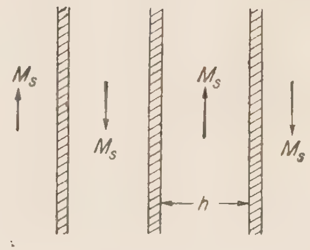

Figure 3. Definition of the thickness, h, of the slice-shaped Weiss domains.

Also the variations in diameter d, which occur in reality, should not be neglected in an improved theory. Experimental discoveries and the more modern theories of seed formation in supercooled solid solutions have made it clear that in many cases when separation occurs there are only quite small deviations from a mean diameter d, so that in such cases, our model is not so very far wrong. All these arguments do not carry sufficient weight to prevent one obtaining a rough approximate formula from our simple model and checking it against experimental results, particularly as such checks will indicate suitable lines along which future improved development can take place.

If with this model we now consider the effect (b) of the inclusions, we obtain the approximate formula (Kersten, 1951):—

$$\left.\begin{aligned} &\mu_a \fallingdotseq K_a = M_s^2\delta^2/K_1 s h \alpha \\ \text{and}\quad &\mu_a \fallingdotseq K_a = M_s^2\delta^2/4K_1 s h \alpha \end{aligned}\right\} \text{ when } d < \delta \qquad \ldots(2)$$

for the 180° and 90° domain walls, respectively. Apart from the symbols already defined, α is the volume factor of the spherical inclusions or

$= (\pi/6)\,(d/s)^3$, h is the width of the Weiss domains, assumed to be in the form of slices as shown in Figure 3,

$$\delta = \delta_{90^\circ} = \sqrt{kT_c/aK_1}$$

δ being the thickness of the 90° wall for a magnetic anisotropy such as that of iron and for a wall parallel to the (100) plane. k is Boltzmann's constant, T_c is the Curie point, a is the lattice constant.

For iron, substituting known values gives $\delta_{90^\circ} = 0{\cdot}4 \times 10^{-5}$ cm. The 180° wall for iron, according to Néel, consists of two 90° walls which are pressed more or less closely together under the influence of internal stresses. For further details see, for example, Bozorth (1951), p. 814.

In order to check whether equation (2) gives the right order of magnitude for slightly impure iron, we will insert the following numerical values: $s = 10^{-5}$ cm and also $s = 10^{-4}$ cm, in accordance with the known range of lengths of the mosaic edges; $h = 10^{-3}$ cm, corresponding to the separation of the Bitter strips often observed in polycrystalline materials (see, for example, Kittel (1949), Figure 12). Then, for iron, from equation (2)

$$\mu_a = \frac{21{\cdot}5^2 \times 106}{4{\cdot}2 \times 10^5} \cdot \frac{0{\cdot}4^2 \times 10^{-10}}{10^{-5} \times 10^{-3}} \cdot \frac{\text{cm}^3\,(\text{gauss})^2}{\text{erg}}$$

and with ergs $= 4\pi$ gauss-oersteds

$$\mu_a = 0{\cdot}14/\alpha \text{ gauss/oersted for } s = 10^{-5} \qquad \ldots(3)$$

or

$$\mu_a = 0{\cdot}014/\alpha \text{ gauss/oersted for } s = 10^{-4} \text{ cm} \qquad \ldots(4)$$

If the volume factor α is 10^{-4}, equation (3) gives, for instance, $\mu_a = 1400$ and equation (4) gives $\mu_a = 140$. The practical values of initial permeability for iron generally lie between these limits (see above). Our approximate formula (2) thus gives generally reasonable results. For the first of the two numerical examples, the condition $d < \delta$ is well fulfilled. For the second example with $\alpha = 10^{-4}$ cm and $s = 10^{-4}$ cm it can easily be shown that d has reached the wall thickness δ. This example thus represents the upper limit of applicability of the approximate formula.

The total content of heterogeneous inclusions is often greater than has been assumed here. It should be noted, however, that the effect of those particles whose diameter approaches the wall thickness is particularly marked. The equivalent value of α which gives the correct value of μ_a in equation (2) will often be smaller therefore than the total volume factor of all the inclusions present.

Finally, if we estimate what value of the volume factor α would give the measured maximum values of μ_a between 10 000 and 20 000, using equation (4) and neglecting the magnetostrictive internal stresses, we obtain a value $\alpha = 10^{-6}$. This is not an unreasonable value for particularly carefully purified iron.

4. SUPERPOSITION OF THE EFFECTS OF MAGNETOSTRICTIVE FORCES AND HETEROGENEOUS INCLUSIONS

Our aim is to obtain an approximate formula which tends to equation (1) for $\alpha \to 0$ and allows the reduction of initial permeability, in the presence of heterogeneous inclusions, to be predicted. Such a formula can be obtained under the simplest possible assumptions if the elastic restriction of wall movement, caused only by the magnetostriction forces, is added to the restriction caused only by the impurities. We thus use the simple expression

$$1/\mu_a = 1/(\mu_a)_{max} + 1/(\mu_a)_F \qquad \text{...(5)}$$

where the subscript $_F$ indicates the effect of impurities and $(\mu_a)_F$ is the initial permeability from equation (2). From equation (5) we finally obtain, by making use of equations (1) and (2), for 180° walls,

$$\mu_a \doteqdot \frac{2}{9}\frac{M_s^2}{\lambda_s^2 E}\,\frac{1}{1 + K_1 sh\alpha/4\lambda_s^2 E\,\delta^2} \text{ when } d < \delta \qquad \text{...(6)}$$

So long as $K_1 sh\alpha$ remains much less than $4\lambda_s^2 E\,\delta^2$, the inclusions cannot lower the initial permeability much below the upper limit set by equation (1). Conversely, there is a large reduction of μ_a due to inclusions if $K_1 sh\alpha$ is equal to or greater than $4\lambda_s^2 E\,\delta^2$.

Furthermore, the approximate equation (6) agrees well with the qualitative considerations, set out in section 2, of the increased sensitivity of iron to impurities being due to its particularly large anisotropy constant $K_1 = 4{\cdot}2 \times 10^5$ erg/cm³. A numerical curve of equation (5) is shown in Figure 1. There $s = 10^{-4}$ cm and $\alpha = 0$, 10^{-5} and 10^{-4} respectively.

Figure 1 shows clearly that a given amount of impurity has a far more damaging effect on the μ_a of iron than on that of the nickel-iron alloys. In each case h was assumed to be 10^{-3} cm. Although the magnetic anisotropy of the alloys with high nickel content is different from that of iron, our approximate formula can also be used for these alloys with a suitable alteration in the definition of the anisotropy constant. It has already been mentioned that, even for 50% nickel, two cases have recently been reported in which increases of μ_a by factors of 2 to 3 above the previously known values have been obtained by careful purification (cf. Figure 1 and Bozorth, 1951, p. 123, Figure 5-26). These new maximum values exceed the theoretical limits set by equation (1). This does not mean that equation (1) cannot still be used to estimate the attainable maximum values of μ_a but it shows that this old formula, which has no sound basis, must not be used except to obtain an estimate of order of magnitude, the accuracy of which is still unknown. The known fall of μ_a in the region of the super lattice phase of Ni_3Fe is at least qualitatively explained by equation (6) since the anisotropy constant K increases considerably after a long period of annealing (Grabbe, 1940).

Figure 1 shows the theoretical value of μ_a, calculated from equation (6), for $\alpha = 10^{-4}$ and $K = 4 \times 10^4$ erg/cm³ at the superlattice point (76% nickel).

Our approximate formula (6) thus agrees with the long-known fact that particularly high initial permeabilities are obtained when a zero magnetostriction point closely coincides with a zero point of the crystal anisotropy. A particularly fine example of this is the Sendust alloy (approx. 85% Fe, 9% Si, 6% Al) (Bozorth, 1951, p. 1000, Figure 4-32).

To what extent the present provisional solution to the problem, stated at the beginning of this paper, will have to be changed and improved later will be shown by further development of the theory, in conjunction with systematic experimental investigations. In this connection, the various solubilities of many alloy components in iron and nickel-iron alloys must be investigated.

DISCUSSION

Dr. K. Hoselitz:

The theory of the initial permeability presented in this paper forms a partial continuation of Prof. Kersten's "inclusion theory". The expressions obtained for μ_a of materials with very finely dispersed impurities are, however, not in such good agreement with experiment as the paper suggests. Inspection of powder patterns of polycrystalline specimens indicates that the value of h observed is nearer 10^{-2} cm than 10^{-3} cm, and hence the values of μ_a calculated for iron would be reduced to values far below those actually found. Moreover, carefully purified iron prepared by Cioffi (1934) had a total impurity content of 0·04%. Thus α would certainly be greater than $4 \cdot 10^{-4}$, giving calculated values of $\mu_a <$ 300 to 3 000. The value measured by Cioffi was 14 000.

Kersten states that a theory of the initial permeability is attended with great difficulties because of the important effect of the domain dimensions. In the theory presented domain dimensions enter as independent parameter (h). Thus, whilst the theory presented attempts to establish relationships between μ_a and h it is felt that a theoretical interpretation of the initial permeability must try to solve the paramount problem of the connexion between h and the amount and distribution of impurities, taking account of the properties of the material, such as magnetocrystalline energy constants, magnetostriction constants, saturation magnetization and others.

Dr. H. P. J. Wijn:

I should like to ask Prof. Kersten if it is known what kind of magnetization process takes place at small field strengths in alloys having a very small crystal anisotropy constant K and also a very small saturation magnetostriction λ_s. Prof. Kersten assumes in his theory that reversible domain-wall displacement is the mechanism which determines the initial permeability but if K and λ_s are both very small, the wall thickness will be very large and perhaps the whole concept of domain walls will not be applicable, so that only rotation processes can occur.

2

COERCIVITIES IN DILUTE FERROMAGNETIC ALLOYS

G. Bate, D. Schofield and W. Sucksmith
(University of Sheffield)

In recent years much attention has been directed, in both the theoretical and experimental fields, to the high coercivity of small particles. Néel (1947a) as well as Stoner and Wohlfarth (1948) have shown that high coercive forces are to be expected when single domain particles exhibit even small shape anisotropy. Many experiments on fine powders (Weil, 1951) have been carried out and coercivities as high as 1000 Oe for iron powders

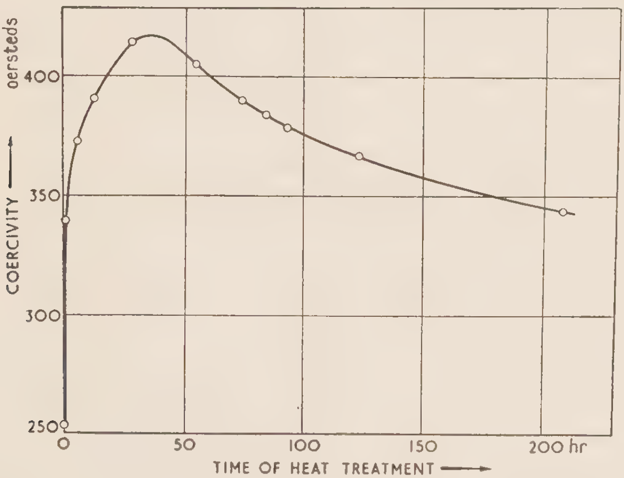

Figure 1. Variation of coercivity with time of heat-treatment at 450°C.

have been measured. It appeared possible to the writers that suitable two-phase alloys, consisting of ferromagnetic "islands" in a matrix of non-ferromagnetic material, would constitute fruitful sources for magnetic investigation, and in this connexion measurements in very high magnetic fields on weakly ferromagnetic copper-nickel and copper-iron alloys (Bitter and Kaufmann, 1939; Bitter, Kaufmann, Starr and Pan, 1941) are not without significance.

Preliminary experiments were therefore carried out on a material readily available, i.e. stainless steel magnetic recording wire, 12% Cr, 12% Ni,

rest Fe (Sucksmith, 1952). When wire of this constitution is cooled rapidly from a high temperature it remains in a single-phase condition of austenitic structure. Cold work, however, facilitates the change to two-phase equilibrium condition, and one of these phases is ferromagnetic. Thus the drawing of the material precipitates the ferromagnetic phase. At this stage the coercivity is relatively low, i.e. about 250 Oe, but subsequent heat-treatment above the phase change temperature at about 300°C results in gradual reversion to a single-phase condition accompanied by the magnetic changes shown in Figure 1. The annealing treatment causes a gradual reduction in the size of the ferromagnetic regions, with the result that there is a marked increase in the number which are small enough to behave as single domains. This causes a sharp increase in coercivity. The later decrease of H_c will be caused by the gradual solution of these regions, until finally a single-phase (paramagnetic) solid solution is produced. Since the intensity of magnetiza-

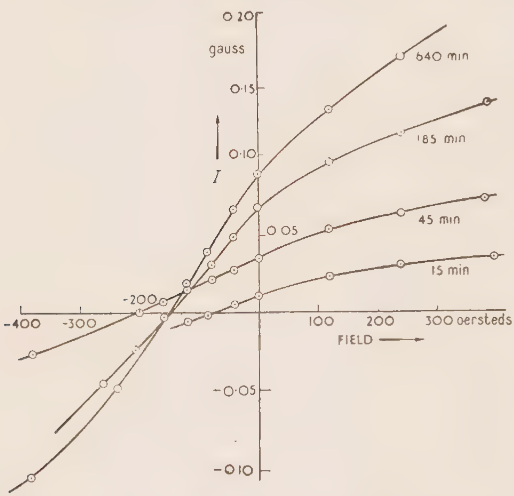

Figure 2. I/H curves for 0·3% iron-copper alloy, heated at 650°C for various times.

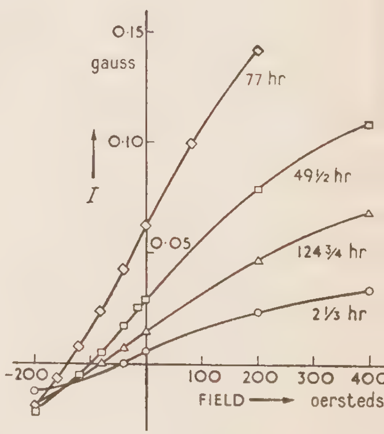

Figure 3. I/H curves for 1½% iron-copper alloy, heat-treated at 350°C.

tion is around 500 Oe, interaction between the closely spaced ferromagnetic aggregates can play a major part, and it was thought desirable to pursue the investigations further under the simpler conditions of a much more diluted ferromagnetic.

The copper-rich alloys of the copper-cobalt and the copper-iron binary systems seem to possess these necessary features. In both cases the solubility in copper is very small at room temperature, i.e. about 0·2%, rising to about 3 to 4% in the neighbourhood of 1000°C. Thus, quenching alloys of compositions between about 0·5% and 2% from appropriate temperatures

might reasonably be expected to produce the supersaturated single-phase state, which could be gradually converted into the two-phase equilibrium state. This in fact proves to be the case. Subsequent annealing precipitates the ferromagnetic component, the non-ferromagnetic one being almost pure copper, and the variation of ferromagnetic properties with heat-treatment can be followed without difficulty.

Results have been obtained which can be briefly summarized as follows. There are evidently three stages, terminating in the development of bulk ferromagnetism, which can, with some difficulty, be identified. Initially the alloy is frozen in the single-phase state, in which the intensity of magnetization is very small, usually exhibiting a field-independent paramagnetism with susceptibilities around 10^{-6}. With continued heat-treatment this grows, until curvature of the I/H curve, together with the appearance of remanence

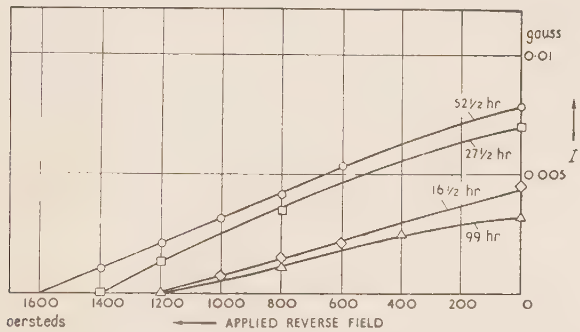

Figure 4. Remanent magnetization of 1% cobalt-copper alloy, heat-treated at 350°C.

and coercivity, indicates the onset of ferromagnetism. This is characteristic of both the cobalt and the more dilute iron alloys. Further heat-treatment of the alloy develops the coercivity with the same general trend as that for the stainless steel referred to above, though of course of a much smaller order of remanent intensity. The magnetization increases progressively with time of anneal in the case of the iron-copper alloys (0·3 to 0·5%) whilst for the cobalt-copper alloys (0·5 to 2·0%) it reaches a maximum after which a steady but small decrease takes place. Typical examples are given in Figures 2 and 3. It should be noted that in all cases the alloys were magnetized in a field of 5000 Oe so that the maximum remanence and coercivity are exhibited. It will be seen that there is no approach to saturation. Even when the measurements are extended to fields of several thousand oersted, approximate linearity between intensity and field still exists. Furthermore the magnetization curves of Figures 2 and 3 were, under the conditions shown, almost completely reversible, the remanence remaining in the direction of the original magnetizing field. It was found that the reverse

field required to reduce the remanence to zero ($H_{rem} = 0$ of table) was many times greater than the coercive field, in sharp contrast to normal ferromagnetics where the corresponding field is not more than 50% greater. An example of the relationship between the applied reverse field and the resulting remanence is shown in the table and Figure 4.

It is clear, therefore, that these magnetization curves are composite in character, and in general consist of three components. There is the "paramagnetic" component, dealt with in the work referred to above, in which the susceptibility is independent of field and increases with heat-treatment. This stage may be assumed to mark the state of aggregation prior to that sufficient for ferromagnetism. There is no coercive force and it is noteworthy that

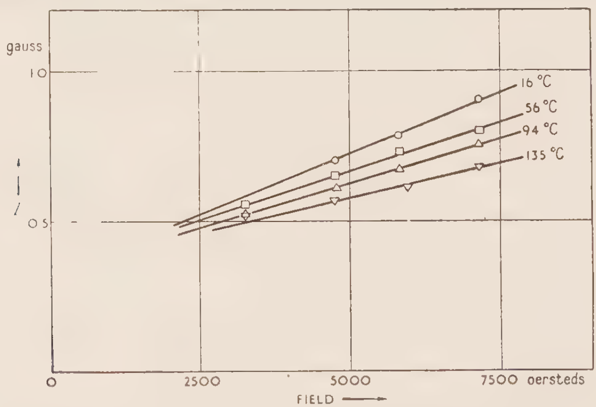

Figure 5. I/H curves at various temperatures for $1\frac{1}{2}$% cobalt-copper alloy, heat-treated at 350°C for 77 hours.

measurements at different temperatures exhibit a susceptibility decreasing with increasing temperature (Figure 5). With the development of measurable coercivity, there is strong evidence of two components, a soft component with H_c of the order 100 Oe, and a harder component whose presence is masked by the softer. Whilst the precise elucidation of H_c for this hard component appears almost impossible, it is not unlikely that it is the order of magnitude of the field required to reduce the magnetization to zero, i.e. about 1000 Oe. This stage falls between the " paramagnetic " and the low coercivities which result from continued heat treatment.

Thus as heat treatment proceeds, we have the initial increase of susceptibility due to the aggregation of ferromagnetic atoms. In time, these aggregates become large enough (and have sufficient nearest neighbours of similar kind) for ferromagnetism to begin, the aggregates being sufficiently small to behave as single domains. Under these conditions the theories of coercivity referred to above become applicable and we may expect abnor-

mally high coercivities if there is departure from spherical shape. As the regions continue to grow with further annealing, they become too large to exist as single domains, so that the coercive force begins to decrease. Obviously there will be considerable overlapping between these stages, and corresponding difficulty of interpretation. The picture drawn is over-simplified, but the general explanation seems not unreasonable. Further work on different aspects of the results is in progress.

Table

Heat-treatment, time in hours	I_{rem}, gauss	H_c, oersted	$H_{rem} = 0$, oersted
$16\frac{1}{2}$	0·0045	140	1 220
$22\frac{1}{2}$	0·006	200	1 400
$27\frac{1}{2}$	0·007	240	1 400
$52\frac{1}{2}$	0·0075	200	1 600
99	0·003	80	1 200

DISCUSSION

Dr. E. P. Wohlfarth:

Although single-domain characteristics are usually associated with particles rather smaller than those used in dust cores, as described by Richards (1953), and are, indeed, more appropriate in a discussion on permanent magnets, it is here suggested that even in powders of dust core size some part at least of the powder aggregate may be magnetically hard. Conversely, the dilute Cu-Fe alloys described by Sucksmith (Bate *et al.*, 1953) may contain a small magnetically soft constituent, apart from the main hard constituent due to the very small iron aggregates produced by appropriate heat-treatment.

That ferromagnetic particles of sufficiently small size are single domains, so that the magnetization process is one purely of rotation under the influence of strong anisotropy forces, was suggested independently just after the war by several workers (cf. Weil, 1951). The anisotropy forces involved may be those due to particle shape, leading, for elongated particles, to coercivities of several thousand, and even for almost spherical particles to coercivities of several hundred oersted; those due to magnetocrystalline anisotropy, leading to particularly large values for cobalt powders; or those due to uniaxial stress. In some powders only a small fraction of the particles may be in the magnetically hard state; this for a number of reasons.

First, the size of most of the particles may be larger than that for which single-domain structure is energetically possible. This critical size depends on the shape and intrinsic characteristics of the powder material, but it is unlikely that particles larger than about 0·1 micron are strictly single domains. On the other hand, even for considerably larger particles a substantial volume fraction of each particle will consist of domain boundaries whose movement in an applied field may be very appreciably impeded due to interference between them. It is suggested, therefore, that on increasing the particle size even well

beyond the critical value its permanent-magnet properties will disappear only gradually and not necessarily as soon as the critical size is exceeded.

Secondly, even for single-domain particles the coercivity due to shape anisotropy alone is smaller for disc-like particles than for needle-shaped ones, and is actually zero for particles having oblate spheroidal shape (Stoner and Wohlfarth, 1948). For an irregularly shaped particle, however, some degree of shape anisotropy must always be present, although the optimum conditions for large coercivity are unlikely to be attained.

Thirdly, unless the particles are widely separated, they will tend to interact, leading to a decrease of coercivity which is in many cases a linear function of packing density. The case of powder particles separated only by narrow ferromagnetic "bridges" has been discussed by Weil (1950).

It is seen, therefore, that for powder aggregates which are essentially hard there may well be a substantial soft magnetic constituent, but at the same time aggregates which are soft may contain a considerable hard constituent. An instance of the second situation is provided by the iron powders discussed by Richards. Here, for the smaller size particles, say 1 to 3 microns, domain-boundary movement may be much less free than for a bulk material, owing to the interference of the relatively few and wide domain boundaries as suggested above. Further, many of the larger particles may well be collections of a few smaller ones sticking together, but not capable of being microscopically resolved as such. An instance of a magnetically hard material with a soft constituent is provided by Sucksmith's experiments on iron particles in copper. This is a particularly simple and illuminating case for which inter-particle interaction will in general be unimportant, and for which the growth of the particles up to and beyond the critical value can be clearly followed by controlled-heat treatment. The foregoing remarks indicate, however, that at any stage of the process not all the iron particles are likely to be in such a state that optimum magnetic hardness is attained. Earlier experiments by Constant and associates show very clearly (cf. Constant, 1945) that this situation does in fact arise in impure copper and brass specimens, and some attempt was made to analyse the results into hard and soft contributions.

The theoretical problem of predicting the magnetic properties of such "two-phase" materials is difficult. Gerlach (1938) notes that the coercivity is not simply an average value of those of the two constituents, but that the coercivity of the soft constituent, even if present only in small quantities, is much more important in determining the bulk coercivity than that of the hard constituent. This may be the reason for the finding of Constant and of Sucksmith that, although the bulk coercivities they measured were appreciable, they do not even approach the extremely large values theoretically attainable under optimum conditions of shape and size. On the other hand, the hard constituent, even if present in small amounts, may require very high fields for complete saturation, and it is this method of analysis that was used in Constant's work.

3

THE INFLUENCE OF SUBDIVISION INTO ELEMENTARY DOMAINS ON THE HIGH-FREQUENCY PERMEABILITY OF FERROMAGNETIC CONDUCTING BODIES

L. Néel

(Laboratoire d'Électrostatique et de Physique du Métal, Grenoble)

It is known that, at very high frequencies, the permeability of ferromagnetic conducting bodies is affected, partly by the inertia of Bloch walls and by the quasi-viscous forces opposing their displacement, and partly by induced micro-currents due to the sub-division of the ferromagnetic substance into elementary domains. These are naturally the factors which present the greatest theoretical interest, as they furnish direct and valuable information on the mechanism of magnetization, and in particular of the very nature of the relaxation of the atomic moments (Kittel, 1951; Becker, 1951).

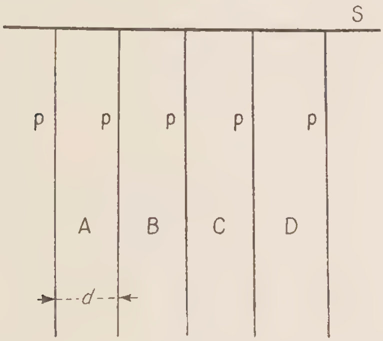

Figure 1. Section through the domains in a plane perpendicular to the surface S and to the boundary walls (p) between domains. The domains are magnetized perpendicularly to the plane of the diagram : A and C from back to front, and B and D from front to back. The applied field is also perpendicular to the plane of the diagram.

But to deduce information of value from experiments on this category of phenomena, it is a question of separating their action from the influence—*a priori* more trivial but always present—of induced micro-currents. Unfortunately, the theory of these micro-currents is not really in a very satisfactory state. Becker (1938b, 1939) has studied the damping of a Bloch wall in the interior of a ferromagnetic conducting substance; but his calculation hardly seems applicable to superficial layers in the presence of skin effect, although this would be essential since the measurements of permeability at high frequencies depend on the theory of skin effect. Kittel has followed the theory of this effect by assuming that the superficial layer of the body is composed of elementary domains, separated by flat and

undeformable walls which are being displaced in a single block during the course of magnetic variations. This last hypothesis is entirely indefensible.

We have taken up the theory again by assuming the superficial layers of the ferromagnetic body to be composed of elementary domains having the shape of flat leaves of a thickness d small compared with their transverse dimensions. As shown in Figure 1, we have assumed that these leaves are disposed perpendicularly to the surface, and are magnetized alternately in opposite directions, following a common direction parallel to the intersection with the surface of the Bloch walls. We have assumed, moreover, that the external field applied

$$H_e = H_0 e^{j\omega t}$$

is parallel to that intersection. Everything then occurs as if we were dealing with a substance of unit permeability within the elementary domains, and as if the walls possessed a superficial magnetic susceptibility equal to $X_a d$ per unit area, where X_a is the initial static susceptibility. For small variations of magnetization, the walls behave like fixed surfaces of discontinuity, and the conditions at the corresponding limits may be written in the following manner:—

$$i_1 - i_2 = (4\pi \chi_0 d/\rho)\,(\partial H/\partial t) \qquad \ldots(1)$$

where i_1 and i_2 are the components along OX of the current densities on either side of the wall, and where H is the OY component of the magnetic field (OX and OY being two rectangular axes situated in the plane of the wall); finally, ρ is the resistivity. Further, we neglect the inertia and the friction of the walls.

It is possible then, starting from Maxwell's equations, and taking condition (1) into account, to develop a rigorous theory (Néel, 1952) which shows that, macroscopically, everything occurs as if the classical skin-effect theory were applicable, provided that the initial static permeability $\mu_a = 1 + 4\pi \chi_a$ is replaced by a certain complex permeability

$$\mu = \mu' - j\mu'' = 4\pi X_a A^2 \qquad \ldots(2)$$

The complex quantity A is given by the expression

$$A = \sum_{n=1}^{\infty} \frac{2r^3(1 + r^2/4\pi X_a \phi_n{}^2)^{\frac{1}{2}}}{\phi_n(\phi^2{}_n + r^2 + r^4)} \qquad \ldots(3)$$

where $\phi_1, \phi_2, \ldots \phi_n$ are the successive roots of the transcendental complex equation

$$\phi \tan \phi = r^2 \qquad \ldots(4)$$

As for the parameter r^2, it is defined by the relation

$$r^2 = ja = j4\pi^2 X_a d^2 \omega/\rho \qquad \ldots(5)$$

To summarize, the real and complex components μ' and μ'' of the apparent

permeability are functions of the single real variable a, defined in (5) and proportional to the frequency.

The calculation of A presents some difficulty as it is fairly hard to calculate the roots of (4), while expression (3) does not in general converge very rapidly. Figure 2 summarizes the results obtained, by giving the values μ'/μ_a and μ''/μ_a as a function of the parameter a. In particular, it can be proved that the real part μ' of the permeability is reduced to half its initial value when $a \doteqdot 7{\cdot}2$.

These results have been obtained, contrary to Kittel's hypothesis, by assuming the wall to be *infinitely flexible*, i.e. by neglecting the surface energy

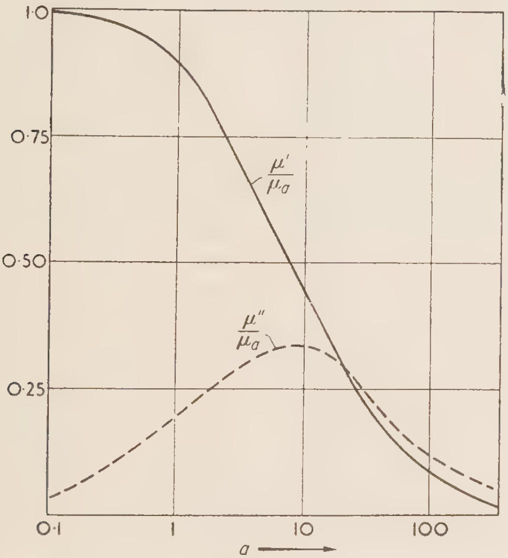

Figure 2. Values of the real and imaginary components, μ' and μ'', of the complex permeability, as functions of the parameter a (equation 5), plotted logarithmically.

of the wall. In order to justify this hypothesis we have made a new calculation of the skin effect, taking into account the value γ of the surface energy of the wall. We have assumed that we are dealing with the same superficial structure as that which has been described above, but, in order to simplify the calculation, we have assumed this time that the thickness d of the elementary domains is small enough for the field and the flux to be considered as functions of two variables only—the time and the depth. In these conditions the apparent permeability is found to be given by

$$\frac{\mu}{\mu_a} = \frac{1 + ja'/\mu_a + 2\sqrt{ja'}}{(1 + \sqrt{ja'})^2} \qquad \ldots(6)$$

where $\quad a' = \gamma d \mu_a{}^2 \omega / 4\rho I_s{}^2$

and I_s is the spontaneous magnetization.

In the case of iron, with $\gamma = 1{\cdot}4$ ergs/cm², $\mu_a = 100$, $\rho = 10\,000$, $I_s = 1700$, it can be proved that, when the thickness d of the domains is greater than 10^{-4} cm, the influence of surface energy is entirely negligible, so that equation (2) is applicable without corrections. The hypothesis of the infinitely flexible wall is therefore justified.

When the thickness of the domains becomes less than 10^{-4} cm, it becomes necessary to take into account the corrections specified in formula (6), but it can then be proved that the reduction in apparent permeability occurs in a range of frequencies so high that it is no longer possible to neglect the friction undergone by the walls in consequence of the relaxation of atomic moments. It is in any case improbable that such thin domains will be found in soft iron.

The application of formula (2) to domains of 20 microns thickness shows that μ' is reduced by half at a frequency of 9 Mc/s, while experiment (Millership and Webster, 1950) shows that a frequency of 340 Mc/s is needed for ordinary annealed soft iron, corresponding to domains of 3·3 microns. As it is easy to obtain 20-micron domains by appropriate mechanical and heat-treatment, it is certainly possible to verify formula (2) for, in the region of 10 Mc/s, the phenomena of relaxation no longer come into play.

4

THE CARDINAL MAGNITUDES OF TECHNICAL MAGNETIZATION

G. C. Richer

Abstract: The true nature of many outstanding problems in applied ferromagnetism can be clarified by restating them in more fundamental terms than has been customary.

A sketch is here given of a simple model of technical magnetization which will enable such restatements to be made by reference to a few cardinal magnitudes whose physical significance is common to all ferromagnetics, but which will, at the same time, provide unambiguous pointers to the structural factors that govern the engineering performance of any given type. The model is based on the experimentally supported concept that, so far as translational processes are concerned, the cyclic behaviour of most ferromagnetics can be closely synthesized by the integration of two normal Gaussian distributions, one for the elastically reversible mechanism of domain-boundary displacement, and the other for the irreversible or Barkhausen mechanism.

The working of the model is illustrated by an analysis of the complex case of the "watt-loss" during alternating magnetization, from which it emerges that the much-discussed "eddy-loss anomaly" can be directly related to the shape of the hysteresis loop.

1. INTRODUCTION

Long-familiar engineering quantities, such as maximum permeability, coercive force, and the "watt-loss" during alternating magnetization, may complexly depend on so many factors that their actual magnitudes have no clear-cut physical significance. This is particularly true of the widely used "watt-loss", which can remain puzzlingly insensitive to major variation in the fundamental properties of the ferromagnetic structure.

An attempt has therefore been made to distil out the nature of the "numbers" without which it will apparently be impossible to frame an unambiguous description of any given ferromagnetic specimen; and to relate these numbers to the basic structural factors on which all variations in engineering performance must ultimately depend.

Brevity will demand a few references to the background to the present outline, as developed in a series entitled "The Physics of Sheet Steel", which appeared in *Sheet Metal Industries* over the period May 1947 to July 1951. For such references it is proposed to use the notation "SMI. 1950/3/25" to denote the relevant year, month, and section number.

2. THE BASIC EQUATION OF TRANSLATIONAL MAGNETIZATION

The adopted treatment is based on the primary concept (Richer, 1947) that over the initial, steep, and knee regions of the normal induction curve the increments dB_π of "irreversible" or "Barkhausen" magnetization, due to

domain-boundary displacements across 180-degree or "anti-parallel" walls, will ideally be such as would result from a normal Gaussian distribution of the probabilities about some characteristic mode H_π of the critical field strength for "Barkhausen reversals", so that

$$dB_\pi/dH = \mu_\pi = \mu_{\pi m}.\ \exp\left[-\beta_\pi(1 - H/H_\pi)^2\right] \qquad \text{...(1)}$$

where μ_π = the differential permeability for Barkhausen or irreversible magnetization
and $\mu_{\pi m}$ = the maximum value of μ_π at H_π.

The secondary concept is that for the increments dB_r of "reversible" magnetization, due to domain-boundary displacements across 90-degree walls, it will be sufficiently near to the truth, for engineering purposes, to put

$$dB_r/dH = \mu_r = \mu_a \,.\, \exp(-\beta_r \,.\, H^2) \qquad \text{...(2)}$$

where μ_r = the differential permeability for reversible magnetization
and μ_a = the initial permeability, as ordinarily defined.

Integrating, equations (1) and (2) will give

$$B = \mu_a \int_0^H \exp(-\beta_r.\, H^2)\, dH + \mu_{\pi m} \int_0^H \exp\left[-\beta_\pi \quad (1 - H/H_\pi)^2\right] dH \qquad \text{...(3)}$$

as the basic equation of translational magnetization.

Equations (1) and (2) are consistent with the experimental finding that the Barkhausen mechanism may be incipiently operative over the Rayleigh region of initial magnetization (Bush, 1950); and for $H \to 0$ they will predict the "Rayleigh Law" (SMI. 1948/6/23(*j*)).

3. ROTATIONAL MAGNETIZATION

To take care of the reversible rotational processes which come into operation as translational magnetization is completed, and which govern the magnitudes of the approach to saturation, an "Akulov" term can be linked with equation (3), in the manner described in SMI. 1950/9/26(*b*). The present discussion, however, will not be concerned with this final stage of the magnetization process, whose characteristics have recently been restated by Lawton and Stewart (1950).

4. TRANSLATIONAL SATURATION VALUE

Translational processes will be complete when all the domain magnetization has been aligned along the magnetically "easy" crystal axes nearest to the external field direction, and the value of B at this point can conveniently be called the "translational saturation value" and denoted by B_t; for any given

order of H_π its magnitude will largely determine the "high-induction permeability."

Under any given experimental conditions the value of B_t will be just as characteristic as the ferric-induction saturation value $(B - H)_s$, and for any given value of the latter will depend only on the crystallographic set-up about the external field direction, i.e. on the "operative lattice orientation".

B_t can usually be assessed with reasonable precision, especially when the elastic or magnetostrictive characteristics, or both, are known (SMI. 1947/6/12; 1950/9/26).

5. BARKHAUSEN SATURATION VALUE

To evaluate B_π, the total B-contribution from Barkhausen magnetization, use can be made of the familiar formula for the area under a normal probability curve, which for the second or Barkhausen term in equation (3) will give

$$B_\pi = \mu_{\pi m} H_\pi \sqrt{\pi/\beta_\pi} \qquad \ldots(4)$$

It will be convenient to refer to B_π as the "Barkhausen saturation value".

6. EVALUATION OF β_π

In most soft ferromagnetics the magnitudes associated with the steep part of the normal induction curve will be almost wholly determined by the Barkhausen term in equation (3), and a working value of β_π for use in equation (4) can be obtained by putting

$$\beta_\pi = (\pi/4)\,(\mu_{\pi m}/\mu_{\pi s})^2 \qquad \ldots(5)$$

where $\mu_{\pi s}$ is the experimental value of B/H at H_π, i.e. at the mid-point of the "middle straight" of the steep part of the B/H curve, whose *slope* at this point will evaluate $\mu_{\pi m}$.

It will be convenient to refer to β_π as the "Barkhausen dispersion index"; for any given value of H_π it will give an inverse measure of the variance of the critical field strength for Barkhausen reversals.

7. EVALUATION OF β_r

With μ_a and B_t known, and B_π established by equation (4), the "reversible" area equation will give

$$2(B_t - B_\pi) = \mu_a \sqrt{\pi/\beta_r} \qquad \ldots(6)$$

so that β_r becomes determinate.

8. THE BASIC EQUATION OF CYCLIC MAGNETIZATION

So long as the underlying constitution of the ferromagnetic structure is not sensibly modified by cyclic variation of the external field—a condition which seems in general to be closely satisfied—the basic equation of cyclic magnetization for the ascending half-cycle of the hysteresis loop will ideally be expected to take the following form:

$$B + B_{max} = \mu_{rm} \int \exp\left[-\beta_c (1 - H/H_\pi)^2\right] dH + \mu_{cm} \int \exp\left[-\beta_\pi (1 - H/H_\pi)^2\right] dH \qquad \ldots(7)$$

with the integration taken over the appropriate cyclic limits of H.

In equation (7), which has been designed to conform to the experimental evidence that the reversible mechanism will tend to act "in phase" with the irreversible mechanism (Tebble, Skidmore and Corner, 1950),

$$\mu_{cm} \doteqdot 2\mu_{\pi m} \qquad \ldots(8)$$

and

$$H_\pi \doteqdot \text{the coercive force } H_c \qquad \ldots(9)$$

Equation (8) reflects the experimentally supported concept that at any given value of H the Barkhausen increments under cyclic conditions will tend to be *twice* the corresponding increments recorded under the normal induction conditions of equation (3).

In equation (7) μ_{rm} will be of the same order of magnitude as, but not necessarily identical with, the initial permeability μ_a in the normal induction equation (3) (Tebble, Skidmore and Corner, 1950). β_c will also differ from β_r, so as to satisfy the condition that the cyclic version of equation (6) shall be given by

$$2(B_t - B_\pi) = \mu_{rm} H_\pi \sqrt{\pi/\beta_c} \qquad \ldots(10)$$

A rational value of μ_{rm}, and hence also of β_c, can be obtained by noting that β_π will normally be sufficiently greater than unity to ensure that Barkhausen magnetization will be largely completed when $H = 2H_\pi$. This means that for $H > 2H_\pi$ the run of the "external" dB/dH curve will be almost wholly governed by the reversible magnitudes, so that a backward and "flat-topped" extrapolation will enable the "internal" order of μ_{rm} to be pretty shrewdly assessed.

It will be seen that, according to equation (7), the reversible component of cyclic magnetization is not ideally anhysteretic, and will therefore make to the residual induction B_r a contribution which will normally be of the order given by $\mu_{rm} H_\pi$.

It is to be expected that the magnitudes of equation (10) will importantly bear on the magnitudes of magnetostrictive hysteresis, and hence also on the vexed problem of "transformer noise".

9. THE CARDINAL MAGNITUDES: PHYSICAL BACKGROUND

The conclusion from Section (8) is that, for $B_{max} \gg B_t$, the cardinal magnitudes of cyclic magnetization can be enumerated and interpreted as follows:—

(*a*) The translational saturation value B_t, which for any given ferric-induction saturation value $(B-H)_s$, as normally determined by the chemical composition, will depend on the operative lattice orientation about the external field direction;

(*b*) The Barkhausen saturation value B_π, which will depend on the proportion by volume in which the ferromagnetic domain structure is such that bulk magnetization is effected by the nucleation and propagation of simple reversals of anti-parallel domain magnetization;

(*c*) The characteristic mode H_π of the critical field strength for Barkhausen reversals, which will reflect the average ease with which such reversals can be achieved, and which is known to depend on the initial content of magnetically unfavourable "dislocation" or strain of the ferromagnetic lattice, with impurities, grain-boundaries and work-hardening as the most familiar causes;

(*d*) The Barkhausen dispersion index β_π, which by reflecting the "variance" of the critical field strength, will depend on the mode of distribution of localized differences in the "strain-content" per unit of volume of the Barkhausen "population", i.e. on the distribution of *differences* in anti-parallel domain-wall conditions;

Table 1. Cardinal magnitudes of cyclic magnetization : typical values

Quantity	Alnico 5	Hard-drawn iron wire	3% Fe-Si oriented strip	4% Fe-Si single crystal, [100] axis	4-79 Permalloy	Supermalloy
$*B_t$ . . . gauss	14 000	15 200	19 200	19 500	8 500	8 000
$*B_\pi$ . . . gauss	12 000	12 400	11 500	15 500	3 400	4 200
H_π . . . Oe	500	5·75	0·15	0·013	0·04	0·004
β_π	20·0	5·00	3·00	80·0	2·80	8·25
$\mu_{rm} (\doteqdot \mu_a)$	2·0	100	1 500	6 000	20 000	100 000
$\beta_c \times 100$	20·0	3·30	0·068	0·030	1·90	0·86

* $(B - H)$ for Alnico 5.

NOTE.—For constructional purposes μ_{cm} is evaluated by equations (4) and (8). The condition for sharply rectangular loops is that B_π/B_{max} shall be not much less than unity, and that the "variance" of the Barkhausen distribution, as reflected by H_π^2/β_π, shall be very small, thus making μ_{cm} very large. Wasp-waisting and similar idiosyncrasies will be generated when the Barkhausen distribution is not "unimodal"; such conditions can be catered for by appropriate sub-division of the irreversible term in equation (7).

(e) The "reversible" magnitudes μ_{rm} and β_c, which can be thought of as depending on the interaction between the non-elastic Barkhausen mechanism and the elastic and magnetostrictive background which governs the initial permeability, as evaluated by the Becker and Kersten type of relationship.

It is to be noted that neither $\mu_{\pi m}$ nor μ_{cm} is a cardinal magnitude in the sense in which B_π, H_π and β_π can be so defined; they are essentially experimental quantities which result from the joint operation of the other three factors.

Typical values of the cardinal magnitudes are given in Table 1.

10. CARDINAL MAGNITUDES v. ENGINEERING PERFORMANCE

The competence of the cardinal magnitudes to "explain" variations in engineering performance can be illustrated by considering the complex case of the "watt-loss" due to hysteresis and eddy currents during alternating magnetization at power-engineering frequencies.

In cyclic magnetization the "reversible" contribution to the residual induction B_r will normally be quite small, and so long as the half-cycle of the hysteresis loop obeys equation (7) it will be permissible to write

$$B_r = B_{loop} \text{ at } 2H_\pi \doteqdot B_\pi; \qquad \text{...(11)}$$

and also to assume that modest differences in the "earing" characteristics of the loop—as predominantly determined by the reversible magnitudes—will not seriously invalidate the familiar empiricism that for any given value of B_{max} the cyclic hysteresis loss

$$W_h \propto H_c B_r \qquad \text{...(12)}$$

or, in terms of the cardinal magnitudes,

$$W_h \propto H_\pi B_\pi \qquad \text{...(13)}$$

Equation (11) tends to be satisfied wherever there is a high degree of "preferred" crystallographic orientation, irrespective of kind or origin. Modestly skew conditions can, however, be roughly catered for by modifying equation (12) to read

$$W_h \propto H_c \,.\, B_r \,.\, \sigma \qquad \text{...(14)}$$

$$\text{where } \sigma = \text{"skewness factor"} = B/B_{loop} \text{ at } 2H_c \qquad \text{...(15)}$$

The cyclic eddy loss according to the classical theory will, under sine-wave conditions and for any given cross-sectional dimensions, resistivity and frequency, depend only on the square of B_{max}. It has long been known,

Table 2. Cardinal magnitudes v. *engineering performance. 3% silicon-iron strip:* 0·0125 *in. thick*

Quantity	1	2	3	4	5	6	7	8	9	10	11	12	13
	H 48	B 915	B 918	NA 265	C 136	C 139	WA 599	A 600	B 914	B 883	A 502	C 137	NA 258
H_c ($\risingdotseq H_\pi$) .... Oe	0·145	0·15	0·135	0·15	0·18	0·18	0·18	0·21	0·12	0·16	0·25	0·35	0·30
H_{max} .... Oe	1·00	1·65	1·50	5·05	2·36	2·90	1·46	2·20	3·40	4·75	4·80	3·25	10·5
* $\mu_{\pi m}$ ($\risingdotseq \frac{1}{2}\mu_{cm}$)	82 500	47 000	59 000	31 000	34 000	28 000	61 000	39 000	45 000	31 500	30 000	25 000	18 500
B_r ($\risingdotseq B_\pi$) .... gauss	11 750	11 950	11 700	6 000	10 300	11 000	12 400	10 800	11 400	9 250	8 750	10 350	5 700
B_{loop} at $2H_c$ ...... gauss	11 750	11 100	10 700	5 000	8 800	9 000	10 200	8 300	8 400	6 900	8 750	9 400	5 200
σ (skewness factor)	1·00	1·08	1·09	1·20	1·17	1·22	1·22	1·30	1·36	1·34	1·00	1·10	1·10
Total loss, watts/Kg, for B_{max} = 15000 50 c/s ..	1·26	1·28	1·27	1·35	1·39	1·43	1·56	1·64	1·62	1·67	1·72	1·84	1·94
† Cardinal number	119	122	123	129	132	140	156	159	169	172	177	180	191

* The normal induction value of $\mu_{\pi m}$ is more accurately and more easily measurable than the loop value of μ_{cm}, and equally competent to reflect the incidence of β_π in equation (16).

† As exploratorily given by: cardinal number (for "watt-loss" grading) = $(H_c\, H_{max}\, \mu_{\pi m}\, B_r \cdot \sigma)^{\frac{1}{4}} \times 10^{-2}$ ...(18)

however, that the actual eddy-loss may greatly exceed the classically-computed value. This much-discussed "eddy-loss anomaly" seems in the main to arise from the fact that in the classical treatment the assessment of the mean cyclic value of $(dB/dt)^2$ is based on the untenable assumption that the operative value of dB/dH remains constant, instead of varying cyclically in accordance with the underlying differentials of equation (7).

By discarding this outworn postulate and substituting the probability concept, it is found that for knee-point order of B_{max} a more rational expectation is that the cyclic eddy-loss

$$W_e \propto (H_{max}/H_\pi)\, B_\pi{}^3\sqrt{\beta_\pi} \qquad \ldots(16)$$

which with equations (4), (8) and (11) will for *experimental* purposes become

$$W_e \propto H_{max}B_r{}^2\mu_{cm} \qquad \ldots(17)$$

(For the mode of development of equation (16) see SMI. 1950/3, 6/25 (*w*) (*x*).)

The statement of equation (17) is that the cyclic eddy-loss will depend

(*a*) not only on B_{max}, but also on the *Barkhausen content* of B_{max}, as virtually given by B_r;

(*b*) on the "steepness" of the hysteresis loop, as reflected by μ_{cm}, which will govern the peak value of dB/dH; and

(*c*) on H_{max}, which will govern the peak value of dH/dt.

When these three factors are taken into account it at once becomes clear that the "total loss" is in essence indivisible, since the eddy-loss no less than the hysteresis loss will be affected by changes in the characteristics of the cyclic magnetization curve.

This view is supported by Table 2, in which, over a wide range of variation in fundamental behaviour, an extremely simple handling of the cardinal magnitudes is seen to lead to an order of agreement between "theory" and practice which can hardly be fortuitous.

Note added in proof

Further experience has shown that for other than "unimodal" conditions the use of equation (11) may tend to exaggerate the operative value of B_π in equation (16), and that such an effect can be largely neutralized by omitting the empirical σ from equation (18).

The author has to thank the Board of Directors of the Steel Company of Wales, Ltd., for permission to publish this paper.

5

IRON LOSSES UNDER SUPERIMPOSED ALTERNATING INDUCTIONS

J. Greig and H. V. Shurmer

(King's College, University of London)

Abstract: Experiments with excitation at 50 c/s and also at a frequency of from 250 to 1000 c/s show that the total loss under superposed excitation may be greater or less than the sum of the losses when the same excitations are applied separately. The increase in loss occurs when the hysteresis loop due to the lower frequency develops re-entrant minor loops due to the higher frequency.

1. INTRODUCTION

The energy losses occurring in ferromagnetic materials subjected to multiple frequency excitation are of direct concern to the designers of electrical machines, and the associated phenomena are of interest in relation both to heavy-current and to light-current electrical engineering. The present investigation deals with the simplest case, that of two-frequency excitation, applied to silicon-iron laminations, the frequencies lying in the range from 50 c/s to 1000 c/s, the higher frequency being a harmonic of the 50-c/s fundamental and in general of smaller amplitude. As it is the non-linear characteristics of the ferromagnetic material which give rise to the interesting features of this problem, it is necessary to carry measurements as far into the non-linear region as possible; and, to obtain results which may be susceptible of interpretation and application, substantially sinusoidal variation of either the component inductions or magnetizing forces must be maintained. Sinusoidal induction was taken as the ideal condition in these measurements.

The immediate purpose of the investigation was to compare the total iron loss in a test specimen undergoing simultaneous excitation at two frequencies with the sum of the losses produced by the same two excitations when applied independently. The experimental results are plotted as curves of a factor k defined by the relation $k = W_t/(W_f + W_h)$, where W_f is the total iron loss for the fundamental induction applied separately, W_h the total loss for the harmonic induction applied separately and W_t the total loss for the same two inductions applied together. It is found that this factor, which would have the constant value unity if the iron-cored coil were a linear circuit element, passes through a minimum value of about 0·9 in the region of low harmonic inductions and increases as the harmonic induction is increased, reaching values of the order of 1·15 at the extremity of the present range of measurement. The losses associated, under combined-frequency excitation, with each of the applied frequencies were also determined for the same range of frequencies and inductions, and an attempt was made to predict from the

complex hysteresis loop the well-known phenomenon that the superposition of a high-frequency ripple reduces the amount of power associated with the low-frequency fundamental upon which it is superimposed.

2. EXPERIMENTAL PROCEDURE

The test specimen consisted of 39 ring stampings of 3·5% silicon-iron, of 10 cm external diameter, 8 cm internal diameter and nominal thickness 0·007 in. The power supply to the test specimen was from a negative-feed-back amplifier arranged to minimize the distortion arising from the non-linearity of the specimen itself. The principle involved is that of obtaining the feed-back voltage from the secondary of the test specimen, thus, in effect, utilizing the specimen as an output transformer of the amplifier. This tech-

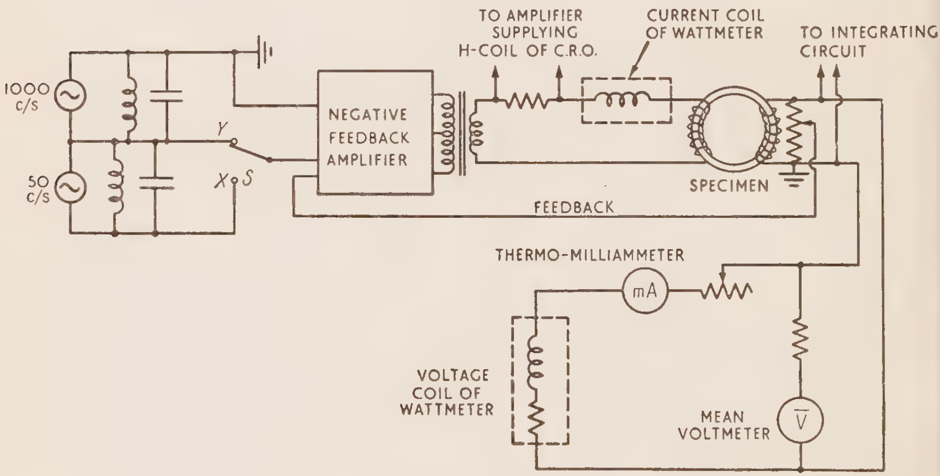

Figure 1. Circuit diagram of apparatus.

nique is due to Dr. Moneypenny of the G.K.N. Research Laboratories and the amplifier described is based on his design. The losses were measured by a reflecting dynamometer wattmeter. Figure 1 shows the general arrangement of the test circuit. The wattmeter volt coil is fed from the secondary of the test specimen, and this, together with the feed-back potentiometer and the mean voltmeter, constitutes a load on the circuit for which allowance has to be made. As the secondary winding is applied as closely as possible to the core, the effect of secondary leakage-reactance has been assumed to be negligible. Provision was made for the continuous display on cathode-ray oscillographs of the dynamic hysteresis loop and of the wave-form of the induced voltage. Harmonic-analyser measurements showed that the negative feed-back was effective in restricting the non-linear distortion of the induced

e.m.f. wave to a harmonic content of less than 5% at the highest inductions at which measurements were made. The reliability of the wattmeter readings when measuring iron loss at a frequency of 1000 c/s, was confirmed by checking against a calorimetric measurement, the agreement being found to be better than 1%. No attempt was made to lock the frequencies of the two sources supplying the amplifier, and there was thus a slow cyclic variation of phase between the two sources. For low-order harmonics this phase variation would produce a cyclic variation of wattmeter reading corresponding to the variation of peak induction from coincidence to opposition of wave maxima. This effect was negligible at harmonic frequencies of 500 c/s and above. It was noticeable, however, at 250 c/s, and values given for this frequency must be regarded as averages for all phase positions.

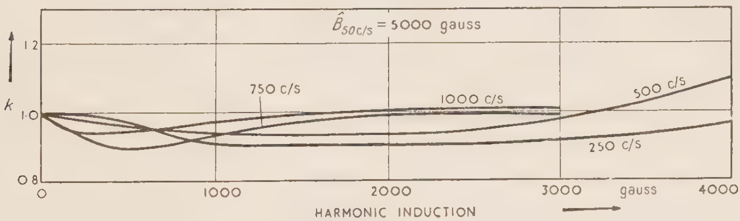

Figure 2.

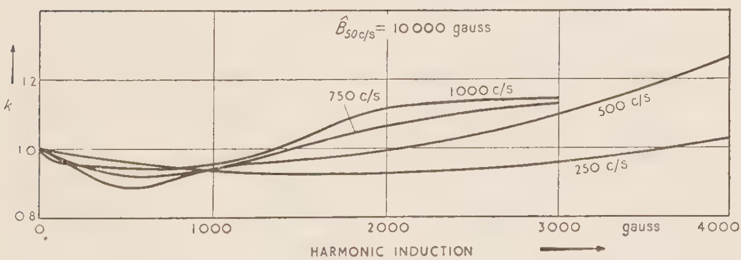

Figure 3.

The factor k as a function of harmonic induction.

Values of the factor k were obtained for a range of harmonic inductions up to 3500 gauss at frequencies of 250, 500, 750 and 1000 c/s superimposed on 50-c/s inductions of 2500, 5000, 7500, 10 000 and 12 000 gauss. Typical curves are plotted in Figures 2 and 3.

The component of power loss associated with each of the applied frequencies was determined experimentally for 1000-c/s inductions up to about 3000 gauss superimposed on the same range as before of 50-c/s inductions. The method of separation was to determine the fundamental component of loss only, by filtering out the harmonic component of search-coil voltage and

applying to the wattmeter terminals only the fundamental component of induced e.m.f. The circuit arrangement used when separating the 50-c/s component in this way is shown in Figure 4 in which it will be seen that a bridged-T filter is employed to suppress the 1000-c/s voltage, the 50-c/s

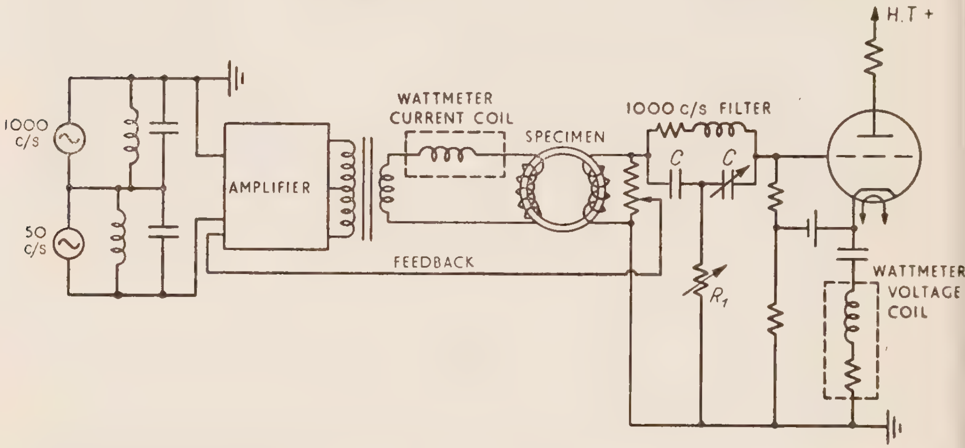

Figure 4. Simplified circuit diagram of apparatus for separation of 50-c/s component from total iron loss.

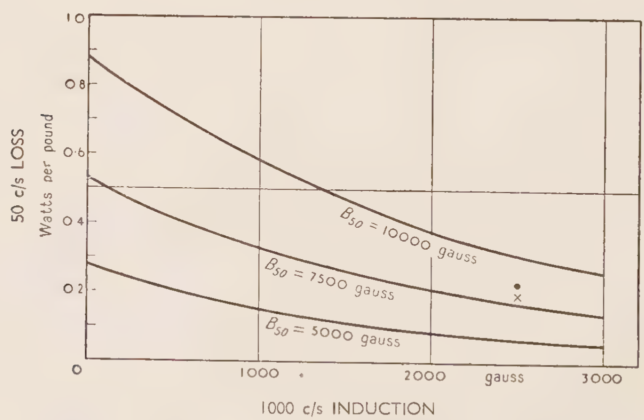

Figure 5. Typical curves showing variation of 50-c/s loss with 1000-c/s induction.

component being transmitted to a cathode-follower which feeds the volt coil of the wattmeter. The impedance presented by the filter network to the search coil was sufficiently high both at the fundamental and at the harmonic frequency not to affect the operating conditions appreciably. Phase shift

and attenuation of the 50-c/s component were negligible in relation to the order of accuracy required. Typical experimental results are given in Figures 5 and 6. These curves show the extent to which the loss associated with one of the component frequencies is affected by variation in amplitude

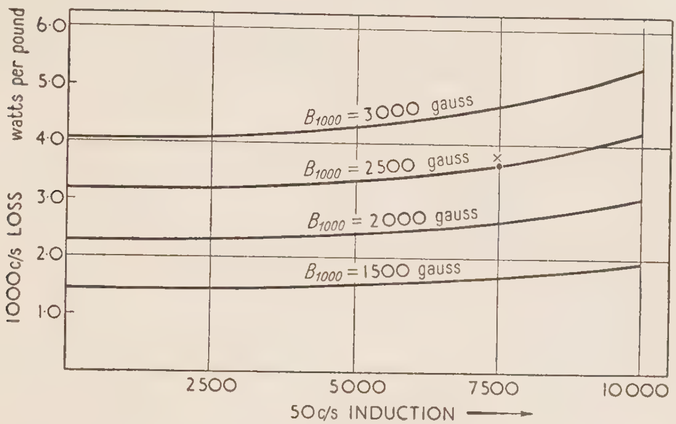

Figure 6. Typical curves showing variation of 1000-c/s loss with 50-c/s induction.

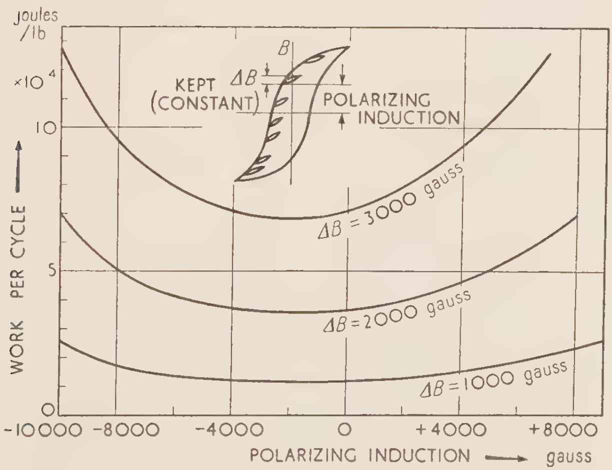

Figure 7. Work per cycle associated with minor loops.

of the other frequency component. In particular the reduction of the 50-c/s component with increase in the 1000-c/s induction is illustrated by Figure 5. All the results are in qualitative agreement with those obtained by Schröter in 1924 using a different method of measurement.

The attempt to interpret some of the phenomena encountered with two-frequency excitation required the provision of static hysteresis loops corresponding to the actual cycle executed by the core material. The direct aim of these static measurements was to determine the areas and slopes of minor loops formed at all possible positions on a major loop. Figure 7, which summarizes a range of results, shows that minor loops of given amplitude are considerably greater in area when formed at the tips of the major loop than when formed on the steeply-rising portions of the main loop in the region of zero flux-density.

3. INTERPRETATION OF EXPERIMENTAL RESULTS

The interpretations put forward for a number of the phenomena observed are based on the following assumptions:—

(*a*) that the eddy-current losses with superimposed alternating inductions are additive;

(*b*) that the hysteresis loss per cycle depends only on the B/H loop, simple or complex, which is traversed and not upon the rate of traverse of individual parts of the loop.

The first assumption implies that the distributions of the systems of eddy currents associated with each of the component fluxes is altered to only a negligible extent by the cyclic changes in permeability resulting from the superposition of one alternating flux on the other. With the laminae used in the present tests, the thickness being 0·0185 cm, and taking a value of 3000 for the permeability, the reduction of flux-density from the surface to the mid-plane of the stamping should, at 1000 c/s, be only of the order of 1%. The flux-density may therefore be considered to remain substantially uniform under all test conditions.

The eddy-current loss for sinusoidal single-frequency excitation is taken to be the difference between the measured total iron-loss and f times the loss associated with the area of the static hysteresis loop corresponding to the peak induction. This hysteresis loss has been shown experimentally to correspond fairly closely with the experimental values of total loss per cycle extrapolated to zero frequency.

Consider first the variation of the factor k in relation to the relative amplitude and frequency of the harmonic induction. Figure 8 illustrates under (a) the simple hysteresis loop and the wave form of H corresponding to sinusoidal time-variation of B. Suppose now that a ripple is superimposed on the B wave as indicated in Figure 8b. If the form of the composite flux-wave is such that B increases continuously to a single positive maximum and thereafter decreases continuously to a single negative maximum so that no subsidiary maxima or minima are formed, then on the second of the foregoing assumptions the hysteresis loop traced will be identical with that

traced previously if the peak value of induction is made the same in both cases. The application of a ripple of larger amplitude is illustrated in Figure 8c. Here subsidiary maxima and minima are formed, and at each of these there is a reversal of direction of tracing round the hysteresis loop with the result that minor loops are formed at points less in number than the order of the harmonic, on the major loop. The energy dissipated per cycle, being $\int H dB$ taken round the complete loop, is represented in the case of a composite loop by the sum of the areas of the main loop and of the minor

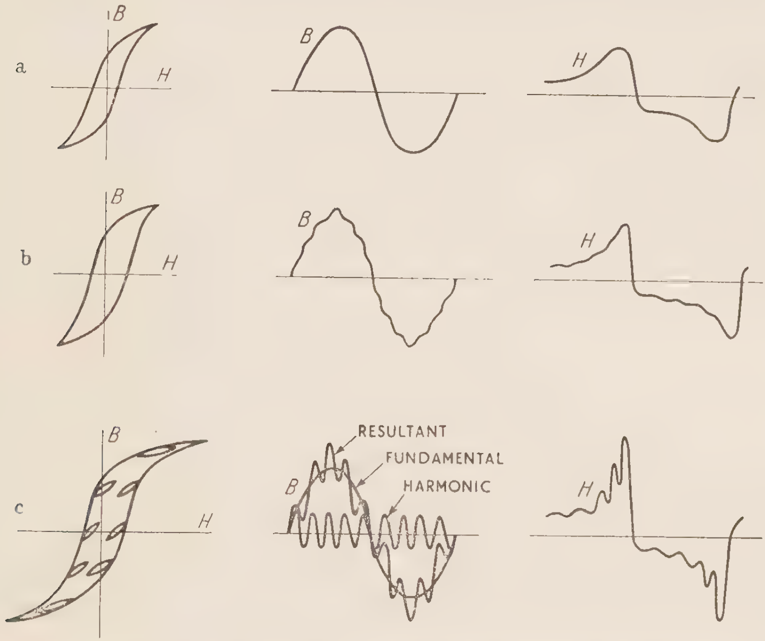

Figure 8. Diagrams to explain theory of hysteresis loss with two-frequency flux.

loops. It therefore follows that if a ripple could be applied such that no minor loops were formed, its application would result in additional hysteresis loss due *only* to any increase in area of the main loop resulting from increased peak induction. Apart from this, "ripple" hysteresis loss would be absent. This hypothesis is consistent with the observation that the value of k can fall below unity, for the absence of the loss which would be associated with a number of cycles of the high frequency may more than compensate for the greater loss in one cycle of the fundamental.

The condition for the formation of a minor loop is a temporary reversal of the direction of tracing of the main loop, thus corresponding to the existence of subsidiary maxima or minima of the flux wave-form, and such

maxima or minima will be formed where the time-rate of change of the subsidiary induction is of opposite sign and becomes greater or less than that of the fundamental induction. Thus the formation of minor loops is mainly dependent upon the relative amplitude and frequency of the harmonic induction. Minor loops will tend to be formed first around the peaks of the fundamental wave and will have larger amplitudes in these regions than on the steeply rising or falling portions of the main wave. It has already been noted that for a given amplitude of minor loop the area increases as the position of the minor loop is displaced towards the tips of the major loop.

On the basis of the foregoing assumptions, an attempt has been made to estimate the value of the factor k from static hysteresis-loop data and a knowledge of the eddy-current losses under single-frequency excitation, the operating conditions chosen being amongst those for which actual test results were available. In each case the peak induction was $B = 10\,000$, the fundamental induction being 7500 and the harmonic induction 2500. The harmonic frequencies were 250, 500, 750 and 1000 c/s. The first step in the calculation was to find the points on the main loop at which subsidiary loops were formed, and to determine their amplitude; that is to say the values of θ for which $dB/d\theta = 0$ in equations of the form

$$B = B_f \sin \theta + B_h \sin (n\theta + \phi).$$

These were determined by plotting tables of values. The hysteresis losses associated with the minor loops were available in the form of sets of curves. The hysteresis loss for the major loop and the eddy-current losses under single-frequency excitation being known, the total loss under superimposed conditions could be computed. The values of k computed in this way are given below. It will be seen that these values agree quite closely with the experimental ones, but in view of the simplifying assumptions and the small range of variations it is only considered significant that the values vary with frequency in a similar way.

Harmonic frequency c/s	k, calculated	k, measured
250	0·911 (for harmonic in phase)	0·910 (average)
500	0·985	0·969
750	1·018	1·021
1000	1·052	1·058

The phenomenon, under double-frequency excitation, of the reduction of the power associated with the fundamental frequency produced by the application of the harmonic frequency may be explained qualitatively by reference to the wave-forms associated with the complex hysteresis loop. It may be

regarded as arising from the lower effective permeability represented by the minor loops as compared with the differential permeability of the major loop at the point at which the minor loop is formed. This means that the change of current required to produce a given change of induction is greater when the minor loop is being traversed than it is for the adjacent region of the main loop. The current produced by the harmonic voltage will therefore tend to be asymmetrical, its positive half-waves being of smaller amplitude than the negative on the rising part of the main wave, and conversely on the

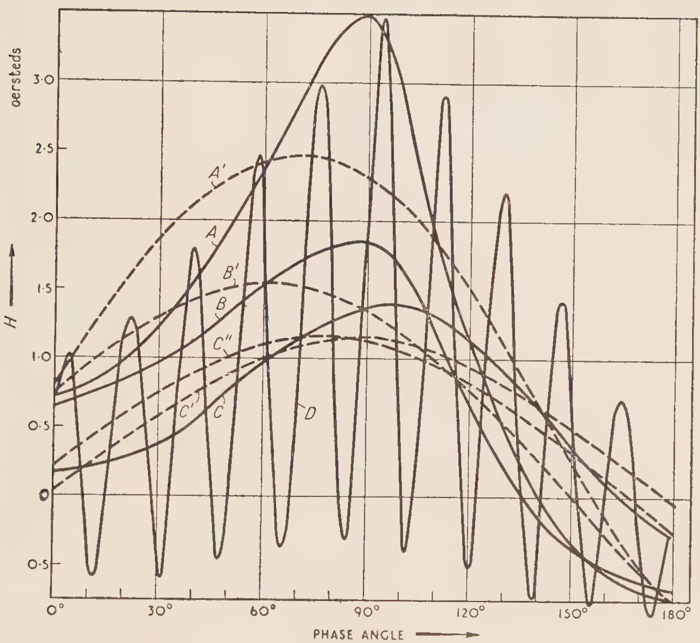

Figure 9. Harmonic analysis of complex wave.

Details of sinoids

Curve	H	ϕ, degrees
A'	2·48	69·1
B'	1·56	61·7
C'	1·17	88·5
C''	1·17	78·5

falling part. This may be regarded as producing a depression of the mean line on the rising slope and at the crest of the main wave and a rise of the mean line on the falling slope, thus, as it were, producing a diminution in amplitude and an equivalent delay in phase of the fundamental. This matter

was examined by carrying out harmonic analyses to determine the fundamental components of the magnetizing current under given single-frequency and superimposed conditions. The conditions chosen were a peak induction of 7500 gauss at 50 c/s and of 2500 gauss at 1000 c/s. In Figure 9 curve B gives the current for the 50-c/s excitation alone and B' represents the fundamental component of the wave. Curve D gives the current wave for the two excitations applied simultaneously, and C'' gives the fundamental component of this wave. It will be seen that the superposition of the harmonic frequency diminishes the amplitude of the fundamental component and retards it in phase. In the figure are also given curve C which is the "mean line" drawn through curve D, the resultant wave, curve C' which is the fundamental component of C, together with curves A and A' which represent 50-c/s excitation alone to a peak induction of 10 000 gauss. The reduction indicated in the fundamental-frequency power is of the same order as that found by experiment.

4. CONCLUSIONS

In addition to the accumulation of experimental data on the losses occurring with two-frequency excitation these experiments suggest two simple qualitative conclusions:—

(*a*) The additional hysteresis loss due to the superposition of two waves, one of which is a harmonic of relatively high frequency, depends not only upon the alteration in peak induction but also upon the extent to which the resultant waveform is re-entrant forming minor loops.

(*b*) Where a reduction of fundamental-frequency power results from the superposition of such a "ripple" component of flux, the reduction is dependent upon the differences between the slopes of minor loops and of the main loop in the same region.

DISCUSSION

Mr. H. Kayser:

The authors have shown that their factor $k = W_t/(W_f + W_h)$, when computed with certain simplifying assumptions, agrees quite well with the directly measured value. This interesting result suggests that, when the two excitations of different frequency are applied simultaneously, instead of separately, no additional phenomena are involved, apart from those arising directly from the quasi-static non-linear B/H relation. This performance under conditions of superposed alternating inductions is thus apparently quite different from that obtained in magnetic recording, where a high-frequency polarizing or premagnetizing current is generally superposed on the audio-frequency signal to increase the strength and reduce the distortion of the recorded signal. If a similar phenomenon is operative here, it is apparently too small to be noticeable.

Mr. S. E. Buckley:

Measurements have been made (Fondiller and Martin, 1921; Deutschmann, 1929; Kalb and Bennett, 1935) on dust-cored loading coils subjected simultaneously to $16\frac{2}{3}$-c/s morse telegraph currents and 1600-c/s telephone currents. This simulates the condition of some telephone lines. It is found that there is an effective increase in both the inductance and the effective resistance of the coil toward the 1600-c/s magnetization and that these increases are at a maximum when the rate of change of the telegraph current is a maximum, i.e. $33\frac{1}{3}$ times per second. The effect is known as "Morse flutter" and it is controlled by limiting the permissible hysteresis factor of the loading coils.

6

NON-LINEARITY IN MAGNETIC CORE MATERIALS AT LOW FIELD STRENGTHS

K. E. Latimer

(Telcon Telecommunications Ltd.)

Abstract: This paper surveys, from the theoretical standpoint, the different types of non-linearity to be expected in magnetic materials, including the ferrites.

An alternative explanation of residual loss of the Jordan type is presented in the Appendix. Like the thermal-agitation model of Néel, this is also based upon Barkhausen discontinuities in the motion of Bloch walls, but follows the general lines of Preisach's explanation. A loss proportional to frequency and to the square of field strength is obtained if the distribution of the irregularities is taken into account. This would appear as a small deformation of the hysteresis loop. This explanation needs experimental confirmation and quantitative verification.

1. INTRODUCTION

The purpose of this paper is to clarify a few aspects of the basic theory of intermodulation and other non-linear effects in magnetic core material at low field strengths, with particular reference to the ferrites.

A distinction is made between the various kinds of non-linear effect which are normally experienced in magnetic core materials such as the ferrites, whose characteristics do not necessarily conform to the usual simplifying assumptions. For example, appreciable departures from the Rayleigh relationship are occasionally experienced in such materials, and the hysteresis may be frequency-dependent.

The practical importance of multi-channel telephony and broad-band transmission systems leads to interest in third-order intermodulation products and in any other non-linear effects liable to fall within the range of frequencies transmitted. The third harmonic of a single sinusoidal input may be of only minor importance, although it may be useful as a datum with which other types of intermodulation may be compared.

It is proposed to consider what intermodulation products may be expected in the following circumstances :—

(*a*) The Rayleigh relationship is not obeyed. (Peterson, 1928. It is remarkable that this important paper was not mentioned by Bozorth (1951).)

(*b*) The characteristics of the material at fundamental frequency are functions of field strength, but the hysteresis loop is a perfect ellipse and harmonics are completely absent.

(*c*) The hysteresis loop is frequency-dependent. (*b*) is a special case of a frequency-dependent loop.

(*d*) The characteristics of the material are independent of field strength but there is a residual loss proportional to frequency.

All these circumstances are capable of causing more non-linear effects than would be estimated from measurements of third harmonic, and the hysteresis factor* (C.C.I.F., 1938) may not in all cases be a reliable guide.

2. DEFINITION OF LINEARITY IN A MAGNETIC CORE

A magnetic core may be regarded as linear over a certain frequency range if any number of sinusoidal fields within this range may be applied without introducing flux components of any other frequencies. It is not sufficient from the communication engineer's standpoint to state that harmonics are absent. The distinction made here is more than a matter of terminology; the mechanism which produces non-linear effects in the broader sense may not be the same as that which produces harmonics.

Thus case (*b*) above is already a non-linear effect from the communication engineer's standpoint. A change of impedance can be regarded as equivalent to the introduction of an unwanted voltage of fundamental frequency. Such a voltage may not be harmful if a purely sinusoidal field is applied, but if the input consists of two or more frequencies present simultaneously, the unwanted component of fundamental frequency will be modulated and will then be equivalent to one or more third-order difference products (Latimer, 1936, especially p. 282).

3. DEFINITIONS OF RAYLEIGH'S RELATIONSHIP

There have been some conflicting statements of Rayleigh's relationship (Rayleigh, 1887; Bozorth, 1951†; Peterson, 1928). Following Peterson, we take as the criterion of a Rayleigh material :—

$$F \equiv a_{11}/a_{02} = 2 \qquad \ldots(1)$$

where a_{11} and a_{02} are coefficients in the expression for the arcs of the hysteresis loop as double power series in terms of h the instantaneous and H the maximum field:—

$$B_{h,H} = a_{00} + a_{10}h \pm a_{01}H \pm a_{20}h^2 + a_{11}hH \pm a_{02}H^2 \ldots(2)$$

In this formula

$$a_{mn} = \frac{1}{m!n!}\left[\frac{\partial B^{mn}}{\partial h^m\, \partial H^n}\right]_{h=0;\; H=0} \qquad \ldots(2a)$$

* The hysteresis factor has always been stated as a number by the C.C.I.F. The symbol μ_2 is often used on the Continent to represent this number.

† In particular, pp. 489 onward. Bozorth devotes much attention to the establishment of the parabolic law and mentions $d\mu/dH$ only in a single sentence which might escape notice.

According to the assumptions made by Peterson, the following relations hold good even for non-Rayleigh material:—

$$a_{00} = 0 \qquad \ldots(2b)$$

$$a_{01} = 0 \qquad \ldots(2c)$$

$$a_{20} = -a_{02} \qquad \ldots(2d)$$

It will be explained later that these assumptions may not be correct. The operation of partial differentiation called for in (2a) cannot be carried out, strictly speaking, because of the presence of Barkhausen noise, and the residual loss may be partly explained by the incorrectness of (2c).

For a coil wound on any ferromagnetic core, it can be shown (Peterson, 1928, p. 774) that, if the impedance is measured as a function of current, the change of reactance divided by the change of resistance is $3\pi F/8$, which has the value 2·35 for a Rayleigh material. This is a convenient test for compliance with the Rayleigh relationship. Even if the hysteresis loop is frequency-dependent, F can be measured with an a.c. bridge and remains a useful constant in its application to engineering problems.

Whereas Peterson found that most metallic ferromagnetic substances satisfied equation (1) fairly well, it has been found that some ferrites, particularly high-permeability specimens of nickel-zinc ferrite, can have a ratio $F \equiv a_{11}/a_{02} = 4$. This is rather an exceptional case.

4. EFFECT OF NON-COMPLIANCE WITH RAYLEIGH'S RELATIONSHIP

Peterson (1928, p. 771) has calculated the magnitude of the third harmonic due to a single sinusoidal input without assuming the Rayleigh relationship. The writer has done the same for the case of the third-order intermodulation products of two sinusoidal inputs, but making some assumptions as to their amplitude ratio and frequency ratio (Latimer, 1936, p. 281). Kalb and Bennett (1935) have made similar calculations of the third-order intermodulation products; although they have not restricted themselves with regard to the amplitude and frequency ratios of the inputs, they have assumed that Rayleigh's relationship holds.

For non-Rayleigh material the writer has shown that the third-order difference products $(2f_a - f_b)$ and $(2f_b - f_a)$ are dependent on a_{11} and a_{02}, especially the former, but that the third-order summation products $(2f_a + f_b)$ and $(2f_b + f_a)$, and the third harmonics $3f_a$ and $3f_b$, are dependent only on a_{02} and not on a_{11}. They are therefore unaffected by a change in F. From this discussion it follows that for non-Rayleigh material the rate of change of permeability with current, a_{11}, is a better measure of the magnitude of the $(2f_a - f_b)$ and $(2f_b - f_a)$ terms than the generally accepted hysteresis factor.

The coefficients of the third-order products have been checked experimentally* by R. A. Brockbank and A. R. A. Rendall for Rayleigh material.

5. THE ELLIPTIC HYSTERESIS LOOP

For various reasons beyond the scope of this article, some absorption mechanism may suppress the higher-frequency components of the flux wave, although non-linearity at fundamental frequency may still be experienced (Wijn and Went, 1951). The previously mentioned calculation of third-harmonic difference products might have been stated by the writer with greater generality to cover this particular case, if only it had been foreseen. The notation previously used now becomes rather inconvenient, because a_{02} is the normal symbol not only in the loop equations but also in expressions for hysteresis loss and third harmonic. In this case we are interested in a_{02} only so far as it affects the hysteresis resistance, and not in its relation to third-harmonic voltage nor as a coefficient in equation (2). Similar considerations apply to a_{11}. The same symbols will, however, still be used, with a prime to indicate a change in meaning.

Starting with the Fourier expansion for the hysteresis loop for a sinusoidal field $h = H \cos pt$,

$$B = b_1 \cos pt + a_1 \sin pt + b_3 \cos 3pt + a_3 \sin 3pt \qquad \ldots(3),$$

we put $a_3 = b_3 = 0$, but retain the usual values for a_1 and b_1 (Peterson, 1928, p. 771), namely

$$\left.\begin{aligned} a_1 &= \frac{8H}{3\pi}(a'_{02}\,|H| + \ldots) \\ b_1 &= H\,(a'_{10} + a'_{11}\,|H| + \ldots) \end{aligned}\right\} \qquad \ldots(4)$$

In equations (4) the symbol $|H|$ is used to denote coefficients which do not change sign with a phase reversal of the input. a'_{10}, a'_{11} and a'_{02} are values determined by a.c. bridge readings and, as mentioned above, have no connection with equation (2).

We now replace the sine-wave input by an applied field consisting of:—

$$h = 2K \cos \omega t \cos pt = K\,[\cos (p + \omega)t + \cos (p - \omega)t],$$

where the frequencies previously referred to as f_a and f_b correspond to the angular velocities $(p + \omega)$ and $(p - \omega)$, ω being small. Repeating the calculations previously mentioned (Latimer, 1936, p. 281), it is found that

* Brockbank (1933) deals with the earlier stages of experimental work on the intermodulation due to two or more tones and describes the test gear used; he also gives typical test results. The theoretical treatment (Latimer, 1936) came later and was finally checked by further unpublished measurements by A. R. A. Rendall using apparatus similar to that described by Brockbank. Brockbank's work is also of considerable interest for its brief reference to variation of intermodulation products with time, a subject on which little was known until very recently.

the results for the $(2f_a - f_b)$ and $(2f_b - f_a)$ components of the flux remain unchanged, the amplitude of each being

$$a'_{02}\frac{16}{15}\frac{K^2}{\pi}\sqrt{F^2 + (8/3\pi)^2}$$

It will be noticed that this result is still mostly determined by a'_{11} and therefore affected by the ratio F, as determined by bridge readings, although Rayleigh's relation ceases to have much meaning. The $(2f_a + f_b)$, $(2f_b + f_a)$, $3f_a$ and $3f_b$ components are all zero.

In a similar way it may be shown that when the applied field consists of a stronger component f_a of amplitude P and a weaker component f_b of amplitude kP, where $k \ll 1$, the result of an elliptic loop is a $(2f_a - f_b)$ component unaltered in amplitude, whereas the $(2f_a + f_b)$, $3f_a$, and $(4f_a - f_b)$ components all vanish. The amplitude of the $(2f_a - f_b)$ component is:—

$$a'_{02} \cdot \tfrac{1}{2}k\, P^2\sqrt{F^2 + (8/3\pi)^2}$$

6. FREQUENCY-DEPENDENT HYSTERESIS LOOP

The case of the elliptic hysteresis loop mentioned above is, of course, a limiting condition which is not likely to be frequently encountered. Normally it is found that most ferrites tend to become more linear at the higher frequencies both in respect of the coefficient a_{11} and in the production of third harmonic (Wijn and Went, 1951). However, since higher frequencies are operative in the latter effect, it tends to disappear first when the fundamental frequency is increased.

The hysteresis loss per cycle in ferrites (i.e. that portion of the loss which is dependent on field strength) has a tendency to increase at first before it finally disappears at high frequencies. It has, however, been shown that a_{11} is more important than a_{02} in respect of $(2f_a - f_b)$ and $(2f_b - f_a)$ components, so that the increase in a_{02} is unimportant. These components must be judged from the magnitude of the impedance change with current at fundamental frequency, whereas the remaining third order terms, and possibly also $(4f_a - f_b)$, must be determined by third-harmonic measurements taken with single-frequency tone at the appropriate frequency. The incompatibility of third-harmonic measurements with hysteresis-factor tests is dealt with by Wijn, 1953.

In addition to the short-term effects discussed here, it is known that long-term variations with time also exist. Snoek (1947, pp. 41-56) discusses the type of disaccommodation due to small amounts of nitrogen or carbon in iron, and also that in certain samples of ferrite where another cause is suspected. Brockbank (1933) mentions briefly the long-term changes in

permeability, hysteresis loss and intermodulation products in silicon-iron, a matter which has been clarified by recent work of Feldtkeller and his colleagues. If a stable hysteresis loop is not established in a single cycle, the above theory of intermodulation does not apply.

7. RESIDUAL LOSS

Definition. It was demonstrated by Jordan (1924) that most magnetic materials can have a component of loss which is proportional to frequency and to the square of the field strength; the loss can thus be represented by a resistance or conductance which is proportional to frequency, but which does not change with current.

There have been some speculations in the past as to the nature of this loss (Ellwood, 1935; Preisach, 1935). Recent work on domain theory by Néel and his colleagues has culminated in an acceptable explanation in terms of Barkhausen discontinuities brought about by thermal agitation of the field (Bozorth, 1951, p. 529; Kittel, 1949).

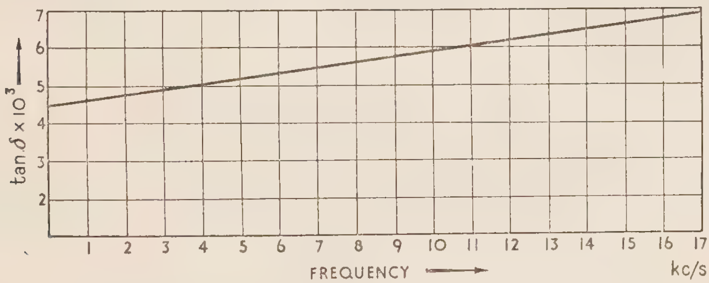

Figure 1. Variation with frequency of tan δ for manganese-zinc ferrite.

In the Appendix it is shown that it is also possible to devise an alternative explanation, still in terms of Barkhausen discontinuities, but without postulating thermal agitation. This mechanism can apparently exist alongside the thermal-agitation model; there may be other explanations besides these. Moreover, since the mechanism of magnetization is believed to be quite different in ferrites from that in metals (Wijn and Went, 1951), whereas residual loss of the Jordan type exists in both, it seems probable that several explanations of residual loss will eventually be found.

Figure 1 shows a plot of the loss angle of a typical ferrite as a function of frequency. It will be seen that over a considerable portion of the low-frequency range the loss angle is more or less constant, i.e. the corresponding loss resistance is proportional to frequency, as stated by Jordan. There is also a smaller component of residual loss which has a loss angle proportional

to frequency, i.e. a resistance proportional to the square of frequency. This could be due to a single relaxation effect or a small amount of eddy-current loss. Residual losses which are proportional to the square of frequency are not a source of non-linearity.

Effects of residual loss. In any material in which part of the residual loss is accounted for by Barkhausen discontinuities, it is possible for a certain type of non-linear effect to occur. A sine-wave field applied to such a material could give rise to an unwanted product consisting of Barkhausen noise modulated at fundamental frequency. Whether such an effect would be observable or not depends upon the dissipation present in the noise spectrum; consequently one would expect such effects to occur at somewhat low fundamental frequencies. The writer is aware of experiments of this kind only at field strengths where hysteresis was predominant, and has seen no attempt to extrapolate down to zero field (Bozorth, 1951, p. 531).

8. EXPERIMENTAL WORK

It has recently been verified that the $(2f_a - f_b)$ and $(2f_b - f_a)$ products, for several coils with ferrite cores in which the hysteresis loop is frequency-dependent, bear a direct relationship to the change of impedance with current, according to the theory given above in sections 5 and 6.

No experiments on Barkhausen noise can yet be reported.

The writer wishes to thank Messrs. Telcon Telecommunications Ltd. for permission to publish this paper. The assistance he has received from unpublished data emanating mostly from the Philips Research Laboratories, Eindhoven, also the co-operation and encouragement of colleagues in the Philips and Mullard organizations, must be gratefully acknowledged.

APPENDIX

Explanation of residual loss of Jordan type

The first attempts to explain residual loss of the Jordan type in terms of Barkhausen discontinuities were those of Ellwood and Preisach, of which the latter is far more detailed.

Preisach thought of the magnetic material as containing a large number of independent "regions" of equal size, distributed throughout the core with a certain frequency of occurrence; each of these regions is characterized by a rectangular hysteresis loop in which the saturation flux density B_s is always the same, but in which the coercive force H_a is variable. In addition, each region is associated with a bias field, so that the loop is symmetrical about the ordinate $h = H_b$. (The symbols H_a and H_b are used instead of Preisach's a and b to avoid confusion with the loop coefficients.)

Figure 2 shows the diagram which forms the basis of Preisach's explanation. The axes are those of H_a and H_b, and the points in the diagram

represent regions of equal volume with every possible combination of values of H_a and H_b. Within the Rayleigh region, the "population density" of such regions is uniform as displayed in this diagram.

When a field is applied to the model proposed by Preisach, the number of regions which reverse their polarity during the cycle is determined by the area ACE of Figure 2. The linear dimensions OA, OC and OE all represent the maximum value H of the applied field, in other words they define an area in which $H_a = H$ and $H_b = 0$, or in which $H_a = 0$ and $H_b = \pm H$, are extreme cases of regions which will just reverse with a maximum field of strength H. The area OBCD represents the number of regions whose polarity remains in the direction last magnetized when the field is reduced from $\pm H$ to zero; in other words, the area is proportional to the remanence.

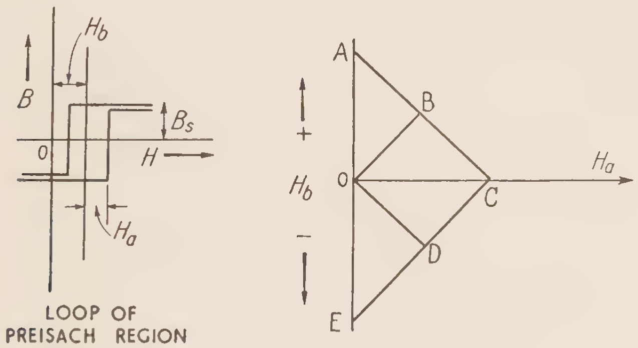

Figure 2. Preisach diagram.

The energy loss per region is proportional to $H_a B_s$, so that a measure of the hysteresis loss can be obtained by taking the first moment of the area ACE about the H_b axis. This is:—

$$\text{Moment} = 2\int_{H_a=0}^{H_a=H} (H - H_a)\, H_a dH_a = \frac{H^3}{3} \qquad \ldots(5)$$

According to this treatment the residual loss which is proportional to H^2 does not appear as part of the area of the hysteresis loop, but must be explained by a time lag, such as that postulated by Néel due to thermal agitation. The Preisach model gives a satisfactory explanation of hysteresis and remanence, but, of course, any hypothesis which results in a hysteresis loop formed by parabolic arcs will do this. The area H^2 of the triangle ABC should be proportional to the flux density, whereas the latter is itself proportional to H, for small fields. Preisach overcame this difficulty by postulating a perfect medium of permeability μ_p in which the regions responsible

for non-linearity are immersed. Bozorth indicates, however, that parts of the hysteresis loop consist entirely of Barkhausen jumps.

The same diagram is capable of representing the irregular motion of the Bloch walls and the power lost in Barkhausen discontinuities. In this case H_b represents the field at which there is an obstacle to Bloch wall movement, and H_a the excess field necessary to overcome the obstacle. The energy loss associated with the jump will be proportional to $B_s H_a^2$, since the loss per unit volume is $B_s H_a$ and the volume itself is proportional to H_a. Since, however, a given motion of the Bloch wall will either consist of a few large jumps or many small jumps, it follows that, in principle, the population density of the regions will be inversely proportional to H_a. Hence, to obtain the loss we must still take the first moment about the H_b axis as in the Preisach model, ignoring the non-uniform population density. So far there is no essential difference between the two models.

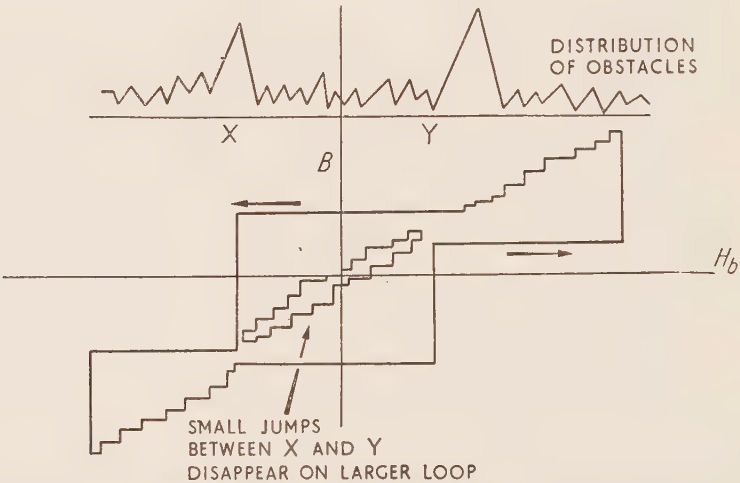

Figure 3. Process of transfer of small irregularities to higher values of H_b

Referring to Figure 3, however, when we consider Bloch wall movements, the occurrence of a particular jump no longer depends on H_a and H_b alone, because the jumps must occur in a particular sequence. In addition, if there happens to be a large obstacle as at X or Y, a large jump will take the place of several small jumps, and a new series of small jumps will then appear at a higher value of H_b. We shall call this the *substitution effect*, because a series of jumps of small H_b are replaced by a new series with higher H_b; the Preisach figure for the positive half-cycle will thus differ from that for the negative half-cycle, although statistically one will be the mirror image of the other.

If the substitution process were complete, as in Figure 3, the number of active regions with a given value of H_a would not increase with the maximum field, as would be indicated by the term $(H - H_a)$ in equation (5), but would remain constant. It is unreasonable, however, to suppose that the substitution effect is complete, and we therefore write $[m_0 + m_1 (H - H_a)]$ in equation (5).

The number of regions contributing to the permeability is now

$$\text{Area} = 2\int_{H_a = 0}^{H_a = H} [m_0 + m_1 (H - H_a)]\, dH_a = 2m_0 H + m_1 H^2 \quad \text{...(6)}$$

and the first moment which determines the losses due to the jumps is

$$= 2\int_{H_a = 0}^{H_a = H} [m_0 + m_1 (H - H_a)]\, H_a\, dH_a = m_0 H^2 + \frac{m_1 H^3}{3} \quad \text{...(7)}$$

Equation (6) contains terms corresponding to a_{10} and a_{11}, although there may be another component of a_{10} if the Bloch wall is sometimes able to

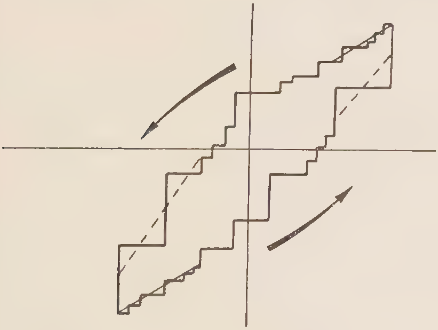

LARGE LOOP

Figure 4. Hysteresis loop, showing Barkhausen jumps.

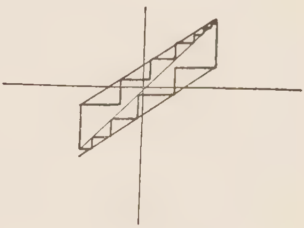

SMALL LOOP

Figure 5. Hysteresis loop due to residual loss alone.

move without Barkhausen jumps. Equation (7) shows a residual-loss term proportional to H^2 and a hysteresis term proportional to H^3, corresponding to the coefficients a_{01} and a_{02}. According to Peterson, the term a_{01} should be zero if the hysteresis loop consists of two arcs which intersect at the loop tips.

If the above hypothesis is correct, and the hysteresis loop consists of a series of Barkhausen jumps which are small at the start of the arc and large at the reversal point, the two arcs of the hysteresis loop (i.e. the smooth curves drawn through the middle of the irregularities) will not meet at the loop tips exactly. The latter will be "blunted" due to the presence of short transition curves which join up the main arcs. If this is admitted, it is

possible for the coefficient a_{01} to have a finite value. Introducing this value into the loop equations it is easy to show that the loop will have an area which is mostly proportional to H^3, but of which there will be a component proportional to H^2. Figures 4 to 6 illustrate this point. Another consequence of this effect is that a_{02} will no longer be precisely equal to $-a_{20}$, but this introduces no new phenomenon. The residual loss due to such loop deformation will, of course, occur once per cycle, like the hysteresis loss, and will thus be proportional to frequency.

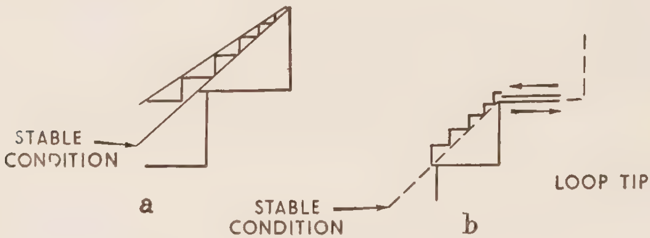

Figure 6. Details of tips of hysteresis loops.

Figure 4 shows a rather large loop, although still in the Rayleigh region, in which the two main parabolic arcs drawn through the middle of the irregularities do not meet at the loop tips. Figure 5 indicates what occurs when only the residual loss is present. The loop now degenerates into a parallelogram. Figures 6a and 6b show the detail of the loop tip. Figure 6a is probably the correct picture, because at the loop tip the change of field is slow and there is plenty of time for a jump to occur. However, the condition shown in Figure 6b might also occur if the Bloch walls are everywhere impeded by obstacles. The nature of the transition curve which joins the main arcs thus has no definite shape, but is liable to vary from cycle to cycle.

The theory advanced in this appendix is of a speculatory nature and requires experimental confirmation. It is also necessary to establish that there is quantitative agreement between the physical quantities involved.

DISCUSSION

Mr. F. F. Roberts:

With regard to Dr. Latimer's discussion of non-linearity, it would seem possible, and desirable in the interests both of the engineer and of the physicist, to eliminate the distinction between harmonic generation and intermodulation. The observed differences in behaviour evidently arise from the fact (demonstrated for ferrites by Wijn, 1953) that the hysteresis is frequency-dependent. If the harmonic or intermodulation product of interest has a frequency below the hysteresis relaxation frequency, then the full value of each will be obtained as computed from the low-frequency hysteresis loop. On the other hand,

if the frequency of interest is above the hysteresis relaxation frequency, then the amplitude of this component will be attenuated by an amount determined by the frequency dispersion of the hysteresis.

With regard to residual loss, there is, on the one hand, no evidence that it is in fact constant at all frequencies, while, on the other hand, network theory tells us that it is possible to construct a finite linear network to match the known residual-loss behaviour, in any given case, within arbitrarily close tolerances, over any specified frequency range. There is no necessary connection between residual loss and macroscopic non-linearity (all processes that convert energy into thermal form must ultimately, on a molecular scale, be non-linear), although Néel's theory of "traînage irréversible" does in fact postulate a physical mechanism connecting them.

Dr. Latimer (in reply):

I agree with Mr. Roberts that it would be desirable to eliminate the distinction between harmonic generation and intermodulation in order to obtain the obvious benefit of having a single factor of merit, for example the hysteresis factor. However, the distinction exists in fact and its elimination is impracticable.

Perhaps in an effort to be brief I have given an over-simplified picture of these rather involved processes. The following summary will perhaps help to rectify this:—

(*a*) Even at low frequencies the various non-linear effects arise from different properties of the loop; the $(2f_a - f_b)$ and $(2f_b - f_a)$ are due mostly to a_{11} and the rest to a_{02} alone. We can only pretend that all these effects spring from a common cause if Rayleigh's relationship is obeyed, and exceptions to this are known. Thinking that most engineers would like to use a_{02} as a factor of merit, I introduced the factor F as the only solution.

(*b*) Mr. Roberts assumes that the shape and size of the low-frequency loop remain unchanged until the hysteresis relaxation frequency is approached. This is incorrect in the case of the ferrites, for between 2 and 50 kc/s an appreciable increase occurs in that part of the loss per cycle which is dependent on field strength, although the cut-off frequency is about 1 Mc/s. From this it is clear that the low-frequency hysteresis loop cannot be used safely as a basis for calculating any non-linear effect at higher frequency.

(*c*) We now revert to the effect mentioned in (*a*), namely that the factor most responsible for third-order difference products is not the hysteresis factor but the constant a_{11}. We can give a_{11} a broader meaning by specifying it in terms of a.c. bridge readings, so that we are no longer restricted to a loop with parabolic arcs, but may even apply it to an elliptic loop. It is now clear that we need to know the value of a_{11} at higher frequencies and different field strengths. On this point there is very little data, but from Dr. Wijn's work there is an indication that a_{11} improves at higher frequencies, though even if this were true on a few samples I should not like to be too dogmatic. Such data may of course be specified equally well in terms of F and a_{02}, both values being those measured at high frequency.

Mr. Roberts's remark in the second paragraph refers to the lack of evidence that the residual loss per cycle is constant at all frequencies. I agree with this: my Figure 1 was the only evidence I had available and I admit that it is insufficient. His point about the ability of a finite network to match any given residual loss was sufficiently convincing to persuade me to suppress that part of the text in preparing the final copy.

I also agree that there is no proved connection between residual loss and non-linearity,

and was only drawing attention to the lack of knowledge on this point. I repeat below the main points in my train of thought:—

(1) That part of the residual loss which is proportional to frequency probably has more than one explanation. So far, two such explanations, that of Néel which is fairly well established, and my own which I advance with diffidence, attribute the effect to Barkhausen irregularities. Two others, that of Dr. Fairweather (1953), who mentioned that it was possible to obtain such a loss from eddy currents under special conditions, and the one mentioned by Mr. Roberts, i.e. a number of relaxations, do not depend on Barkhausen.

(2) If this loss can be attributed to Barkhausen effect, there is a possibility, but not a certainty, that part of the fundamental wave is converted into Barkhausen noise, appearing externally.

(3) Barkhausen noise has been observed when hysteresis is present, but I am unaware of any experiment in which the noise is related to the field strength in such a way that we may say that over a certain range it depends on the cube of the field and over another range on the square. This is the result I would expect, i.e. the Barkhausen noise would be related to the sum of the hysteresis and residual losses.

My remarks on residual loss were only very tentative, but were intended to lead to an exchange of views and some discussion. I am quite prepared to be convinced that I am mistaken.

7

FREQUENCY-DEPENDENCE OF MAGNETIZATION PROCESSES IN FERRITES AND ITS RELATION TO THE DISTORTION CAUSED BY FERRITE CORES

H. P. J. Wijn

(Philips Laboratories, Eindhoven)

Abstract: Magnetization curves of ferrites have been measured as a function of frequency and it appears that two dispersion mechanisms occur. The relation between the dispersion frequency of the initial permeability μ_a and the value of μ_a at low frequency has been investigated for samples of nickel-zinc ferrite with increasing zinc-content; the greater part of μ_a is caused by a rotation of the spins in the Weiss domains. The dispersion of the permeability corresponding to magnetic fields of the order of magnitude of the coercive force of the ferrite always occurs at a lower frequency, and is attributed to a relaxation of the irreversible Bloch-wall displacements. As a consequence of the last-mentioned dispersion, the distortion caused by coils with a ferrite core can decrease with frequency, and even vanish.

Total losses of the ferrite are given as a function of induction and frequency, and the relation between distortion and hysteresis resistance is discussed.

1. INTRODUCTION

It is common knowledge that in a wide frequency range the use of ferrites for coil cores in high-quality resonance circuits gives an advantage over the laminated or powder cores hitherto used. From a certain frequency, however, depending on the kind of ferrite, the core losses increase considerably with frequency and the value of the self-inductance of the coil decreases. The cause of this phenomenon seemed to be satisfactorily explained by Snoek (1948) as a natural gyromagnetic resonance of the magnetic spins, i.e. a spin resonance caused by the simultaneous action of the applied radio-frequency magnetic field and the internal polarizing fields, which latter can originate from crystal anisotropy and internal strains in the ferrite.

Measurements on magnesium ferrite by Welch et al. (1950), Roberts (1951), and Rado et al. (1950) show two dispersions for the initial permeability. Rado ascribes the low-frequency dispersion to a Bloch-wall resonance, the dispersion at about 1500 Mc/s being due to a Snoek-type spin resonance.

Since more and more use is being made of manganese-zinc and nickel-zinc ferrites at high inductions, for instance for high-frequency transformers and deflection rings in television sets, we studied the phenomena occurring in them by measuring a large part of their magnetization curves at several frequencies. These materials have a high resistivity, so it is possible to examine both the frequency-dependence of the simultaneous rotation of the spins

in a Weiss domain and the frequency-dependence of the displacement of the Bloch walls between them, without their being disturbed by eddy-current effects. For the magnetization curve two different dispersions are found which are related to these two kinds of magnetization processes.

It will be shown that for frequencies higher than about ½ Mc/s some ferrites have a linear magnetization characteristic and do not cause distortion when used in transformers at high frequency. The results of the measurements of total losses in ferrites as a function of induction and frequency are given, and finally the consequences of the results of these measurements are discussed in connection with the usual method of deriving the distortion from the hysteresis resistance. It appears that this method cannot generally be applied to ferrites at frequencies above about 50 kc/s. A general survey of the physical and chemical properties of ferrites is given by Snoek (1947), Polder (1950), and Went and Gorter (1951). The methods of measurement used in obtaining some of the results given in this paper have been described by Polder (1950).

2. MAGNETIC DISPERSION PHENOMENA IN FERRITES

(*a*) **Dispersion of the initial permeability of ferrites.** If losses occur, the initial permeability* μ_a of a ferrite can be regarded as a complex quantity (Polder, 1950), $\mu_a = \mu' - j\mu''$. The quantities μ' and μ'' as a function of frequency have already been given and discussed for different ferrites by Beljers and Snoek (1949) and also by Polder (1950). In Figure 1 similar results of measurements by C. M. v.d. Burgt are given for five nickel-zinc ferrites with decreasing zinc content. The measuring method is the same as given by Polder (1950), but the frequency range is extended to 3000 Mc/s. As always, μ'' increases sharply at a definite frequency which frequency is higher for smaller low-frequency initial permeability of the ferrite. That this dispersion is related to a resonance phenomenon follows from the small increase of μ' just before its decrease, and from the fact that for Grade E the value of $\mu' - 1$ becomes negative at 3000 Mc/s. The nature of this resonance is intimately related to the origin of the initial permeability of the ferrites, i.e. whether it is due to reversible Bloch-wall displacements or to rotations in unison of the spins in each Weiss domain.

Starting from Döring's conception (1948) of the apparent mass of a moving Bloch wall, Becker (1951) derived a formula for the resonance frequency of such a wall:

$$\omega_0 = \gamma I_s \sqrt{\frac{\pi\delta}{l.\,\chi_{0\,disp}}} \qquad \ldots(1)$$

where γ is the magneto-mechanical ratio, 17 Mc/s-oersted,

I_s is the saturation magnetization in gauss/cm³,

* A magnetic field having the value H in a previously-demagnetized ferrite core will cause in that core an induction B, such that $B = \mu H$. The permeability μ will generally depend on H and the limit of μ for $H = 0$ is called the initial permeability μ_a of the ferrite.

χ_{0disp} is the initial susceptibility at low frequency, caused by reversible Bloch-wall displacements,

δ is an average thickness of the Bloch wall, and

l is the average distance between two Bloch walls.

The resonance frequency for the natural gyromagnetic resonance as given by Snoek (1948) is

$$\omega'_0 \,.\, \chi_{0rot} = \frac{2}{3}\gamma I_s \qquad \ldots(2)$$

where χ_{0rot} is the initial susceptibility at low frequency caused by a simultaneous rotation of the spins in the Weiss domains, and $\omega_0'/2\pi$ is the frequency at which the imaginary part of the susceptibility has a maximum.

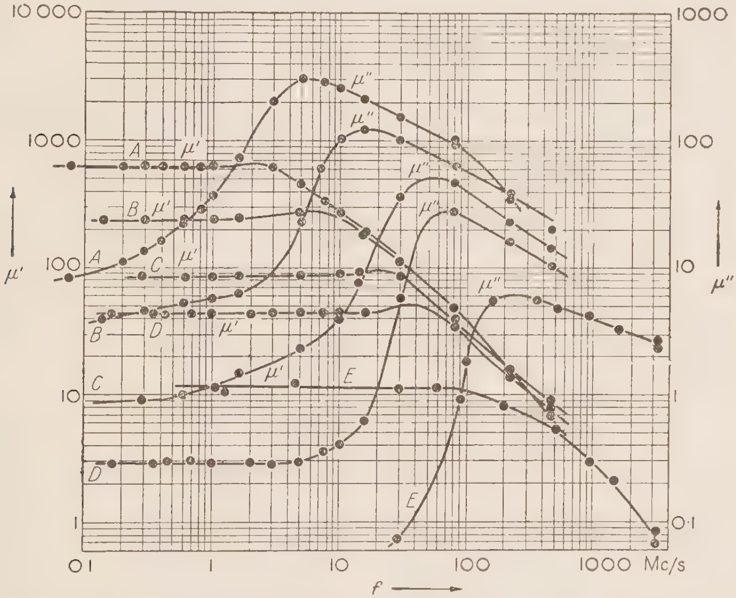

Figure 1. Variation with frequency of the real and imaginary parts, μ' and μ'', of the initial permeability: for various nickel-zinc ferrites (see Table 1). Note the different scales for μ' and μ''.

The two formulae show a great difference as to the dependence of the resonance frequency on the initial permeability. For wall displacements this frequency will always increase at most by $1/\sqrt{\chi_{0disp}}$ with decreasing permeability, since δ decreases at the same time. In the case of rotation processes, ω_0 increases in proportion to $1/\chi_{0rot}$; thus a comparison of the resonance frequency with χ_0 for different ferrites can give an answer to the question as to which kind of magnetization process causes this dispersion.

In Table 1 the values given for χ_{0rot} are those which, calculated according to equation (2), correspond to the measured resonance-frequency $\omega_0'/2\pi$ of the nickel-zinc ferrites of Figure 1. Since, for a simple gyromagnetic resonance, the permeability has dropped at the resonance frequency, to half of its low-frequency value, in the polycrystalline ferrites we have designated $\omega_0'/2\pi$ as the frequency at which $(\mu' - 1)$ has dropped to half of its low-frequency value. From the table it follows that for the whole series of nickel-zinc ferrites an excellent agreement exists between the initial permeability derived from the resonance frequency according to Snoek's equation (2) and the measured one. If the frequency for which μ' has a maximum was put in equation (2) as a resonance frequency, we still find the relation between initial susceptibility and resonance frequency as predicted by this formula for different ferrites, though the product of their corresponding values is too small by a factor 1·5. This indicates that for the most part the initial permeability of these ferrites is the result of a simultaneous reversible rotation of the electron spins of a Weiss domain from their equilibrium position in the internal field into the direction of the applied external field.

Table 1.—Comparison between the measured initial permeability and the permeability derived from the gyromagnetic resonance frequency for nickel-zinc ferrites

Grade	Chemical composition in mol % (balance Fe_2O_3)		Gyromagnetic resonance frequency* as determined from the measurements of Figure 1 $\nu_0' = \omega_0'/2\pi$ Mc/s	Saturation magnetization I_S, gauss/cm^3	Initial permeability according to equation (2)		Measured initial permeability μ_a
	NiO	ZnO			$\mu_{arot}-1 = 4\gamma I_S/3\nu_0'$	μ_{arot}	
A	17	33	8	292	776	777	640
B	25	25	30	332	236	237	240
C	33	17	75	321	91	92	85
D	40	10	140	283	43	44	44
E	49	1	350	197	12	13	12

* i.e. the frequency for which $(\mu' - 1)$ has dropped to half of its low frequency value.

Attention is drawn to the peculiar shape of the μ''/frequency curves of Figure 1. For instance, for Grade E, μ'' increases sharply above a rather definite frequency to a maximum and then decreases slowly. Polder (1953) deals in greater detail with these questions.

(*b*) **Dispersion of irreversible Bloch-wall displacements in ferrites: magnetization curves of ferrites as a function of frequency.** The single-valued function which gives the relation between the amplitude H_{max} of a sinusoidal field and the maximum of the induction B_{max} in the ferrite core will be called the "magnetization curve" of the ferrite at the frequency of the field H.

This curve is plotted from measurements carried out on a ring-shaped specimen of the ferrite with two windings. The current through the primary is a measure of the field strength and the rectified secondary voltage is a measure of the maximum induction in the core. A detailed discussion of the measuring method and some of the results have already been given (Wijn and Went, 1951).

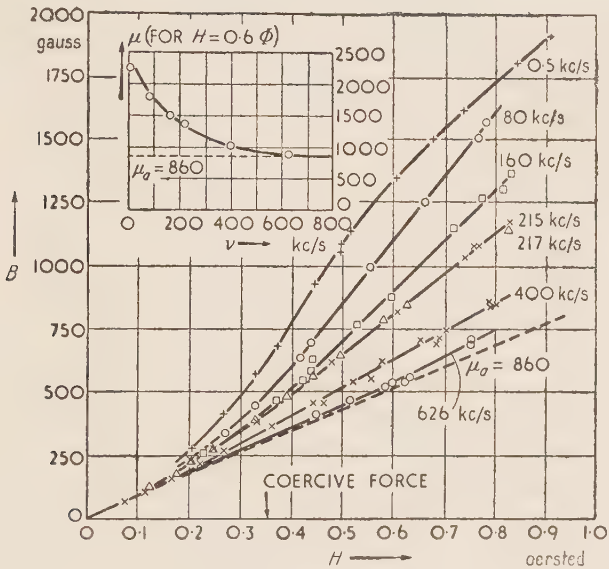

Figure 2. Magnetization curves at various frequencies for the manganese ferrite I, which has high initial permeability. Inset: Variation with frequency of μ at $H = 0{\cdot}6$ oersted.

In Figure 2 the magnetization curves are given for the manganese ferrite I for several frequencies ($\mu_a = 860$, and chemical composition in mol %, 43·5MnO and 56·5 Fe_2O_3). The curve for 0·5 kc/s has the typical shape; i.e. for sufficiently low field-strengths $B_{max} = \mu_a H_{max}$, while for higher fields the peak-amplitude permeability μ increases with increasing H_{max}, reaches a maximum value for $H_{max} = 0{\cdot}6$ oersted and then decreases monotonically to the value 1 for very high field-strengths. The shape of the magnetization curve of this ferrite depends upon the frequency of the field, and for high frequencies it becomes a straight line, its slope being the same as the initial slope of the low-frequency magnetization curve, μ_a. Thus the above-defined peak-amplitude permeability μ for a definite H_{max} depends on frequency. This is illustrated in the inset of Figure 1, which shows the change with frequency of the permeability at 0·6 oersted. For this ferrite

a sharp distinction can be made between two kinds of magnetization processes. One process gives rise to μ_a, which is frequency-independent up to 626 kc/s (μ_a drops to half of its initial value only at 5 Mc/s), and a second process gives an important contribution to the magnetization at field strengths of about the coercive force, H_c. The second process is already very frequency-dependent from 100 kc/s onwards. Both these dispersions have been found for all measured ferrites with an initial permeability of about 500 and higher, and in every case the dispersion of μ_a is found to take place at a higher frequency than the dispersion of the permeability for field-strengths of about H_c.

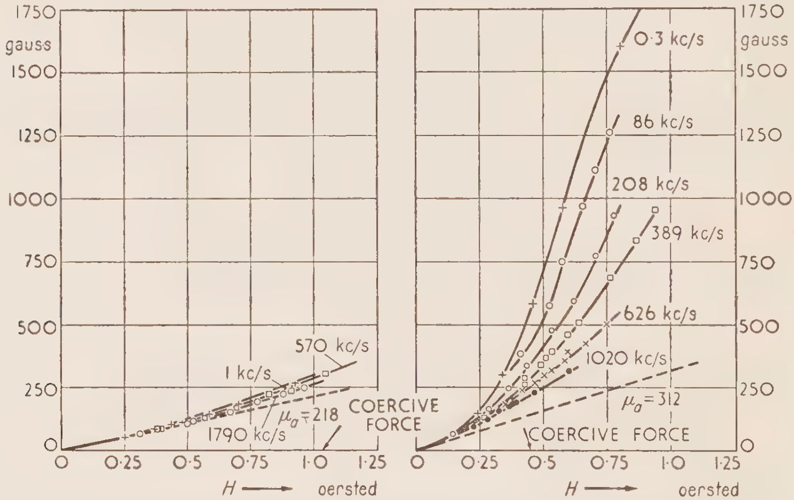

Figure 3(*a*) Figure 3(*b*).

Magnetization curves for nickel-zinc ferrites: (*a*) ferrite II, having initial permeability 218, porosity 14·6%; (*b*) ferrite III, similar initial permeability, porosity 3·2%.

A still better insight into the nature of the magnetization processes can be obtained from the measurements of ferrites with the same chemical composition but different porosities. In Figures 3a and 3b the magnetization curves for several frequencies are given for the ferrites II (chemical composition 25 NiO, 25 ZnO, and 50 Fe_2O_3) and III (27 NiO, 23 ZnO and 50 Fe_2O_3), which have porosities of 14·6 and 3·2% respectively. This difference in porosity has been obtained by firing at different temperatures, and it is seen that it does not have much effect on the initial permeability, which is 218 for the porous and 312 for the non-porous material. (This difference can be partly accounted for by the unequal densities of the ferrites.) The gyromagnetic resonance frequencies, 30 Mc/s and 18 Mc/s respectively, are in good agreement with this. A much greater difference, at least at low

frequency, is found between the magnetizations at a field-strength of about 1 oersted. But, as can be seen from the figures 3a and 3b, this difference disappears at high frequency because the magnetization curve of ferrite III depends on frequency in the same way as the curve for the ferrites with a high permeability. In ferrites a small porosity gives rise to a frequency-dependent magnetization process, which makes an important contribution to the magnetization even in small fields. This process is to be ascribed to Bloch-wall displacements (Wijn and Went, 1951).

(*c*) **Third-harmonic distortion in ferrites at different frequencies.** In what follows the ratio of the amplitudes of the third harmonic V_3 and the fundamental V_1 of the open-circuit secondary voltage of a transformer with ring-

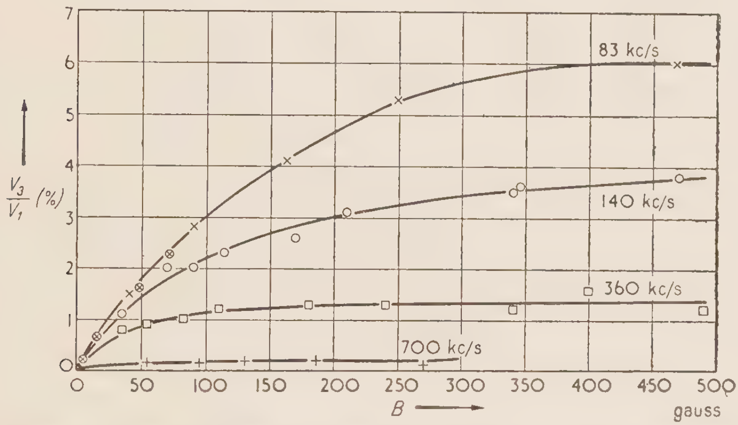

Figure 4. Ferrite I: distortion against induction at various frequencies. ⊗ distortion at 2 kc/s calculated from the hysteresis resistance by equation 3.

shaped core will be called the distortion of the core material when the current through the primary, wound tightly on the core, is sinusoidal. This is permissible since the hysteresis loop is symmetrical with respect to the origin ($H = 0$, $B = 0$), so that only odd harmonics can occur, and because the fifth and higher harmonics are at least an order of magnitude smaller than the third; moreover, we wish to study the distortion as a function of frequency and it has been found that the higher harmonics behave similarly to the third harmonic. The distortion measurements have been carried out with a selective voltmeter (Wijn and Went, 1951).

Figure 4 gives for the ferrite I the distortion V_3/V_1 for four frequencies, and it is seen that this quantity depends very much on frequency, being almost absent at 700 kc/s. Thus for this ferrite the shape of the hysteresis loop must likewise change with frequency: at low frequency it is the well-known loop with sharp tips, whereas at high frequency B is a linear function

of H and only a phase shift between the two can occur (see section 3(a)), giving rise to an elliptical loop. For all ferrites investigated the frequency dependence of the magnetization curve and the distortion go hand-in-hand.

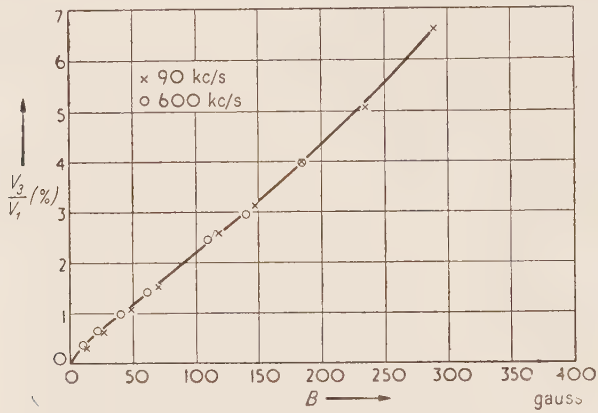

Figure 5. Frequency-independent distortion in ferrite II.

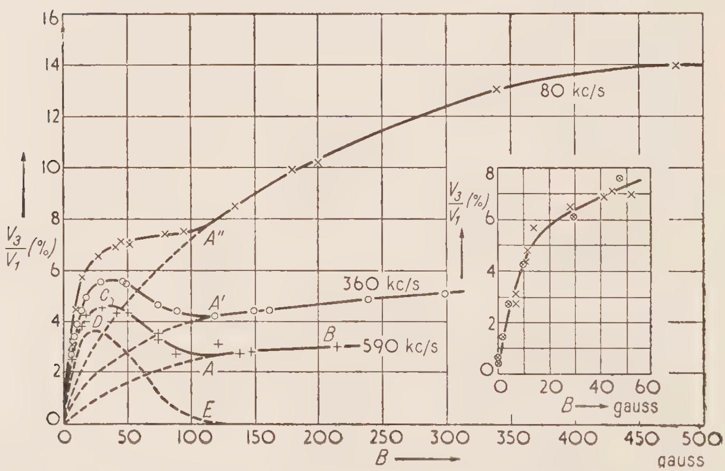

Figure 6. Ferrite III: distortion against induction at various frequencies.
Inset: × distortion measured at 80 kc/s with selective voltmeter.
⊗ distortion at 2 kc/s calculated from the hysteresis resistance by equation 3.

It has already been seen that for ferrites with a lower initial permeability no dispersion of the magnetization curve occurs below 1 Mc/s. The results of the distortion measurements of ferrite II, given in Figure 5, are in agreement with this. Sintering of this kind of ferrite at a high temperature

considerably affects the shape of the magnetization curve and makes it dependent on the measuring frequency, as we have just seen. The distortion also shows a peculiarity. Not only is it high at low frequencies compared with that of the other ferrites, but it also shows a very remarkable dependence on induction, especially at 590 kc/s; see Figure 6. One can regard the distortion of these ferrites sintered at a high temperature as being composed of two parts: superimposed upon the frequency-dependent distortion is the frequency-independent distortion given by the curve ODE. From the measurements described in section 3(*b*) it will follow that both distortions are caused by an irreversible magnetization process.

3. TOTAL LOSSES IN FERRITES AS A FUNCTION OF INDUCTION AND FREQUENCY

(*a*) **Total losses measured with a calorimeter.** Since the shape of the hysteresis loop of ferrites can be frequency-dependent, we measured the total losses. These are a measure of the area of the B/H loop. At high field-strengths the induction in the core is not sinusoidal and the total losses cannot be measured with sufficient accuracy in a bridge or resonant circuit, so we determined these losses directly by means of a calorimeter. The calorimeter is made of glass and is filled with olive oil to prevent as far as possible both eddy-current losses and dielectric losses. A sinusoidal current flowed in a coil wound on a ring-shaped ferrite core: and we measured at several frequencies the relation between the maximum induction B_{max} and the total losses for a number of ferrites.

(i) *Total losses of ferrites with frequency-independent magnetization curve.* Nickel-zinc ferrite IV (chemical composition in mol % 25 NiO, 20 ZnO and 55 Fe_2O_3) has frequency-independent magnetization and distortion curves, and it is therefore a suitable ferrite for measuring the total losses as a function of frequency. The resistivity of this material being 52 ohm-cm, eddy-current losses can be neglected if the smallest dimension of the sample is some millimeters, as was actually the case. At low frequency, for instance at 50 c/s, the total losses are substantially caused by the irreversible Bloch-wall displacements. The area of the hysteresis loop at 50 c/s was determined by means of an integrating circuit and the result is given in the lowest curve of Figure 7. Since for this ferrite the hysteresis loop closes at about 3000 gauss, the loss per cycle still increases considerably with increasing induction at 1000 gauss.

In the same figure the total losses per cycle determined with the calorimeter are given at 117, 336 and 490 kc/s. At all frequencies the losses increase similarly with the induction ($W_{tot} \propto B_{max}{}^{2\cdot 4}$), and for a given induction the loss per cycle increases with frequency. For this ferrite the distortion at 490 kc/s is still the same as that at low frequency, so that the "hysteresis" loop at 490 kc/s is formed by the low-frequency hysteresis loop and the

ellipse corresponding to a phase shift between B and H determined by the additional losses per cycle at 490 kc/s compared with those at 50 c/s.

(ii) *Total losses of ferrites with frequency-dependent magnetization curve.* As an example for this sort of ferrite the total losses are given for ferrite I. The magnetization curves and the distortion at different frequencies are already known from Figures 2 and 4. From the results of the loss measurements given in Figure 8 it appears that in this case also the total losses per cycle for a constant induction increase with frequency, but that at the same

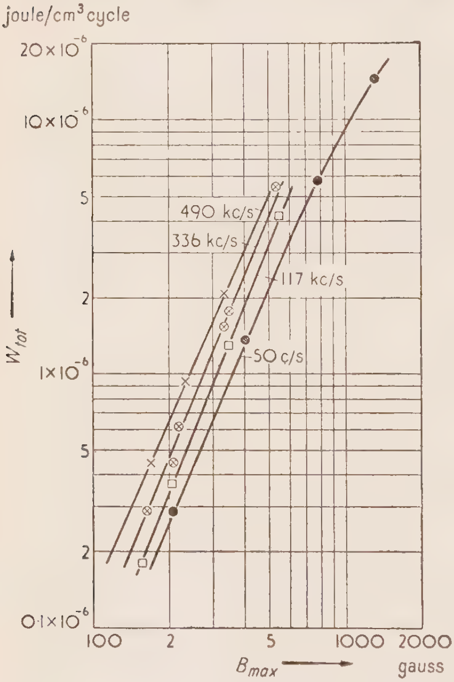

Figure 7. Variation with B of the total losses at several frequencies for ferrite IV, which has a frequency-independent magnetization curve.

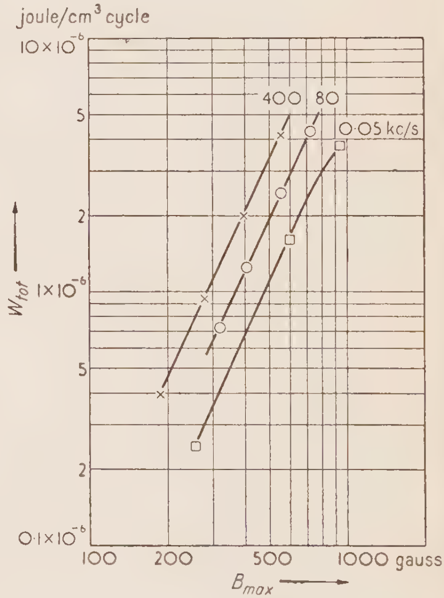

Figure 8. Variation with $B_{max.}$ of the total losses at several frequencies for ferrite I, which has a frequency-dependent magnetization curve.

time the distortion decreases. The low-frequency hysteresis loop with sharp tips gradually changes at high frequencies into an ellipse corresponding to a phase shift δ between B and H, which could be verified with an oscilloscope. The loss coefficient tan δ, which is determined by the total losses per cycle, is not a constant, but increases with B_{max}. The resistivity of this ferrite is 1·2 ohm-cm, and the smallest dimension of the sample is 3 mm. Therefore the losses at 400 kc/s cannot be attributed to eddy currents. Moreover, a

similar increase of the loss per cycle with frequency is found for ferrites with a much higher resistivity.

(*b*) **Relation between hysteresis resistance and distortion in ferrites.** In telecommunication engineering the distortion caused by core material at low inductions is usually derived from its hysteresis resistance, and the requirements for distortion are always expressed by imposing an upper limit on the hysteresis resistance. As we have seen, a coil with a core in which losses are generated can be treated as self-inductance L in series with resistance R. In general R, like L, will depend on the coil current. The current-dependent part of the total resistance is called the hysteresis resistance R_h of the core.

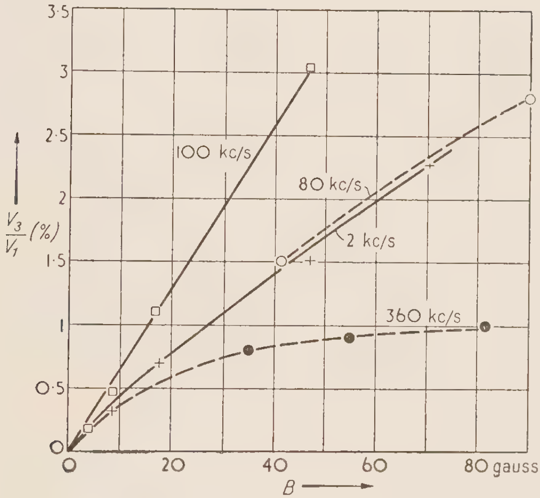

Figure 9. Ferrite I: distortion against induction. Broken curves, measured with a selective voltmeter; full curves, calculated from the hysteresis resistance by equation 3.

For sufficiently small fields the relation between R_h and the distortion due to irreversible magnetization processes in magnetic materials is given (Peterson, 1928) by

$$V_3/V_1 = 0{\cdot}6\ R_h/2\pi f L \qquad \text{...(3)}$$

where f is the measuring frequency. For the ferrites I and III the hysteresis resistance has been measured at 2 kc/s as a function of the induction in the core, the distortion then being calculated according to formula (3). The result is given in Figure 4 and in the inset of Figure 6, which show good agreement between the distortion derived from the hysteresis resistance at 2 kc/s and the distortion determined by a selective voltmeter at low frequency.

Hence it follows that in the case of ferrite I the frequency-dependent part of the magnetization curve to an *irreversible* magnetization process. Thus we have established that in ferrites with an initial permeability of at least 500 a dispersion frequency exists for the irreversible Bloch-wall displacements which is much lower than the gyromagnetic resonance frequency dealt with in section 2(*a*). From the agreement between the two distortion measurements for ferrite III it is to be concluded that the frequency-independent distortion given by the curve ODE in Figure 6 is also caused by an irreversible process.

At high frequencies equation (3) does not hold for ferrites, since the total losses per cycle increase at different frequencies with approximately the same power of the induction (see section 3(*a*)) but at a given B_{max} they increase with frequency. In agreement with this the measured hysteresis resistance increases more than linearly with frequency, and according to equation (3), the distortion should also increase with frequency. Figure 9 gives as an example the distortion derived from the hysteresis resistance of ferrite I at 2 kc/s and 100 kc/s. From this it might be concluded that the distortion at 100 kc/s is higher than that at 2 kc/s, but, as is known from the results in Figure 4, the contrary is the case. In Figure 9 the distortion measured with the selective voltmeter at 80 kc/s is given for comparison. The conclusion to be drawn from the above is that if it is desired to know the distortion at a high frequency, as is often the case where ferrites are used, the distortion must be measured directly at the desired frequency, for instance with a voltage analyser. To deduce the distortion from the hysteresis resistance measured at high or low frequency may give erroneous results.

DISCUSSION

Prof. R. Feldtkeller:

A fall in the distortion factor of the flux density with increasing frequency has been observed also with normal transformer laminations. The fall takes place between magnetizing forces of 10 and 50 mA/cm and frequencies between 1 and 200 c/s. The frequencies are so low that the fall in distortion cannot be attributed to eddy currents. Another effect is also observed in the same range of magnetizing force. Assume that the transformer lamination has been demagnetized by a magnetizing force of diminishing amplitude. After a rest period of several hours, i.e. after the residual effects of the strong magnetizing forces at the beginning of the demagnetizing process have died away, it is suddenly energized by an alternating magnetizing force of constant amplitude. At the beginning of the excitation, the distortion factor has a certain value. It slowly falls with time, reaching a minimum, for example, after half an hour, and then rises during the next few hours to its final value. This effect is referred to as "creep".

If the shape of the hysteresis loop is investigated with a cathode-ray oscilloscope during the creep, it is found that, at the start of excitation, the loop has a pronounced "waist" which disappears in the course of a few hours. The loop finally assumes the usual form consisting of two parabolae. The creep of the distortion factor can be explained, in view

of these observations, in the following way: The distortion due to the tips of the hysteresis loop is superimposed on a temporary distortion which is caused by the "waist" effect and is opposite in phase. At the start, the temporary distortion predominates. After some time this has fallen to the same order of magnitude as the permanent distortion due to the tips of the loop and approximately compensates for it. After a further lapse of time the temporary distortion disappears completely so that only the permanent distortion remains.

The creep is temperature-dependent in the same way as the Richter after-effect; only the relaxation times are temperature-dependent and not the magnitude. The physical origin of the creep could thus be the movement of atoms in the lattice.

Mr. F. F. Roberts:

An interesting feature of Dr. Wijn's results is that the low-frequency initial permeability, where domain walls are presumably free to move in phase with the applied alternating field, is essentially equal to the high-frequency permeability for all values of field, which is in turn ascribed entirely to spin rotation alone. This situation is quite different from that described by Galt, Matthias and Remeika (1950) for a monocrystalline nickel ferrite specimen. While it is understandable that the residual intergranular voids in sintered ferrite will tend to prevent large-scale domain wall movements, it is difficult to draw the line between the small-scale movements of strongly-hindered walls and simple rotational processes occurring to some extent independently in different crystallites. It would seem quite possible to have small-field hysteresis phenomena in a sintered material without any coherent domain-wall effects. The domain-wall concept itself may not be very fruitful for such materials, particularly where the crystallite dimensions are comparable with the thickness of a wall as usually calculated.

What is the origin of the relaxation mechanism associated with the hysteresis in sintered ferrites? How does the relaxation frequency vary with temperature in the cases discussed in the paper?

Dr. Wijn (in reply):

The phenomenon of the gyromagnetic resonance of rotating electron spins might be a basis for the explanation of the measured relaxation effects of irreversible domain-wall displacements found in some ferrites. During the passage of a domain wall, the spins must rotate from their equilibrium position into the new one prescribed by the growing Weiss domain. Under the influence of an external magnetic field having a frequency ν_{displ}, and an amplitude of the order of the coercive force, the domain wall will be displaced a distance l in $1/\nu_{displ}$ seconds, if l is the average length of a Weiss domain.

The passage of a 180° domain wall will cause a change of 180° in the orientation of a spin within $\delta \cdot \dfrac{1}{\nu_{displ}}$ sec., when δ is the wall thickness. This time corresponds with a rotation frequency ν_{rot} given by the formula $\nu_{rot} = l\nu_{displ}/\delta$, and relaxation effects can be expected when ν_{rot} has the order of magnitude of the gyromagnetic resonance frequency ν_{res} of the ferrite. It is found experimentally that ν_{displ} is proportional to ν_{res}. Moreover, ν_{displ} is low for very dense ferrites which will probably have larger Weiss domains than material with a large amount of pores.

As regards the temperature dependence of the relaxation frequency, we have found that for a NiZn ferrite (grade A) this frequency increases by a factor of about 2 when the temperature is decreased from 80 to —80°C.

8

HYSTERESIS INTERMODULATION IN DIRECTIONAL FILTERS

V. G. Welsby

(Post Office Engineering Research Station)

Abstract: Hysteresis distortion of signal waveforms in a two-band communication system, using filters for directional discrimination, produces unwanted circuit noise. This can be avoided by the use of air-cored filter coils, but at the expense of increased size and lower Q-factors. This paper investigates the problem of using ferromagnetic cores in the filters in such a way that both losses and distortion are kept to a minimum for given coil dimensions.

1. INTRODUCTION

The hysteresis of iron-cored coils causes waveform distortion which produces signals at unwanted frequencies in communication systems. Its effect can be reduced to any desired extent by introducing air-gaps into the cores, but this may be accompanied by a reduction in the "Q" of the coils which can be restored only by an increase in their physical dimensions. The relationship between the hysteresis distortion at low flux-densities and the value of Q can be calculated for simple waveforms and for materials which obey the Rayleigh law. Even for complex waveforms and for materials which do not rigidly follow this law, it is possible to establish an approximate relationship which is sufficiently accurate to form a valuable guide in the design of circuits such as wave filters.

This paper considers first, in general terms, the relationship between the Q of an iron-cored coil and its hysteresis properties, and then suggests its application to a problem which arises in the design of filters which must meet certain requirements for both Q and hysteresis and, at the same time, must have the smallest possible dimensions.

Usually one of the requirements of a communication system is that it shall be capable of passing information simultaneously in both directions. On long transmission lines with intermediate repeaters, it is common practice to avoid instability by using different frequency bands for the two directions of transmission. Figure 1 shows schematically the circuit of an intermediate repeater for such a system. It is seen to consist essentially of a common amplifier, serving to amplify signals in both directions, and two sets of " directional filters ", each comprising a high-pass and low-pass filter pair.

The problem under discussion first arose in connexion with the design of

submerged repeaters for deep-sea cables in which it is essential that the volume of the filters should be kept to a minimum and yet that they should meet very stringent requirements as regards hysteresis distortion and pass-band loss.

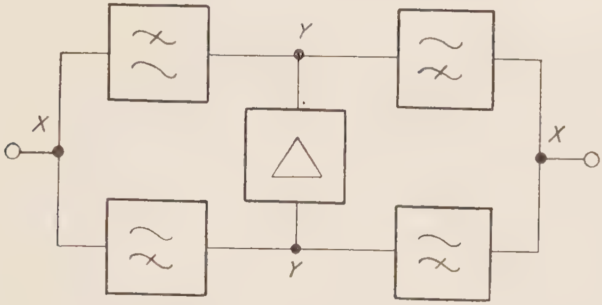

Figure 1. Schematic diagram of "two-band" repeater. "Line" junctions X; "amplifier" junctions Y.

2. INTERMODULATION IN DIRECTIONAL FILTERS

If the coils and condensers of the directional filters were ideal, it would merely be necessary to ensure that, over the pass-band of each filter, the other one produced sufficient attenuation to prevent unwanted feedback around the loops formed by the amplifier and each filter pair. Real coils and condensers, apart from the fact that their losses cause undesirable attenuation in the filter pass-bands, may cause further trouble due to non-linearity of their impedance characteristics. It is well known that the simultaneous application of two or more sinusoidal voltages to a slightly non-linear impedance will produce a distorted current waveform which can be analysed into components at the applied frequencies and also at integral multiples of these frequencies and sums and differences of the multiples. In other words, the current which flows in response to any applied signal voltage will contain components corresponding to the applied signal, together with a series of "intermodulation" or "cross-modulation" products which did not appear in the original signal. It follows therefore that impedance non-linearity in the components of the directional filters will cause signals, transmitted in one band, to produce unwanted intermodulation products, distributed over a relatively wide frequency range, some of which will fall within the frequency band allocated to the opposite direction of transmission. In a multi-channel carrier telephony system, intermodulation generally shows up as an unintelligible but disturbing background noise which is unpleasant and which impairs the articulation standard of the telephone circuits. If some or all of the channels are used for telegraphy, the effect of intermodulation is to increase the probability of errors in

transmission, thus lowering the grade of service available. Although intermodulation products may not be audible (as for example in a telegraph system) the expression " intermodulation noise" is used generally to describe the interference products which appear in one band due to signals transmitted in the other.

Although solid-dielectric condensers are not entirely free from non-linearity, it is the hysteresis effect in coils with ferromagnetic cores which is usually the main cause of intermodulation in filters. Obviously, magnetic hysteresis can be avoided altogether by using air-cored* coils, but only at the expense of increased power losses and filter pass-band attentuation. The design problem thus reduces to that of using the ferromagnetic core material in such a way that both the losses and the hysteresis non-linearity are kept within allowable limits.

We shall next discuss briefly the question of hysteresis from the point of view of the circuit designer.

3. HYSTERESIS DISTORTION

If a sinusoidal alternating magnetizing-force H is applied to a ferromagnetic core and instantaneous values of the flux-density B plotted against corresponding values of H, the familiar "hysteresis loop" is obtained. The formation of a closed loop instead of a straight line does not necessarily mean that a coil wound on the core would have a non-linear impedance, but merely that the phase of B has been displaced relative to that of H. If there is no distortion, the waveform of B will also be sinusoidal and the loop will be an ellipse. B can be analysed into two components, one in phase and the other in quadrature with H, so that if $B = \mu H$, the permeability μ must be regarded as a complex quantity. The actual hysteresis loop is not an ellipse, however, so that the waveform of B will be distorted and will contain, in addition to the fundamental-frequency components, a series of harmonic-distortion-components which will induce corresponding harmonic e.m.f.'s in the coil. The hysteresis loop can be defined in terms of current and induced e.m.f. in the coil by:—

(*a*) the ratio of quadrature voltage to current (i.e. the reactance of the coil),

(*b*) the ratio of in-phase voltage to current (i.e. the part of the total resistance of the coil which is due to hysteresis),

(*c*) the ratio of the voltage component at each harmonic frequency to the in-phase fundamental voltage (i.e. the amount of distortion produced).

These quantities will be denoted respectively, by L (henries), R_h (ohms) and k_n, where the latter is referred to as the nth order "voltage distortion factor".

* i.e. coils with non-magnetic cores.

They are all functions of the r.m.s. current in the coil, but the relationship between them is very complicated. At the relatively low flux-densities used in filter coils it is possible to evolve a fairly accurate theory based on the empirical Rayleigh hysteresis law. This states that the hysteresis loop is given by an equation of the form

$$B = \mu_R \hat{H} \pm \tfrac{1}{2}\alpha\,(\hat{H}^2 - H^2) \qquad \text{...(1)}$$

where the $+$ and $-$ signs refer to the two sides of the loop. μ_R is the real part of the complex permeability (i.e. it is the ratio between the in-phase component of B and the applied H) and α is a constant. Feldtkeller (1949a) has pointed out that experimental results consistently show that α is not a constant but actually a function of $\hat{H}$. He suggests that it is given by an expression of the form

$$\alpha = a + b/(\hat{H}_B + \hat{H}) \qquad \text{...(2)}$$

where a, b and $\hat{H}_B$ are constants for a given material.

Feldtkeller also states that b is positive for nickel-iron alloys which have been carefully purified, and negative in alloys with a considerable proportion of impurities. It is to be expected that, for some alloys, an intermediate condition will be found where b is practically zero so that α is, in fact, a constant. Such materials will obey the Rayleigh law exactly.

If H is given by $\hat{H}$ cos ωt, we have

$$\begin{aligned} B &= \mu_R \hat{H} \cos \omega t \pm \tfrac{1}{2}\alpha \hat{H}^2 (1 - \cos^2 \omega t) \\ &= \mu_R \hat{H} \cos \omega t \pm \tfrac{1}{2}\alpha \hat{H}^2 \sin^2 \omega t \end{aligned}$$

Thus B is the sum of two components, one of which is sinusoidal and in phase with H and the other is proportional to a periodic function of ωt such that

$$\begin{cases} f(\omega t) = \sin^2 \omega t & (0 \leq \omega t \leq \pi) \\ f(\omega t) = -\sin^2 \omega t & (\pi \leq \omega t \leq 2\pi) \end{cases}$$

$f(\omega t)$ can be expanded into a Fourier series of the form

$$f(\omega t) = \frac{8}{\pi}\left(\tfrac{1}{3} \sin \omega t - \frac{1}{3.5} \sin 3\omega t - \frac{1}{3.7} \sin 5\omega t - \text{etc.}\right)$$

so that

$$B = \mu_R \hat{H} \cos \omega t + \frac{4\alpha \hat{H}^2}{\pi}\left(\tfrac{1}{3} \sin \omega t - \frac{1}{3 \cdot 5} \sin 3\,\omega t - \text{etc.}\right)$$

The induced voltage is proportional to dB/dt.

$$\frac{dB}{dt} = -\,\omega \mu_R \hat{H} \sin \omega t + \frac{4\alpha \hat{H}^2 \omega}{\pi}\left(\tfrac{1}{3} \cos \omega t - \tfrac{1}{5} \cos 3\,\omega t - \text{etc.}\right)$$

By definition,

$$k_3 = \frac{4\alpha\hat{H}^2\omega}{(\omega\mu_R\hat{H}) . 5\pi} = \frac{4}{5\pi} \cdot \frac{\alpha\hat{H}}{\mu_R}$$

and

$$\frac{R_h}{\omega L} = \frac{4\alpha\hat{H}^2\omega}{(\omega\mu_R)\hat{H}3\pi} = \frac{4}{3\pi} \cdot \frac{\alpha\hat{H}}{\mu_R}$$

or

$$k_3 = \frac{3}{5} \cdot \frac{R_h}{\omega L} \qquad \text{...(3)}$$

Equation (3) shows that there is a simple relationship between the voltage distortion factor and the ratio of the hysteresis-loss resistance to the reactance of the coil. It will be noted that this relationship still holds, even though both μ_R and α are both actually functions of $\hat{H}$.

This result has a useful practical application, since it enables the distortion factor to be predicted from simple impedance measurements. In the particular case of a toroidal coil of N turns, wound on a core of cross-sectional area A and mean magnetic path length l, there is a simple relationship between B, H and the impedance of the coil (Welsby, 1950).

It is found that

$$R_h = \frac{16\sqrt{2\pi}}{3} \cdot \frac{\alpha}{\mu_a{}^{3/2}} \cdot \frac{I}{\sqrt{Al}} \cdot fL_0{}^{3/2} . 10^{3\cdot 5} \qquad \text{...(4)}$$

or

$$R_h = F_h\, IfL^{3/2} \qquad \text{...(5)}$$

where

$$F_h = \frac{16\sqrt{2\pi}}{3} \cdot \frac{\alpha}{\mu_a{}^{3/2}} \cdot \frac{1}{\sqrt{Al}} . 10^{3\cdot 5} \qquad \text{...(6)}$$

F_h is defined as the "hysteresis factor" of the coil. For a given core it is independent of frequency and inductance :

$$k_3 = \frac{3}{5} \cdot \frac{R_h}{\omega L} = \frac{3}{10\pi} \cdot F_h I\sqrt{L} \qquad \text{...(7)}$$

For a toroidal core, F_h is proportional to $\alpha/\mu_a{}^{3/2}$ and inversely proportional to the square root of the core volume.

If a narrow air-gap of length g, is introduced into the core, equation 6 still holds, but μ_a is reduced to an effective "gapped" value of μ_g, where

$$\mu_g = \frac{\mu_a}{1 + g/l.\mu_a} \qquad \text{...(8)}$$

Assuming that the presence of the air-gap has not affected the distribution of flux density in the core, F_h should be reduced to F_{hg}, where

$$F_{hg} = F_h(\mu_a/\mu_g)^{3/2} \qquad \text{...(9)}$$

For any shape of core, F_h will always be proportional to α and inversely proportional to the square root of the core volume, but the factor of proportionality depends on the core. If μ_g is taken to represent the "inductance ratio" of a coil of any shape (i.e. the ratio of inductances with and without the core) it is still approximately true to say that F_h is inversely proportional to $\mu_g^{3/2}$. The error involved will obviously increase as μ_g is made smaller.

Equation 9 leads to the idea of reducing the hysteresis distortion of a coil by using air-gaps to "dilute" the core material. In practice, this works very well for real air-gaps in cores of relatively high permeability (e.g. laminated or ferrite cores), but it is found that, if the permeability of a powder-core material is varied by varying the proportion of insulant in it, the change of F_h is considerably less than would be expected. This is possibly due to non-uniform flux density throughout each particle and to the fact that each particle is not completely homogeneous. It may be accentuated by the fact that powder-core materials of low intrinsic permeability are generally intended for use at high frequencies, with the result that, in commercial cores, the "dilution" is usually accompanied by a reduction of particle size. This effect is shown in Table 1, which gives typical measured values of F_h for three toroidal powder-cores of identical dimensions composed of molybdenum-permalloy powder pressed with varying space factors and for three ferrite pot cores, made of the same material, but with different air-gap lengths (Latimer and Macdonald, 1950).

Table 1

Core type	Material	Effective μ	F_h
1828/6	powder-core	15	3·5
1828/16	,,	26	5
1828/15	,,	50	7
W 36/8	ferrite	20	2·3
R 36/9	,,	35	5
Y 36/9·5	,,	60	12

4. VARIATION OF Q WITH PERMEABILITY

As already mentioned, the hysteresis loss can generally be neglected in filter coils so that, if the total effective resistance of a coil is R, it can be expressed in the form

$$R/fL = F_e f + F_c + K/f \qquad \ldots(10)$$

where F_e and F_c are the eddy-current and residual loss factors respectively and $K = R_{dc}/L$ where R_{dc} is the d.c. resistance of the winding. As μ is varied, provided the flux distribution remains unchanged, F_e and F_c will

both be directly proportional to μ, and K will be inversely proportional to μ. We can thus write

$$R/fL = A\mu + B/\mu$$

where $$A = (F_e f + F_\epsilon)/\mu \quad \text{and} \quad B = \mu R_{dc}/fL$$

and A and B are independent of μ.

Now Q will be a maximum when R/fL is a minimum, i.e. when

$$(d/d\mu)(R/fL) = 0$$

or when $A - B/\mu^2 = 0$.

Denoting the optimum value of μ by μ_1, we have

$$\mu_1 = \sqrt{B/A}$$

For this value of μ_1

$$R/fL = 2\sqrt{AB}$$

and the maximum value of Q is Q_1 where

$$Q_1 = 2\pi fL/R = \pi/\sqrt{AB}$$

For any value of μ, Q is given by

$$Q = \frac{2\pi}{A\mu + B/\mu} = \frac{2\pi/\sqrt{AB}}{\mu\sqrt{B/A} + (1/\mu)\sqrt{A/B}}$$

or $$Q = \frac{2Q_1}{(\mu/\mu_1 + \mu_1/\mu)} \qquad \text{...(11)}$$

A curve of Q/Q_1 plotted against μ/μ_1 (Figure 2a) shows that for small variations of μ from its optimum value μ_1, the fall in Q is not very great. For example, the use of an air-gap to reduce the permeability to half the optimum value would reduce the hysteresis factor by a ratio of nearly 3 to 1, with a fall in Q of only 20 per cent. For large changes Q becomes almost proportional to μ so that, for a gapped core, Q then tends to change as $F_h{}^{3/2}$.

Suppose that the type and size of a coil and the material of its core have been chosen. For a given frequency range, there will be an optimum permeability and a definite value of hysteresis associated with it. It is only possible to obtain a further decrease in hysteresis factor at the expense of a fall in Q and therefore of increased filter loss.

Effect of coil Q on filter losses. It will be assumed that the high-pass and low-pass filters are of the image-parameter type and that the usual Zobel "x-termination" method is used to combine them at the junction

points. It can be shown that the loss per section can be expressed approximately as p/Q db (Scowen, 1947) where p is given by Table 2 for various values of the parameter m, which determines the ratio between the cut-off frequency and the frequency of peak attenuation of each section. $x = f/f_0$ or f_0/f where $x<1$ and f_0 is the cut-off frequency of the filter concerned.

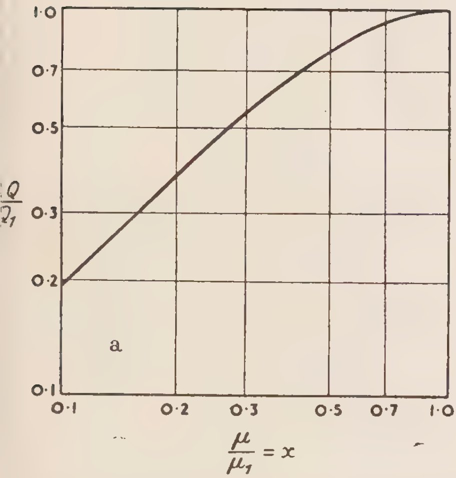

Figure 2a. Effect on Q and on filter losses when the permeability μ is reduced below its optimum value μ_1 by the introduction of a narrow air-gap.

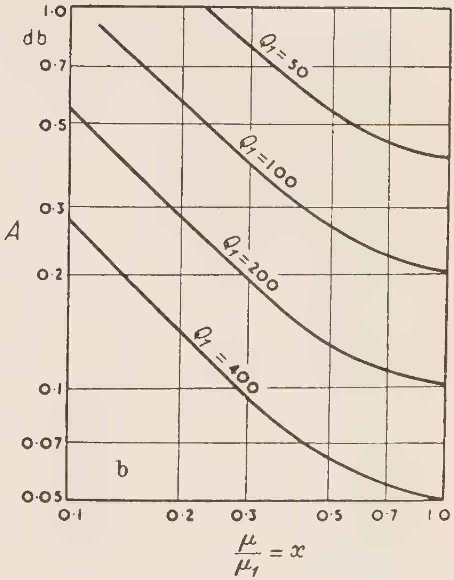

Figure 2b. Q_1 is the maximum value of Q; A is the average attenuation per section for $f/fc = 0{\cdot}9$ (low-pass) or $fc/f = 0{\cdot}9$ (high-pass).

Table 2

x	p, db.				
	$m = 1{\cdot}0$	$m = 0{\cdot}8$	$m = 0{\cdot}6$	$m = 0{\cdot}4$	$m = 0{\cdot}3$
0·6	5·7	5·5	5·3	4·2	2·6
0·7	7·9	7·3	7·3	5·5	4·8
0·8	11·1	10·5	10·5	9·0	9·0
0·9	17·3	18·9	20·8	22·0	23·5

The Table is based on the assumption that the condensers contribute a negligible amount of loss and that the filter sections chosen are those which each have a single coil and three condensers (one of which may have zero or

infinite capacitance). In order to obtain some idea of the relative magnitude of the quantities involved, it will be assumed that it is desired to work at frequencies up to 0·9 of the cut-off frequency (1/0·9 for the high-pass filters). Table 2 shows that, for estimating purposes, the maximum pass-band loss, for any normal m-value, will then have an average value of about $20/Q$ db per section. By combining this result with Figure 2a, the curves of Figure 2b have been produced. These show, for coils with various maximum Q values, the effect on the pass-band loss at 0·9 of cut-off as the permeability is reduced by means of an air-gap. For powder-core materials the eddy-current factor generally depends in a more complicated way on the apparent permeability,* with the result that the curves obtained above may not be directly applicable to coils with cores of this type. They give a general guide, however, to the way in which the pass-band loss is increased by a reduction in permeability below the optimum value.

5. APPLICATION TO FILTER DESIGN

Consider the simple case of a coil of inductance L shunted across or connected in series with a matched transmission line having a resistive characteristic impedance R at all frequencies. It is easy to show that the ratio of third harmonic and fundamental power levels P_3/P_1 is proportional to $F_h^2P_1/f$ and is a function of the ratio $\omega L/R$. It is convenient to express this result in terms of an arbitrary reference frequency f_0 and the ratio $f/f_0 = x$. P_3/P_1 is then proportional to $F_h^2P_1/f_0$ and is a function of $2\pi f_0 L/R$ and of the parameter x. If the coil forms part of a low-pass filter, the impedance conditions are rather more complicated but it can be seen that, if f_0 is taken as the cut-off frequency, $2\pi f_0 L/R$ is now a constant and P_3/P_1 will still be proportional to $F_h^2P_1/f_0$ and will be a function of x.

The harmonic-signal/noise power ratio is thus independent of the impedance of the circuit, but it improves at a rate of 3 db per octave as the cut-off frequency is raised. In practice we are concerned with the transmission of energy which is distributed over a given band of frequencies, and the question arises as to whether the distribution of the resulting intermodulation products can be predicted in the same way as the harmonics of a single transmitted frequency. Theoretically, this problem cannot be solved by the usual methods of analysis because the shape of the hysteresis loop is itself a function of the wave-form of the magnetizing force, so that the law connecting the total intermodulation power and the transmitted power is not necessarily the same as for a sinusoidal signal. Fortunately, at the low flux-densities with which we are concerned here, this distinction is more of academic than practical interest and need not be considered further. It can be assumed that the ratio of total third-order intermodulation

* Low-permeability cores are generally intended for use at high frequencies and would probably have a smaller average particle size than high-permeability ones using the same material. Lack of uniformity in the flux distribution and in the properties of the particles will also complicate the problem.

power to the total transmitted power is also proportional to $F_h^2 P_1/f_0$ where f_0 is an arbitrary reference frequency whose value determines the frequency scale. In this case P_1 and P_3 refer to the total fundamental power and third-order intermodulation power respectively. Although mathematical analysis would be extremely difficult, the prediction of the ratio P_3/P_1 and of the frequency distribution of P_3 for each of the individual coils of a pair of filters can be based on the results of systematic measurements, using random-noise signals distributed over a suitable frequency band. Unfortunately space does not permit its inclusion here, but the author hopes to include it in a later publication.

6. CONCLUSIONS

It has been shown that, for design purposes, the hysteresis factor of a coil (obtained either from bridge measurements or harmonic measurements using a sinusoidal input) can be used as a guide to the relative intermodulation distortion produced when the coil forms part of a highpass-lowpass filter pair. The absolute value of the distortion cannot be calculated directly, but can be estimated from the results of systematic measurements using random-noise signals.

Acknowledgment is made to the Engineer-in-Chief of the Post Office Engineering Department for permission to use the information contained in this paper.

9

PHYSICAL ASPECTS OF LOSSES IN SOFT MAGNETIC MATERIALS

D. Polder

(Bristol University)

Abstract: Unambiguous classification into hysteresis, eddy-current and residual losses is difficult or impossible, as ignorance of the physical processes involved results in unsatisfactory definitions of these losses. Even "permeability" is ambiguous, especially for material having large domains.

The distinction between losses giving loss angles which do or do not vary with frequency in a particular way is, in many cases, of little physical significance. In many ferrites, the variation of hysteresis with flux is not in accordance with the Rayleigh law. Several physical processes are discussed which contribute or may contribute to losses in different frequency ranges.

1. INTRODUCTION

This paper aims at giving a physical discussion of the classification and the origin of losses in soft magnetic materials. Unambiguous classification of different types of losses is extremely difficult, and standard denominations must be used with great care. Confusion is possible because of a different approach of the engineer and the physicist to the general problem, manifesting itself, for instance, in a possible difference of opinion as to what is the obvious meaning of a term such as permeability, hysteresis loss or eddy-current loss. Partly the difficulties originate from the incompleteness of our understanding of the fundamental physical processes involved, which makes it difficult to disentangle their individual effects.

The last remark applies particularly to experiments with higher flux amplitudes. For this reason we shall confine our attention mainly to the physical aspects of low-amplitude phenomena and shall not touch upon hysteresis and similar processes.

Though much of the work described in this paper is well known and some observations are of an entirely trivial nature, a short and qualitative review of the present situation may be opportune. As a result of fundamental research, and the development of new magnetic materials, several aspects of magnetism and of magnetic losses have become more clearly understood and this progress will eventually affect the practical application of ferromagnetic materials.

2. CLASSIFICATION OF LOSSES

In this paper we shall only discuss phenomena which give energy dissipation inside the core material itself, disregarding dielectric losses caused by

external a.c. electric fields. For the classification of losses it is important to consider the dependence on the amplitude of the a.c. field, on the frequency and on the size of the specimen. Further information may be obtained from the effect of biasing fields or temperature and other factors. In order to simplify the discussion we assume no biasing field. A possible classification is the following:—

(*a*) Initial losses, which, even in the limit of vanishingly small fields, contribute to R/L or Q^{-1} of a core. Initial losses are due to phenomena linear in H and B. They show proportionality of the energy loss per cycle with the square of the a.c. field. Therefore, we may define a second type :

(*b*) Losses in addition to the previous losses found in experiments with higher $\hat{B}$.

Eddy currents, dimensional resonance, carbon in solid solution and gyromagnetic resonance may all contribute to the initial loss. As far as linearity holds they do not give rise to higher harmonics. A sub-classification can be made in size-dependent phenomena, to be discussed in section 3 (first two examples) and size-independent phenomena, discussed in section 5 (last two examples). A further characterization by means of the dependence on frequency will be seen to be not unambiguous. The energy dissipation per cycle in a quasi-static experiment contains no contribution from initial losses as defined above.

A sub-classification of (*b*)-type losses is difficult for several reasons. For instance, hysteresis loss per cycle only has a definite meaning for a quasi-static B/H loop. At higher frequencies and in conducting materials one has the well-known difficulty of cross-effects of eddy currents and hysteresis. If certain simplifying assumptions are made, such as frequency-independence of the local hysteresis loops, the cross effects can be evaluated, at least in principle. The calculations are extremely complicated, involving much numerical work, and have been carried out for very simple cases only. Furthermore, the basic assumptions are questionable, e.g. it is not known whether the disregard of micro-eddy currents is at all justified, especially in thin sheets.

For this reason one usually prefers a phenomenological definition of hysteresis loss. It has been defined as that part of the whole loss per cycle obtained by linear extrapolation to zero frequency. At higher frequency the physical significance of this procedure is nil. The usual argument based on the different frequency-dependence of hysteresis and eddy-current losses does not apply any more if the flux pattern inside the individual sheets or particles is materially affected by eddy currents. A further disadvantage is that some residual losses are automatically included in this definition of hysteresis loss.

In ferrites the difficulties with respect to the meaning of hysteresis loss are of a different nature. As shown by Wijn and Went (1951) the shape of

the B/H curve of many ferrites is not independent of frequency if one considers frequencies of the order 10^5 c/s. Furthermore, it is found that at sufficiently high frequencies practically no higher harmonics are produced in these ferrites, in contradistinction to what happens at low frequencies at the same B. On the other hand, the observed energy dissipation per second is more than proportional to the square of the amplitude of the field, so that the loss is not simply of the type (*a*). As we do not have a precise physical picture of what actually happens in these materials it seems premature to decide upon a classification of losses at high inductions. Work along the lines reported by Wijn will be of great importance to clear up these points.

A point of practical interest may be added here. At small, but not vanishingly small, $\hat{B}$, hysteresis loss is commonly defined as that part of R/L proportional to $\hat{B}$. The hysteresis coefficient h is defined by $(R/L)_{hyst} = \mu h \hat{B} f$. The proportionality with $\hat{B}$ exists if hysteresis is of the Rayleigh type (Bozorth, 1951, p. 492), and in that case the amount of higher harmonics is a simple function of μ and h. In the ferrites studied by Wijn, a term proportional to $\hat{B}$ also exists and h may be defined accordingly. It must be kept in mind, however, that such a figure for h may give a totally wrong impression of the distortion. At the high frequencies considered above, the actual distortion is much smaller, since the loss mechanism is of an entirely different nature.

For constructional purposes, therefore, it appears desirable to have available independent figures for losses and distortion with a specification of the $\hat{B}$ values and frequencies for which they are valid.

3. SIZE-DEPENDENT INITIAL LOSSES

Apart from magneto-mechanical resonance losses, which are only appreciable very near the frequencies of mechanical resonances of the specimen, eddy-current losses and dimensional-resonance losses are important losses which depend on the dimensions of the ferromagnetic specimen.

The size-dependence of both eddy currents and dimensional resonance follows immediately from Maxwell's equations. In the eddy-current case the dissipation of energy in the form of Joule heat is a direct consequence of the flow of current. In the less well-known case of dimensional-resonance losses, the displacement current $\partial D/\partial t$ is an important factor determining the flux pattern inside the core. It may be extremely large if the apparent permittivity of the material is large. Since a displacement current itself is non-dissipative, losses are found in the region of frequency near certain resonance frequencies. For the lowest of these frequencies the wavelength of the electromagnetic wave inside the material is of the order of the smallest dimension of the specimen (Brockman, Dowling, and Steneck, 1950). Both the conductivity and the imaginary part of the susceptibility contribute to the dissipation in the resonance region.

Some of the better conducting ferrites show these phenomena at frequencies above 1 Mc/s; in other ferrites and in metals, dimensional-resonance effects are usually of no practical importance (Polder, 1950). In this connexion it should be pointed out that, strictly speaking, the distinction between eddy-current losses and dimensional-resonance losses is artificial. These names refer to solutions of the same Maxwell's equations for rather different values of the constants. If an estimate is wanted of the losses in a homogeneous ferrite core, the best thing is to work it out with the aid of the actual dimensions and the frequency-dependent values of the complex permeability and permittivity.

It follows from the foregoing paragraph that it does not make sense to characterize ferrite materials with an eddy-current loss coefficient e, in contradistinction to inhomogeneous materials made from powders or sheets. In the last-mentioned materials size effects are determined by the dimensions of the ferromagnetic particles or thickness of the sheets. The usual practical application of the materials is in a frequency range where the skin-depth is larger than the dimensions just mentioned. This makes the contribution to R/L from eddy currents proportional to f^2.

The proportionality to f^2 is commonly used for the definition of eddy-current losses in inhomogeneous core materials by an analysis of the very-low-amplitude value of R/L in terms of a part $\propto f$ and one $\propto f^2$. Thus, if μ' is the real part of the effective permeability,

$$R/L \doteq \mu' cf + \mu' ef^2 \doteq 2\pi f (\tan \delta_m)_{eff}$$

δ_m is the effective magnetic loss angle of the material, c is called the residual-loss coefficient (Legg, 1936). It must be remembered that by doing so, any loss mechanism for which the magnetic loss angle is proportional to f, as may happen in the case of losses due to interstitial carbon, is automatically included as eddy-current loss. Since there is no reason to assume that other loss mechanisms will necessarily give a constant angle in a wide frequency range, the usual way to separate eddy-current and residual losses seems rather arbitrary from a physical point of view. In fact, if losses are investigated in a wide frequency range, a simple analysis of this type breaks down anyway.

A further remark about eddy-current losses in inhomogeneous core materials must be made here. Let there be no other loss mechanism contributing to the term $\propto f^2$ in R/L. In that case one might hope to be able to predict the actual figures from the particle dimensions, the resistivity and the permeability of the magnetic component. Apart from trivial though troublesome reasons, such as inadequate insulation, we have at least two possible causes for appreciable disagreement with experiment, even at extremely low flux densities.

First we have the well-known difficulty that magnetic particles or sheets

are never homogeneous in resistivity or in permeability (Peterson and Wrathall, 1936). Generally speaking this will lead to higher eddy-current losses than expected.

A second reason is of a more fundamental nature. It is well known that the initial permeability of soft metallic ferromagnetics is mainly due to reversible wall displacements. The application of a field will give rise to a large change of flux in the region which the domain wall happens to pass, while little change is found elsewhere. Micro-eddy currents will be set up. Their combined pattern will have some resemblance to the pattern expected from a naïve picture of homogeneous permeability, but the details will be entirely different. This effect has been suggested by Stewart (1950) and emphasized by Williams, Shockley and Kittel (1950), who estimate that, for a special example, the total loss may be as much as a factor 3 higher than expected. The details depend to a large extent on the actual domain geometry and, therefore, the resulting anomaly may be susceptible to changes in the condition and the dimensions of the ferromagnetic particles. It should be pointed out that this interesting explanation of the eddy-current anomaly must not be confused with hysteresis due to wall displacements. In both cases the dissipation is due to micro-eddy currents, but hysteresis is a non-linear phenomenon connected with irreversible displacements, while the present discussion refers to a reversible motion governed by linear laws. It is quite possible that at higher flux-densities different effects contribute to the eddy-current anomaly.

4. DIGRESSION ON PERMEABILITY

The term permeability is used in practice with a great number of different meanings. Especially in a discussion on the fundamental interpretation of experimental results, it is always very desirable to define as precisely as possible what permeability is meant. For our paper we use $\mu = \mu' - j\mu''$ for the complex initial permeability in the sense of Maxwell's equations for periodic phenomena. We make the usual assumption that it is possible to define μ for any small specimen of a homogeneous ferromagnetic substance containing many Weiss domains. The last restriction is essential in view of the anomalous properties of particles consisting of only one or a few domains (Kittel, 1949). The contributions from wall displacements and rotational processes, but also from micro-eddy currents, to the permeability are automatically accounted for in this definition. In particular, the phenomenological description of the damping of wall motion at high frequencies (cf. section 5), either because of eddy currents or by other causes, is simply a frequency-dependent complex permeability. In the same way all loss mechanisms to be discussed in section 5 are described in terms of complex permeability in the Maxwellian sense.

The question arises whether this procedure is always justified. This is

not an entirely academic question as will be seen. In the first place micro-eddy currents depend on domain geometry and are, in principle at least, implicitly dependent on size and shape of the specimen, in contradistinction to what is wanted for Maxwell theory. Secondly and more strikingly, if the frequency is high or the domains are large, so that the skin-thickness begins to be of the order of the domain size, the distinction between micro-eddy currents and macro-eddy currents breaks down, the definition of permeability mentioned above is no longer possible and a more detailed treatment is necessary to describe the properties of the material in a physically significant way.

Because of its practical value, the effective complex initial permeability is often used in technical literature for the description of non-homogeneous materials such as powder cores. The figures automatically account for all eddy-current and other losses in or outside the individual particles or sheets. For homogeneous materials, such as ferrites, the effective permeability only has a meaning as a figure characterizing the behaviour of an actual core, thus accounting for the dimension-dependent eddy currents or resonances if present.

5. SIZE-INDEPENDENT INITIAL LOSSES

We shall discuss:—

(*a*) Losses of the Snoek type.

(*b*) Richter- and Jordan-type losses.

(*c*) Gyromagnetic resonance losses.

(*d*) Losses connected with damping of wall motion.

Let us first discuss (*a*) and (*b*), losses which are found at under, say, 1 Mc/s. As a result of work by Snoek (1939, 1941, 1942, 1947), we have a clear physical picture of at least one possible contribution to residual losses: the loss in body-centred metals containing a small amount of impurities such as C or N. The one characteristic frequency ν_0 of this typical relaxation phenomenon is the inverse of the time required to establish preferential distribution of impurities over different inter-lattice positions induced by magnetostrictive stresses. The maximum loss is found near the strongly temperature-dependent relaxation frequency ν_0; for $f \ll \nu_0$ we have $\tan \delta \propto f$, i.e. $R/L \propto f^2$; for $f \gg \nu_0$ a small constant contribution to R/L is left.

We may think of other mechanisms, characterized by more than one relaxation frequency. As an example we mention the small thermo-elastic or thermomagnetic losses of the type first discussed by Zener (1937, 1938). From a physical point of view the classification of residual losses into Richter losses with frequency-dependent loss angle and Jordan losses with constant loss angle has not much significance. The existence of a relaxation frequency will give rise to frequency-dependence, but a distribution of relaxation

frequencies may easily give a virtually constant loss angle over a wide frequency range as has been shown for the dielectric case by Gevers (1946). Such a classification tends to obscure the fact that we simply have not got a satisfactory physical picture of a certain amount of residual loss in homogeneous and non-homogeneous ferromagnetic materials.

Losses (*c*) connected with the rotational processes in magnetization and (*d*) originating from the friction experienced by a moving Bloch wall, may be important at or above 100 kc/s. Because of the minor importance of rotational processes for the initial permeability of metallic high-permeability ferromagnetics, the latter type of loss should be predominant in these materials. Experiments by Galt (Galt et al., 1950) indicate that wall displacements are also important for the initial magnetization of a ferrite single crystal.

A difference of opinion appears to exist with regard to the contribution from wall displacements to the initial permeability of sintered ferrites. On the one hand Rado and collaborators (1950) claim to have detected dispersion of wall displacement susceptibility in a special ferrite sample, on the other hand Went and Wijn (1951) present rather convincing arguments that, at least in a number of ferrites, the initial permeability is practically only of rotational origin. The authors of both papers agree that rotational losses occur in any case at some frequency in ferrites. We discuss rotational losses first.

Each magnetic dipole in a demagnetized ferromagnetic may be thought of as being bound to an equilibrium position by an effective internal magnetic field. This field has a different value and direction in different parts of the material, and is composed of the actual internal magnetic field and a fictitious field describing the effects of crystal anisotropy and magnetostriction. The motion of a dipole with respect to its equilibrium position meets a frictional force of unknown origin. The friction has been postulated theoretically by Landau and Lifshitz (1935) and is clearly demonstrated in experiments on gyromagnetic resonance in large external fields (Kittel, 1951). The same mechanism will provide damping of gyromagnetic resonance in the effective internal fields. The natural precession frequency of the dipoles is proportional to, and the rotational permeability μ_{rot} of the material is inversionally proportional to, the average strength of the internal field. From this the very approximate formula

$$2\pi f_r \doteqdot \frac{2}{3}\left(\frac{e}{mc}\right)\frac{4\pi M_{sat}}{\mu_{rot} - 1} \text{ where } e/mc \doteqdot 17 \text{ Mc/s-gauss}$$

suggested by Snoek (1948) may be qualitatively understood. It predicts the frequency f_r of the a.c. field for which maximum resonance and, therefore, maximum resonance loss will occur. Insertion of the actual low-frequency permeability for μ_r predicts the position of the (first) peak of μ'' in many

ferrites (Wijn and Went, 1951; Polder, 1950; Rado, Wright and Emerson, 1950) within a factor of 3 or so. This suggests that rotational processes are at least as important as wall displacements in ferrites. The peak in μ'' is found at frequencies ranging from 5 Mc/s to 500 Mc/s for ferrite materials with permeabilities varying from 1000 to 10. A pronounced tail in μ'' at the high-frequency side can be explained by resonance frequencies, greatly increased because of the creation of internal magnetic charges in the region between domains during the precessional motion (Polder, 1951). In powdered ferrites or ferrites containing a large amount of non-magnetic phase around small particles, the a.c. magnetic charge at the domain boundaries should be very important. It may be expected to give rise to distinct resonance at frequencies f_1 of the order $2\pi f_1 \fallingdotseq (e/mc)\, 4\pi M_{sat}$. Polder and Smit, 1953). Of the two resonances it is likely that a second peak sometimes found in ferrites (Rado et al., 1950 ; Welch et al., 1950) above 10^3 Mc/s must be interpreted in this way. We wish to mention that our interpretation is at variance with the one suggested by Rado et al.

In metallic ferromagnetics damping of domain-wall motion is mainly due to micro-eddy currents (Becker, 1938a). It accounts for a steady drop of the real part of the (Maxwellian) permeability and increased loss angle (also the effective loss angle) at frequencies above 100 Mc/s. The relaxation frequency of this phenomenon is of the order

$$f_2 \fallingdotseq \rho c^2/\mu l^2$$

where ρ is the resistivity (c.g.s. units) and l the average domain size. The precise calculation of the effect is complicated by the skin-thickness being of the same order as the domain size at these frequencies, so that only domains near the surface play a role (Kittel, 1946).

In non-metallic ferromagnetics the experimental findings are not yet conclusive. Referring to Went and Wijn's paper (1951) and our foregoing criticism of Rado's interpretation of very-high-frequency losses for very small $\hat{B}$ in sintered ferrites, we believe that there is no definite evidence of initial wall-damping losses in these materials. In a ferrite single crystal domain-wall-motion losses are reported at small field-amplitudes in the 100 kc/s region (Galt et al., 1950). For this reason we shall only mention two suggestions which have been made in theoretical work. Döring (1948) has shown that the equation of motion of a wall contains a term which can be interpreted as the mass of a wall and which is a result of the inertia associated with the precessional motion of the magnetic dipoles in a moving wall. If at the same time the wall is bound to a position of lowest energy we may expect resonance and resonance losses at the frequency f_3 of natural vibration of the wall. Since the binding force is stronger the lower the displacement permeability, we can understand qualitatively the approximate relation

$$2\pi f_3 \fallingdotseq (e/mc)\,.\,4\pi M_{sat} \sqrt{\delta/l(\mu - 1)_{disp}}$$

δ is the domain wall thickness.

For ferrites this gives $\jmath_3 \doteqdot 100$ Mc/s, if a substantial contribution from wall displacements to the permeability is assumed.

Kittel (1951) has shown that the damping mechanism effective in gyromagnetic resonance can also provide a frictional force on a moving wall. While in non-conducting materials eddy-current damping is negligible, the last-mentioned friction might be considerably stronger than in metals. Whether this is so depends on the interpretation of the broad gyromagnetic-resonance curves of ferrites in large external fields (Beljers, 1949). If the broadening is due to damping, an estimate leads to a relaxation frequency for the wall motion of the order of 10^7 c/s. This would obscure the previously discussed inertia effect. There is still the possibility, however, that the broad curves are simply composed of a great number of overlapping narrow curves. In that case the estimate is too low. As mentioned before, the theoretical speculations reproduced in the last two paragraphs have not yet found a convincing experimental confirmation.

DISCUSSION

Dr. M. Kornetzki:

Introduction

The following facts can be contributed towards the explanation of the causes of loss in ferrites:—

Figure 1 shows the loss factor $(\tan \delta)/\mu$ of some nickel-zinc-ferrites (with various relative initial permeabilities μ) as a function of frequency. The losses have been extrapolated to

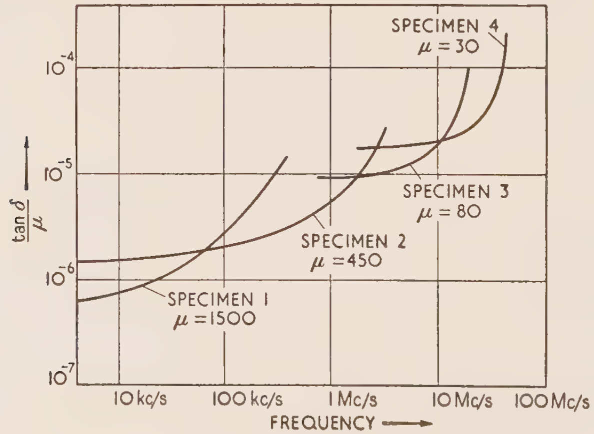

Figure 1. Variation with frequency of the loss factors of various nickel-zinc ferrites.

zero magnetizing force, so that we are dealing only with residual losses. At very low frequencies, they each begin with an initial value $[(\tan \delta)/\mu]_0$ which, as usual, will be defined as the residual loss. As the frequency is increased, the loss rises, slowly at first and then

more rapidly. It is known that this rise depends on spin-precession. This may either be a case of precession of the spins in the whole domain (Snoek) or of the inertia of the Bloch walls (Döring and Becker), which may also be caused by spin-precession. For the following discussion it is immaterial which of the two effects predominates. It is known that the precession motion of the spins is damped and that the loss factor of ferrites must rise as the precession frequency is approached. We are interested here, however, in the *cause of the damping* of the precession motion; this cause has not yet been clearly explained. One can think of two possibilities :—

(1) The above-mentioned initial value $(\tan \delta)/\mu$ and the damping of the precession may have completely different causes;

(2) the precession may be damped by the same effect as that which causes the basic loss $[(\tan \delta)/\mu]_0$. Then it should be possible to establish a relationship between the two parts of the loss curve.

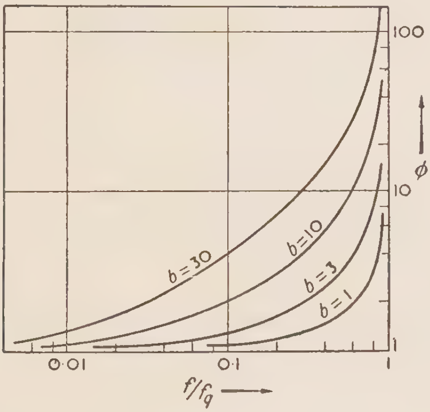

Figure 2. The function $\phi' = 1 + b\,\dfrac{f/f_q}{1-(f/f_q)^2}$

Results

A decision was attempted in the following way:—

The loss curves of Figure 1 are plotted on the usual logarithmic scale. It is seen that they are not alike, their curvature being quite different. The left-hand curve, which applies for a ferrite with an initial permeability of 1500, is slightly curved. The curves lying further to the right have relatively greater curvature, the greatest being that of the right-hand curve, which was measured on a ferrite with an initial permeability of 30.

It was found that the curves can be approximated by a function of the form

$$\phi' = 1 + b\,\frac{f/f_q}{1-(f/f_q)^2}$$

f is the test frequency, f_q is a resonant frequency which is yet to be determined and b' is a factor also to be determined. Two possibilities can be tried:—

(*a*) $$\frac{\tan \delta}{\mu} = \left(\frac{\tan \delta}{\mu}\right)_0 \left(1 + b\,\frac{f/f_q}{1-(f/f_q)^2}\right) \qquad \ldots(1)$$

(*b*) $$\frac{\tan \delta}{\mu} = \left(\frac{\tan \delta}{\mu}\right)_0 + c\,\frac{f/f_q}{1-(f/f_q)^2} \qquad \ldots(2)$$

If (*a*) were true, so that the basic loss $\left(\frac{\tan\delta}{\mu}\right)_0$ appeared as a *multiplying factor* in the precession attenuation, one would have to assume that both losses have the same cause. If, on the other hand, the two losses were merely *additive* it could be assumed that the spin precession is *not* damped by the same cause as that which determines the loss as low frequencies.

To decide the matter, the function ϕ' was plotted, on the same scales as the loss curves, as a function of the relative frequency f/f_q. Figure 2 shows the function ϕ' with various values of b' between 1 and 30. It is now possible to make these curves coincide with those of Figure 1 and, in this way, to determine b and f_q. The table shows the result.

Nickel-zinc-ferrite, Specimen No.	Initial permeability μ	$\left(\frac{\tan\delta}{\mu}\right)_0 \times 1\,000$	b approx.	f_q, Mc/s	$c \times 1\,000$, approx.
1	1500	0·006	30	0·7	0·18
2	450	0·015	10	4·5	0·15
3	80	0·09	1·5	20	0·14
4	30	0·18	1	48	0·18

It is seen that b assumes different values between 1 and 30 for the various ferrites. If the factor c in equation (2) is calculated from the relationship

$$c = b[(\tan\delta)/\mu]_0 \qquad \ldots(3)$$

the values given in the table are obtained. It is seen that c is roughly constant for the various ferrites; varying only between $0{\cdot}14 \times 10^{-3}$ and $0{\cdot}18 \times 10^{-3}$. It follows from this result that equation (1), which leads to varying values of the parameter b, is less accurate than equation (2).

Conclusions. Since equation (2) gives roughly constant values for the parameter c, the following conclusions can be reached about the loss curves:—

The losses are composed of two independent parts. $[(\tan\delta)/\mu]_0$ represents the actual residual loss, in which precession effects play no part. The damping of the precession effects causes the loss factor $c\,\frac{f/f_q}{1-(f/f_q)^2}$. c has a mean value of $0{\cdot}016 \times 10^{-3}$. Both losses add to form the total loss. The cause of the damping of the spin precession is thus different from that of the basic loss.

It is yet to be determined whether c is the same for all ferrites or applies only for the Ni-Zn-ferrite investigated here.

Additional remarks. These effects become particularly clear if the loss curve is plotted over the relative frequency f/f_q. As shown in Figure 3, all the curves are very much alike, at least in the initial portion. The dotted line shows the function

$$\phi = 0{\cdot}16 \times 10^{-3}\,\frac{f/f_q}{1-(f/f_q)^2}$$

in which c has been assigned the mean value of $0{\cdot}16 \times 10^{-3}$.

The curves, at least over the initial portions, are parallel to the function ϕ and are merely displaced by the amount $[(\tan \delta)/\mu]_0$. In the neighbourhood of f/f_q they deviate to a greater or lesser extent from the function ϕ because the latter tends to infinity at this point.

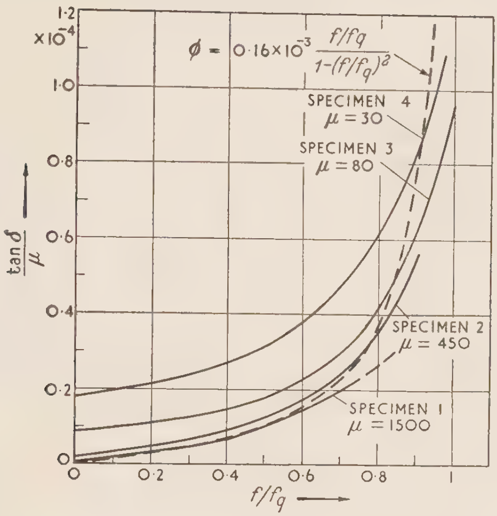

Figure 3. Dependence on the reduced frequency f/f_q of the loss factors of various nickel-zinc ferrites.

At $f = 0$ the curves start with a finite slope. The ferrites investigated thus have an *apparent* eddy-current factor c/f_q. This is practically inversely proportional to the permeability. It is known that Snoek has published the for nula

$$f_p = \gamma I_s/\mu$$

where f_p is the gyromagnetic boundary frequency, I_s the saturation magnetizing force, $\gamma = 2.10^{-6}$ gauss^{-1} . sec^{-1}. If f_p is compared with the frequency f_q introduced in this paper, it is found that

$$f_p = (3 \text{ to } 5) f_q$$

It is clear that the above tentatively-introduced function ϕ, which can be deduced from the equation for a harmonic oscillator, is only a first rough approximation. A more exact function must contain a damping term to ensure that the function ϕ remains at $f = f_q$.

Summary. The frequency-dependent losses of nickel-zinc-ferrites with permeabilities of 30 to 1500 can be approximated by a simple function. From the form of this function it is concluded that the spin precession, which causes the rise of the magnetic loss angle at high frequencies, is damped by some effect other than that which determines the loss angle at low frequencies.

Dr. Polder (in reply):

Generally speaking, it does not seem possible to describe the complex permeability of sintered ferrites as a function of frequency with the aid of only one damped resonance mechanism if the whole frequency range between, say, 10 Kc/s and 1 000 Mc/s is considered.

Several investigators have tried to account for the observed curves by using expressions involving either a damped resonance term and a relaxation term or more resonance terms. In particular, loss curves showing two maxima as observed by Rado et al. (1950) and by Welch et al. (1950) would necessitate the introduction of more resonances.

From a theoretical point of view it does not seem likely that a simple analysis of this type should give a precise description of the experimental curves. A closer inspection of the theory of natural ferromagnetic resonance (i.e. precessional resonance in demagnetized samples) shows that this phenomenon is considerably complicated by the magnetic interaction between different parts of the material which have different directions of magnetization and take part in the resonance process each in a different way. One would expect a great number of different modes of precession with natural frequencies extending over a considerable frequency range, rather than one or two well-defined resonance frequencies. The precise frequency dependence of resonance losses depends to a large extent on the actual arrangement of the Weiss domains in the material and, therefore, among other factors, on the way the sintered material is prepared.

Prof. R. Feldtkeller:

The magnetic relaxation effects can be classified as follows:—

1. *The initial-permeability region*

Material demagnetized by an alternating field of diminishing amplitude and then allowed to rest for several hours.

Experimental results extrapolated to zero field strength and flux density. For sinusoidal magnetizing force $H = \hat{B} \cos \omega t$, the flux density $B = \hat{B} \cos (\omega t + \phi_B)$ is also sinusoidal, its amplitude $B = \mu_a \hat{H}$ being exactly proportional to the amplitude of the magnetizing force. The laws of linear network theory apply here. It is thus sufficient to know either the frequency response of $\hat{B}$ and ϕ_B for all frequencies or the time response of B after a sudden change of d.c. magnetizing force from 0 to H in order to be able to calculate the behaviour of the relaxation effects for any given variation of magnetizing force.

The following effects are so far recognized:—

1(*a*) *Jordan after-effect*

Wide spread of relaxation times (1 : 10^8), no measurable temperature-dependence of relaxation times.

1(*b*) *High-frequency Jordan after-effect*

Narrow spread of relaxation times (1 : 10), no measurable temperature-dependence of relaxation times. Variation of intensity with temperature not yet measured. (Restoration of the disturbed temperature equilibrium within the particles of powder cores.)

1(*c*) *Richter after-effect*

Medium spread of relaxation times (1 : 10^3). Relaxation times vary with temperature in accordance with $\tau = \tau_\infty \exp(-\theta/T)$ with θ = 9000 to 10 000°K. No measurable variation of intensity with temperature. (Movement of dissolved C and N atoms in α-iron after the passage of a 90° wall.)

2. *Rayleigh region*

Material demagnetized by alternating field of diminishing amplitude and allowed to rest for several hours.

For sinusoidal magnetizing force $H = \hat{H} \cos \omega t$, the flux density is no longer sinusoidal but must be represented by a Fourier series:

$$\begin{aligned} B = &\hat{B}'_{\omega} \cos \omega t + \hat{B}''_{\omega} \sin \omega t \\ &+ B'_{3\omega} \cos 3\,\omega t + B''_{3\omega} \sin 3\omega t \\ &+ \ldots\ldots\ldots\ldots\ldots\ldots \end{aligned}$$

Linear network laws do not apply. Thus the response of B to a sudden change of H cannot be calculated, even if all the coefficients of the Fourier series for B are known for a given sinusoidal magnetizing force. The theory of quasi-linear networks is generally applicable.

The following effects are recognized:—

2(*a*) The components $\mu_{LR} = \hat{B}'_{\omega}/\hat{H}$ and $\mu_{RR} = \hat{B}''_{\omega}/\hat{H}$ of the fundamental-frequency permeability vary with frequency. They have limiting values which are reached after the alternating magnetizing force has been applied for a long time. (Silicon-iron, ferrites.) No variation with temperature has been measured.

2(*b*) The harmonic permeability

$$\mu_p = \sqrt{\hat{B}'^{2}_{p\omega} + \hat{B}''^{2}_{p\omega}}/\hat{B} \qquad (p = 3, 5, \ldots)$$

varies with frequency and has a limiting value which is reached after the alternating field has been applied for a long time. No measurable variation with temperature.

The following effects appear to be significant:—

2(*c*) The variation with frequency of the combination-frequency permeability

$$\mu_{p \pm q} = \sqrt{\hat{B}'^{2}_{p\omega 1 \pm q\omega 2} + \hat{B}''^{2}_{p\omega 1 \pm q\omega 2}}\ /\hat{H}\ (p \text{ and } q \text{ integers})$$

and its limiting value after the alternating field has been applied for a long time.

2(*d*) The variation of flux density after the magnetizing force has suddenly changed from 0 to H.

In addition the following effects have been observed:—

2(*e*) Variation of the components μ_{LR} and μ_{RR} with time after the application of an alternating magnetizing force. (Creep of the permeability.)

2(*f*) Variation with time of the harmonic permeability μ_p ($p = 3, 5, \ldots$) after the application of an alternating magnetizing force. (Creep of harmonics.)

The relaxation times vary with temperature according to $\tau = \tau_{\infty} \exp(-\theta/T)$ with θ of the order of magnitude of 10 000°K.

No measurable variation of intensity with temperature.

2(*g*) Variation with time of the combination-frequency permeability μ_{p+q} after the simultaneous application of two alternating magnetizing forces of the same amplitude with a small frequency separation. (Creep of the combination frequencies.)

3. *Region where the magnetizing force is comparable with the coercive force*

Material demagnetized by alternating field of diminishing amplitude and allowed to rest for several hours:—

3(*a*) Variation of the flux density B with time after the d.c. magnetizing force has suddenly increased from 0 to H.

3(*b*) Variation with time of the magnetizing force H for linear growth with time of the flux density B (step-impulse of the coil voltage).

3(*c*) Variation with time of the reversible permeability after the d.c. magnetizing force has suddenly increased from 0 to H.

Material magnetized to saturation for a considerable time by a large d.c. magnetizing force H_s:—

3(*d*) Variation with time of the flux density B after the d.c. magnetizing force has suddenly decreased from H_s to H, particularly when $H = 0$ (remanence) or $H = —H_c$ (coercive force).

3(*e*) Variation with time of the reversible permeability after the d.c. magnetizing force has suddenly decreased from H_s to H, particularly when $H = 0$ (remanence) or $H = — H_c$ (coercive force).

Material magnetized to saturation for a considerable time by a large alternating magnetizing force H:—

3(*f*) Variation with time of the reversible permeability after sudden demagnetization (disaccommodation, temporary decrease in slope of small loops).

Since, in the region of large magnetizing forces, neither the theory of linear networks nor that of quasi-linear networks is available to relate the result of one experiment with a different one, a large number of experiments, each with new results, can be imagined and are, in fact, necessary, e.g. tests with two consecutive changes of the d.c. magnetizing force in the same direction (two-level step function) or in the opposite direction (impulse function).

Mr. A. C. Lynch:

The suggested types of residual loss may be summarized thus:—

Observed characteristics	Names		Suggested mechanism	References
strongly dependent on frequency and temperature	Richtersche Nachwirkung	traînage reversible	migration of foreign atoms through the lattice	Néel, 1951; Feldtkeller, 1953a; Dunton, 1953
nearly independent of frequency; slightly dependent on temperature	Jordansche Nachwirkung	—	thermal effects of magnetostriction	Zener, 1937; Polder, 1953
	—	traînage irreversible	thermal activation of domain-wall movements	Néel, 1951; Street, 1953; Barbier, 1953
—	—		effects of non-uniform flux distribution	Fairweather, 1953

The magnetostriction mechanism should disappear in Mumetal-type alloys; so any frequency-independent loss observed in them may be ascribed to thermal activation (except in so far as conditions are modified by any binder present in powder cores, as verbally suggested by Dr. Kornetzki).

Dr. D. Polder:

I feel that in a fundamental discussion on the physics of losses, the use of standard names may be extremely misleading unless we know very precisely what component of the losses we want to indicate. In order to obtain real understanding of the fundamental processes it is absolutely essential to describe in great detail the procedure by which the particular component has been isolated from the experimental loss data and, moreover, to investigate whether this procedure is at all significant. A classification which is useful from the practical point of view of characterizations of materials does not necessarily make sense as regards the physical interpretation of the observed facts.

10

FERROMAGNETIC RESONANCES, HYSTERESIS AND RESIDUAL LOSSES IN FERRITES AND METALS

F. F. Roberts

(Post Office Engineering Research Station)

Abstract: The Döring-Becker domain-wall resonance mechanism is essentially a special case of ordinary spin resonance in a thin sheet of the material. The wall-resonance frequency is simply related to the coercive force, and the wide distribution of local coercive-force magnitudes required to account for the Rayleigh loop hysteresis therefore implies a wide frequency range over which magnetic dispersion and absorption must occur.

1. INTRODUCTION

The subject of spin-precession resonance inside magnetic domains has been treated in detail by Kittel (1951) and Van Vleck (1951), while the domain-wall resonance effect has been examined theoretically by Döring (1948) and Becker (1951). The possibility of these two resonance mechanisms, together with their associated damping effects, has increased the scope for the physical interpretation of the experimental permeability/frequency characteristics found by various workers for both metals and ferrite materials. While it has been clear that domain-wall resonance must itself ultimately be ascribed to a precession-resonance effect, the connection between the two has not been obvious, and it is one object of the present contribution to point out a simple connection between them. The way in which this connection is established opens up further possibilities in the correlation of the frequency dispersion and the amplitude non-linearity of permeability. The so-called residual loss can be regarded, at least in part, as arising from a particular distribution of magnetic "barrier heights" and appears to be correlated with the Rayleigh loop mechanism as already understood. An additional mechanism to that of Néel (1950) thus seems to be possible for his "traînage".

2. DOMAIN-WALL RESONANCE AS A FORM OF SIMPLE PRECESSION RESONANCE

In an element of domain wall far from specimen or crystal boundaries and from inclusions or other imperfections, the spins are in a state of neutral equilibrium, the forces of magnetocrystalline anisotropy and of exchange just counterbalancing one another. Such a domain-wall element can be displaced slowly by an arbitrarily small externally-applied field, if the effects of neighbouring wall elements upon it can be neglected. As has been emphasized by Néel, the component of magnetization normal to the wall must, under equilibrium conditions, be constant through the wall cross-section from the

domain on one side to that on the other, and the local direction of magnetization in the wall thus rotates skew-fashion about the normal as one passes from one domain to the other. In the mid-plane of the wall the component of magnetization I_y parallel to this plane will have a direction $\bar{y}$ lying symmetrically between the two adjoining domain magnetization directions, and a magnitude in general less than the saturation value I_{sat} of the material. For our present purpose we neglect the constant normal component of magnetization and represent the domain wall by a sheet of small but finite thickness enclosing the mid-plane of the real wall and uniformly magnetized to the intensity I_y in the direction $\bar{y}$ parallel to its surface. Furthermore, we consider the effect of an external field h only in so far as it influences the spins contained in this thin sheet, that is, we neglect any incidental small spin rotations produced in all the spins inside the two adjacent domains. Under these conditions the components of magnetization parallel to the surfaces of the sheet in the two bounding domains are independent of h and may be neglected. Micro-eddy currents will likewise be neglected, although they would be present under dynamic conditions in the case of a metal or a high-conductivity semi-conductor. We shall thus consider, as the sole effect of importance in our present context, the influence of the applied field h on the component of the spins in the wall represented by I_y. For simplicity we shall suppose h to be in the plane of the sheet and perpendicular to $\bar{y}$.

Thus, when h is an alternating field, the spins in the sheet may be regarded as in the first place attempting to oscillate in the plane about the direction $\bar{y}$, but because of their gyroscopic properties they will be forced to precess about the direction $\bar{y}$, resulting in the appearance of an oscillating magnetization component normal to the sheet. The behaviour is then closely analogous to that discussed by Kittel in connection with the demagnetizing corrections in microwave gyromagnetic-resonance experiments, and the resonance frequency is given by

$$f_0{}^{disp} = 2{\cdot}8\sqrt{B_y H_y} \quad \text{Mc/s} \qquad \ldots(1)$$

where $B_y = H_y + 4\pi I_y$, if we assume substantially free electron spins without orbital interaction (the numerical factor 2·8 would otherwise be slightly different). In our present context the field H_y represents the constraining force acting on the spins in a given element of the sheet due either to neighbouring elements (equivalent surface tension of domain wall) or to the presence of crystalline imperfections in the region occupied by the element.

Thus we see that simple precession resonance of the spins within a single domain and the so-called domain-wall resonance of Döring and Becker are essentially different forms of the same general phenomenon, and it is at once clear why the wall-resonance frequency should normally be lower than

the simple precession-resonance frequency. For in the latter (neglecting specimen-shape or domain-shape anisotropy) we have the simple relation

$$f_0^{rot} = 2{\cdot}8\, H_{anis}\ \mathrm{Mc/s} \qquad \ldots(2)$$

where H_{anis} is the internal field representing magnetocrystalline anisotropy, and we assume there is no external static magnetizing field. Now H_{anis} is of the order of 100 Oe or more for pure materials, whereas H_y is of the order of the coercive force, and may thus be 0·1 Oe or less, while B_y, depending both upon the material and the type of domain wall concerned, may be of the order of 5000 gauss. Thus f_0^{rot} would be some 5 times f_0^{disp} in such a case. In the case of high-permeability alloys and mixed ferrites, the same general tendency for f_0^{rot} to exceed f_0^{disp} appears to prevail.

In order to check the agreement between our result (1) and that of the Döring-Becker theory, consider the case of a so-called 90° wall having the domain magnetizations parallel to the plane of the wall on each side, but with an angle of 90° between one another. (This may not in general be the type of 90° wall having lowest energy, but it is the simplest for our present purpose.) For such a wall we shall have

$$I_y = I_{sat} \qquad \ldots(3)$$

and I_y will lie along the internal bisector of the two domain magnetization directions. We assume that the wall is held in stable equilibrium in the absence of an external field by an internal field H_y parallel to I_y. Let an external static field h, small compared with H_y, be applied in the plane of the wall and perpendicular to H_y. The direction of the resultant field will then rotate by $\tan^{-1}(h/H_y)$ or approximately h/H_y radian, and the spins in the mid-plane of the wall will rotate by an equal amount in sympathy. If we assume that the effective wall-thickness is δ, over which the spin-direction in our case changes by 90°, then the rotation is equivalent to a wall displacement of

$$d = (h/H_y)\,(2/\pi)\,\delta \qquad \ldots(4)$$

Thus, if l is the distance apart of similarly-moving domain walls, the total magnetization averaged over the whole specimen in the direction of h changes by

$$(d/l)\,(I_{sat}/\sqrt{2}) \qquad \ldots(5)$$

and hence the initial magnetic susceptibility arising from the wall displacement is

$$\begin{aligned} \chi_0^{disp} &= (d/l)\,(I_{sat}/h\sqrt{2}) \\ &= (\delta/l)\,(I_{sat}/H_y)\,(\sqrt{2}/\pi) \qquad \ldots(6) \end{aligned}$$

If we insert H_y in terms of χ_0^{disp} from (6) in our relation (1) we obtain, making use of (3) and neglecting H_y in comparison with $4\pi I_{sat}$:

$$f_0^{disp} = 2{\cdot}8\sqrt{4\pi I_{sat}(\delta/l)\,(I_{sat}/\chi_0^{disp})\,(\sqrt{2}/\pi)}$$
$$= 2{\cdot}8\,.\,2^{5/4}\,.\,I_{sat}\sqrt{\delta/l}\sqrt{/1\chi_0^{disp}}\ \text{Mc/s} \qquad \ldots(7)$$

which differs from Becker's result only in having a factor $2^{5/4}$ in place of $\sqrt{\pi}$. This discrepancy arises in part from our over-simplified model of wall displacement in terms of χ_0^{disp} and in part from a difference in the type of 90° wall considered here as compared with that in Becker's discussion. In essence the two results are identical.

3. DISCUSSION

The expression of the domain-wall resonance frequency f_0^{disp} in the form of our relation (1) rather than in the Döring-Becker form (7) brings out the mechanism of the effect as no more than a special case of the better-known spin-precession resonance, and makes it clear that the dependence on δ/l apparent in (7) is accidental. It is of course true that δ and l and χ_0^{disp} will all be functions of the anisotropy, and of the density of lattice imperfections that also determine H_y. But H_y has a more direct experimental significance. As already noted, H_y arises from lattice imperfections, which may vary from gross inclusions of foreign matter visible to the naked eye to atomic dislocations extending their influence only over a small number of nearby cells of the crystal lattice. The magnitude of H_y effective for a domain-wall element will therefore vary according to the location and orientation of the element in the lattice. For some positions H_y will be negative, that is, oppositely directed to the sense that I_y would have if a wall could be located there, and such positions will obviously be unstable. Certain values of the externally applied field h will bring some wall elements to unstable positions, where H_y is going through zero. It is plausible (for example, on the assumption that some wall elements do not move at all, but happen to have their initial H_y oppositely directed to h) that the value of h required to cause such instability is comparable with the initial H_y value for the affected elements. This value of h may be termed the local coercive force for the element. From what has been said above, a wide distribution in magnitude of local coercive force is to be expected, and just such a distribution is required to account for the Rayleigh loop hysteresis behaviour of most ferromagnetics. Néel (1950) has introduced the further concept of thermal fluctuations in the local coercive force, and has shown that such fluctuations could lead to a magnetic loss angle nearly constant over a very wide (logarithmically) frequency range, corresponding to the " residual loss" actually observed in many ferromagnetics.

It now seems possible to put forward an alternative (or an additional) explanation of "residual loss", at least over part of the frequency range, making use of the same wide distribution of local coercive force and hence of our H_y, for this H_y distribution will lead directly to a distribution of f_0^{disp} and hence to dispersion of the magnetic permeability and a corresponding "absorption" over a broad frequency range. In this explanation, however, the precise shape of the dispersion and absorption characteristic will depend not only on the distribution of f_0^{disp}, but also, and probably to a major extent, on the frequency variation of the magnetic losses associated with the domain-wall resonance. On this account we should expect marked differences between the behaviours of ferromagnetic metals and ferrites, not only because of micro-eddy currents in the metals, but also because microwave resonance line-widths suggest that some other mechanism of strong spin-precession damping is present in the metals (Kittel, 1951 ; Van Vleck, 1951).

It is interesting to consider as a quantitative example, a high-permeability alloy having a coercive force $H_c = 0{\cdot}1$ oersted and $4\pi I_{sat} = 5000$ gauss. If we assume $H_y = H_c$, then equation (1) gives for the main wall-resonance frequency $f_0^{disp} \doteqdot 63$ Mc/s. Above this frequency the domain-wall contribution to the initial permeability must be negligible, but the rate of cut-off at lower frequencies will depend on the damping involved, as well as on the density distribution of local coercive-force values. If the Rayleigh hysteresis law is still valid down to a field as low as $0{\cdot}001\ H_c$, then there will be some domain-wall elements having resonance frequencies as low as about 2 Mc/s and therefore, given damping, showing absorption at frequencies down to perhaps a tenth of this.

While considerable evidence has accumulated of natural resonances of various kinds in the ferromagnetic ferrites, corresponding evidence for the metals is much more scanty. The most impressive of the latter is that of Wieberdink (1948, 1951) and Kronig (1948), who found a sharp resonance in a 60/40 Ni-Fe alloy wire at a frequency of about 300 Mc/s. The experimental techniques tend to become difficult with the metals at such frequencies on account of the small depth below the surface that can be explored and the possibility that this superficial layer may not be typical of the bulk metal. There is some possibility that a transmission technique described elsewhere (Roberts, 1953a) might be used to demonstrate wall-resonance effects in the interior of a specimen.

In the case of sintered polycrystalline ferrites, the work of Went and Wijn (1951) strongly suggests a distribution of f_0^{disp} over the kilocycle frequency range. The work of Galt et al. (1950) on single-crystal ferrite samples shows further that f_0^{disp} decreases to very low values at low temperatures, at least in the case of nickel ferrite. Unfortunately it is not known whether H_c varied in the same way for this specimen.

Acknowledgment is made to the Engineer-in-Chief of the Post Office Engineering Department for permission to make use of the information in this paper.

DISCUSSION

Dr. H. P. J. Wijn:

From this theory of the ferromagnetic resonance phenomena in ferrites it follows that the domain-wall resonance frequency should be proportional to the coercive force H_c of the ferrite. We have found that H_c for Ni-Zn ferrites can be varied by a factor of 4 by firing the ferrites at different temperatures. Nevertheless, the resonance frequency for the initial permeability remains practically constant. This suggests that the resonance found in ferrites (Wijn, 1953) is not related to domain-wall displacements.

Mr. F. F. Roberts (in reply):

The theory given relates primarily to material that is at least approximately monocrystalline. It might be applied to sintered polycrystalline ferrites either if each domain wall extended over a large number of crystallites and could move across them while preserving its identity, or if each domain wall had a well-defined existence only within a given crystallite. In the latter case, which seems the more probable, the externally measured H_c value for the bulk material would not be simply related to the internal H_c value involved in the theory, and one could not at once conclude from Dr. Wijn's experimental results that domain-wall effects may be dismissed from further consideration.

(*Further discussion relevant to this Paper appears on pages* 82-89.)

11

RELAXATION PHENOMENA IN CARBONYL IRON

T. A. Dunton

(The Mond Nickel Company Limited)

Abstract: The magnetic after-effects which occur in carbonyl iron are briefly reviewed together with the theory of the temperature-dependent after-effects. Measurements of the time-decrease of permeability at the remanence point of compressed powder-cores of C-type carbonyl iron show that two distinct modes of relaxation occur. The first mode is reversible and is characterized by a range of time-constants. Although this behaviour resembles that found in solid and laminated iron and silicon-irons, it is difficult to reconcile with the accepted theory of carbon and nitrogen diffusion, but this may be due partly to the high internal stress and small grain-size of compressed powders. The second mode, which becomes discernible after some days, is irreversible and is probably due to metallurgical ageing.

1. INTRODUCTION

When the magnetic field surrounding certain ferromagnetic bodies is rapidly changed, the magnetic conditions within the material do not instantaneously follow the changes, the delay being longer than can be accounted for by eddy currents. This additional time-lag or "after-effect" arises from more than one source and may extend, at room temperature, over times varying between milliseconds and days. Under alternating conditions short-time after-effects are reflected as losses in the associated electrical circuits.

There are two main types of after-effect, characterized by their relationship to frequency and temperature.

(*a*) Richter after-effect is strongly temperature-dependent and its associated loss angle varies markedly with frequency, the curve relating loss angle to frequency having the shape of a Gaussian curve. This form of after-effect, which occurs only in certain materials, obeys the principle of superposition.

(*b*) Jordan after-effect is always measured under alternating conditions, and the associated losses are often called "residual" losses, since they cannot be accounted for by hysteresis or eddy currents. These losses are independent of the temperature and depend only slightly on the frequency.

There is a further form of after-effect, known variously as "time-decrease of permeability", "disaccommodation", or "after-effect of the permeability" which is possibly another aspect of Richter after-effect; this appears as an increase in the initial permeability each time the magnetic field is changed, followed by a gradual decrease to an equilibrium value.

2. MAGNETIC AFTER-EFFECTS IN SOFT CARBONYL IRON

The first observations of magnetic after-effect were those of Ewing (1885) and Rayleigh (1887) on iron. They both found that the effect was most conspicuous in very soft well-annealed iron. It was to these and other early magnetometric measurements (Tobusch, 1908) that Jordan (1924) referred in support of his assumptions that a certain proportion of the energy losses occurring in iron wires situated in an alternating field were due to after-effects. Jordan also found that these losses were greater in iron than in steel wires, by a factor of three. The most exhaustive work on the after-effect in carbonyl iron and its dependence on the magnetic and metallurgical condition was carried out by Richter (1937) and by Schulze (1938), the former using ballistic and magnetometric methods, while the latter made measurements in the frequency range 60 to 5000 c/s.

After a change in the magnetic field, change of induction with time may be represented by an exponential law with a range of time-constants, i.e. by an equation of the form

$$B = B_0 \int_0^\infty \frac{g(\tau)\ \exp\ (-t/\tau)}{\tau}\ d\tau$$

Satisfactory agreement with experimental results may be obtained if the distribution of time constants, $g(\tau)$, is considered as constant and equal to $1/(\ln \tau_2/\tau_1)$ between the limits τ_1 and τ_2 and equal to zero outside these limits. When measurements are made under alternating-current conditions the loss angle due to the after-effect is given by

$$\tan \delta = \{K/(\ln \tau_2/\tau_1)\} \{\tan^{-1} \omega\tau_2 - \tan^{-1} \omega\tau_1\} \qquad \ldots(1)$$

where K is a constant and ω the angular frequency. It has a maximum at $\omega_m = 1/\sqrt{\tau_1\tau_2}$. The ratio τ_2/τ_1 is about 20 to 30 for carbonyl-iron strip.

The relationship between after-effect and temperature may be obtained by writing the time constant, τ, related to one particular point on the decay curve, as

$$\tau = \tau_0 \exp(-Q/RT) \qquad \ldots(2)$$

where Q is an energy of activation. Richter obtained a value for Q of 20 000 cal/mole, which was in close agreement with the activation energy associated with mechanical after-effect.

From equations (1) and (2) it may be seen that if $\tan \delta$ is plotted against the temperature with the frequency as parameter, a family of bell-shaped curves results, the height of which is a measure of the after-effect. These curves will be superimposed upon the temperature-independent Jordan after-effect. Schulze found that the relationship between the angular frequency, ω_m, and the temperature at which the maximum loss occurs, i.e.

$\log \omega_m = \text{const} - Q/RT$, gives a value for the activation energy, Q, equal to that found by Richter.

That the Richter after-effect is a property not only of the material but of its condition was demonstrated by Schulze. In the "as-rolled" state, in which the metal has suffered 90% reduction, frequency-dependent after-effect (measured at $H = 0, B = 0$) does not occur but only Jordan after-effect. After heating in hydrogen for two hours at 450°C, although crystal recovery takes place, no Richter after-effect is apparent. Upon heat-treatment in hydrogen at higher temperatures the Richter after-effect then progressively increases together with recrystallization. If the material, fully recrystallized at 1000°C, is worked, the Richter after-effect decreases and becomes zero at about 2·3% deformation. At the remanence point the Richter after-effect is only about one-quarter that of the original recrystallized material; it can be increased slightly by a demagnetizing treatment but can be fully restored only by a short heat-treatment at 450°C or above.

The Jordan after-effect remains substantially the same in all conditions.

The third type of after-effect, time-decrease of permeability, also occurs to a marked extent in massive carbonyl iron, as has been demonstrated by Snoek (1938), who also showed that this time-decrease and Richter after-effect are but two aspects of the same phenomenon. He ascribed this phenomenon to the elastic after-effect existing in the 180° boundaries separating the domains, the coupling between the magnetic and elastic effects being the local magnetostrictive strain. If, after a magnetic disturbance, the domain boundary loses potential energy in the course of the material adapting itself to the local strain, then, at low temperatures, the decay of permeability may be written, in terms of reluctivity, as

$$r = r_1 + r_2 \{1 - \exp(-t/\tau)\} \quad \ldots(3)$$

where r_1 is the restraining force due to the permanent strains and r_2 is the additional force required for the boundary to be in equilibrium. At higher temperatures, since the time constant is related to temperature by equation (2), the permeability decays so quickly that no delay is observed, and in its place Richter after-effect is found, which may be expressed by an equation analogous to (3), i.e.

$$\mu = \mu_1 + \mu_2 \{1 - \exp(-t/\tau')\}$$

where

$$\mu_1 = 1/(r_1 + r_2), \quad \mu_2 = 1/r_1 - 1/(r_1 + r_2) \text{ and } \tau' = \tau(r_1 + r_2)/r_1.$$

r_1 is not constant throughout the material; thus, although the time-decrease of permeability may be expressed in terms of a single relaxation time, magnetic after-effect will involve a distribution of time constants, since

r_1 occurs in the power of the exponential. On laminations of well-annealed carbonyl iron Snoek found a time constant of 250 seconds at $-24{\cdot}6$°C and 1460 seconds at $-36{\cdot}6$°C, giving a value of $Q = 17\,000$ cal/mole which agrees reasonably well with that found by Richter.

The metallurgical cause of time-decrease of permeability is impurity atoms of carbon and nitrogen. This has been demonstrated (Snoek, 1939) by subjecting the iron to a high-temperature heat-treatment in moist hydrogen, after which the material shows no disaccommodation. Upon the reintroduction of a very small quantity of carbon or nitrogen (as little as 0·008%), the effects reappear.

To explain the mechanism by which the impurity atoms cause elastic after-effect, and through it magnetic after-effects, Snoek developed a geometrical lattice theory in which it is assumed that the impurity atoms are situated in the octahedral sites of the body-centred-cubic α-iron lattice. In the unstrained condition, since the x, y and z positions are crystallographically equivalent, the foreign atoms will be evenly distributed over these three positions and there will be an equal exchange of places under the action of thermal forces. If, however, the lattice is elastically stretched, for instance, in the z direction, the $0, 0, \frac{1}{2}$ and the $\frac{1}{2}, \frac{1}{2}, 0$ positions will be preferentially occupied, since the external loading will thereby be countered. Elastic after-effect, and hence magnetic after-effect, and time-decrease of permeability are explained, therefore, by an interchange of places over distances of the order of the lattice parameter. Thus, being dependent upon a diffusion process, after-effects will be strongly influenced by temperature, according to equation (2). From a knowledge of the diffusion rates of carbon and nitrogen and τ_0, the diffusion path-lengths are calculated as $2{\cdot}3 \times 10^{-8}$ cm for carbon and $0{\cdot}86 \times 10^{-8}$ cm for nitrogen, which are of the order of the dimensions of the crystal lattice and in keeping with the theory.

Fahlenbrach (1948) has investigated the time-decrease of permeability, measured over a period of 10 minutes at temperatures ranging from -200°C to the Curie point. He found that in both soft iron and in carbonyl iron an after-effect occurred between 500°C and 700°C with perhaps an additional region in carbonyl iron between 300°C and 500°C. It has been suggested (Snoek, 1950) that this after-effect is the result not of diffusion of impurities but of elastic relaxation caused by grain-boundary slip.

3. TIME-DECREASE OF PERMEABILITY AT THE REMANENCE POINT IN COMPRESSED C-TYPE CARBONYL-IRON POWDERS

For some applications of magnetic materials, e.g. cores for use in telephone loading coils, the permeability should be little affected by a transient polarizing field (C.C.I.F., 1938). The change in permeability, which is in effect the difference between the initial permeability and the incremental permeability at the remanence point, is often termed magnetic instability. During an

investigation of instability of carbonyl-iron powder-cores we have studied the variation with time of the permeability after the core has suffered transient polarization. The materials tested were C-type carbonyl-iron powders containing about 0·05% carbon and 0·02% nitrogen, and having mean particle diameters of about 5 microns. After decarburizing, the slightly sintered powders were lightly ball-milled to powder form, insulated with 0·8% by weight of a cellulose lacquer, heat-treated at 125°C for 16 hours and pressed to form toroids of 4 cm mean diameter and 1 sq. cm cross-section. For most cores, the pressure used was 96 tons/sq.in. and all cores were heated at 100°C for 24 hours to consolidate them. The measuring field-strength was 15 mOe but, because of the demagnetizing factor, the true internal field-strength was much lower.

4. EXPERIMENTAL RESULTS

The course of permeability with time, after applying a polarizing field of 92 Oe for 5 seconds, is illustrated in Figure 1, for a sample having the composition 0·012% C, 0·016% N_2, 0·002% S, 0·25% O_2. The general shape of the curve is that of an exponential decay, but it cannot be charac-

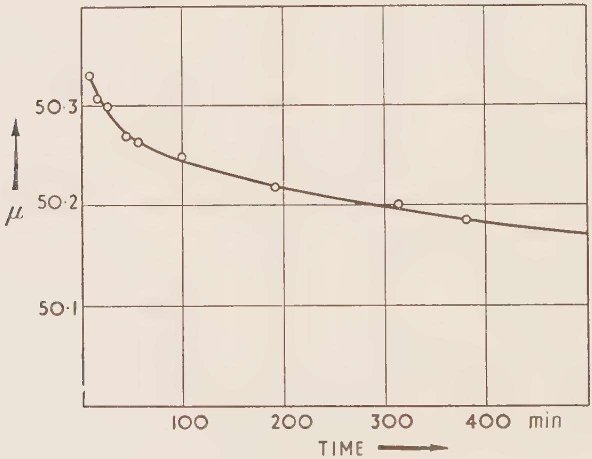

Figure 1. Variation of permeability with time after transient polarization.

terized by a single time of relaxation. There is a rapid fall in permeability over the first hour and then the curve flattens considerably, but even after several days the permeability continues to fall. The results at room temperature are shown again in Figure 2, together with curves obtained by measurement at 37°C and at 0°C, the ordinate now being the percentage change from the initial, i.e. the 5-minute, value. At all temperatures the

first portion of the curves is similar, the rate of change of permeability being slightly lower at the higher temperatures.

At 20°C, after some two or three thousand minutes, instead of approaching

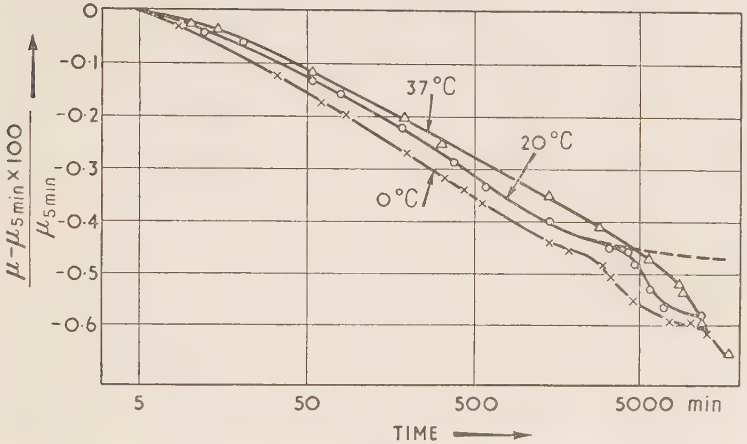

Figure 2. Variation of permeability (as percentage) at various temperatures after transient polarization.

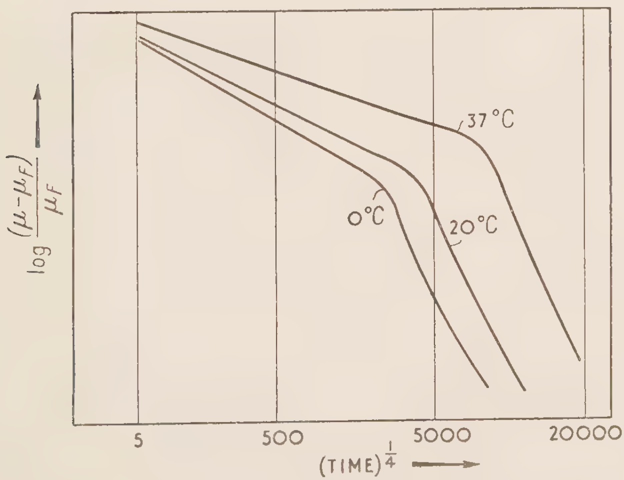

Figure 3. Permeability after polarization plotted against $(\mathrm{time})^{\frac{1}{4}}$.

some equilibrium value as indicated by the extrapolated dotted line, the permeability continues to fall and does not reach a final value until later. The same effect can be discerned at the other temperatures. The discon-

tinuity in the gradual decrease of permeability can be shown more distinctly by a plot of log $(\mu - \mu_F)/\mu_F$ against $t^{\frac{1}{2}}$ where μ_F is the final permeability (Figure 3). This is a rather arbitrary method of presentation, derived from an expression of the type $(\mu - \mu_F)/\mu_F = A \exp(-Bt^n)$ which has been used in the past (Webb and Ford, 1934) to express the course of time-decrease of permeability. It thus appears that there are two courses of time-decrease having widely different relaxation characteristics. The time at which the second fall becomes prominent increases with the temperature.

Figure 4 illustrates the behaviour of the permeability on a further application of the polarizing field. The core was polarized and the permeability

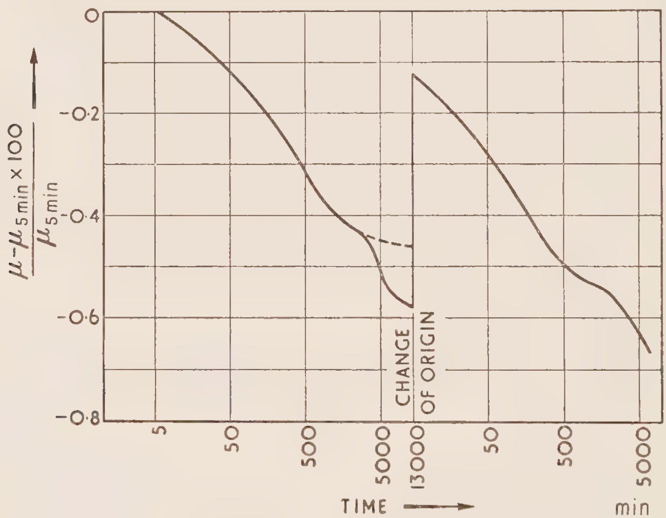

Figure 4. Percentage change in permeability with time after a first and a second polarization.

plotted over 9 days, by which time it had fallen by 0·58%. After a second polarization the permeability increased by 0·46%, and thus did not return to its original value; the difference is equal, within experimental error, to the difference between the extrapolated value of the first part of the curve and the value actually measured after 13 000 minutes. The shape of the decay curve after the second polarization is similar to that after the primary polarization. It may be considered that the decrease of permeability with the shorter relaxation time is reversible, whereas the longer time-decrease is not. If the material suffers a second polarization shortly after the first, the permeability again reaches its initial maximum.

Although the main interest in this work has been concerned with the behaviour of the incremental permeability at the remanence point, some powder-cores have been demagnetized by a decreasing alternating field from the same peak value of 92 Oe, and it has been found that the magnitude of the decrease, measured after 72 hours, is the same as that at the remanence point. The effect of successive polarization and demagnetization is presented in Figure 5. Again it is seen that the high permeability obtained after the primary magnetization is not repeated.

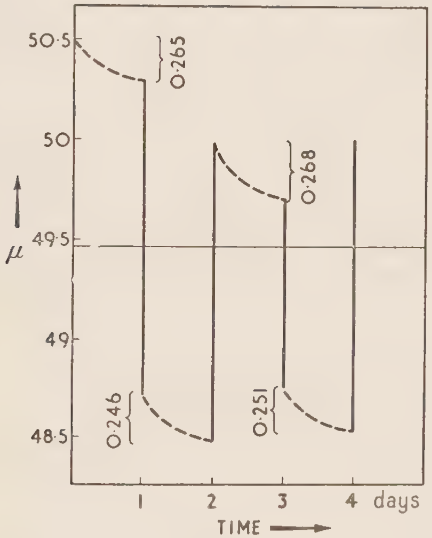

Figure 5. Permeability/time curves on successive polarization and demagnetization.

Time-decrease of permeability is stated to be caused by mechanical as well as by magnetic shocks, but with carbonyl-iron powder cores the effect was comparable with the experimental error. Since powder-cores are mechanically weak the vibration could not be very severe, but nevertheless it was much greater than that which cores would undergo in normal handling. Similarly, vibrating a core after it had been magnetically shocked had little effect upon the magnitude of the decrease after 72 hours.

Although 100 tons/sq.in. is quite a common moulding pressure for powder-cores, such high pressures are not always used; measurements have therefore been made on cores formed under a series of moulding pressures. An example of the results obtained is presented in Table 1.

Table 1. Effect of moulding pressure on the time-decrease of permeability

Pressure, tons/sq.in.	Permeability	Time-decrease of permeability, %
24	20·5	0·33
36	27·5	0·39
48	35·7	0·47
60	39·1	0·52
72	43·8	0·60
84	47·0	0·61
96	49·7	0·58

Here the permeability change after 72 hours increases with the moulding pressure up to about 70 tons/sq.in. and then remains constant. In their application, powder-cores can often be considered as homogeneous bodies with inherent physical properties, but the interpretation of the behaviour of powder-cores must be in terms of the properties of the ferromagnetic component. There are a number of theoretical relationships which are qualitatively confirmed in practice, between core permeability μ, particle permeability μ_m, and packing fraction p (Howe, 1946; Colombani, 1950). Howe has derived the expression

$$\mu = \frac{\mu_m - 2(1-p)(\mu_m - 1)/3}{1 + (1-p)(\mu_m - 1)/3}$$

which gives upon differentiation and assuming $\mu_m \gg 1$,

$$\frac{d\mu}{\mu} = C\frac{d\mu_m}{\mu_m}$$

where $C = \dfrac{9p}{(1+2p)\{3 + \mu_m(1-p)\}}$ and increases with p.

Thus the time-decrease of permeability should be augmented by an increase in the forming pressure. Since, from the figures in Table 1 for pressures above 70 tons/sq.in., the percentage decrease of core permeability is constant, the percentage decrease in the particle permeability must have fallen.

Materials have been tested which have had carbon and nitrogen contents ranging from 0·08% to less than 0·001%. Although for these samples the time-decrease of permeability has not been equal, no strong correlation has been found with the percentage of carbon, nitrogen or any other impurity elements. Heat-treatments of the powders in inert gases or in vacuo at temperatures up to 500°C prior to pressing have similarly had little effect.

5. DISCUSSION OF RESULTS

Although magnetic after-effects have been observed for some years, there are as yet no complete explanations of all the types in their various aspects; in particular, the Jordan after-effect is little understood. It seems reasonably certain that, within restricted temperature ranges, carbon and nitrogen cause temperature-dependent magnetic after-effect and the allied time-decrease of permeability in carbonyl iron, though, as Néel (1951) has pointed out, the manner in which these atoms affect the domains and their boundaries may not be as first visualized by Snoek.

The results reported here show that the time-decrease of incremental permeability is mainly a function of the reversible permeability, since the amplitude is almost the same at remanence ($\Delta\mu = 0{\cdot}267$) as in the demagnetized condition ($\Delta\mu = 0{\cdot}248$). It is thus of the Richter type and not of the type dependent upon irreversible magnetic changes which has been investigated by Street and Woolley (1949a, 1949b), Maeda (1950a, 1950b) and others. The changes of permeability with time, however, though having the general characteristics of previously published results on solid and laminated carbonyl iron and silicon-irons, differ in detail and cannot be conveniently explained on the theory developed by Snoek. The first obvious difference between the previous work and that reported here is the time constant; with massive carbonyl-iron samples it has been found to be of the order of seconds at room temperature whereas we have found it to be of the order of 10^4 seconds. Furthermore, the time-constant does not take a single value at each temperature, neither do the time-constants move rapidly towards smaller values as the temperature is increased; on the contrary, the mean time-constant tends to increase with temperature. If, therefore, the increase of permeability after a change in the magnetic field is caused by the presence of carbon and nitrogen atoms, then the subsequent decrease with time is not solely dependent upon diffusion of these atoms. Silicon-irons, as measured by Webb and Ford (1934), give relaxation times of the order that we have found, but again the details differ since the effect has not now been found to be dependent upon the time of application of the measuring current, nor has the amplitude of the time-decrease been found to decrease rapidly with rise in temperature.

Snoek's hypothesis is that the iron lattice is in an essentially stress-free condition before the application of the disturbing magnetizing field, which is far from the initial condition in compressed powder-cores, since internal stresses within the particles equivalent to stresses of tens of tons/sq.in. have been measured (Taylor, 1953). These strains certainly modify the usual magnetic properties of materials, preventing for instance the free movement of the domain boundaries, with a consequent lowering of the permeability. It is to be expected that they will also influence after-effects. A further difference between compressed powders and massive materials is the difference

in grain size, the crystal size of the powder being less than 2000 Å. From the work of Schulze it appears that grain size considerably influences the degree of after-effect. Thus, in rolled strip where the crystals are very small, there is no frequency-dependent after-effect and it only arises with the onset of recrystallization. The small amplitude of the time-decrease, compared with that obtained on massive samples, if the time effects arise from the same cause, is therefore probably due to the high internal strains and small crystal size of the particles. This is confirmed by the fact that as internal stress is increased by raising the compacting pressure the time-decrease of the particle permeability is reduced.

Although it is difficult to account for time-decrease of permeability in terms of carbon and nitrogen diffusion, yet, if the origin of the effect lies in the presence of these atoms in solution in the α-iron, the degree will not be expected to vary much until the carbon and nitrogen contents are reduced to about the limit of solubility, which will probably be very low in heavily strained material. We found that on reducing the content of these elements the material becomes more deformable and hence has a higher permeability and time-decrease, and although materials with carbon contents below 0·001% have been tested no point has been observed at which the trend is reversed.

The second stage of the permeability decay probably arises from metallurgical ageing. Measurements made on unpolarized cores show a slight fall of permeability with time, but the main evidence for ageing is that upon a second application of the polarizing field, after a time long enough for this decay to have taken place, this second loss of permeability is not recovered, indicating that permanent changes have occurred in the material.

The above work was carried out in the laboratories of The Mond Nickel Co. Ltd., to whom the author is indebted for permission to publish this paper.

DISCUSSION

Mr. C. E. Richards:

The time-decrease in permeability of powder-cores is shown to be temperature-dependent and to have a constant of 10^4 seconds compared with a few seconds for massive iron. Can this in any way depend on the plastic binder flowing because of magnetostriction pressure, and only allowing a slow return to normal when the magnetic substance tries to resume its original shape ?

Mr. Dunton (in reply):

It is unlikely that flowing of the plastic binder under the action of magnetostrictive pressures can account for the observed effects. Under extreme conditions when all the magnetostrictive strain is directed towards reducing the air gaps, that is, when the core retains its original shape, the change of permeability will not be greater than 0·03%. If any change of shape occurs, the change in permeability will be less than this value. Any slow return of the plastic to its equilibrium position could therefore only account for a very small part of the total observed permeability change.

(*Further discussion relevant to this Paper appears on page* 86.)

12

RICHTER-TYPE AFTER-EFFECT OF THE PERMEABILITY IN SILICON-IRON LAMINATIONS

R. Feldtkeller

(Technische Hochschule, Stuttgart)

Abstract: The Richter after-effect depends, as Snock has shown, on relaxed movements of carbon atoms within the crystal lattice. It is better to define the Richter after-effect in terms of the reciprocal of the complex impedance rather than the complex impedance itself or the loss factor. The intensity and spread of the relaxation times is independent of temperature, but the mean relaxation-time is strongly temperature-dependent. In all cases so far investigated, the Richter after-effect is accompanied by a limiting of the initial field strength for the smallest Barkhausen jumps and an anomalous hysteresis-free increase of permeability with the amplitude of the a.c. field.

1. THE PHYSICAL ORIGIN OF RICHTER AFTER-EFFECT

The elements oxygen, nitrogen and carbon form solid solutions with the crystal lattices of α-iron and γ-iron. In the α-lattice, only two types of inclusion positions are available to the foreign atoms—the mid-points of the edges*, and the mid-points of the tetrahedra formed by two corners and two cell mid-points. Only the foreign atoms at the mid-points of the edges can make a contribution to the Richter after-effect.

If the material is unmagnetized and free from stress, the foreign atoms will distribute themselves irregularly along the three edge-directions. The individual included atoms are practically independent of each other, since only a few hundredths of one per cent are soluble in α-iron.

Figure 1. Foreign atoms in the α-lattice seek, for vertical extension, the mid-points of the vertical edges (or horizontal faces).

If the lattice is stretched in the vertical direction, the energy of the foreign atoms on the vertical edges is reduced and that of those on the horizontal

* These are equivalent to mid-points of surfaces. For consider the body-centred lattice as made up of two interpenetrating cubic lattices: then the mid-points of the edges in one lattice are the mid-points of the surfaces in the other lattice.

edges is increased, so the foreign atoms will seek the vertical edges (Figure 1). This change of position obeys the probability laws of thermodynamics, and therefore occurs more rapidly as the temperature is increased. The waiting time of a foreign atom, from the moment of stretching, is called the relaxation time. For two absolute temperatures T_1 and T_2, the relaxation times τ_1 and τ_2 are given by

$$\tau_1/\tau_2 = e^{-U/kT^1}/e^{-U/kT^2}$$

If the relaxation time τ_∞ refers to temperature $T = \infty$,

then $\tau = \tau_\infty \, e^{-U/kT} = \tau_\infty \, . \, e^{-\theta/T}$

U/k, or θ, is called the activation temperature and, for carbon and nitrogen in α-iron, it lies between 9000 and 10 000°K. Between room temperature and 100°C, the relaxation time falls to about a thousandth part.

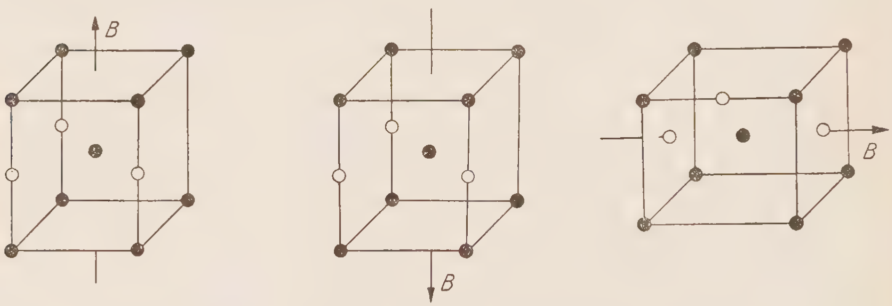

Figure 2. Change of magnetization through 180° causes no change of position, but if through 90° causes the foreign atoms to change their positions.

From our knowledge of magnetostriction we can assume that, in a spontaneously-magnetized Weiss domain, the foreign atoms will lie preferentially along the cube edges which are parallel to the direction of spontaneous magnetization. If we reverse the direction of spontaneous magnetization by means of an external field, all the foreign atoms can remain in their places; but if the direction of magnetization is rotated through 90°, they will change position after the relaxation time has elapsed, and seek edges of the cube which lie parallel to the new direction of magnetization (Snoek, 1947, p. 46).

Bozorth and his colleagues have shown that in silicon-iron both 180° and 90° domain-boundaries are present (Bozorth, 1949; 1951, p. 537). Figure 3 shows in principle how these boundaries come together. The domain boundaries are held quasi-elastically in this formation by mechanical stresses and small inclusions of foreign matter.

If the induction is changed by a fixed amount ΔB, by a field directed from bottom to top, the boundaries will shift to the right into the position

shown by the dotted line. The flux between the old position and the new one will change its direction. In the inclined strips, the change will be 180° and in the central shaded rectangle it will be 90°. The energy which is necessary to maintain this shift is made up of the following parts:—

(*a*) The energy necessary to shift the inclined 180° boundaries to the right against their elastic bonds to the rest position.

(*b*) The energy necessary to shift the vertical 90° boundary to the right against its elastic bond to the rest position.

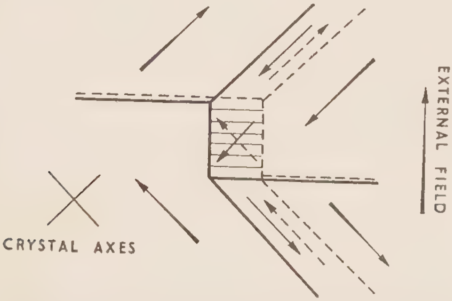

Figure 3. Positions of the domain boundaries before and after a change of magnetic flux.

(*c*) The energy necessary to rotate the direction of magnetization of the shaded region through 90° from the preferred direction set up by the inclusion of foreign atoms. This force component disappears after the relaxation time when the foreign atoms have taken up their new positions in the lattice.

We thus obtain the graph of induction and field strength shown in Figure 4.

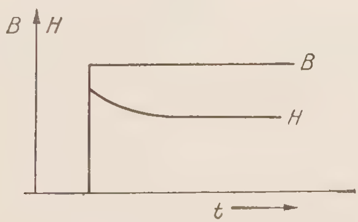

Figure 4. A jump in flux-density results in a jump in field-strength, followed by a fall to a lower value.

This transition of the field strength from the height of the peak to the low final value was discovered by Richter (1938), and was named Richter after-effect.

If the induction B is caused to jump rapidly up and down, the field strength makes large jumps because the foreign atoms have no time to change their positions. If, however, the jumps of induction follow each other sufficiently slowly for the foreign atoms to complete their change of position, then the mean amplitude of the alternating field becomes smaller (Figure 5). On changing to a sinusoidal change of induction, a large variation of field strength, i.e. a large value of $1/\mu$, is found at high frequencies, whilst at

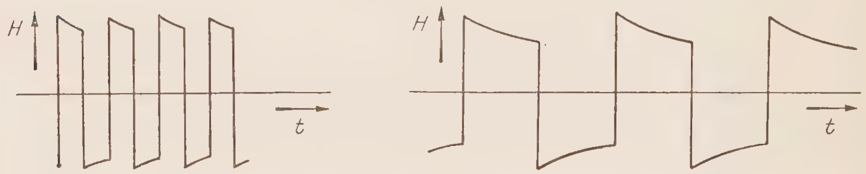

Figure 5. Variation of field-strength for fast and slow alternations of flux density.

low frequencies, the variation of field strength is small, corresponding to a small value of $1/\mu$. The transition from high to low frequencies is accompanied at medium frequencies by a phase difference between induction and field strength. $1/\mu$ here becomes complex. The properties of Richter after-effect can be particularly well studied by measuring the complex permeability and plotting its reciprocal (Schulze, 1938).

2. GRAPHS OF THE RECIPROCAL OF THE COMPLEX PERMEABILITY

If the graphs of the complex permeability $\mu = \mu_{LR} - j\mu_{RR}$ and its reciprocal $1/\mu = 1/\mu_{LP} + j1/\mu_{RP}$ are obtained by means of an a.c. bridge and are freed from the influence of hysteresis and eddy currents by calculation, the curves of Figure 6 (Wilde, 1949) are obtained. The curves of the reciprocal are obviously simpler to discuss than the curves of the complex permeability itself, since they differ in form only by a parallel shift along the ordinate axis although their frequency scale varies widely.

Looking at Figure 3 again, the narrow strips in which the direction of the flux changes have parts in which it changes through 180° and parts in which it changes through 90°. These parts lie magnetically in cascade and not parallel to one another. By the rules of magnetic circuits, the magnetic stress in this case is obtained from two summations. The first summation $\Sigma l_{180°}\Delta B/\mu$ is taken over the region in which the flux direction jumps through 180° and is independent of time. The second summation $\Sigma l_{90°}\Delta B/\mu(t)$ is taken over the region in which the flux direction jumps

only through 90° and depends on time as a result of the position-change effect of the foreign atoms. We thus obtain the apparent permeability as

$$\frac{1}{\mu^*}=\frac{1}{\mu}\,\frac{\Sigma l_{180°}}{l}+\frac{1}{\mu(t)}\,\frac{\Sigma l_{90°}}{l}$$

From this it is understandable that the curves of $1/\mu$ are simpler than those of μ.

We obtained the curves by extrapolation to zero field-strengths. They refer thus to the initial permeability and so to the quasi-elastic movements of the domain boundaries and not to Barkhausen jumps. They thus obey the basic laws of linear a.c. theory, namely the simple superposition law, the laws of conformal representation which govern the relationship between the real and imaginary parts of a complex quantity, and finally the well-known relationships between time functions and frequency functions. It is thus immaterial, in principle, whether the Richter after-effect is obtained by pulse experiments or by measurements at various frequencies. The frequency response method is easier because it is simpler to carry out measurements over a wide frequency range than over a wide time range. Speaking practically, it is possible to measure a quantity between 10 c/s and 10 kc/s and to plot a graph. It is hardly possible, however, to obtain and to reproduce in a paper an oscillogram which enables effects to be recognized which may last 10 milliseconds or 10 seconds.

3. INITIAL PERMEABILITY

We denote by initial permeability the value assumed by the permeability for negligible field strength and negligible eddy currents. It is obtained by extrapolation of the measured values to zero field-strength and by elimination of the effects of eddy currents by calculations. One obtains then, not a single value, but a curve of the form shown in Figure 6. It runs from the *relaxed initial permeability* μ_{a0} at which the curve starts on the ordinate axis for the frequency $f=0$, to the *unrelaxed initial permeability* $\mu_{a\infty}$ at which the curve ends on the axis again for $f=\infty$.

The relaxed initial permeability is determined by the mechanical stresses and small inclusions of foreign matter which bind the domain boundary quasi-elastically in its position of rest (Kersten, 1943b). The unrelaxed initial permeability is smaller because, in the regions in which the flux direction rotates through 90°, the foreign atoms wait in their old positions in the lattice and do not respond to the new flux direction until the relaxation time has elapsed.

The transformer laminations which were investigated had, at room temperature, a relaxed initial permeability of $\mu_{a0}=455\mu_0$ but an unrelaxed

initial permeability of $\mu_{a\infty} = 310\mu_0$. The relaxed initial permeability is thus 50% greater than the unrelaxed initial permeability, a sign that the Richter after-effect is of appreciable magnitude.

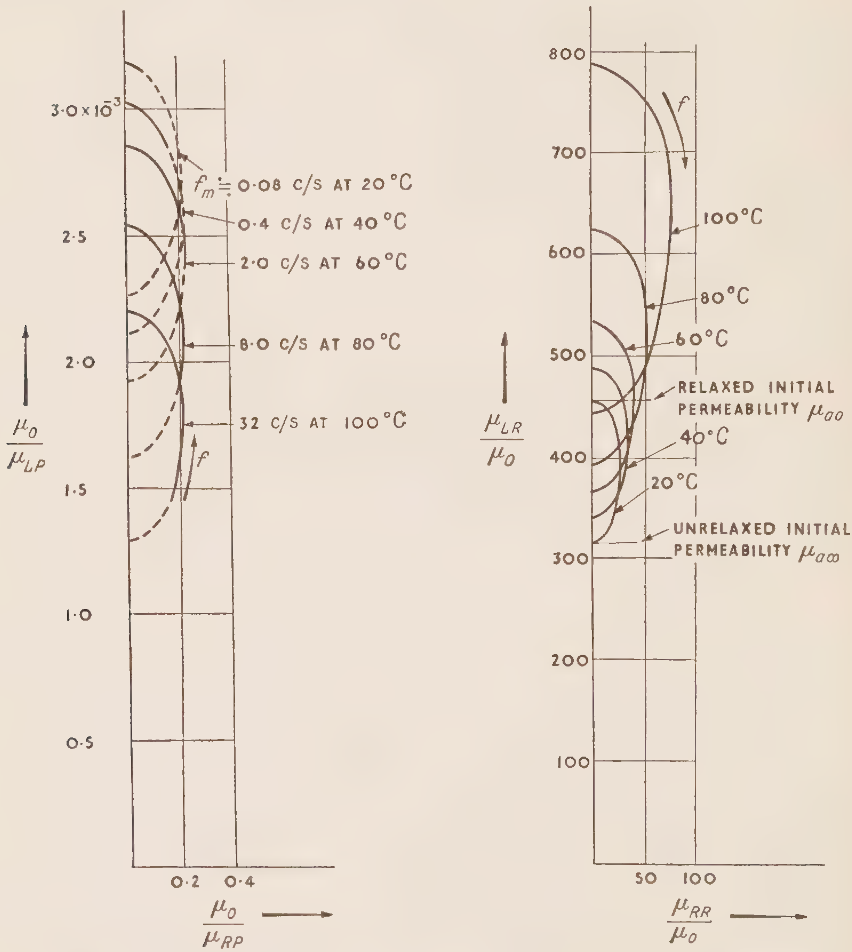

Figure 6. Curves of complex impedance and its reciprocal, for Richter after-effect.

4. TEMPERATURE-DEPENDENCE OF THE INITIAL PERMEABILITY

Between 20 and 100°C the relaxed initial permeability μ_{a0} increases by $325\mu_0$ from $455\mu_0$ to $780\mu_0$. In the same temperature range the unrelaxed initial permeability $\mu_{a\infty}$ increases by only $130\mu_0$ from $310\mu_0$ to $440\mu_0$. It would be wrong, however, to conclude, from the difference between the

increases of the two initial permeabilities, that the intensity of the relaxation effects on which the Richter after-effect depends is a function of temperature. We can discuss the Richter after-effect only in connection with the reciprocal of the permeability, not the permeability itself.

From Figure 6 we see that the reciprocals of the relaxed and unrelaxed initial permeabilities differ by a *temperature-independent* value of $1{\cdot}0 \times 10^{-3}$ $(1/\mu_0)$ and we can thus conclude that the intensity of the Richter after-effect is independent of temperature.

The unrelaxed initial permeability $\mu_{a\infty}$ of the transformer lamination investigated had a flat minimum at about 0°C and was $800\mu_0$ at a temperature of −50°C.

5. DISTRIBUTION OF RELAXATION TIMES

The theory of after-effect gives, with respect to the intercepts of the complex curves on the ordinate axis, a singly infinite family of curves if one assumes that the distribution of the relaxation times follows a Gauss error curve about their mean value. A parameter of this family of curves is the degree of scatter of the relaxation times. Thus the scatter can be obtained from the form of the curves.

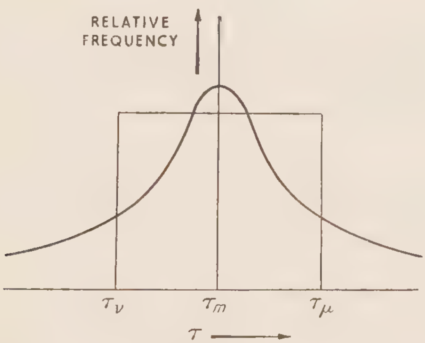

Figure 7. Distribution curve of the relaxation-times and its approximation by a rectangle.

To define the scatter we use the rectangle which best approximates to the distribution curve and encloses the same area as the latter (Figure 7) (Feldtkeller, 1950). The scatter can then be clearly defined by the ratio τ_μ/τ_ν. By comparing the measured curves with the calculated family of curves, the transformer lamination investigated is found to have a Richter after-effect value of $\tau_\mu/\tau_\nu \doteqdot 10^3$. To this ratio belongs not only a definite form of curve but also a definite frequency scale. We can thus compare not only the shapes of the calculated and measured curves but also the frequency scales and, if

both agree well with each other, then we shall have more confidence in the conclusions drawn from the measurements. Unfortunately there is no physical explanation for this large scatter of relaxation times.

6. TEMPERATURE RESPONSE OF THE RELAXATION TIMES

The curves of the reciprocal of the complex permeability in Figure 6 have the same form at different temperatures and also the same frequency scale if the frequency is expressed in terms of the mid-frequency of each curve. We can conclude from this that the scatter of the relaxation times is independent of temperature and that only the mean relaxation time τ_m varies with temperature.

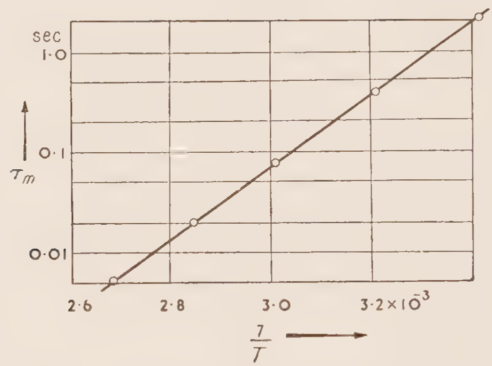

Figure 8. The mean relaxation-time τ_m plotted against reciprocal of absolute temperature.

This mean relaxation time τ_m is the reciprocal of the mean angular frequency ω_m of each curve. We can thus obtain the mean relaxation times simply from Figure 6. If we express them on a logarithmic scale over the reciprocal of the absolute temperature T, we obtain the straight line shown in Figure 8, as we might have expected from the above-mentioned formula $\tau = \tau_\infty \,.\, e^{-\theta/T}$ for the relaxation times of position-change effects.

The slope of the straight line gives the activation temperature $\theta = 9600°$K. The ordinate axis intercept gives the relaxation time $\tau_\infty = 1{\cdot}85 \times 10^{-14}$ sec, from which the mean diffusion path can be estimated as about $2{\cdot}5 \times 10^{-8}$ cm by assuming a value of $D = 20 \times 10^{-3}$ cm^2/sec for the diffusion constant, as measured for carbon in α-iron. These figures confirm the physical explanation of the Richter after-effect.

7. TEMPERATURE RESPONSE OF RICHTER AFTER-EFFECT

To describe the temperature dependence of the Richter after-effect clearly and quantitively, it is best to draw the curves of the inverse of the complex permeability for two or more temperatures as shown in Figure 6. Now it is not easy for everyone to read curves in the complex planes, and it is desirable to find a quantity which exactly expresses the Richter after-effect, directly in terms of temperature with frequency as a parameter or in terms of frequency with the temperature as a parameter.

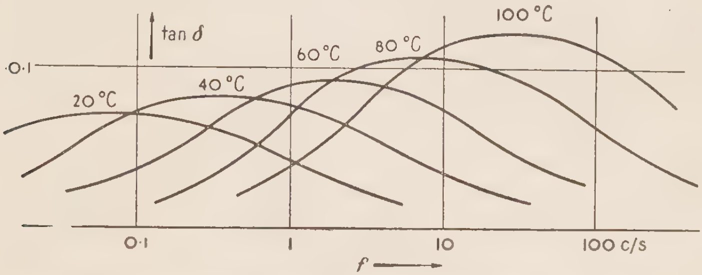

Figure 9. The loss factor caused by Richter after-effect, as a function of temperature and frequency.

Similar relaxation phenomena have been investigated in dielectric materials. Here the loss factor is expressed in terms of the frequency with the temperature as a parameter. If the same is done with the Richter after-effect, the curves of Figure 9 are obtained. This shows clearly the shift of the

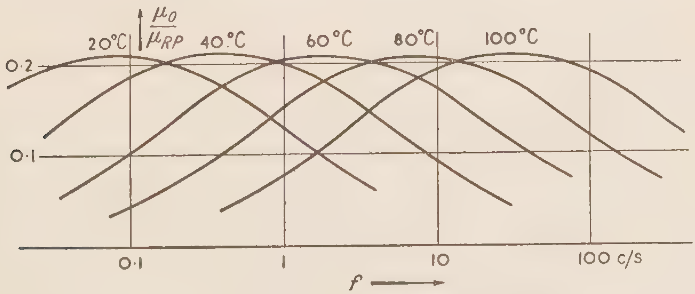

Figure 10. Imaginary part of complex permeability, produced by Richter after-effect, as a function of temperature and frequency.

maximum of the Richter after-effect, with rising temperature, towards higher frequencies, but it produces the false impression that the Richter after-effect increases in intensity with increased temperature. In reality this expresses only the increase of the relaxed initial permeability μ_{a0} with temperature, which affects the loss factor tan δ but has nothing to do with the Richter

after-effect. A true representation of the Richter after-effect is only obtained when not the loss factor but the imaginary part of the reciprocal $1/\mu_{LP}+j1/\mu_{RP}$ of the complex permeability is plotted against frequency, as shown in Figure 10.

8. ANOMALOUS DEPENDENCE OF PERMEABILITY ON FIELD STRENGTH

Transformer laminations which show strong Richter after-effect always show also certain hysteresis anomalies. Hysteresis can be denoted by the rise of permeability with field strength. The hysteresis-loop theory of Rayleigh gives a linear rise of permeability. In laminations with Richter after-effect, however, the permeability is constant at low field strengths. Then follows, for a field strength of a few mA/cm onwards, a very steep rise (Figure 11) (Feldtkeller, 1943).

For ferromagnetic materials which obey the Rayleigh theory, such as nickel-iron alloys and carbon-free silicon-iron, the first Barkhausen jumps take place at immeasurably small field strengths which lie far below 1 mA/cm.

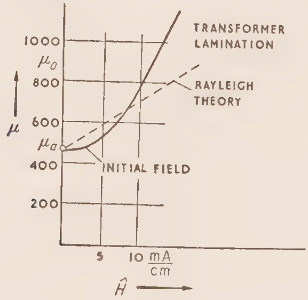

Figure 11. Rise of permeability with the amplitude of the alternating field.

For transformer laminations with Richter after-effect, the field strength necessary for the slightest Barkhausen jumps to begin is 2 to 5 mA/cm. This starting field strength corresponds to a flux density of about 1 gauss. The saturation flux density is of the order of 20 kilogauss. It can therefore be assumed that the smallest Barkhausen jumps occur when the domain boundaries have moved by about one ten-thousandth part of the width of a Weiss domain. If this is assumed to be about 0·1 mm we obtain quasi-elastic extensions of about 10^{-5} mm, i.e. of the order of thickness of the domain boundary wall itself.

9. CURVES OF COMPLEX PERMEABILITY

The curves of complex permeability too, in so far as they depend on hysteresis, show characteristic anomalies for transformer laminations with marked Richter after-effect. From the Rayleigh theory, this curve should be a straight

line making an angle of 23° with the ordinate axis and carrying a linear frequency scale. For the transformer lamination whose Richter after-effect we have been discussing, the curve shown in Figure 12 was found. It is straight, but it does not carry the linear frequency-scale mentioned in

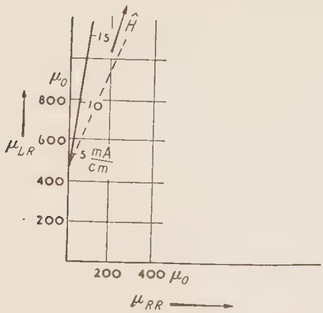

Figure 12. Curve of complex permeability due to hysteresis, for a transformer lamination.

section 8 and it makes an angle of about 8° with the ordinate axis instead of 23° (Feldtkeller, Wilde, and Hoffmann, 1951). This hysteresis property can be explained as follows:—

Preisach (1935) has given a theory of the hysteresis loop. Part of the flux has no hysteresis and is proportional to the magnetizing force. The factor of proportionality is the initial permeability. The other part of the flux has hysteresis. It is represented by an infinite number of elementary loops, of the rectangular form shown in Figure 13, superimposed on each

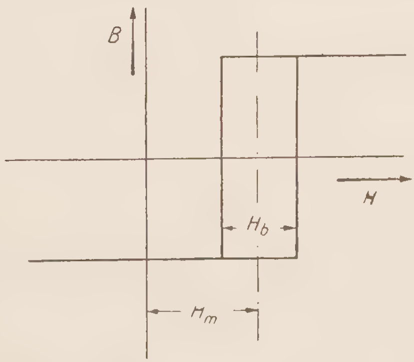

Figure 13.
Elementary hysteresis loops.

other. All widths H_b of the elementary loops and all mean magnetizing forces H_m are equally probable. These assumptions suffice to make the branches of the hysteresis loop obey the Rayleigh equations.

Preisach's hypothesis must be changed in two respects. First it must be assumed that small loops do not occur for which the mean magnetizing force H_m is smaller than the initial magnetizing force H_s, but that all mean magnetizing forces greater than the initial value are equally probable. Secondly, it must be assumed that the domain boundary walls, corresponding to elementary hysteresis loops with smaller values of H_b, and which thus have already reached their elastic limit at small field strengths, have a stronger elastic bond to their rest position than the domain boundaries corresponding to hysteresis loops of greater width. Then the permeability on which the hysteresis is based increases with flux density, and the component μ_{LR} of the complex permeability increases relatively faster than the component μ_{RR}.

This is only another method of saying, as can be confirmed for example by measuring the hysteresis loop with a fluxmeter, that for the transformer lamination which was investigated the slope of the tangents at the tips of

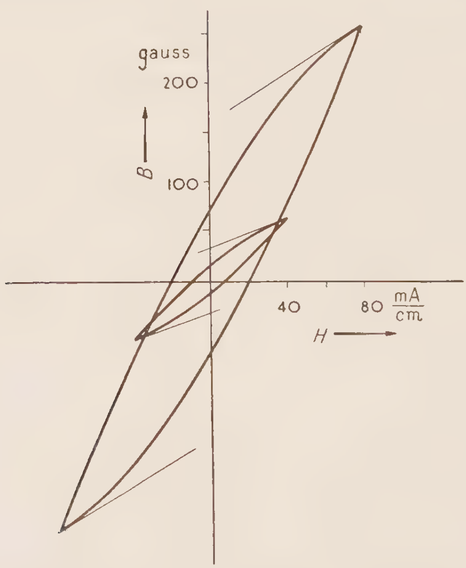

Figure 14. The return tangents at the tips of the hysteresis loops for a transformer lamination become steeper with increasing amplitude.

the loop showed a marked increase with increasing amplitude of the alternating field-strength (Figure 14) whilst, according to the Rayleigh theory, the slope should have remained constant (Feldtkeller, 1949a, p. 39).

Nothing is yet known of the physical connection between this effect and the Richter after-effect, which it always accompanies.

DISCUSSION

Dr. H. P. J. Wijn:

Prof. Feldtkeller finds for silicon-iron a Richter-type after-effect, which he explains as due to a diffusion of carbon as discovered by Snoek. While Snoek thinks the after-effect is due to the displacement of 90° walls, Prof. Feldtkeller concludes from the results of his measurements given in Figure 6 that the special arrangement of 90° and 180° walls, as given in his Figure 3, causes the after-effect. It will therefore be of interest to measure the after-effect in silicon-iron at different biasing field strengths, in order to vary the ratio of the numbers of 90° and 180° walls present in the material.

Prof. Feldtkeller (in reply):

Dr. Wijn has asked what considerations have led to the particular configuration of Bloch walls shown in Figure 3. My reply is that the required configuration must satisfy two conditions:—

(1) In addition to the 180° walls, which to a first approximation, determine the initial permeability, it must also contain 90° walls since, according to Snoek's explanation, the Richter after-effect (movement of carbon atoms) occurs only in regions over which a 90° wall has passed.

(2) The curves of complex permeability and its reciprocal show that the Richter after-effect mainly influences the reciprocal of the complex permeability. The region over which the 90° wall passes must therefore take up a position so that it acts as an air-gap with respect to the strip of flux which changes its direction.

I have searched among the many illustrations published by Bozorth and his colleagues, for one which corresponds to both these conditions and have found it in Figure 11-53, Bozorth, 1951. Figure 3 of my paper is a part of this diagram.

(*Further discussion relevant to this Paper appears on page* 86.)

13

JORDAN-TYPE AFTER-EFFECT (RESIDUAL LOSS) IN POWDER-CORES

R. Feldtkeller

(Technische Hochschule, Stuttgart)

Abstract: The method suggested by Jordan for separating the losses is not sufficient. The separation of losses must be based on the complex permeability $\mu_{LR} - j\mu_{RR}$. Eddy currents change only μ_{RR}. As a result of eddy currents, μ_{RR} increases proportionally with frequency. The Jordan after-effect changes μ_{LR} and μ_{RR}. μ_{LR} falls with frequency, to a first approximation as its logarithm. μ_{RR} has a flat maximum. If it is assumed that the relaxation times are distributed about the mean value in accordance with a Gaussian error curve, it is possible to calculate the complex permeability curve corresponding to the Jordan after-effect. The elimination, by calculation, of the eddy currents from the measured complex permeability must lead to a curve of the predicted type. This is a useful criterion for determining the eddy-current loss coefficient.

The Jordan method of loss separation ascribes the variation of the residual-loss coefficient with frequency to eddy-current effects.

1. INTRODUCTION

The inductance and loss angle of a dust-cored coil depend on frequency and current. This is partly due to the d.c. resistance of the winding, and partly due to the magnetic losses. The only method of determining the physical constants of the a.c. effects is the measurement of the impedance Z of a test coil for various frequencies and currents. It is not convenient, however, to discuss the behaviour of the impedance itself. It is better to subtract from it the d.c. resistance of the winding R_g and then to divide the result by the frequency, the square of the number of turns W and the ratio of core cross-section to magnetic path-length A/l. This removes the effect of arbitrary core dimensions and coil data.

A complex quantity

$$\mu = \frac{Z - R_g}{j\omega W^2 A/l} \qquad \ldots(1)$$

is obtained, having the dimensions of permeability, which is represented in the complex plane as the complex permeability of the powder-core under test. Figures 4 and 5 show curves of measured complex permeabilities. The problem immediately arises of analysing the measured values of permeability to obtain the effects of hysteresis, eddy currents and residual loss. This cannot be done without certain physical assumptions.

Jordan (1924) investigated, not the complex permeability, but the loss factor. He assumed that the variation of the loss factor with magnetizing

force depended only on hysteresis, and that the eddy-current and residual losses were exactly proportional to magnetizing force.

For eddy currents, this hypothesis can be justified without any further assumptions. The change of inductance as a result of eddy currents is only a second-order effect, and to a first approximation the loss factor is proportional to the frequency; and for small magnetizing forces, the hysteresis effect is superimposed on the eddy-current effect but is itself unchanged (Feldtkeller, 1949b, 1949c).

For residual loss, Jordan's hypothesis has a physical meaning. It means that, in the parts of the ferromagnetic material over which a domain boundary has passed and which have changed their direction of magnetization, relaxation effects occur which are independent of the amplitude of movement of the domain boundary, and that additional relaxations of the start of Barkhausen jumps, as assumed by Preisach, are unimportant. It is not possible to raise serious objections to these properties of residual loss.

On the other hand, Jordan made a further suggestion to which there are certain objections. He assumed that the effect of residual loss on the loss factor was independent of frequency. This must mean physically that all possible relaxation times from $\tau = 0$ to $\tau = \infty$ may occur equally frequently. It is far more probable that they group themselves around a mean value according to a normal distribution curve, even if the standard deviation is large.

This mean value is determined by the material constants and the dimensions. If this assumption is made, however, it removes from the Jordan method of the analysis of the losses the most important part of its hypothesis. The residual-loss coefficient would become frequency-dependent, and it would no longer be possible to determine which part of the frequency response should be attributed to eddy currents and which to residual loss.

It is necessary to seek a further criterion. This is found when, in addition to the frequency variation of the loss factor, that of the inductance (i.e. of the permeability) is considered. Here the eddy-current and residual loss effects differ (Feldtkeller and Hettich, 1950). We will next study this difference, making use of the curves of the complex permeability in the complex plane.

2. THE FUNDAMENTAL CURVES OF COMPLEX PERMEABILITY

Figure 1 shows the calculated complex permeability curves for a flat lamination and a circular cylinder of homogeneous material with no hysteresis. The curves for a toroid of circular cross-section, i.e. the usual core shape, do not differ greatly from these, and even the curves for a core with an air-gap or a dust-core have the same form. Only the beginning of the curves is of interest. We find that the component μ_{RR} is proportional to frequency, whilst μ_{LR} is practically constant (Wolman, 1924; Dwight, 1929).

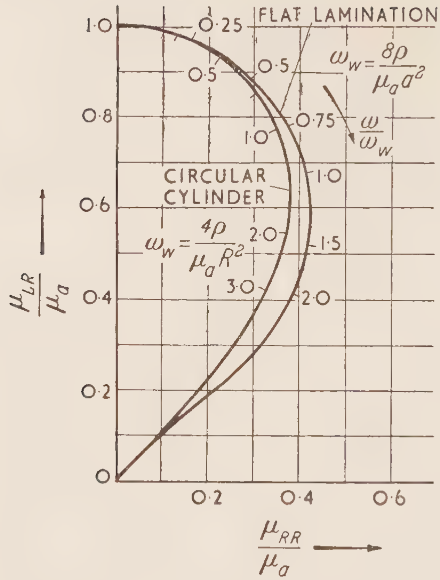

Figure 1. Effect of eddy currents on the complex permeability of a flat lamination and a homogeneous circular cylinder.

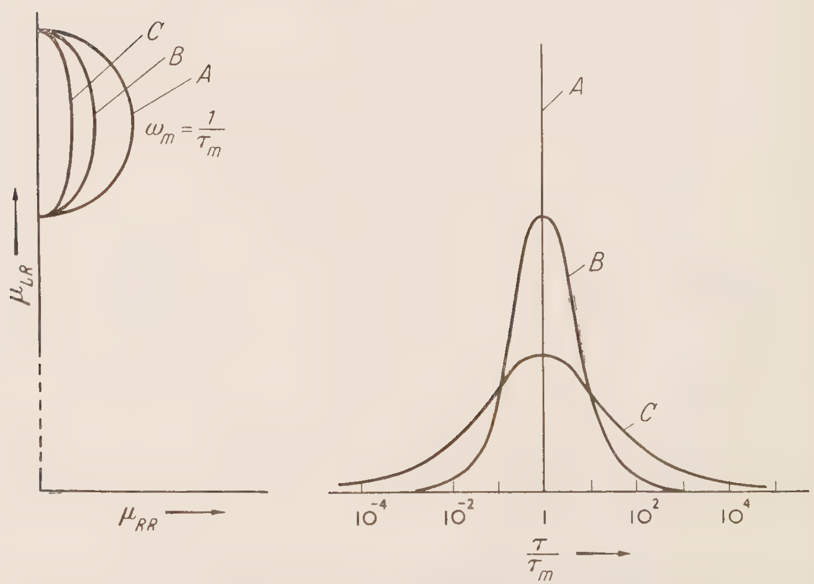

Figure 2. Effect of residual loss, with a given distribution of relaxation times, on the complex permeability.

Figure 2 shows the calculated effect of residual loss on the complex permeability. It is assumed that the part μ_n of the initial permeability μ_a is associated with the residual loss. In reality, μ_n is something like a hundred times smaller than μ_a but in the diagram this component has been greatly exaggerated for the sake of clarity. It is further assumed that the relaxation times τ group themselves according to a Gauss probability curve about their mean value. The line A shows the case where only one relaxation time exists, i.e. in which a sudden change of magnetizing force results in an exponential change of flux density; the corresponding curve is a semicircle. B and C are cases with increasing spread of the relaxation times about their mean value; the curve assumes an elongated form similar to a semi-ellipse.

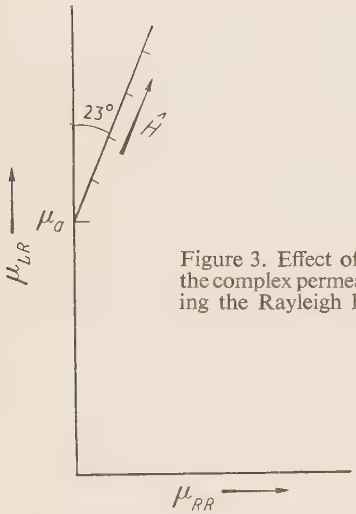

Figure 3. Effect of hysteresis on the complex permeability, assuming the Rayleigh hysteresis law.

In the middle frequency range, the decrease of the component μ_{LR} is then roughly inversely proportional to the logarithm of the frequency, the component μ_{RR} passes through a very flat maximum and there is a definite relationship between the two components (Schulze, 1938 ; Wilde, 1949). Finally, Figure 3 shows the effect of hysteresis on the complex permeability. The Rayleigh hysteresis loop theory can be used to calculate the corresponding curve, which is found to be a straight line, making an angle of 23° with the ordinate axis and carrying a linear magnetizing-force scale. Thus there is a particularly close relationship between the two components μ_{LR} and μ_{RR} of the complex permeability.

The curves of Figures 1 to 3 must be used as a guide when discussing measured curves of complex permeability.

A warning must be given against using measured values of μ_{RR} or of the

loss factor μ_{RR}/μ_{LR} alone as a basis for analysis. Owing to the smallness of the residual loss, the measurements are very difficult and a relatively large degree of uncertainty is therefore attached to the measured results. Systematic and unsystematic measuring errors can usually be distinguished if the values of the components μ_{LR} and μ_{RR} are checked, one against the other. For example, in a frequency range where μ_{RR} is independent of frequency, the decrease of μ_{LR} must be inversely proportional to the logarithm of frequency ; in fact μ_{LR} must fall by $(2/\pi)\ln(f_2/f_1) \,.\, \mu_{RR}$ when the frequency is raised from f_1 to f_2. Thus, for example, it must fall by 0·44 μ_{RR} when the frequency is doubled. No method of measurement should be adopted for the study of residual loss which does not permit the application of this criterion.

3. ANALYSIS OF COMPLEX IMPEDANCE AT LOW FREQUENCIES

Powder-cores with permeabilities of 50 μ_0 and over usually have such large eddy-current losses that they can only be used in the voice-frequency range. It is therefore sufficient to analyse their complex permeability between 0·5 and 16 kc/s.

Figure 4 shows the measured values of complex permeability for a Sendust core for two magnetizing forces of 50 and 100 mA/cm respectively. The analysis of these curves gave the following results :—

(*a*) The curve for 50 mA/cm can be obtained from that for 100 mA/cm by a parallel shift in a direction which makes an angle of about 20° with the ordinate axis. This parallel shift shows the pure influence of the hysteresis. By shifting the curve in the same direction by the same amount once more, the extrapolated curve A is obtained for zero magnetizing force $H = 0$, thus eliminating the effect of hysteresis.

(*b*) The increase of μ_{RR} with increasing frequency is partly due to eddy currents but may also be due to residual loss. The two effects cannot be separated directly.

(*c*) The fall of μ_{LR} with increasing frequency has nothing to do with eddy currents, but is due only to residual loss. If it is possible to assume a Gaussian distribution of relaxation times then, from Figure 2, a curve can be sought which best fits this change of μ_{LR} with frequency. It can be shown that the frequency response of μ_{LR} leads to the choice of one particular curve. This is shown as curve B in Figure 4.

(*d*) If our hypothesis is correct, the difference between curves A and B must be due to eddy currents and therefore must lie horizontally and must be proportional to frequency. This can be checked by moving the points of curve A horizontally by amounts proportional to frequency, the constant of proportionality being chosen to make the curve fit curve B as closely as possible. As curve C shows, this agrees satisfactorily. The remaining error in loss factor is only about 3.10^{-4}, an amount which generally does not

exceed the error of measurement to a sufficient degree to enable any conclusions to be drawn about possible errors in the hypothesis.

The analysis shows that the relationship between the complex permeability and the magnetizing force depends only on the frequency-independent hysteresis and that, for very small magnetizing forces, residual loss appears, in addition to eddy-current loss.

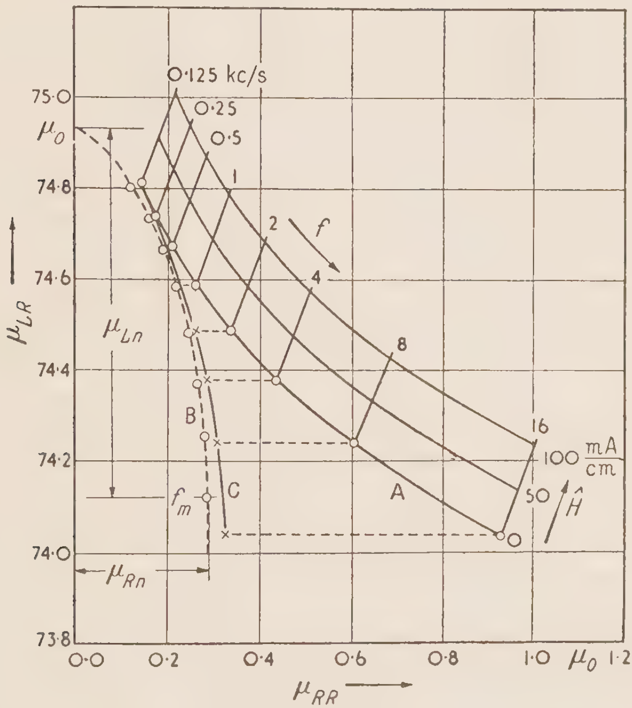

Figure 4. Measured complex permeability of a powder-core and its analysis into hysteresis, eddy-current, and residual loss effects.

4. JORDAN AND RICHTER RESIDUAL LOSS

The differences between Jordan-type loss and another effect discovered by Richter in 1936 are shown in Figure 5. On the left is the curve of Jordan residual loss at room temperature. The mean frequency is 20 kc/s. If the temperature is raised, the initial permeability rises. The curve shifts upwards along the ordinate axis, keeping its shape and size unchanged and still having a mean frequency of 20 kc/s. The residual loss is thus due to an effect whose magnitude and time-constant are practically independent of temperature.

Figure 5 shows also, on the right, the curve for Richter residual loss for transformer laminations. The mean frequency is 0·1 c/s for room temperature and 20 c/s for 90°C. This effect is not independent of temperature but operates about 200 times faster at 100°C than at room temperature.

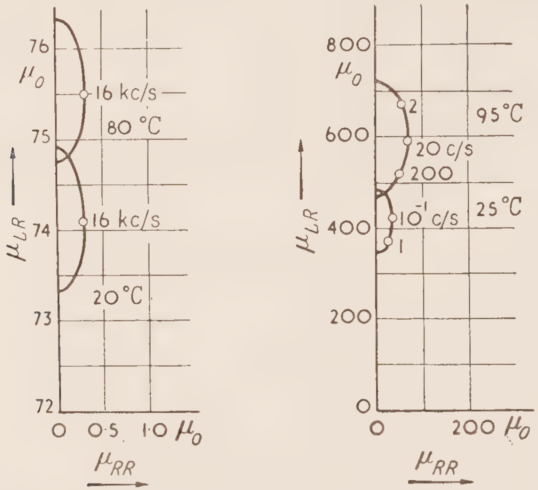

Figure 5. Curves of Jordan-type residual loss for a powder-core (left) and Richter-type residual loss for a laminated transformer core (right).

In powder-cores, also in carbonyl-iron powder-cores, only the temperature-independent Jordan residual loss is found. This is strange, because in carbonyl-iron laminations, above all, the temperature-dependent Richter effect is found, and was first discovered (Richter, 1937); it was only later that it was also found in transformer laminations by Wilde and Bosse (1943).

The fact that the Jordan effect is independent of temperature leads to the conclusion that it is due to the dissipation of heat which is produced in the parts whose length changes in the direction of the magnetization. The characteristic temperature response of the Richter effect points to diffusion phenomena of foreign atoms in the crystal lattice of the α-iron. The carbonyl-iron powder also contains foreign atoms. Since the Richter effect is lacking here, it must be assumed that the effect of change of magnetization occurs in a different way in powder from that in laminations, and that it does not allow the foreign atoms to leave their positions in the crystal lattice.

5. EDDY-CURRENT COEFFICIENT

If it is assumed that the eddy-current coefficient C_w, the hysteresis coefficient C_h and the residual loss coefficient C_n are independent of frequency, the

effective resistance of a coil, in so far as it depends on core losses, can be expressed as

$$R_k = C_w f^2 L + C_h f \hat{H} L/\sqrt{2} + C_n f L \qquad \text{...(2)}$$

in which f is the measuring frequency, $\hat{H}$ the peak magnetizing force and L the inductance (Deutschmann, 1931).

Since $\quad L = W^2 \mu_{LR} A/l$

and $\quad R_k = \omega W^2 \mu_{RR} A/l,$

$$\text{then} \quad \frac{R_k}{fL} = 2\pi \frac{\mu_{RR}}{\mu_{LR}}$$

$$\text{Thus} \quad 2\pi \frac{\mu_{RR}}{\mu_{LR}} = C_w f + C_h \hat{H}/\sqrt{2} + C_n$$

$$\text{and} \quad \frac{d}{df}\left(2\pi \frac{\mu_{RR}}{\mu_{LR}}\right) = C_w.$$

The variation of μ_{LR} with frequency can be neglected in comparison with that of μ_{RR}, so that

$$C_w = 2\mu \, . \, \frac{1}{\mu_{LR}} \, . \, \frac{d(\mu_{RR})}{df} \qquad \text{...(3)}$$

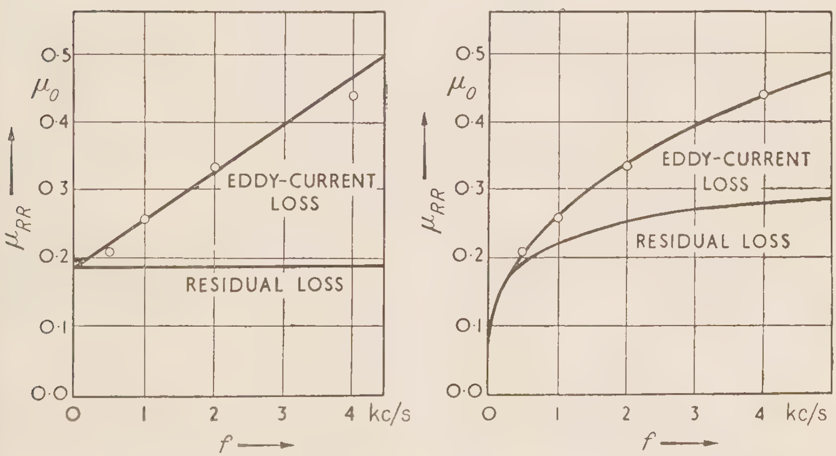

Figure 6. Approximate and exact separation of the component μ_{RR} of the complex permeability into eddy-current and residual loss effects.

Figure 6 shows on the left the measured values of μ_{RR} in a frequency range

of 0·5 to 4 kc/s. A straight line has been drawn through the measured points, with a slope of

$$\frac{d(\mu_{RR})}{df} = \frac{0{\cdot}27\mu_0}{4\ \text{kc/s}}$$

With $\mu_{LR} = 75\mu_0$, we get

$$C_w = 6{\cdot}28 \,.\, \frac{1}{75\mu_0} \cdot \frac{0{\cdot}27\mu_0}{4\ \text{kc/s}} = 5{\cdot}7\ \mu\text{sec.}$$

For comparison, the right-hand side of Figure 6 shows the component μ_{RR} of the residual loss, which has been taken from Figure 5. The eddy-current loss is responsible only for the difference between this curve and the measured curve. Thus, in equation (3), the value

$$\frac{\Delta\mu_{RR}}{\Delta f} = \frac{0{\cdot}15\mu_0}{4\ \text{kc/s}}$$

must be substituted, giving the true eddy-current coefficient

$$C_w = 6{\cdot}28 \,.\, \frac{1}{75\mu_0} \cdot \frac{0{\cdot}15\mu_0}{4\ \text{kc/s}} = 3{\cdot}1\ \mu\ \text{sec.}$$

The true eddy-current coefficient thus has only about half the approximate value which would have been obtained by the assumption that the residual loss was independent of frequency.

6. REPRESENTATION OF RESIDUAL LOSS

So far the effects of eddy currents, hysteresis and residual loss have been represented by the three coefficients C_w, C_h and C_n in equation (2). There is no reason why the eddy-current coefficient should not be expressed as a parallel quantity, provided it is determined as shown above.

The hysteresis coefficient C_h in equation (2) only describes completely the effect of hysteresis on the complex permeability provided the Rayleigh hysteresis theory holds.

The curve of complex permeability resulting from the Jordan residual loss can be represented by the half-length on the ordinate axis (μ_{Ln} in Figure 4) and the maximum distance from the ordinate axis (μ_{Rn}) and also by the mean frequency f_m and the magnitude of the component μ_{Lm} at that frequency.

From Figure 4 the following values are obtained :—

$$\mu_{Ln} = 0{\cdot}8\ \mu_0 \qquad \mu_{Rn} = 0{\cdot}3\ \mu_0$$
$$f_m = 16\ \text{kc/s} \qquad \mu_{Lm} = 74{\cdot}1\ \mu_0$$

If the relaxation times of the residual loss effect are grouped according to a Gaussian distribution curve about their mean value, these values enable the form of the curve and its frequency scale to be determined.

DISCUSSION

Mr. C. E. Richards:

It is shown that only Jordan-type loss is found in carbonyl-iron powder-cores whereas the temperature- and frequency-dependent Richter loss occurs in carbonyl-iron laminations. We should probably try to forget that it is carbonyl iron which seems to act inconsistently as there seems no metallurgical reason why it should behave uniquely; the data presented are likely to be special examples of the general behaviour of iron powders and iron laminations.

High-permeability powder-cores, including those made from carbonyl powder may be compressed at not less than 100 tons/sq.in. Schultze (1938) has shown that Richter-type loss does not occur in heavily-worked metal but only after recrystallization, and that quite small deformations of the recrystallized metal cause the disappearance of the loss. It seems likely that a soft-iron core made at 100 tons/sq.in. will have been deformed sufficiently to cause this to happen.

If Schultze is correct Richter loss would only be expected in those few carbonyl-iron cores which are made of recrystallized metal not heavily compressed. The ordinary process of decarburizing is carried out at too low a temperature for recrystallization to occur though there is stress relief.

Prof. Feldtkeller (in reply):

In order to be able to answer the important questions with certainty, exact measurements of the complex impedance of many cores must be made, over wide ranges of frequency and temperature. The manufacturing processes used for these cores must be systematically varied and accurately known.

Einsele and Baur (1952) have already shown that the after-effect consists of two components. The low-frequency component, whose origin is unknown, has a very wide distribution of relaxation times. The high-frequency component has a very narrow spread of relaxation times. Its mean relaxation time coincides with the time taken for the restoration of the disturbed temperature equilibrium in a powder particle, this is an important clue to the physical origin of this component. I am convinced that the exact analysis of reliable measured curves will shed further light on the cause of Jordan after-effect.

(*Further discussion relevant to this Paper appears on page* 86.)

14

THE THERMAL-AGITATION AFTER-EFFECT

J. C. Barbier

(Laboratoire d'Electrostatique et de Physique du Métal, Grenoble)

Abstract: Measurements of the variation of magnetization as a function of time, throughout the whole hysteresis range and on various substances, show the existence of an irreversible after-effect. The experimental results agree well with the hypothesis of a fluctuating after-effect field proposed by Néel. They show that, for a given ferromagnetic substance, the after-effect may be characterized by the same constant s_v, to a close approximation, in the whole range of hysteresis.

1. INTRODUCTION

Measurement of the losses of a ferromagnetic substance, submitted to an alternating field, shows the existence of residual losses when the losses due to hysteresis and induced currents have been eliminated. These residual losses can be connected with the magnetic after-effect observed in quasi-static experiments. Hence the interest in knowing the nature of the after-effect and the laws which it obeys.

At least two kinds of after-effect may be distinguished. The first arises from the diffusion of atoms of carbon or of nitrogen in the crystalline lattice of iron. This after-effect is observed only in certain substances; Néel (1951) has developed the theory of it. The other has its origin in the thermal fluctuations of the spontaneous magnetization. It affects all ferromagnetic substances, and may also coexist with the first type. This is the irreversible or thermal-agitation after-effect discovered by Preisach (1935) and of which Néel (1950, 1951) has clarified the general theory. In the light of the results of which we give an outline, we shall try to discuss the validity of the hypothesis stated by Néel.

2. GENERAL EXPRESSION OF THE AFTER-EFFECT

According to Néel everything occurs as if on the applied field there were superimposed a fluctuating field $H_i(t)$, sometimes positive, sometimes negative, and whose absolute value increased as a function of time according to the law

$$H_i(t) = S_v\,(Q + \log t)$$

where S_v and Q vary only slowly as functions of $\log t$. The variation of magnetization due to the after-effect, $\Delta I(t)$, is connected with this field by the expression

$$\Delta I(t) = cH_i(t) = cS_v\,(Q + \log t)$$

where c is the irreversible differential susceptibility. c has a very large value

in the neighbourhood of the coercive field. It is in this region that Courvoisier (1945), then Street and Woolley (1949), have observed the irreversible after-effect, while we (Barbier, 1950) pursue the study of this after-effect in the Rayleigh region. We have then systematically extended our measurements to the whole range of hysteresis. All the results agree and establish that the variations of magnetization are proportional to log t; in our experiments we have used intervals of time ranging from 1/40 sec. to 4.10^6 sec.

Kronenberg has found that the variations, as a function of time, of the apparent remanent magnetization after saturation were proportional to log t for periods of more than a year.

3. STUDY OF THE CONSTANT OF AFTER-EFFECT IN THE WHOLE RANGE OF HYSTERESIS

We have characterized the after-effect by the constant S_ν which it is possible to determine experimentally. S_ν is given approximately by

$$S_\nu = \Delta I/c(\log t_1 - \log t_2)$$

where ΔI represents the variation of magnetization between two instants t_1 and t_2, subsequent to the process of variation of the applied field. The fluctuating nature of the fictitious after-effect field is represented by the proportionality of $I(t)$ to c. This can be made evident by the comparison of S_ν and S_ν' given by

$$S_\nu' = \Delta I/(a + c)\,(\log t_1 - \log t_2)$$

in which a represents the differential reversible susceptibility and $(a + c)$ the total differential susceptibility.

At numerous points in the range of hysteresis we have determined S_ν and S_ν'. Here, for example, is a series of results obtained with an Alnico.

(a) After-effect at the point B of remanent magnetization in the Rayleigh region (Figure 1 : by the path OAB) : when the magnetizing field varies from 20 Oe to 100 Oe, c varies from 0·004 to 0·02; S_ν remains equal to 1·65 Oe while S_ν' varies from 0·0224 Oe to 0·113 Oe.

(b) After-effect for the same value of remanent magnetization obtained by a different process (Figure 1 : by the path OA′B′D′B). We now observe an increase of the remanent magnetization as a function of time. c varies with the field H and thus with the field H_3 necessary in order to return to the point B.

Table 1

c	0·055	0·10	0·13	0·19
S_ν	1·60	1·60	1·75	1·80
S_ν'	0·24	0·41	0·55	0·71

(c) After-effect in a field $-H_2$, at the point C′, of nearly zero magnetization (Figure 1 : by the path OA′B′C′).

Table 2

c	0·05	0·08	0·095	0·12	0·15	0·16	0·25	0·36	0·55
S_v	1·70	1·60	1·60	1·65	1·70	1·75	1·60	1·60	1·55
S_v'	0·28	0·34	0·40	0·48	0·60	0·65	0·75	0·90	1·0

On some samples of Oerstit (Grades Oe 400 and Oe 120), kindly presented by M. Kronenberg, we have been able to compare the values of S_v and S_v'

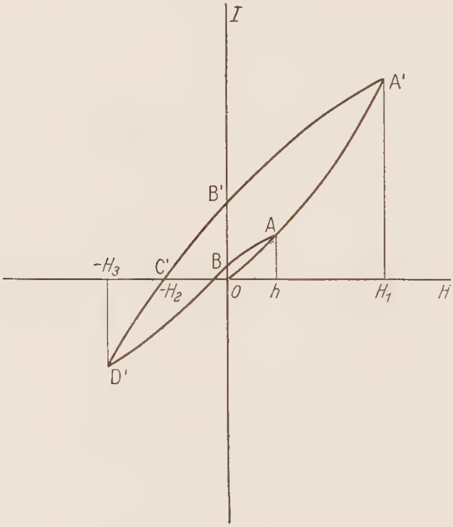

Figure 1. Different approaches to the same value of remanent magnetization.

for very different magnetizations. From his measurements of the apparent remanent magnetization after saturation, we have deduced S_v and S_v' after having measured a and c. On the same samples, we have also determined S_v and S_v' in the Rayleigh region, for remanent magnetizations about a thousand times weaker. For the Oerstit 400, for example, we have found that when c became 45 times greater, S_v' became 16 times greater whilst S_v was increased by only about 20%.

Thus for large variations of magnetization, of field strength and of irreversible differential susceptibility, S_v remains sensibly constant, while

S_v' varies widely. The variations of magnetization due to the after-effect therefore seem to be closely proportional to the irreversible differential susceptibility. These results confirm the fundamental hypothesis of the existence of a *fluctuating after-effect field.*

4. STABILIZATION OF THE REMANENT MAGNETIZATION

Theory and experiment show that the remanent magnetization which varies as a function of time as a result of the after-effect may be stabilized by applying an alternating field $H \sin \omega t$ decreasing from a value H_0 down to zero. This alternating field produces an effect equivalent to that which would have been produced by the fluctuating after-effect field. If the field H_0 has been sufficient, the magnetization is stabilized and becomes independent of the time of observation. In the Rayleigh region, it is easy to calculate the remanent magnetization which remains after this treatment.

$$I_r' = \tfrac{1}{2}b\,(H - H_0 + S_v \log t/\tau)^2$$

where t is the time of application of the magnetizing field H, and τ a time of the order of $1/\omega$ and b the Rayleigh constant. We have verified experimentally the exactness of this formula.

We have verified also that, in conformity with the theory, following annealing at a temperature T, the remanent magnetization diminishes and becomes independent of the time of observation. There has again been stabilization. A rise in temperature of about 50°C is sufficient to make the after-effect disappear.

5. GENERALITY OF THE THERMAL-AGITATION AFTER-EFFECT

The results quoted relate to magnetically hard substances. But the thermal-agitation after-effect affects all ferromagnetic bodies. For very soft substances, for example, nickel-zinc ferrite, we have found values of S_v of the order of 10^{-3} for coercive fields of the order of 0·3. For a soft iron S_v was around 5.10^{-4}. The measurements of Lliboutry (1950) have given, for mild steels, values of S_v of the order of 10^{-3}. From Courvoisier's results relating to a hard steel, we find $S_v = 0{\cdot}116$ with $H_c = 15$ Oe.

Our measurements on very varied substances show that S_v is nearly proportional to the coercive field.

Néel's theory predicts that S_v is inversely proportional to the square root of the Barkhausen discontinuities. The results concerning the magnetically hard substances quoted above in section 3 seem to prove that the volume of these discontinuities remains sensibly constant in the whole range of hysteresis. For substances which are magnetically softer, one may expect greater variations in the volumes of Barkhausen discontinuities, and thus greater variations of S_v in the range of hysteresis.

6. CONCLUSIONS

The particularly simple results of the quasi-static experiments which have just been explained agree well with the theory proposed by Néel. They allow some of the properties of irreversible after-effect to be stated:—

- the irreversible after-effect affects all ferromagnetic substances;
- the variation of magnetization is very nearly proportional to log t ;
- for a given substance, this after-effect can be characterized by a constant which is expressed in oersteds and which, at least for magnetically hard substances, keeps sensibly the same value in the whole range of hysteresis;
- the variation of magnetization is proportional to the irreversible differential susceptibility.

Néel has established that with the irreversible after-effect there are associated, in an alternating field, losses of energy which are represented by a loss angle proportional to the after-effect constant S_v. We have undertaken some measurements of this loss angle. The results, as yet incomplete, will be published later.

(*Discussion relevant to this Paper appears on page* 86.)

15

A STUDY, WITH THE AID OF ELECTROPOLISHING, OF THE BEHAVIOUR OF SOFT MAGNETIC MATERIALS OVER A WIDE FREQUENCY RANGE

I. Epelboin

(Faculty of Sciences, Paris)

Abstract: This paper deals with nickel-iron alloys having a very low magnetostriction. Their behaviour in a large range of radio frequencies is briefly shown, and the results obtained with the aid of electropolishing are developed, including the macroscopic magnetic texture and the texture due to shape.

1. INTRODUCTION

Eddy currents have a considerable influence on the behaviour of high-permeability metallic substances in alternating fields, and it is often found necessary to calculate them. This is very complicated, however, even if the material is of simple geometric shape such as a tape or wire.

We write

$$\mu' - j\mu'' = |\mu| e^{-j\alpha} = F(f) \qquad \ldots(1)$$

for the complex effective permeability, that is to say, that which is measured when the specimen is placed parallel to the magnetic field of frequency f. If both the magnetic induction B and the field H are small, they may be considered as sinusoidal and the magnetic and electrical skin-effects may, in principle, be calculated from Maxwell's equations:—

$$\left.\begin{array}{l}\text{curl } H = \sigma \\ \text{curl } E = -\,\partial B/\partial t\end{array}\right\} \qquad \ldots(2)$$

Even in this simple case, however, it is necessary to know, first, the duration of stabilization of the magnetization due to the various phenomena of after-effect, and second, the distribution of the permeability within the substance. This distribution is determined on the microscopic scale by the division of the substance into elementary domains and on the macroscopic scale by a non-uniform distribution of the magnetization in the thickness of the specimen wire or tape (macroscopic "texture").

2. ISOTROPIC MAGNETIC MATERIAL

An isotropic magnetic specimen which is so poor a conductor that macroscopic eddy currents are not produced allows the function $F(f)$ to be predetermined by considering solely the microscopic texture. This is the case for example for fine magnetic powders coated in an insulating dielectric (Abadie

and Epelboin, 1948; Pistoulet, 1952): given the effective permeability $|\mu|\ e^{-j\alpha}$ corrected for the influence of the permittivity, it is possible to calculate the microscopic eddy currents with the aid of relatively simple models of elementary domains in which the vectors of magnetization are orientated at 90° and in which the displacements of the Bloch walls are proportional to the applied field (Polivanov, 1948). Figure 1, relating to 80/20 nickel-iron powder (grain size 60 to 95 microns) shows the experimental characteristics μ' and μ'' as a function of the frequency, compared with the calculated characteristics for a domain thickness of 1·5 microns and a conductivity $6{\cdot}3 \times 10^4\ \mathrm{ohm^{-1}\ cm^{-1}}$ of the metal.

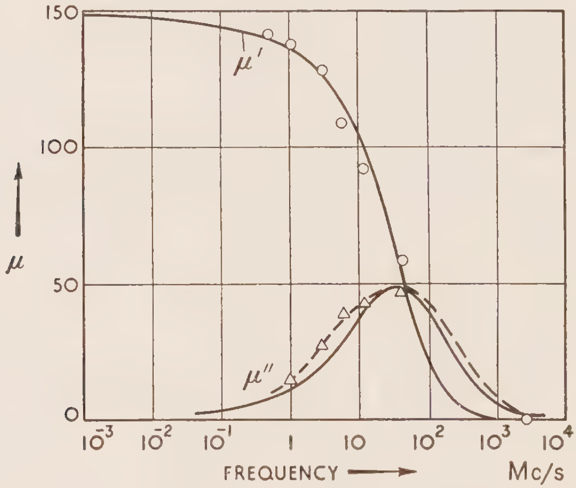

Figure 1. Components of the complex permeability of 80/20 nickel-iron powder, obtained by extrapolation, showing agreement of the experimental results (broken line) and theoretical curves (full line), from equation (2).

For centimetre waves, the calculation of eddy currents is complicated by the natural gyromagnetic resonance which produces demagnetizing fields in the powder. One can, however, eliminate these disturbing fields by inducing an artificial gyromagnetic resonance with the aid of a superimposed d.c. magnetic field (Griffiths, 1946). It can then be shown (Pistoulet, 1952), that the characteristics $|\mu|\ e^{-j\alpha}$ represented in the complex plane, for f constant and H_a variable, become circular beyond a certain value of the superimposed field, thus permitting the calculation of the gyromagnetic constant g corrected for the influence of the eddy currents. For the Permalloy powder quoted in Figure 1 it has been found that $g = 2{\cdot}25 \pm 0{\cdot}06$ (Pistoulet, 1952) at $\lambda = 1{\cdot}25$ cm.

3. HIGH-PERMEABILITY METALLIC SUBSTANCES

Even in a very narrow range of frequencies, eddy currents have a considerable influence on the characteristics $|\mu|\, e^{-j\alpha} = F(f)$ of massive metallic substances of high permeability. To determine the distribution of the permeability in a magnetic substance and in consequence its influence on the characteristics $F(f)$, we have used a technique which consists of electropolishing the specimen after thermal treatment to discover the macroscopic magnetic texture.

In what follows, we limit ourselves to a case which is relatively simple but usual in telecommunications technique—that of high-permeability

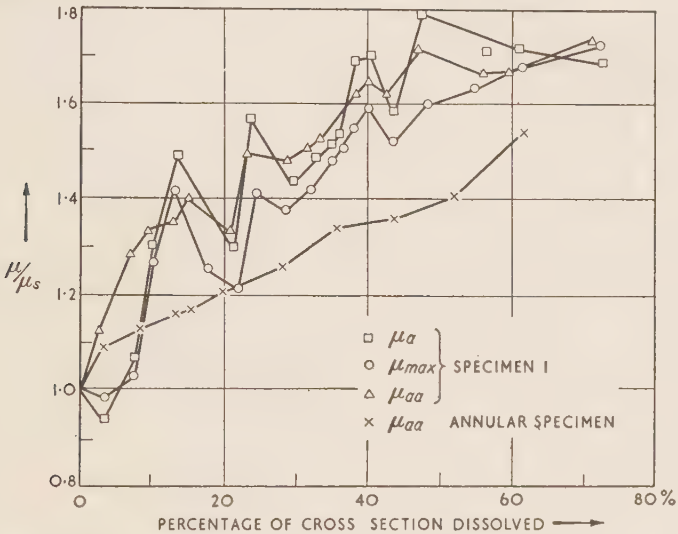

Figure 2. Permeability as a function of the cross-section dissolved by electropolishing. Initially, thickness of tape = 300 microns, maximum permeability μ_{max} = 80 000, static permeability μ_a = alternating permeability μ_{aa} = 20 000. The annular specimen was obtained from Specimen 1; initially its permeability μ_{aa} = 4000.

nickel-irons (such as molybdenum-Mumetal). Suitably annealed, this alloy presents two advantages:—

(*a*) It obeys the Rayleigh laws and therefore in very weak fields there is no appreciable after-effect, either thermal-agitation or diffusion (Néel, 1951). The coefficients of magnetization are defined with the aid of the variation of the permeability of amplitude $\mu_a + 2bH_1$ as a function of the applied field H_1, and in the absence of eddy currents, this variation becomes identical with the initial magnetization curve taken by Ewing's method without static change-over (Gilardin, 1951; Epelboin and Gilardin, 1952).

(*b*) The composition of the alloys gives a constant of magnetostriction small enough for us to neglect the stress energy. In studying the variation of the function $|\mu|\, e^{-j\alpha} = F(f)$ at low temperatures, one can separate the influence of the magnetic-anisotropy energy from that of the magneto-crystalline energy: the latter, indeed, increases at low temperatures while the magnetic anisotropy remains constant (Weil, 1951). The low value of the stress energy may be checked in the specimen itself by measuring the inverse magnetostriction effect (Langevin, 1951) and verifying the similarity of the shapes of the initial-permeability curves for μ_a and μ_{aa}, the static and the alternating cases, and of the maximum permeability μ_{max}, as a function of the section of the tape. In Figure 2 we have reproduced, as a function of the section dissolved by electropolishing, the variations of μ_a, μ_{max} and μ_{aa} of specimen 1, a tape having an initial thickness 300 microns, initial permeability 15 000 and maximum permeability 80 000.

4. MACROSCOPIC MAGNETIC TEXTURE (TAPES OF NORMAL THICKNESS)

Tapes of normal thickness, that is to say a few tenths of a millimetre, have been studied by subjecting them to successive electropolishings after thermal treatment. This has allowed us to show that the macroscopic magnetic texture, or in other words the distribution of the permeability through the thickness of the tape, is assimilable into a continuous function $\mu(z)$, where z represents the distance from a point on the central plane and $\mu(z)$ the permeability. To reach a value for $\mu(z)$, one measures the mean permeability $\bar{\mu}(z)$ of a tape of thickness $2z$ and applies the formula

$$\bar{\mu}(z) = (1/z)\int_0^z \mu(z)dz \qquad \ldots(3)$$

Then, knowing different values of $\mu(z)$, one may deduce its curve. If we consider two points situated at distances $|z|$ and $|z| + |dz|$ from the central plane, we may agree to call the texture positive when we have $\mu(z) > \mu(z + dz)$.

However, to be able to determine $\mu(z)$ from equation (3) it is necessary to be sure that the electropolishing does not modify the properties of the main body of the tape. It is for this reason that in earlier publications (Abadie and Epelboin, 1948; Epelboin and Marais, 1949) we have pointed out that before defining the type of texture, we have taken the precaution of polishing two identical specimens, one on one face, the other simultaneously on both faces, in order to determine the same function $\mu(z)$. Otherwise, introducing the expression $\mu(z)$ into the equations (2) in order to calculate the contribution of the macroscopic texture to the propagation of the eddy currents often causes mathematical difficulties. That is why we

are limited to the study of particularly stable tapes having a texture of which the analytical form is easily handled, for example

$$\mu(z) = \mu_z(1 + tz/d)^{-2} \quad (t>0) \qquad \ldots(4)$$

where d = thickness of tape (Polivanov, 1948).

This form of $\mu(z)$ leads to quite simple expressions for the magnetic and electrical skin-effects which we have verified experimentally (Epelboin and Marais, 1949).

5. AN ATTEMPT TO INTERPRET THE MACROSCOPIC TEXTURE

For the last two years we have believed that the macroscopic texture is bound up with the diffusion of impurities during the course of thermal treatment; with a metal having low stress energy, it would be caused by a magnetic-anisotropy energy created by the inclusions and cavities in the interior of the substance. X-rays have not always detected these heterogenities; for example, the tape of Figure 2 has a crystalline parameter, constant through its thickness to about $\pm$ 0·0005 Å (this approximation corresponds, moreover, to the limits of the errors in measurement). Quenching in water, however, is liable to produce a selective chemical attack sufficiently intense to cause, for a depth of 10 to 15 microns, a contraction of the lattice of the order of 0·003 Å, due to the appearance of a solid phase revealed by a few very weak diffraction spots which cannot be confused with a spot due to a superlattice of the $FeNi_3$ type (Wyart and Epelboin, 1949).

The whole of the results obtained up to the present, thanks particularly to the use of electropolishing, support this explanation of the texture by the diffusion of impurities and we quote three studies which constitute at the same time a simple means of determining $\mu(z)$.

(*a*) If the macroscopic magnetic texture is an anisotropy produced by inclusions and cavities after thermal treatment, two identical tapes having undergone the same anneal should present similar $\mu(z)$ functions even if one of them has been submitted to mechanical stresses. This has been verified with the flat specimen (No. 1) of Figure 2 and the same tape No. 2, which has been cold-worked after thermal treatment, making it into the shape of an annular ring. This last operation has brought the initial permeability (μ_{aa}) down from 15 000 to 4000, but the characteristics μ_{aa} as a function of the dissolved section seem to show that the curves $\mu(z)$ have the same shape in the two cases despite a welded butt-joint which had to be made at the ends of the tape to give it its annular form.

(*b*) If the macroscopic magnetic texture is due to the diffusion of traces of impurities, it is normal that metallic tapes of different thicknesses taken

from the same cast, and undergoing the same thermal treatment, should show the same texture in the outer layers. This would explain for example why two tapes taken from the same cast and having undergone the same thermal treatment, but of respective thicknesses $2L$ and $2l$ ($L > l$) should have textures such that that of the second (thickness $2l$) could be deduced from that of the first (thickness $2L$) by cutting out from the middle of the latter a band of thickness $2(L - l)$ (Figure 3). This has been verified (Epelboin and Marais, 1949) on tapes of molybdenum-Mumetal annealed at 1100°C in commercial hydrogen which showed, for thicknesses greater than

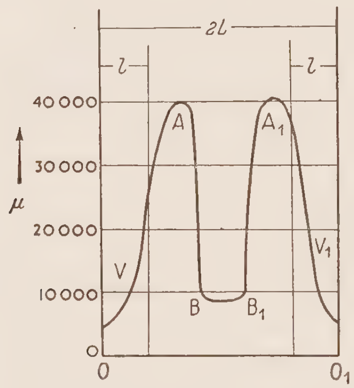

Figure 3. The relation between the macroscopic magnetic textures of two tapes of different thicknesses.

0·35 mm, partially negative textures. This relation is approximate as it cannot be applied to very thin tapes, but it has the advantage of being valid in the case of other very soft magnetic materials such as Supermalloy or pure iron, and it explains why the initial permeability of tapes of many materials is at its maximum for a certain thickness, the thickest presenting a partially negative texture. On the other hand, tapes of molybdenum-Mumetal 0·25 to 0·50 mm thick, annealed at 950°C in purified electrolytic hydrogen, all have the same initial permeability, 40 000; this makes us suppose that they have no pronounced macroscopic magnetic texture and upholds the interpretation of the texture as a diffusion of impurities. It is as well to note, however, that a reservation must be made on the subject of surface layers since $\mu_{max}(d)$ diminishes below a certain thickness of tape and we will give an explanation of this later.

(*c*) The origin of the magnetic texture may also be studied by making a separation of the magnetic losses in a relatively narrow range of frequencies. The variation of tan α (see equation (1)) as a function of the frequency is the same for a tape of macroscopic texture $\mu(z)$ as for a homogeneous tape of

permeability $\mu_m(d)$ and having an apparent conductivity σ_a calculated according to

$$\frac{\sigma_a}{\sigma} = \frac{3}{a^3} \frac{1}{\mu_m^2(d)} \int_0^d \mu_m^2 (z)\, z^2 dz \qquad \text{...(5)}$$

where σ is the measured conductivity.

It is now possible to obtain the function $\mu(z)$ by separation of the Jordan losses extended as far as values of tan α equal to 0·4. This permits us to show that superficial electropolishing (weight of dissolved alloy less than 10%) is capable of diminishing the apparent conductivity by several tens per cent, not by diminution of σ which varies in general by several per cent, but by a significant diminution of $\mu(z)$. The study of σ_a/σ at low temperatures shows that the texture remains very nearly unchanged, from which it can be deduced that it is practically independent of the magnetocrystalline energy; on the other hand, this latter makes the initial permeability vary considerably (Abgrall, 1951; Abgrall and Epelboin, 1952). For example, while the temperature varies from + 20° to − 180°, it is found that the initial permeability of a 50-micron tape decreases from 15 000 to 3500; on the other hand σ_a/σ remains practically constant around 1·3, showing that the texture is associated with a magnetic anisotropy.

6. TEXTURE DUE TO SHAPE (VERY THIN TAPES)

It is above all the study of very thin tapes which shows that the magnetic texture is associated with a demagnetizing effect. Below a certain thickness, the anomaly σ_a/σ increases considerably when the tape is made thinner, whatever the procedure employed. Thus a 3-micron lamination gave $\sigma_a/\sigma = 18$ and it may be seen from Figure 4 that σ_a/σ increases when a tape undergoes successive electrolytic thinning; this is not accompanied by an increase in the Jordan constant (Abgrall, 1951; Abgrall and Epelboin, 1952). The permeability remains practically constant (15 000) and the increase of σ_a/σ could be explained by a modification of the structure according to the extent to which the tape is thinned. This appears, moreover, as a small decrease in σ (a few per cent) and, for lesser thicknesses, by an important modification to the shape of the curve $\mu = F(H)$ of which the curvature changes sign ; for very small thicknesses the concavity is turned downwards (Figure 5), while for thicker tapes it is turned upwards (Figure 6); finally, the maximum permeability is produced for higher fields when the tape is thinner (Figure 4).

A simple calculation shows that these results no longer permit the magnetic texture of very thin tapes to be represented by a continuous function; this is, moreover, in conformity with the presumed structure of the Weiss domains, whose dimensions are of the same order as the thickness of the tapes we are studying.

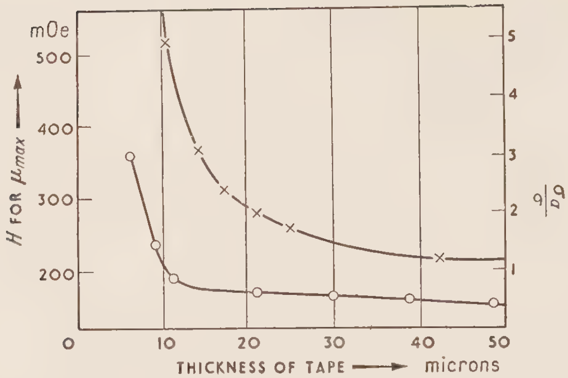

Figure 4. —x—x—x—, variation of σ_a/σ for a 50-micron tape subjected, after annealing, to successive electro-polishings. The initial permeability remains in the order of 16 000. —o—o—o—, variation with thickness of H_m for maximum permeability. The tapes of various thicknesses were obtained by electropolishing 50-micron tape and annealing in pure hydrogen.

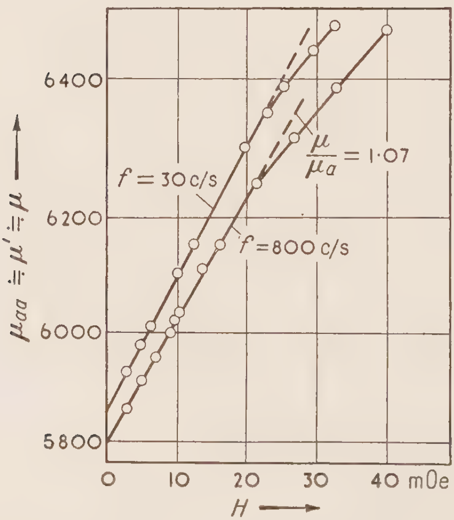

Figure 5. Variation of permeability with field for a tape 7 microns thick, obtained by electro-polishing a 50-micron lamination and annealing in pure hydrogen at 900°C.

We have supposed that the anomalies of very thin tapes are associated with a texture due to shape, or in other words with magnetic anisotropy caused by a demagnetizing field appearing this time on the surface of the tape and which would be due to imaginary free magnetic poles by a mechanism analogous to that which gives rise to the increase of coercive field in finely-divided powders (Néel, 1946).

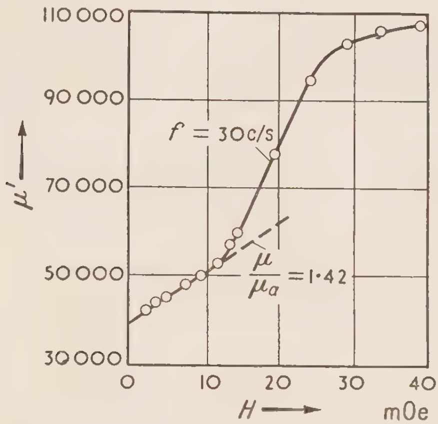

Figure 6. Variation of permeability with field for a tape 200 microns thick, annealed in pure hydrogen at 900°C. The curve $\mu = F(H)$ relating to the static case has a similar shape.

In order to differentiate between the influence of the magnetic after-effect and that of the texture of shape, we have studied the tapes at varying temperatures. The results obtained at temperatures down to that of liquid nitrogen (Abgrall, 1951; Abgrall and Epelboin, 1952) confirm the relative stability of the texture, again allowing us to think that it is independent of the magnetocrystalline energy. These results do not, however, mean that the characteristic function $F(f)$ is not influenced by the magnetocrystalline energy, and the study at low temperatures of very-high-permeability tapes even shows the contrary. Thus, at 20°C, in the 50-micron tape already quoted as having an initial permeability of 15 000, the characteristics $F(f)$ change their sign between $-59°$ and $-98°$ and this is accompanied at $-121°$ by a very slight diminution (7%) of σ_a/σ. We think that these anomalies may be connected with an after-effect introduced by the growth of magnetocrystalline energy, which latter is capable of modifying the time of stabilization of the diffusion through magnetocrystalline couplings (Néel, 1951). This after-effect may be shown even more clearly by making the temperature follow a cycle between $-180°$ and $+20°$; the permeability

then assumes lower values (the difference may reach 15%) and if the temperature is then held constant the permeability starts slowly to increase. This phenomenon is independent of the texture due to shape and consequently of the magnetic anisotropy, as it still exists when two-thirds of the tape thickness has been removed by electropolishing. Similar results have been obtained, although less clearly, with the resistivity.

The behaviour of soft magnetic materials is therefore considerably influenced by the magnetic textures which appear to be due to the energy of magnetic anisotropy. This is even more clear in the case of wires than in that of tapes as their form allows the simultaneous study of the magnetic and electrical skin-effects.

(*Discussion relevant to this Paper appears on page* 188.)

16

ON THE THEORY OF RESIDUAL AND STRATIFICATION LOSSES

A. Fairweather

(Post Office Engineering Research Station)

Abstract: The losses observed with conducting ferromagnetics in alternating fields are greater than would be expected from measured values of their permeability and (d.c.) resistivity. Such losses often vary with field strength in the same way as eddy losses. If they also vary with frequency in the way usually associated with eddy losses they are described as "extra" or "excess" eddy losses; if they do not, they are described as "residual" losses. But a significant part of such losses may be eddy losses of two types not considered hitherto, and which are increased by residual domain-orientation. One of these types of loss can also arise as a consequence of certain methods of measurement. An elementary analysis is given of stratification loss at low frequencies.

1. INTRODUCTION

It has been known for many years that the calculated and the experimentally-observed behaviour of magnetic materials subjected to an alternating field do not agree. In particular, the energy losses exceed those predicted in the usual way and contain components which vary with frequency in a manner which has not yet been satisfactorily explained.

In 1916 McLachlan considered that such differences might be due to a variation of permeability in the body of material. Jordan in 1924, followed by Scott in 1930, suggested that the cause might be some kind of magnetic lag or viscosity. This topic was pursued by Preisach in 1935 and by Richter in 1937 and 1938; the latter established a correlation between mechanical and electrical behaviour. In 1935 and 1936 Peterson and Wrathall showed that much of the discrepancy between theory and experiment was consistent with the presence of a surface layer of low permeability: the possibility of such a layer had been surmised long ago by Heaviside in 1888. Peterson and Wrathall also concluded in 1936 that the effect of magnetic lag was far too small to account for the observed results. In the same year, Dannatt attributed excess eddy losses to the presence of cross fluxes: in this he anticipated one of the suggestions put forward in the present paper. Also in 1936, Legg remarked that the manner in which some of the extra, or "residual", losses vary with frequency is not that which would be expected from a loss arising from magnetic viscosity. The possibility that residual and eddy loss might, perhaps, be related, since both are proportional to the square of the field strength, appeared to him unlikely because residual loss did not vary as the square of the frequency. In 1937 Reed discussed Peterson and Wrathall's equations and their application to experiments. The well-known "onion-skin" structure of certain carbonyl-iron powders led the present author in

1944 to examine the possibility that low-permeability skins might be responsible for some of the extra losses encountered in powder-cores. A theory was worked out, and measurements were made on cores employing powders as prepared and after etching. Although the experimental technique at that time was not very good, there appeared to be a significant improvement after etching.

The present paper falls into two parts. In the first part, the conventional theory of eddy losses in magnetic materials is criticized and it is suggested that a significant portion—perhaps most—of the extra eddy and residual losses may be eddy loss. A little experimental evidence is given in support of this view. In the second part of the paper, a new but strictly elementary analysis is given of stratification loss for a few core shapes of interest, at frequencies such that shielding is negligible.

2. THE CALCULATION OF EDDY LOSS; THE LONGITUDINAL AND TRANSVERSE PULSATION LOSSES; THE DEVIATION LOSSES

The usual calculations of eddy currents in conducting bodies are essentially the same whether the body is magnetic or not: they differ only in the inclusion of a numerical factor to take account of permeability values greater than unity. This is not, however, an adequate description of the significant differences between a magnetic and a non-magnetic material. One outstanding difference is explicit in both the early Weber-Ewing molecular magnet theory and its later development, the Weiss domain theory. Adjacent domains are separated by finite, but not sharply-defined, transition regions, known as domain "walls", throughout which electron spins progressively change in direction: the centre of a domain wall is an unstable region. The basic process giving rise to the familiar magnetization curve is the change with field strength of the directions of groups of spins. For weak fields, and in particular for bodies which do not resemble one or more separate domains (i.e. "bulk" material, not fine powder and perhaps not thin strip), these rotations are largely confined to, but not entirely restricted to, the domain wall. Since they result in a movement of the wall, the magnetization process in such circumstances is often described as one of "wall displacement" or "domain growth". For bodies approximating to an aggregation of separate domains (e.g. insulated powders of sufficiently small particle size) it seems inevitable that the process must be one of nearly uniform rotation throughout the body of each domain.

This picture has several important consequences, some of which may be summarized as follows :—

(*a*) The distribution of flux in a magnetic body subjected to a steady magnetic field is not adequately described by calculations from the bulk geometry of the body. The flux follows tortuous paths determined by domain orientation and field strength. There are components of flux in directions

perpendicular to that of the field: these will be described as "transverse". The component in the same direction as that of the field will similarly be described as "longitudinal". For completely random domain orientation, there is no net transverse flux for a given specimen: other orientations may, however, give rise to transverse fluxes in lengths of the specimen exceeding a few domains.

(*b*) In an alternating field, both components of flux give rise (by transformer action) to eddy losses: these will be referred to as transverse and longitudinal "pulsation" losses respectively. In practice, the smallness of the longitudinal component is ensured by appropriate shaping (e.g. lamination): but it does not necessarily follow, and in practice it often does not, that the same result is also achieved for the transverse one*.

(*c*) In an alternating field, the configuration of the flux paths does not remain constant, but deviates about a mean corresponding to that for zero field. This process of "flux swinging" gives rise (by dynamo action as distinct from transformer action—the distinction is somewhat artificial but it illustrates the point at issue) to another component of eddy loss which will be described as "deviation loss".

The mechanism is essentially the same whether magnetization proceeds by smooth rotations uniformly distributed throughout the body of a domain or by sudden swings localized at the centre of a domain wall. In both situations there would be a strong correlation between deviation loss and mechanical properties. For smooth rotations the amplitude and angular velocity of rotation and, therefore, the deviation loss would be simply related to the frequency and strength of the applied field. For sudden swings amplitude and velocity would not necessarily be related to the field frequency, provided it were sufficiently low. Neither would they necessarily be simply related to the maximum value of the applied field. They would, however, be expected to depend upon the type of domain boundary involved.

Consider, for example, domain-oriented materials of the kind discussed by Bozorth and Dillinger in 1935, prepared by annealing certain alloys in a magnetic field. One effect of such treatment is to orient otherwise randomly distributed magnetostrictive stresses in such a way as to favour magnetization in a specified direction at the expense of magnetization in directions at right angles. By this means a material is obtained which has a very high maximum permeability, a very low coercive force and a very low hysteresis loss at high flux-densities; it also has the now well-known rectangular hysteresis loop.

On demagnetization, either forced at room temperature, or perhaps occurring naturally during the process of cooling to room temperature, half of the domains reorient themselves in the opposite direction. The process of measurement at low field strengths involves remagnetization

* A helical coil can introduce an additional small transverse component.

proceeding largely by domain growth at 180° boundaries, with corresponding spin rotations of 180° in the vicinity of such boundaries. The situation which obtains in such circumstances in a sheet of thickness comparable with the dimensions of a single domain is now of special interest. Thus the rotations can occur about axes either parallel to the surface of the sheet or at right angles to it. In either case, deviation loss is likely to be significant because of the 180° swings; but if the rotations take place about axes parallel to the surface of the sheet, eddy currents are induced in planes parallel to the surface of the sheet and large deviation losses are to be expected.

Consider now the more common, nominally isotropic, materials. It is, perhaps, not unreasonable to suggest that in such materials the domains are unlikely ever to be oriented completely at random. The departure from randomness increases rapidly if the thickness is reduced so as to include only a few domains. Significant structural defects are nearly inevitable, and heat treatment is done, almost invariably, in the earth's magnetic field. Random orientation is, of course, not necessary to ensure the absence of permanent magnetization, or of directional behaviour in specimens which are long compared with a few domains.

Thus there are at least three possible components of eddy loss and only one of them, the longitudinal pulsation loss, is treated, even approximately, in the usual theories. Furthermore, only two of them, the longitudinal and transverse pulsation losses, vary necessarily as the square of the frequency: the third, the deviation loss, is unlikely to do so. This may be seen by consideration of a simple system which is, perhaps, not altogether irrelevant to the problem under consideration.

Consider a thin circular magnetic disc which is mechanically constrained and situated in a uniform alternating magnetic field applied in a direction perpendicular to the axis of rotation of the disc. The direction of magnetization of the disc is everywhere parallel to the faces of the disc and is not coincident with the direction of the applied field: this direction of magnetization is supposed to change with field strength. Since the disc is circularly symmetrical about its axis of rotation, a change in the direction of magnetization can be regarded as a rotation about this axis. The point of interest is the relative motion between the body of the disc and the flux which traverses it: it is immaterial, therefore, whether the flux is regarded as rotating, and the disc as stationary, or vice versa.

Two mutually independent and orthogonal systems of eddy currents flow in the disc. One is the usual "pulsation" system which is unaffected by the changing direction of the flux: the other is a "rotation" system arising from this change.

For simplicity, the instantaneous magnitude of the angular deviation, ϕ, will be supposed proportional to the instantaneous magnitude of the applied field, and to vary sinusoidally with time. The corresponding maximum

deviation, θ, is proportional to the maximum field strength and at a frequency $\omega/2\pi$

$$\phi = \theta \sin \omega t$$

The instantaneous magnitude of the induced voltage is proportional to $\partial\phi/\partial t$, so the instantaneous power, P, can be written

$$P \infty \alpha \theta^2 \omega^2 \cos^2 \omega t$$

Mechanical considerations suggest that θ must inevitably decrease with increase of ω: a choice must be made of a suitable function to represent this decrease. A function of the form $(a - b\,\omega)$ is inadmissible: on squaring, it leads to a loss proportional to a power of ω higher than the second, which is contrary to experience: it also leads to negative power components which are repugnant. A suitable form is

$$\theta = a + b/(p + \omega) \quad (\text{where } p \ll b/a)$$

On substituting into the equation for the instantaneous power with $p \to 0$, it follows that for both instantaneous and average powers

$$P \propto a^2\omega^2 + b^2 + 2ab\omega.$$

The second and third terms represent power components which are respectively independent of and directly proportional to the frequency. All three terms are of course directly proportional, through θ, to the square of the maximum field strength.

Thus it appears that the usual assumption that eddy-current losses are always proportional to the square of the frequency, is incorrect; so, therefore, is the one that a loss varying as some other function of the frequency, e.g. the so-called "residual" loss in conducting magnetic materials, must necessarily arise wholly from some more obscure cause.

Résumé and experimental results. The main implications of the preceding discussion may be summarized briefly as follows: Residual and extra eddy loss in conducting ferromagnetics may, perhaps, be eddy loss: in particular, they may be eddy loss of "deviation" type which is increased by residual domain orientation, which increases as the material is made thinner. For the production of low-loss materials, every effort should be made to secure homogeneity and completely random domain orientation; this implies fine domain structure.

Experiments were done with specimens of 100-micron 65% nickel-iron which differed only in the magnetic conditions obtaining during annealing. With one a field was applied which was sufficient to ensure nearly complete domain orientation; with another, the Earth's field only was involved; and with another the Earth's field was reduced by a factor of at least 10. According to the above theory, additional loss should have been very evident for the

first, much less so for the second and still less so for the third. The results are given in Figure 1.

Intentional domain-orientation gave the expected increased loss, but

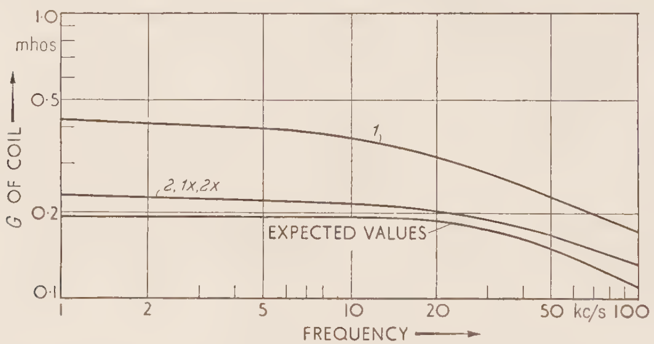

Figure 1. Losses in 65% nickel-iron after various anneals: 1, magnetic anneal; 1x, zero-field anneal; 2 and 2x, "ordinary" anneals.

reduction of the Earth's field had no appreciable effect. This suggests either that the remaining field was important, or that the domain structure was significantly coarse.

3. ELEMENTARY THEORY OF STRATIFICATION LOSS WHEN SHIELDING IS NEGLIGIBLE

The problem is: A measurement is made of the properties of a magnetic core in an alternating field of frequency low enough for shielding to be ignored; the eddy losses are observed to be greater than would be expected from the measured values of average permeability and (d.c.) resistivity; are these extra losses consistent with the hypothesis that the core has a skin of low permeability? And, if they are, what is the skin thickness required? Accordingly, we examine the behaviour of a core of constant resistance and constant average permeability (i.e. constant total permeance; constant total flux in a specified field; or constant inductance of test coil) as the flux in the kernel of the core is increased at the expense of that in a thin skin.

If residual loss were, in fact, eddy loss of either transverse-pulsation or deviation type, then it would be affected by stratification and the two contributions would not readily be separable. This would apply also to any loss (e.g. hysteresis loss at high flux densities) which varies with field strength at a rate faster than that corresponding to simple proportionality.

The result of an elementary loss calculation depends on the assumption made regarding the eddy-current paths: the solutions given for specific finite cross-sections are based on the assumption that the currents flow in circuits

similar to the boundary of the cross-section. The variables are defined in Figure 2: it is, perhaps, worth emphasizing that B is the average flux density, B_1 that in the kernel and B_2 that in the skin; these quantities are, of course, directly proportional to the corresponding permeabilities. The flux

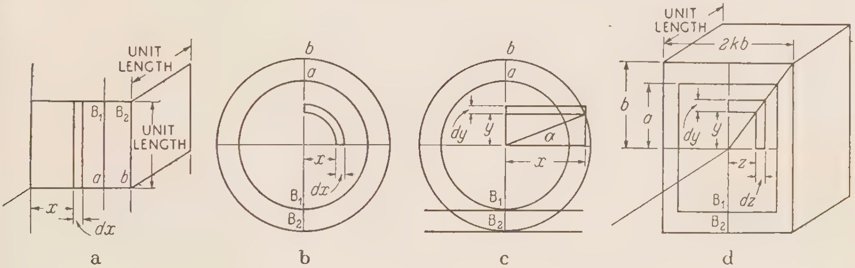

Figure 2. Diagrams to define the symbols used in Section 3.

carried by the skin is ultimately assumed to be small. The suffix x, as in E_x, defines a quantity "at x": and v, in P_v, a power per unit volume.

The stratified sheet (Figure 2a)

$$E_x\,(0 \leqslant x \leqslant a) = \sqrt{2}\pi f B_1 x$$

$$E_x\,(a \leqslant x \leqslant b) = \sqrt{2}\pi f\,[B_1 a + B_2\,(x - a)]$$
$$\fallingdotseq \sqrt{2}\pi f B_1 a$$

$$R = \rho/dx$$

$$P \fallingdotseq \frac{2\pi^2 f^2}{\rho}\left\{\int_0^a B_1{}^2 x^2 dx + \int_a^b B_1{}^2 a^2 dx\right\}$$

$$\fallingdotseq \frac{2\pi^2 f^2}{\rho}\cdot\frac{B_1{}^2 a^2}{3}\,(3b - 2a)$$

$$P_v \fallingdotseq \frac{2\pi^2 f^2}{3\rho}\cdot\frac{B_1{}^2 a^2}{b}\,(3b - 2a)$$

$$\fallingdotseq \frac{2\pi^2 f^2}{3\rho}\,.\,B^2 b\,(3b - 2a) \qquad \text{(for } B_1 a = Bb\text{)}$$

$$\frac{P_v\,(a \neq b)}{P_v\,(a = b)} \fallingdotseq 3 - \frac{2a.}{b}$$

Measurements are often made with the aid of a coil employing the magnetic material as a core: the energy dissipated in the core appears as a contribution to the effective resistance of the coil. The results may be expressed in terms either of the series resistance R_s and inductance L_s of the coil or the equiva-

lent parallel components G and L. If the series representation is used, then it follows (as in the non-stratified case in Legg, 1936, Eqn. 11) that

$$R_s \doteqdot \frac{16\pi^3}{3\rho} \,.\, b(3b - 2a)\, \mu L_s f^2$$

$$\frac{R_s}{\omega L_s} \doteqdot \frac{8\pi^2\mu}{3\rho} \,.\, b(3b - 2a) f$$

Reed has shown numerically that, when eddy-current shielding is negligible, Peterson and Wrathall's equations reduce to (cf. Reed, 1937, Eqn. 17)

$$\frac{R_s}{\omega L_s} \doteqdot \frac{26{\cdot}2\mu}{\rho}\, b\,(3b - 2a) f$$

which is identical with the result just obtained. If the parallel representation is used, and if $\omega LG \ll 1$, then $L_s \doteqdot L$ and $R_s \doteqdot \omega^2 L^2 G$; $R_s/\omega L_s$ can, therefore, be replaced by ωLG.

$$\frac{R_s/\omega L_s\,(a \neq b)}{R_s/\omega L_s\,(a = b)} \doteqdot \frac{\omega LG\,(a \neq b)}{\omega LG\,(a = b)} \doteqdot 3 - 2\frac{a}{b}$$

thus providing a means of deducing a, and hence $(b - a)$, from the results of an experiment at one frequency. If measurements are available in a range of frequencies, then the desired information can be obtained graphically by extracting $(R_s/\omega L_s) \,.\, 1/f$ from a plot of $R_s/\omega L_s$ versus f (or $\omega LG/f$ from ωLG versus f): this is the method adopted by Reed.

The stratified cylinder (Figure 2b)

$$P_v \doteqdot \frac{\pi^2 f^2 B^2 b^2}{\rho}\left(\frac{1}{4} + \ln\frac{b}{a}\right)$$

The stratified sphere (Figure 2c)

$$P_v \doteqdot \frac{3\pi^2 f^2 B^2 b}{2a^4}\left\{\frac{b^5}{15}\left[\left(1 - \frac{a^2}{b^2}\right)^{\frac{1}{2}}\left(3\frac{a^4}{b^4} - \frac{a^2}{b^2} - 2\right) + 2\right] + a^4 b\left[\ln\frac{1 + (1 - a^2/b^2)^{\frac{1}{2}}}{a/b} - \left(1 - \frac{a^2}{b^2}\right)^{\frac{1}{2}}\right]\right\}$$

The stratified bar (Figure 2d)

$$P_v \doteqdot \frac{2\pi^2 f^2 B^2 b^2}{\rho}\;\frac{k^2}{k^2 + 1}\left(\tfrac{1}{4} + \ln\frac{b}{a}\right)$$

Thanks are due to Mr. A. G. F. Thomas of Standard Telephones and Cables Ltd., who supplied the experimental material and carried out a magnetic and an "ordinary" anneal; to Messrs. E. V. Walker, R. E. S. Walters, and E. J. Frost, who carried out a "zero-field" and an "ordinary" anneal; and to Mr. P. C. Jones who made the measurements. Acknowledgment is made to the Engineer-in-Chief of the Post Office for permission to make use of the information contained in this paper.

17

A CALORIMETRIC METHOD OF FINDING THE TOTAL LOSS IN FERROMAGNETIC SPECIMENS SUBJECTED TO AN ALTERNATING MAGNETIC FIELD

L. F. Bates, A. V. Davies and D. J. Harper
(The University of Nottingham)

Abstract: A direct method for measuring the total heat losses in strip, tube or rod specimens of ferromagnetic materials under conditions of high flux-density is described. The method consists of applying a field of chosen amplitude to the specimen for a known number of complete cycles, recorded by a counting circuit. The heat generated in the specimen is measured by a thermocouple system which is calibrated in a simple manner. Some preliminary measurements are described.

1. INTRODUCTION

The apparatus described below was designed to enable rapid direct measurements of losses to be made in the region of high flux densities and frequencies between 10 and 500 c/s on ferromagnetic specimens of a size which could easily be given different annealing and other treatments in the laboratory (e.g. strips of transformer sheet some 15 to 30 cm long and 1 cm wide), and which would give accurate results when the waveforms of both field and flux were non-sinusoidal.

The only method giving accurate results with no wave-form or frequency limitations is the calorimetric method. Earlier calorimetric methods (e.g. Wilson, 1946, and Greig and Kayser, 1948) are lengthy and tedious owing to the great care which must be taken in obtaining an accurate cooling correction and calibration. However, if the heating period can be reduced to the order of one second, the method becomes adiabatic and no cooling correction need be applied. Moreover, in open-circuit measurements calibration can be effected by passing a current through the specimen itself. An apparatus employing these principles has been devised.

The total loss in the specimen when subjected to an alternating magnetic field for a short time (up to four seconds) is measured from its temperature rise by means of a thermocouple system which is calibrated by passing a direct current through the specimen. The average value of the maximum induction is measured by means of a rectifier voltmeter.

2. THE APPARATUS

(*a*) A block diagram of the apparatus is shown in Figure 1. The output from an oscillator is delivered to an amplifier and a gate circuit. The purpose

of the gate circuit is to connect the amplifier to the solenoid which contains the specimen for a chosen interval of time and also to send a pulse to a counter circuit for each cycle during this interval; from the number of pulses, the frequency being known, the time of application of the field can be found.

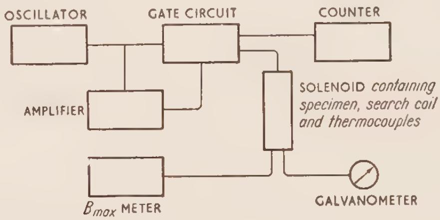

Figure 1. Block diagram of apparatus.

The specimen is mounted in the solenoid and has a search coil wound on it and a thermocouple system attached to it. The search coil is connected to a meter which measures the mean value of the E.M.F. induced in it, from which the average value of the maximum induction, B_{max}, can be found. The thermocouple system is connected to a sensitive galvanometer whose deflection gives the loss in the specimen during the time of application of the field when the system is calibrated.

(*b*) The oscillator is resistance-capacitance tuned with good frequency and amplitude stability. The frequency ranges from 5 to 500 c/s. The wave-form can be varied from sinusoidal to square.

(*c*) The amplifier is of push-pull type giving up to 10 W output. Its output is connected to the solenoid via a quick-acting relay and an a.c. ammeter.

(*d*) The gate circuit has the following functions to perform:—

(1) To switch on the output from the amplifier to the solenoid as the output passes through zero, (2) switch off as the output passes through zero again after a short time interval, (3) send a pulse to the counter circuit each cycle, (4) allow the time interval to be varied. The circuit is shown in Figure 2.

The valve V_1 produces an approximately square wave. This is differentiated and triggers V_2 of the first flip-flop circuit. R_1 and C_1 are chosen to have a time constant of about 1 millisecond. The output taken from the cathode thus consists of square negative pulses as the input passes through zero. This output is applied to the grids of the pentodes V_4 and V_5, which are normally cut off.

The circuit is operated by depressing the switch K. This raises the grid of V_5 to cathode potential and V_5 sends a negative pulse to V_6 of the second

flip-flop. When the first negative pulse from the first flip-flop reaches the grid of V_5, a positive pulse is sent to V_6, thus triggering the second flip-flop. Three effects follow. The relay in the anode of V_7 operates, connecting the amplifier to the solenoid. A large negative pulse is sent from the anode

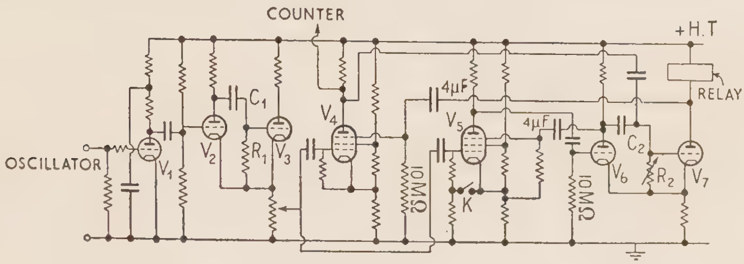

Figure 2. Gate circuit.

of V_6 to the suppressor of V_5, cutting it off, and a large positive pulse is sent from the anode of V_7 to the suppressor of V_4, which then conducts and sends a square positive pulse to the counter circuit each cycle.

After an interval decided by the time-constant of R_2 and C_2, which can be varied up to a maximum of four seconds, the circuit flops back, the relay operates and a negative pulse cuts off V_4. The delay is synchronized to an exact number of cycles by applying positive pulses to the grid of V_7 from the anode of V_4.

(*e*) The counter employs two type G.C. 10A "Dekatron" counter valves. The circuit is shown in Figure 3. The square pulses from the anode of V_4

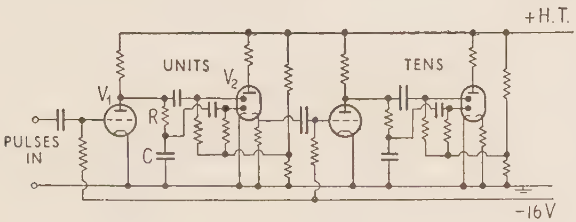

Figure 3. Counter circuit.

are amplified and inverted by V_1 and applied to the first guide ring of the "Dekatron" V_2. The pulses are delayed by RC and applied to the second guide ring. The output from the output cathode is amplified and applied to the second "Dekatron". The number of hundreds is estimated, no hundreds counter being used.

(*f*) The average value of the maximum induction is found in the usual

way from the mean value of the voltage induced in a search coil wound on the specimen. Assuming no even harmonics are present, the mean voltage $\bar{e}$ is $4naf\,B_{max}$ where n = number of turns of the search coil, f = frequency and a = area of cross-section of the specimen at search coil. To find the mean value a rectifier voltmeter of the form shown in Figure 4 is used. The

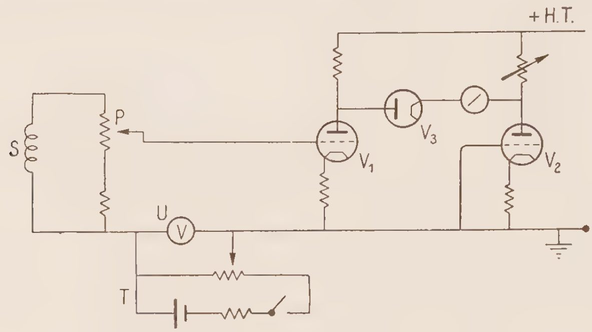

Figure 4. Meter circuit.

search coil S is wound near the middle of the specimen. The potentiometer P has a number of fixed positions and imposes a negligible load on the search coil. One search coil can thus be used for the whole range of B_{max} values and frequencies without moving the specimen. The circuit T is used to apply a direct voltage to V_1, measured by the voltmeter U.

An E.M.F. applied to the grid of V_1 is amplified and rectified, and the deflection of the galvanometer G is proportional to the mean value of the amplified and rectified wave. G has a period much longer than that of the lowest frequency used. Negative feedback is used to improve stability and linearity. The only adjustment required is to adjust the potentiometer on the anode load of V_2 so that G just registers zero or an infinitesimal current.

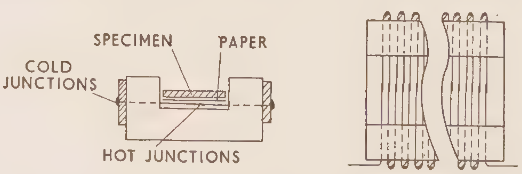

Figure 5. The thermocouple system.

(g) The solenoid is of circular cross-section of internal diameter 3 cm and length 60 cm. It is uniformly wound with ten layers of 500 turns each on a Micanite former and gives a field of 112 Oe/A.

(h) The thermocouple system consists of sixty copper-constantan couples made from 35 S.W.G. wire mounted non-inductively in an ebonite holder

5 cm long, as shown in Figure 5. The cold junctions are soldered to small lengths of stout copper wire to prevent rapid temperature variations. The hot junctions are insulated from the specimen by waxed paper 0·001 cm thick. Good thermal contact is obtained by smearing both sides with glycerine. The system is connected in series with a sensitive galvanometer, critically damped. The scale is placed 2 m distant. Deflections normally range from 5 to 50 cm and can be read to 0·1 mm.

3. THE METHOD OF MEASUREMENT

The apparatus has so far been used with strip specimens 15 to 30 cm in length, 1 cm wide and about 0·04 cm thick. The strip is first wound near the centre with some five hundred turns of 46 S.W.G. d.c.c. copper wire, insulated from the specimen by a thin layer of waxed paper. It is placed in a holder to centralize it in the solenoid and the thermocouple system clamped to it. Search coil and thermocouples occupy the central 7 cm of the specimen. The average value of the maximum induction required is then set as follows: The B_{max} meter is adjusted and the value of $\bar{e}$ for the required B_{max} and frequency, found from $\bar{e} = 4naf\ B_{max}$, divided by 2 to allow for the half-wave property of the B_{max} meter, is applied to the grid of V_1 by means of the circuit T. This voltage is removed, the amplifier connected to the solenoid and the output adjusted until the galvanometer G registers the same deflection. To avoid over-heating the specimen when setting B_{max} for the thermal measurements, a rheostat is switched in in place of the solenoid and the current through it measured with the same amplifier output setting. The thermal measurements are now made by depressing switch K and noting the thermocouple galvanometer deflection.

The output is checked before and after each thermal measurement. Finally, the calibration is carried out. The gate circuit is used to switch the calibrating current on and off. Its duration is found by setting the frequency at 50 c/s and counting the number of cycles.

The deflection of the thermocouple galvanometer is found for various current values. From the slope of a graph of deflection against the square of the calibrating current, and a knowledge of the resistivity of the specimen, the number of ergs generated per cm length of the specimen to give unit deflection can be found. Hence from the thermocouple galvanometer deflection the loss in the specimen at given values of B_{max} and frequency can be found.

4. PERFORMANCE AND RESULTS

The B_{max} meter has been tested for linearity both with alternating and direct applied voltages. The direct voltages were applied by the circuit T (Figure 3) and the alternating voltage by tapping a known fraction of a sine wave whose mean value was accurately known, by means of potentiometer P.

The meter is very nearly linear up to 0·6 volt input, and the alternating and direct readings agree almost exactly. It has also been tested by applying to the potentiometer a distorted wave-form of sufficient amplitude to ensure the accuracy of an ordinary rectifier voltmeter reading mean values. The amplification is assumed to be constant during the short interval between calibration and measurement of $\bar{e}$. The accuracy is limited by slight fluctuations in the diode current which necessitate frequent adjustment.

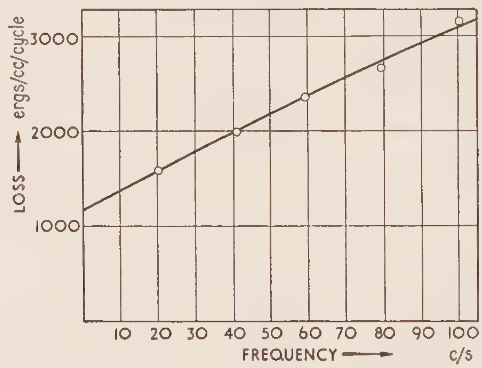

Figure 6. Variation of loss with frequency in a specimen of high-loss silicon-iron; $\hat{B}$=10 000 gauss.

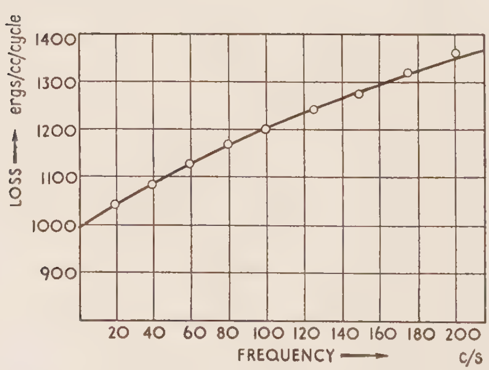

Figure 7. Variation of loss with frequency in a nickel tube specimen; $\hat{B}$=900 gauss.

Graphs of deflection of the thermocouple galvanometer against time of application of a constant amplifier output at fixed frequencies have been obtained. They are straight lines passing through the origin for times up to five seconds, whence it is assumed that heat losses during the interval of time used in measurements (a maximum of four seconds) are negligible.

The thermocouple system gives a deflection of 1 mm for a loss of some

150 ergs per cm length of specimens of the size so far used, corresponding to a loss of some 4000 ergs/c.c. Deflections are consistent to about 1 mm in the normal range of deflection 5 to 50 cm.

Power supplies are stabilized power packs except in the case of the B_{max} meter which works from batteries.

A few preliminary measurements have been made. Figure 6 shows a loss/frequency graph obtained with a strip of 4% silicon-iron sheet at a B_{max} of 10 000. Figure 7 gives the results obtained with a nickel tube 9 mm in external diameter and 0·046 cm thick.

DISCUSSION

Mr. H. Kayser:

One of the principal reasons for the unpopularity of calorimetric methods of measurement is the lengthy experimental period required and the tedious calculations arising from the need to apply cooling corrections. These drawbacks seem to have been successfully removed by arranging that the total heating period is short (4 seconds being given as the limit), and that, as a direct result of this, the cooling correction becomes negligibly small. This development will be highly welcome if it can be shown that there are no serious drawbacks due to transient effects which may have to be considered if very short heating periods are used.

First, there are thermal transients which are unlikely to have the same effect with magnetic-loss heating, corresponding to the test conditions, and the pure conduction-current heating occurring during calibration. That such transients can be important has been shown by MacGregor-Morris and Grisdale (1939), working on dielectrics. By the use of dummy specimens (Greig and Kayser, 1948) or other carefully chosen test, a check can readily be made that the calorimeter is operating satisfactorily as a transfer instrument.

Secondly, it is necessary to ensure that there are no significant errors due to transient effects in the magnetic behaviour of the specimen. Such effects are known to exist at low inductions, where Webb and Ford (1934) studied the time decrease of permeability, and Feldtkeller during this discussion has referred to the remarkable change of shape of B/H loops which he has found taking place over periods of several minutes. It is to be expected however, that such transient effects are negligibly small at the high inductions referred to in this paper.

Mr. A. C. Lynch:

Although the sensitivity of this method is much in advance of that previously reached with calorimetric apparatus, it is still far short of that attainable with a.c. bridges. It detects losses of about 30 ergs/second, whereas bridges will detect losses of the order of 0·01 ergs/second.

Prof. Bates (in reply):

As Mr. Kayser remarks, transient effects corresponding to those found by MacGregor-Morris and Grisdale might exist. In their experiments a thin layer of dielectric of low thermal conductivity was surrounded by large masses of metal of high conductivity, and a large transient, due to the change of temperature distribution with time, was found. In our case the opposite conditions hold, a thin strip of metal being surrounded by material of

low conductivity, and the transient might be expected to be much smaller. A calculation similar to that used by MacGregor-Morris and Grisdale shows this transient to be negligibly small. Another transient was introduced in their experiments by the fact that calibrating heater and specimen were separate; this corresponds in our case to the fact that whereas the direct-current heating during calibration and the hysteresis heating are sensibly uniform, eddy-current heating increases from the middle towards the surface of the specimen.

In the light of Mr. Kayser's suggestion, we used a dummy specimen to estimate the magnitude of this effect. It was necessary to produce a given quantity of heat in a specimen with more than one distribution of that heat. This was done by constructing a specimen of two strips of specimen material, insulated from one another by very fine mica. Either strip could be heated separately by direct current. This gave a much more non-uniform distribution than that found in the magnetic heating experiments, as the specimen was much thicker and the mica has high thermal resistance. For a given heat release in either strip the thermocouple galvanometer deflections for the two cases differed at most by 3%. We are therefore confident that thermal transients play little part in the actual measurements.

Magnetic transients would be expected to be negligibly small, but in any case they should be non-linearly dependent on the time of application of the field, and show as a curvature or intercept on the time-of-application/deflection graph, as, indeed, might the first type of transient mentioned above.

The present method was developed to work under conditions where bridge methods are unsuitable, i.e. at high flux densities where both B and H are non-sinusoidal. The great sensitivity which makes bridge methods so useful in testing communication materials is not required here.

18

A SCREENING-FACTOR TECHNIQUE FOR PERMEABILITY DETERMINATION AND SOME EXPERIMENTAL RESULTS

F. F. Roberts

(Post Office Engineering Research Station)

Abstract: The attenuation of an electromagnetic wave on passing from one surface to the other through a sheet of magnetic alloy depends upon the permeability of the material. Simple probe units are described for impressing and picking up the exploring wave, and a theory of the attenuation caused by the insertion of the specimen between them is outlined. Preliminary experimental results at a frequency of 4 Mc/s suggest that the permeability of thin nickel, Radiometal and Mumetal strip material may be much lower perpendicular to the surface than parallel to it. Such anisotropy could arise from the domain structure within the strip.

1. INTRODUCTION

The technique and theory to be outlined were developed as a possible method for determining the magnetic properties in the interior, as distinct from the surface, of solid materials, metallic or otherwise, at radio frequencies. This technique consists in the measurement of the overall insertion loss suffered by an electromagnetic signal transmitted from one major surface to the other of a thin sheet or slab of the material, the signal propagating through the body of the material. Preliminary experimental results will be quoted which are in reasonable agreement with the present theory for non-magnetic sheets but indicate that the magnetic permeability of 0·001-inch nickel strip measured normal to the surface of the strip is of the order of unity, while that of a similar Mumetal sample (un-annealed) in this direction is also considerably lower than the permeability as usually measured parallel to the length of the strip. The theoretical approach adopted has similarities to that of Schelkunoff (1934), and the general conclusions are consistent with those of King (1933).

2. OUTLINE OF MAGNETIC TRANSMISSION TEST ARRANGEMENT

The sample of material to be tested is pressed lightly between two identical probe units, one energized from a radio signal generator and the other feeding a communications-type radio receiver.

Each probe unit (see Figure 1) consists of a hollow thick-walled brass cylinder of 1 inch outside diameter and $\frac{3}{4}$ inch long. One end of it is closed by a thick wall integral with the rest, and this wall is pierced with a central circular hole of $\frac{1}{4}$ inch diameter. The outside surface of this end wall is ground flat, in order to permit close and uniform contact with the sample

on test. Inside the brass cylinder is a half-turn loop of about $\frac{1}{4}$ inch diameter in a plane through the axis of the cylinder, centred on this axis, and with its nearest point about $\frac{1}{4}$ inch behind the outer flat surface.

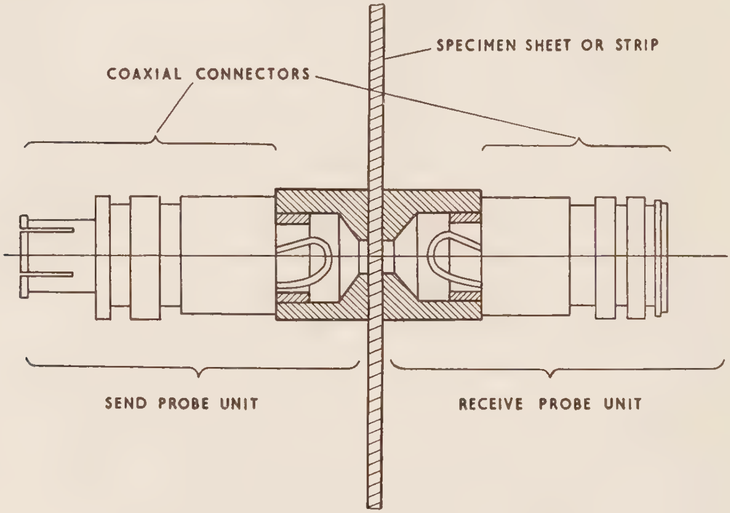

Figure 1. Assembly of probe units and specimen.

The majority of measurements have so far been made at 4 Mc/s. The basic loss of the probe units placed face to face without any sample is about 100 db, so that the measurement of sample insertion losses greater than about 40 db has not yet been possible.

3. SUMMARY OF PREVIOUS THEORIES OF ELECTROMAGNETIC SCREENING

Roston (1948) has distinguished the behaviour of screening materials for (i) the radiation field, (ii) the electric induction field, and (iii) the magnetic induction field, and has implied that for (i) the insertion loss is simply t/d nepers, where t = screen thickness and d = depth of eddy-current penetration. It is suggested that (ii) obeys the same law and likewise the component of (iii) parallel to the surface of the screen. Finally Roston states that for the component of (iii) normal to the screen the insertion loss depends only on the "surface impedance" of the screen and is independent of the thickness if $t > 2d$. That the insertion loss does not depend significantly on the angle of incidence of the magnetic field upon the metal surface in the case of plane waves and plane surfaces can be seen from treatment by Stratton (1941) of this situation. Now plane waves correspond with Roston's radiation field, while the characteristic property of an induction field is its

curvature about the source. It would seem, in general, more appropriate to consider the curvature of the field as the cause of the different screening effect, as may be seen from the theory of cylindrical screens (Schelkunoff, 1934). Schelkunoff's theory treats wave propagation in air and in solid bodies in terms of generalized transmission lines in which several modes of propagation are possible. This approach is a very powerful one, since it can draw upon the now extensive theory of guided waves and can provide relatively simple models from which the allowable approximations in any particular case can be reliably determined. King's theory (1933) is also implicitly a wave theory, but is more restricted than Schelkunoff's by the omission of all but the symmetrical cases, and it does not offer the physical interpretation of the latter work.

4. THE PRESENT THEORY

The transmission line concept. In the general screening situation energy passes from a signal source to a receiver via one or more possible paths, and it is desired to find the increase in overall received-signal attenuation caused by the insertion of the screen in such a way as to intercept some or all of these paths. In the cases in which we are here interested it will be assumed that the screen intercepts all of the possible paths by which significant energy can pass between source and receiver. Further, in the experimental arrangement considered (described in Section 2), all of the significant paths are along the same physical route, i.e. through the sample or the air space between the holes in the two probe units; the different paths consist of different modes of wave propagation over this particular physical route.

Now we may represent any individual path, over which there is a single mode of wave propagation, by an equivalent transmission circuit, as follows. The equivalent generator impedance is equal to the characteristic impedance of the hole in the sender probe unit for the wave mode concerned. The equivalent load impedance has the same value, as the probe units are identical, and these impedances are given by standard wave-guide theory for a circular guide cross-section equal to that of the probe hole. The sample is thin compared with the hole diameter, and it is assumed that the energy propagates through the sample with negligible leakage around the edges, i.e. into the adjacent portions of the sample material outside the cylinder joining the two probe holes. The inside of this cylinder is considered as an intermediate section of wave guide whose impedance and propagation functions can again be found from standard theory, and this may be represented as a symmetrical 4-terminal network inserted between the generator and load impedances.

The insertion loss of the sample for any given path may then be obtained from standard network theory (Guillemin, 1935) as follows :—

$$\ln |E_R/E_R'| = \alpha t - \ln |1 - r_S r_R| + \ln |1 - r_S r_R e^{-2\gamma t}| \text{ nepers} \qquad \ldots(1)$$

where $E_R{}'$ = received voltage with sample inserted
E_R = received voltage with probe faces in contact
$\gamma = \alpha + j\beta$ = propagation function of sample
r_S = voltage reflection coefficient of generator impedance relative to characteristic impedance of sample
r_R = ditto for receiver impedance
t = sample thickness.

The first term on the right-hand side of equation (1) above represents the transmission loss, the second term the reflection loss, and the third term the interaction loss. The reflection loss, although apparently negative, is in general a true loss, since r_S and r_R can never exceed unity in magnitude, but it can give a small gain under certain conditions. The interaction "loss" can become a considerable gain in thin samples, but is negligible in electrically thick samples, on account of the exponential factor.

Since the sample is here assumed uniform in magnetic and electric properties throughout its thickness, and the equivalent generator and receiver impedances are equal, we have :—

$$r_S = r_R = r = \frac{Z - Z_0}{Z + Z_0} = \frac{1 - z_0}{1 + z_0} \qquad \ldots(2)$$

where Z = equivalent generator and receiver impedance,
Z_0 = characteristic impedance of sample,
$z_0 = Z_0/Z$ = normalized impedance of sample-filled waveguide relative to empty guide of same cross-section.

Wave mode involved. For the probe unit described in Section 2 the wave mode involved is essentially a pure circular H_{11} mode. At the test frequency of 4 Mc/s employed, the plane-wave wavelength in air is 75 m, so that the $\frac{1}{4}$-inch-diameter probe hole is far below cut-off, and the propagation is in the evanescent state. Even if the probe units were constructed with perfect symmetry of the desired type, higher order modes would be excited, but these will be attenuated more rapidly in the empty guide, and it is only a question of making the length of the probe hole sufficient to suppress these modes to unimportant proportions.

Impedance and propagation functions. For any given H-mode of propagation in waveguide the normalized impedance of a sample-filled section, relative to an air-filled section of the same diameter, is given by

$$z_{0H} = \mu \sqrt{\frac{1 - (\lambda_0/\lambda_c)^2}{\mu\epsilon - (\lambda_0/\lambda_c)^2}} \qquad \ldots(3)$$

The propagation function has the form :

$$\gamma_0 = \frac{2\pi j}{\lambda_0}\sqrt{\mu\epsilon - (\lambda_0/\lambda_c)^2} \qquad \text{...(4)}$$

In these formulae

μ = relative magnetic permeability of sample material,

ϵ = relative dielectric permittivity of sample material,

λ_0 = wavelength of plane waves in air at the test frequency,

λ_c = wavelength of plane waves in air at the cut-off frequency of the empty guide,

$j = \sqrt{-1}.$

Now in the case of non-conducting ferromagnetic materials, such as ferrites, μ and ϵ are primarily real quantities in the frequency range of present interest. In the case of metals, however, while μ may still be primarily real, ϵ becomes primarily an imaginary quantity. (For in a metal at any radio frequency the component of ϵ due to the bound electrons is negligible compared with that due to the conduction electrons.) The effective permittivity of a metal may in fact be written:

$$\epsilon = -4\pi j/\omega\rho \qquad \text{...(5)}$$

where $\omega = 2\pi \times$ frequency and ρ = bulk resistivity of the metal.

For the metal samples and the frequency in which we are at present interested, we have:

$$(\lambda_0/\lambda_c)^2 \gg 1 \quad \text{and} \quad |\mu\epsilon| \gg (\lambda_0/\lambda_c)^2 \qquad \text{...(6)}$$

so that (3) and (4) approximate closely to:

$$z_{0H} \fallingdotseq j\frac{\lambda_0}{\lambda_c}\sqrt{\frac{\mu}{\epsilon}} \qquad \text{...(7)}$$

and

$$\gamma_0 \fallingdotseq \frac{2\pi j}{\lambda_0}\sqrt{\mu\epsilon} \qquad \text{...(8)}$$

Thus for the H_{11} mode at 4 Mc/s with our probe unit, copper has:

$$z_{0H} \fallingdotseq (1-j)\, 6{\cdot}94 \,.\, 10^3 \times 1{\cdot}37 \,.\, 10^{-6}$$
$$\fallingdotseq (1-j)\, 9{\cdot}5 \,.\, 10^{-3}$$

while a ferromagnetic alloy having $\mu = 10^4$ and ρ = 45 microhm-cm has:

$$z_{0H} \fallingdotseq (1-j)\, 6{\cdot}94 \,.\, 10^3 \times 7 \,.\, 10^{-4}$$
$$\fallingdotseq (1-j)\, 5$$

i.e. its impedance now exceeds that of air for the same wave.

While γ_0 may contribute significantly to the screening effect for very thin and very thick screens, there may be a considerable range of practical conditions for which γ_0 is relatively unimportant and for which the reflection loss term in (1) contributes nearly all the useful insertion loss.

Expected insertion losses for particular cases. The propagation and impedance constants, the transmission, reflection and interaction losses and the resultant insertion losses have been computed for each of the screen materials and thicknesses for which measurements have been made. The relevant known or assumed properties are given in Table 1, together with the resultant insertion losses for a frequency of 4 Mc/s with the probe units described in Section 2.

Table 1

No.	Material	Thickness microns	Resistivity microhm-cm	Resultant insertion loss				
				$\mu = 1$	10	100	1000	10 000
1	Aluminium	5	2·8	14·4	—	—	—	—
2	Copper	23	1·7	31·2	—	—	—	—
3	,,	50	1·7	39·1	—	—	—	—
4	Nickel	27	7·2	19·9	21·6	37·1	108·6	—
5	Radiometal	55	45	11·5	13·0	27·3	90·2	—
6	Mumetal	33	60	6·4	7·1	13·5	47·2	154·6
7	,,	60	60	10·3	11·7	25·5	85·2	275
8	Titanate ceramic	1 800	$\epsilon = 30$	9·0	—	—	—	—
9	Ferrite ceramic	1 800	$\epsilon = 40\,000 \underline{/-20^\circ}$			43·7 for $\mu = 800\underline{/-30^\circ}$		
10	Air	1 800	$\epsilon = 1$	9·0	—	—	—	—

In the cases where there is an approximate impedance match the reflection "loss" becomes a slight gain, and the interaction loss is then negligible (although in most of the cases considered the rising transmission loss alone largely determines the latter result). The interaction "loss" can become a considerable gain, but never a serious loss.

It is particularly interesting to note how slowly the total insertion loss rises initially as the assumed magnetic permeability is raised. This behaviour is due to the initial decrease of reflection loss exceeding that of interaction gain. If the sample is made very thin, so that the transmission loss becomes very small, it is readily seen that the total loss is determined by:

$$\left|\frac{1 - r^2 e^{-2\gamma_0 t}}{1 - r^2}\right| \longrightarrow \left|\frac{1 - r^2(1 - 2\gamma_0 t)}{1 - r^2}\right| \longrightarrow \left|1 + \frac{2r^2\gamma_0 t}{1 - r^2}\right| \qquad \ldots(9)$$

If now $|z_0| \ll 1$, so that $r \to (1 - 2z_0)$ and $r^2 \to (1 - 4z_0)$ or $(1 - r^2) \to 4z_0$, and $r^2 \to 1$, then (9) becomes

$$1 + \gamma_0 t/2z_0 \qquad \ldots(10)$$

But from (7) and (8) we have

$$\gamma_0/z_0 \doteqdot 2\pi\lambda_c\epsilon/\lambda_0^2$$

so that, making use of (5), (10) becomes:

$$1 - 2\pi j t\lambda_c/\lambda_0\rho c \qquad \ldots(11)$$

where c = velocity of light in air.

Thus, within the restrictions stated above, the insertion loss of a thin enough screen is independent of its magnetic permeability. The loss is, however, frequency-dependent through the term λ_0.

We cannot extrapolate (11) to obtain the static screening effect because the second approximation (6) becomes invalid at low frequencies. At extremely low frequencies, (3) and (4) become:

$$z_{0H} \doteqdot \mu \qquad \ldots(12)$$

and

$$\gamma_0 \doteqdot 2\pi/\lambda_c \qquad \ldots(13)$$

Then (9) becomes

$$1 + \frac{\pi t}{\lambda_c}\frac{(\mu - 1)^2}{\mu} \qquad \ldots(14)$$

for H waves, and is of the same form as the classical magneto-static result (King, 1933).

The ferrite sample has an intermediate behaviour owing to its considerable electrical thickness relative to the probe hole diameter and the wave mode considered.

5. SOME EXPERIMENTAL RESULTS

In this section some preliminary measurements on non-magnetic and magnetic materials will be quoted and briefly commented upon. The materials and thicknesses are listed in Table 1. Mumetal samples were measured both in the cold-rolled and annealed conditions, and all the measurements given below were made at 4 Mc/s, with the probe units described in Section 2. The accuracy of insertion loss measurement is about $\pm$ 1 db below 20 db, progressively becoming worse as the spurious crosstalk and noise level is reached at about 40 db. The results are given in Table 2.

Table 2

Sample No. and condition	Measured insertion loss, db	
1	10	
2	30 to 36	
3	40	
4	16 to 17	
5	10 to 16	10 db "as received", 16 db some days later.
6, cold-rolled and electropolished ..	2	Actual sample thickness may be only 30 microns near edge of probe hole.
6, annealed	10	
7, cold-rolled	14	
7, annealed	40	
8, minus 10	0	
9, minus 10	20 to 30	Accuracy limited by greater basic loss.

The measurements on the relatively thick non-metallic samples were made in terms of the change of received signal when the sample was withdrawn to the side of the gap between the flat faces of the probe units, these faces still being in contact with the samples to maintain their separation constant.

No change of insertion loss was found for any of the magnetic samples as these were rotated relative to the plane of polarization of the transmitted waves.

Comparison between Tables 1 and 2 shows a low observed loss for the aluminium foil. This is probably related to imperfections in the foil revealed as numerous very small pinholes when the foil is held up to a strong light. The agreement for the copper samples is satisfactory, and likewise for the titanate ceramic. The ferrite ceramic result is qualitatively as expected, but the measurement accuracy is inadequate to permit any precise conclusions. In the case of the magnetic metal samples, however, the experimental results do seem to throw useful new light on the permeabilities involved.

Thus for nickel it appears that the effective permeability cannot be significantly greater than unity, unless the resistivity of the sample were notably greater than the figure assumed. For the Radiometal and the un-annealed Mumetal samples the permeability must be below 100: the un-annealed electropolished specimen gives an anomalously low insertion loss, possibly arising from fringing field effects around its rather thin edges just beyond the boundaries of the probe holes. The thicker annealed Mumetal sample has an effective permeability of over 100, while for the thinner annealed sample it appears to be under 10. But further tests on a more uniform 40-micron Mumetal un-annealed sample gave only 3 to 4 db insertion loss.

6. INTERPRETATION OF RESULTS

The permeability values which must be put into the theory to give agreement with the measured insertion losses for the un-annealed magnetic metals, and even for the thinner annealed Mumetal, are much below the values usually measured for the same materials in the same form. The discrepancy may in part be due to the presence of higher order H_{1n} modes, for these must have smaller λ_c values, leading (up to a point) to smaller reflection losses, which can in turn be made up by higher transmission loss associated with higher μ. The expected high μ values would, however, in most cases give much greater transmission losses than the measured insertion losses (i.e. for the un-annealed samples).

One remaining consideration perhaps contains the clue to the discrepancy. The magnetic field used in the ordinary measurement of permeability is essentially everywhere parallel to the surface of the sample, whereas in our H_{11}-mode measurements the field has a component normal to this surface. In our theory we have assumed the permeability to be isotropic. Now it seems very reasonable on physical grounds (see below) that the μ value normal to the surface of a thin specimen may be much lower than that parallel to the surface. It would be expected that this type of anisotropy, having low μ parallel to the direction of propagation of our H_{11}-waves, would modify the wave mode so as to stretch the H-field pattern in the direction of propagation, thereby reducing the phase and attenuation constants, and also the normalized impedance. The total insertion loss would then fall, and the material would behave like one having a low isotropic μ value.

The physical reasonableness of a low μ normal to the surface of a thin sample follows at once from the domain-wall displacement theory of ferromagnetic permeability. For nearly all the domains are magnetized in a direction parallel (or nearly so) to the surface, only a small volume of "closure" domains at the edges being magnetized normal to the main surface. Hence wall displacements can hardly contribute much permeability normal to the surface. In a thick sample on the other hand, internal domains can exist magnetized normal to the surface, and their growth and contraction under the influence of the normal field can contribute a large permeability in this direction.

There is also a possible mechanism of a low and isotropic permeability in annealed Mumetal—although in fact this behaviour has not yet been observed experimentally. Low μ could appear at the frequency of measurement because this frequency happened to be somewhat above the domain-wall displacement resonance frequency (e.g. as discussed by Becker, 1951). Although this resonance frequency is of the order of 10^2 to 10^3 Mc/s for iron and nickel, it is probably considerably lower for alloys having high permeability at low frequencies.

7. FURTHER DISCUSSION

Two further points arise from the preceding Section: (i) Can we determine the permeability parallel to the surface by means of our transmission technique ? (ii) Can we explore the interior of a sample for possible systematic variations of permeability with depth below the surface ?

(i) In theory we can use purely transverse H (relative to the direction of propagation) by employing the circular E_{01} wave mode, replacing the loop by a straight axial wire in each probe unit. This mode results, however, in a reflection loss quite out of range of the present measuring set-up. Such extremely thin films would be needed to obtain a measurable insertion loss that doubt would exist as to the proper electrical resistivity. Nevertheless, such experiments may be of value.

(ii) The insertion loss theory given at length in Section 4 is valid at any frequency, and measurements of insertion loss over a wide frequency range, on comparison with the calculated values, would in the first place indicate how μ might be changing with frequency. Only certain types of permeability variation with frequency are physically possible. Variations of measured insertion loss inconsistent with these could be interpreted in terms of a more elaborate theory in which the sample is treated as a succession of two or more layers of different permeability.

Insertion loss measurements on a number of samples of different thicknesses would be valuable if it could be assumed that μ did not change for physical reasons as the thickness was changed. Insertion phase-shift measurements, coupled with the relevant theory parallel to that of equation (1), would enable the same information to be obtained with fewer test frequencies.

8. CONCLUSIONS

The transmission theory outlined in the preceding Sections appear to be adequate for the experimental arrangement described, and to be capable of extension to a wide range of other possible arrangements. Satisfactory agreement between theory and experiment has been obtained for non-magnetic materials, and the observed discrepancies for magnetic metal strip samples strongly indicate that the permeability is much lower perpendicular than parallel to the surface of thin samples.

Considerable further work is desirable (*a*) to improve the sensitivity of the experimental set-up, (*b*) to carry out measurements over as wide a range of frequencies as possible, and (*c*) to extend the measurements to thicker and to much thinner samples, especially of high-permeability alloys. It would be interesting to attempt Faraday rotation measurements on thin metal samples using this technique with the circular H_{11} mode, the receive probe unit serving as a polarization analyser on a null-position basis.

Acknowledgment is made to the Engineer-in-Chief of the Post Office Engineering Department for permission to use the information given in this paper.

DISCUSSION

Mr. P. R. Bardell:

To what extent may the very low measured values of transverse permeability in metal strip be attributed to the self-demagnetizing effect resulting from the low value of the ratio of length to thickness of specimen?

Mr. F. F. Roberts (in reply):

This self-demagnetizing effect is automatically allowed for in the reflection-loss term of the theory.

19

IRREVERSIBLE MAGNETIC-VISCOSITY EFFECTS

R. Street and J. C. Woolley

(The University, Nottingham)

Abstract: An account is given of the activation energy theory of irreversible magnetic viscosity. The theory is applied to the two cases when the field applied to a specimen undergoing magnetic viscosity is changed (1) discontinuously or (2) continuously. The latter result is of direct interest when measurements of magnetic viscosity are made on specimens having non-zero demagnetization factors. The experimental results which are presented are shown to be in good agreement with the predictions of the theory. Finally, the formal relationship between the present theory and that of Néel is discussed briefly.

1. INTRODUCTION

As pointed out by Néel (1951), magnetic-viscosity effects may be divided into at least two different classes which are described as reversible and irreversible magnetic viscosity. Experimentally, the two classes are most clearly distinguished from each other by their sensitivity to temperature. The enormous temperature-sensitivity of reversible viscosity may be explained on the hypothesis advanced by Snoek (1947, p. 37) that impurity atoms diffusing through the lattice are responsible for the time-variation of intensity of magnetization. Irreversible magnetic viscosity is relatively little affected by changes in temperature. It is now generally agreed that irreversible magnetic-viscosity phenomena are essentially due to thermal activation of the fundamental domain processes responsible for the magnetization of a ferromagnetic material, and two formal theories of the phenomenon have been proposed by Néel (1951) and Street and Woolley (1949a).

Reversible magnetic viscosity can occur only in certain substances while all ferromagnetic materials should exhibit irreversible magnetic-viscosity effects. In the work summarized in this paper a study was made of the irreversible magnetic viscosity occurring in a permanent-magnet alloy, but it is believed that the results are applicable, at least in general form, to all materials exhibiting irreversible magnetic viscosity.

Direct measurements of magnetic viscosity are usually made by suddenly changing the field applied to a specimen at zero time and then following the change in its intensity of magnetization, either by means of a magnetometer or a ballistic galvanometer. The object of the work described here was to determine the influence on magnetic viscosity of (*a*) small discontinuous field changes applied after the beginning of the experiment, and (*b*) the continuously variable demagnetizing field set up by the increasing intensity of magnetization of the specimen. As will be seen below it is possible to

describe both these effects in terms of the formal theory of magnetic viscosity (Street and Woolley, 1949a); in the analysis a parameter is introduced which is related to the volume of the material affected by the activation process.

2. THE ACTIVATION-ENERGY THEORY OF IRREVERSIBLE MAGNETIC-VISCOSITY

The fundamental assumption at the basis of the theory* is that over certain ranges of the magnetization curve of a ferromagnetic specimen, following an initial sudden increase in the applied magnetic field, there are domains (or regions of domains) having their magnetization vectors in orientations of metastable equilibrium. It is supposed that transitions to more stable orientations may take place by thermal activation, i.e. the thermal agitation

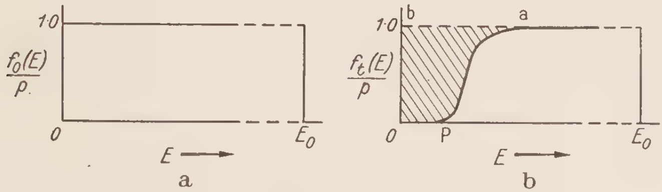

Figure 1. Distribution of activation energies.

of the material supplies the necessary activation energy for such transitions to occur. In the analysis it is necessary to know the initial numbers of domains having activation energies lying within a range E to $E + dE$, i.e. the initial distribution function $f_0(E)dE$. Good agreement between the predictions of the analysis and the experimental results is obtained if it is assumed that $f_0(E)$ is a constant for those domains which are activated during the time required for a magnetic-viscosity experiment. Thus $f_0(E)dE$ may be replaced by pdE, where p is a constant independent of E. The idealized distribution function is represented in Figure 1(a).

As thermal activation proceeds the value of $f(E)$ for the lower E values will progressively and significantly diminish with time. The distribution function $f_t(E)$ at time t after the beginning of the experiment has the form indicated in Figure 1(*b*) ; the hatched area OPab represents those domains which have been activated in time t. It is next assumed that on the average each of the domains so activated contributes the same amount $\bar{i}$ to the holomagnetization of the specimen and thus $\bar{i}$ (area OPab) represents the increase in intensity of magnetization, due to magnetic viscosity, in time t. It may be shown that the profile, Pa, the lower energy limit of the distribution function, moves to the right of the diagram at a speed inversely pro-

*Street and Woolley, 1949a, 1950

portional to the time which has elapsed from the beginning of the experiment (see Section 3 below). It therefore follows that the area swept out by Oa, and hence the intensity of magnetization of the specimen, increases logarithmically with time. This is the type of time-dependence observed experimentally using specimens exhibiting irreversible magnetic viscosity and is characteristic of the phenomenon.

3. DISCONTINUOUS CHANGES OF APPLIED FIELD

When the magnetic field applied to a specimen is changed discontinuously the magnetostatic energy of the domains is also changed. If the total change of energy consequent upon the change in applied field exceeds the activation energy of any set of domains, this will be activated and hence will make an irreversible contribution to the intensity of magnetization of the specimen. This case has already been considered (Street and Woolley, 1950). In the present paper the case where the applied-field change is not directly and instantaneously responsible for an irreversible increase in the intensity of

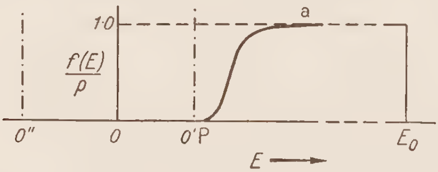

Figure 2. Activation energies in an external field.

magnetization will be discussed. The situation may be represented diagrammatically as in Figure 2. In this diagram O is the origin of the axis of activation energy in the absence of any change in the external field. When an increment in external field ΔH_e is applied it will be assumed that the resulting change in domain energy may be represented by a change in the origin of the activation energy axis. ΔH_e will be defined as having a positive sign if its application results in a decrease in activation energy. Thus in Figure 2 it is assumed that positive ΔH_e changes the origin of activation energy from O to O'; a negative ΔH_e serves to displace the origin from O to O''. Qualitatively, then, the time rate of increase of the intensity of magnetization should respectively increase or decrease when positive or negative increments of field are applied. This is in fact observed, as may be seen from the typical results plotted in Figure 3. A quantitative analysis of the process will now be given; for simplicity the ideal case applicable only to a specimen having zero demagnetization-factor will be considered. The results obtained from an analysis taking into account the effect of non-zero demagnetization-factor are essentially similar, and it is intended to publish this elsewhere.

The rate at which domains are being activated, at a constant absolute temperature T, is given by the usual equation

$$df(E)/dt = - Cf(E) \exp(-E/kT) \qquad \ldots(1)$$

where $f(E)$ is the number of domains having activation energies lying between E and $E + dE$ at time t, and C is a constant. Equation (1) may be integrated to give :—

$$f(E) = p \exp[-Ct \exp(-E/kT)] \qquad \ldots(2)$$

after inserting the initial condition that $f_0(E) = p$.

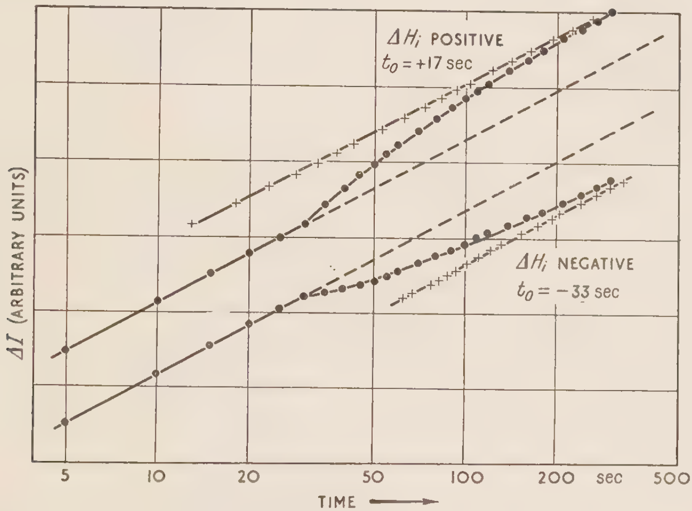

Figure 3. Time rate of increase of magnetization in a typical material.

Now the position of the profile Pa along the E-axis of Figure 2 can be conveniently defined as that value of E for which $f(E) = \frac{1}{2}p$. Hence the position of the profile E at time t may be derived from (2):—

$$\tfrac{1}{2} = \exp[-Ct \exp(-E/kT)] \qquad \ldots(3)$$

The rate at which the mid-point of the profile moves to the right of the diagram in Figure 2 is given immediately from (3) by differentiation, for $dE/dt = kT/t$. Hence, so long as sufficient time has elapsed from the beginning of the experiment for the profile to be completely formed, the area it sweeps out, and hence the increase in holomagnetization, will be proportional to ln t or

$$\Delta I = K + S \ln t \qquad \ldots(4)$$

where K and S are constants. The breakdown of this relation for values

of $t \to O$ may be seen from Figure 1*b*, for in this time range the profile has not reached its equilibrium form and the rate of increase of ΔI will be less than the value given by $1/t$. Our experimental observations show, however, that equation (4) accurately represents the time variation of ΔI, at least for times $t > 0{\cdot}5$ sec. Barbier (1953) has shown that for certain specimens the logarithmic relation holds for times t as small as $0{\cdot}025$ secs. (The interpretation of our experimental results for $t < 0{\cdot}5$ sec. is uncertain due to the disturbing effects of eddy currents.)

Consider now the situation which exists when a change ΔH_i occurs at time t_1. (In the ideal case of a specimen possessing zero demagnetization coefficient, $\Delta H_e = \Delta H_i$.) Just before ΔH_i is applied the position E_1 of the mid-point of the profile (with respect to the origin O of the E-axis) is given, from equation (3), by

$$\tfrac{1}{2} = \exp\left[-Ct_1 \exp\left(-E_1/kT\right)\right] \qquad \ldots(5)$$

Immediately after the application of ΔH_i the origin of the activation-energy axis moves to some point, say O' (Figure 2) where $OO' = E'$, the change in activation energy of the domains. Now E' is some function of ΔH_i and may be written $E' = F(\Delta H_i)$. The distance of the mid-point of the profile from the new origin of activation energy O' is now $(E_1 - E')$. When ΔH_i is positive the increased rate of recession of the profile at time t_1 is exactly equal to the rate of recession which occurred at some earlier time $(t_1 - t_0)$ where t_0 is defined by:—

$$\tfrac{1}{2} = \exp\left[-C\,(t_1 - t_0) \exp - (E_1 - E')/kT\right] \qquad \ldots(6)$$

The case when ΔH_i is negative is exactly similar in form.

Thus the time variation of ΔI for times $t > t_1$ will be of the form $S \ln (t - t_0)$, i.e. the change in the origin of activation energy has been transformed into a change in the time origin. If ΔH_i is positive, both t_0 and E' are positive, whereas if ΔH_i is negative both t_0 and E' are negative.

From equations (5) and (6)

$$\ln\, t_1/(t_1 - t_0) = E'/kT = F(\Delta H_i)/kT \qquad \ldots(7)$$

This relation may be shown to hold also for specimens with non-zero demagnetization coefficients (Street, Woolley and Smith, 1952).

The first point to be settled experimentally is whether the observed time-variation of ΔI for times $t > t_1$ can be represented in the form $S \ln (t - t_0)$. In Figure 3 the experimental results have been replotted with a change in the time origin $= t_0$. (The methods of computing t_0 from the observations need not be considered here.) It will be seen that to a good approximation the time-variation of ΔI does conform to an equation of the form $S \ln (t - t_0)$ as predicted, for both positive and negative values of ΔH_i.

The predictions of equation (7) have also been checked by the following experiments:—

(i) With ΔH_i kept constant in magnitude and sign, t_0 has been determined for a range of values of the time of application of ΔH_i, i.e. t_1. In Figure 4, curve (a) shows a typical set of results, plotting $(t_1 - t_0)$ as a function of t_1 with $\Delta H_i = +1{\cdot}00$ oersted. As predicted from equation (7) there is a linear relation between $(t_1 - t_0)$ and t_1 for constant $F(\Delta H_i)$. Curve (b) shows a similar set of results obtained with $\Delta H_i = -1{\cdot}00$ oersted and again linear dependence is observed.

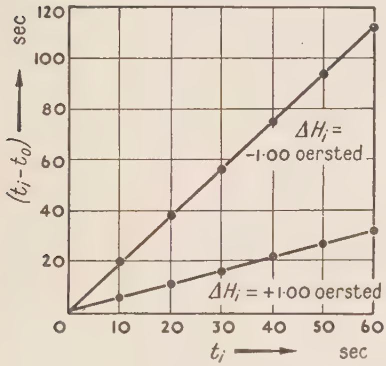

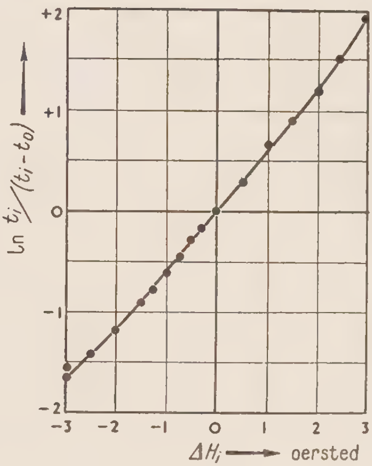

Figures 4 and 5. Experimental checks of equation (7).

(ii) Experiments were carried out with values of ΔH_i varying from $+3{\cdot}00$ to $-3{\cdot}00$ oersteds and the results are plotted in the form $\ln t_1/(t_1 - t_0)$ against ΔH_i in Figure 5. It will be seen that within the limits of experimental error $\ln t_1/(t_1 - t_0)$ is a linear function of ΔH_i*, and thus from equation (7)

$$F(H\Delta_i) = q\Delta H_i = E' \qquad \ldots(8)$$

where q is a constant which may be determined from the experimental results.

The results presented above thus justify to a rather remarkable extent, considering the approximations made, the assumption that a change in the applied internal field results in a simple change in the activation energy of the domains which take part in magnetic viscosity. The experimental conclusion that the change in activation energy is linearly proportional to the change in internal field can now be applied to a consideration of the case (b) of Section 1.

* At least within the range $-2 < \Delta H_i < +2$ oersted.

4. CONTINUOUS VARIATIONS OF FIELD

If the intensity of magnetization of a specimen subject to magnetic viscosity increases with time according to a relation of the form given in equation (4) then, if the demagnetization coefficient, D, is not zero, the internal field varies by $-D(\Delta I)$ when the external field remains constant. From Section 2, the resulting effect on the magnetic viscosity can be represented by considering that the origin of the activation-energy axis moves continuously to the left of the diagram in Figure 2. The displacement of the origin from its initial position at any time t will then be given by

$$-qD(\Delta I) = -qD(K + S \ln t) \qquad \ldots(9)$$

Thus for specimens of identical material, but differing in their demagnetization coefficients, the larger rates of change of ΔI with time will be observed for specimens of smaller demagnetization coefficients, and vice versa. This behaviour is observed experimentally as may be seen from the results plotted in Figure 6. (From these results, the logarithmic variation of ΔI with time

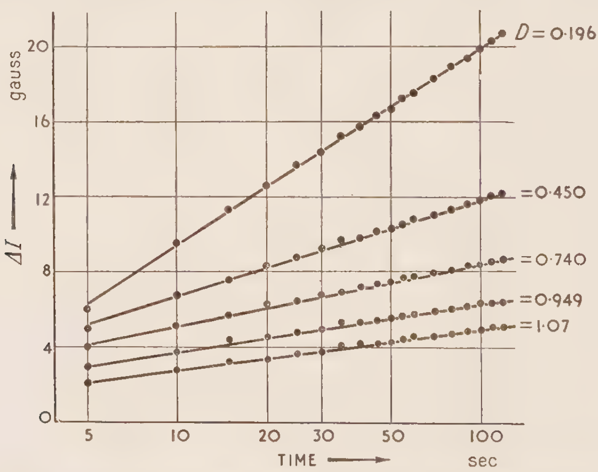

Figure 6. Effect of demagnetization coefficient on magnetic viscosity.

is not appreciably affected by the variable demagnetizing field. An analytical demonstration of this result, *ab initio*, appears to be intractable.)

If, at time t, $f(E)dE$ is the number of domains having activation energies lying between E and $E + dE$, *measured from the origin of activation energy at time zero*, then the rate of activation of these domains at t will be from (9):—

$$-df(E)/dt = Cf(E) \exp[-(E+qDS \ln t+m)/kT] \qquad \ldots(10)$$

where m is written for qDK. It can be shown (Street, Woolley and Smith,

1952) that this equation, on solution, gives

$$\Delta I = S_0(1 - qDS/kT) \ln t \qquad \ldots(11)$$

for the time-dependence of the intensity of magnetization, where $S_0 \bar{t} = pkT$. S_0 is in fact the slope of the $\Delta I/\ln t$ graph which would be obtained using an ideal specimen with zero demagnetization-coefficient.

Equation (11) only gives the increase in magnetization due to irreversible activation phenomena. In addition since the demagnetizing field changes with time there will be a corresponding reversible change of the intensity of magnetization. The observed time-dependence of magnetization will be

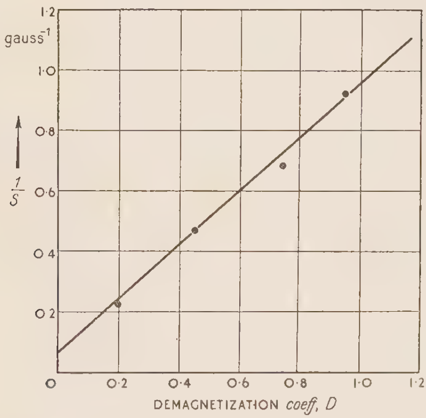

Figure 7. Experimental check of equation (13).

the algebraic sum of the reversible and irreversible contributions and is given by an equation of the form

$$\Delta I = [S_0(1 - qDS/kT) - D\chi_{rev} S] \ln t \qquad \ldots(12)$$

where χ_{rev} is the reversible susceptibility of the material. Comparison of equations (12) and (4) leads to

$$1/S = 1/S_0 + D(q/kT + \chi_{rev}/S_0) \qquad \ldots(13)$$

Equation (13) may be checked directly from the experimental results shown in Figure 6 and knowing χ_{rev} a value of q/kT may be derived. The result is shown graphically in Figure 7, in which the reciprocals of the slopes of the lines in Figure 6 are plotted against D. The straight line obtained confirms the predictions of (13), within the limits of experimental error, and from the slope of the line $q/kT - 0{\cdot}83$ oersted^{-1}. The latter value agrees well with the value of $q/kT = 0{\cdot}82$ oersted^{-1}, obtained by the method of discontinuous field-variation described in Section 3, using the

longest specimen of the set. The good agreement between these values, determined by independent experimental methods, demonstrates the value of the formal theory and justifies the necessary approximations made in its development.

5. COMPARISON WITH NÉEL'S THEORY

Since it has been assumed above that magnetic viscosity is due to the activation of irreversible domain processes, it follows that there should be a formal relation between the parameters characteristic of the magnetic viscosity and the irreversible susceptibility. This relation has been derived (Street, Woolley and Smith, 1952) and is

$$qS_0/kT = \chi_{irr} \qquad \text{...(14)}$$

where χ_{irr} represents the irreversible susceptibility of the material of the specimen. Hence from (14)

$$kT/q = S_0/\chi_{irr} \qquad \text{...(15)}$$

S_0/χ_{irr}, and hence kT/q, is in fact equal to the fictitious-field constant introduced by Néel to account for irreversible magnetic viscosity; this is referred

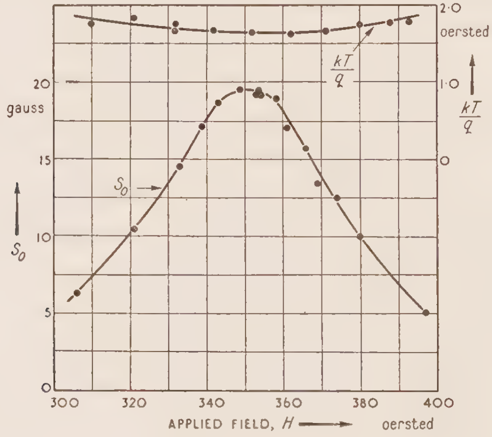

Figure 8. Experimental check of equation (15).

to as S_v (e.g. by Barbier, 1953). It thus appears possible to link up in a formal way the treatments of magnetic viscosity, one starting from the postulate of a fictitious field and the other from a consideration of activation processes.

Measurements have been made on a specimen of Alnico having a coercive force of 350 oersteds, to determine the quantities kT/q and S_0 at different points on the hysteresis cycle of magnetization. The results are plotted on Figure 8, and it will be seen that although S_0 varies widely over the cycle,

the value of kT/q is reasonably constant and independent of the point at which measurements are made. The latter observation confirms that reported by Barbier (1953).

6. PHYSICAL INTERPRETATION OF THE RESULTS

From equation (8) it can be seen that the quantity q is the coefficient relating the change in activation energy to the change in internal field. By using a somewhat simplified model of the magnetization process, and assuming that magnetization proceeds by movement of boundary walls, it is possible to

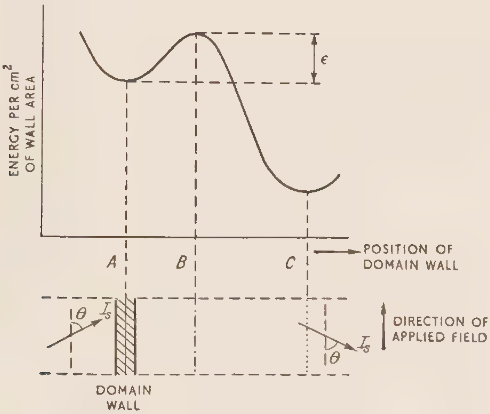

Figure 9. Model to illustrate activation-energy of a domain wall.

interpret q in a rather more definite physical form. Consider the variation of the energy of a system of two domains as a function of the position of the boundary wall separating them, assuming constant internal field conditions. The situation envisaged is sketched in Figure 9. As a result of the previous magnetic treatment let the boundary wall occupy the mean position A. Due to thermal agitation, the nature of which does not enter into the argument, the boundary wall will oscillate at random. The activation energy ϵ per sq. cm. of wall area is indicated on Figure 9 and is the difference in energy with the boundary wall at positions B and A. Suppose now that the internal field changes by an amount ΔH_i. The resulting change in the *difference* of the energies of the system (per sq. cm. of wall area) with the wall at B and A is $2 \cos \theta . I_s . \Delta H_i . \delta l$, to the first order in ΔH_i, where δl is the distance from A to B. If the mean area of the boundary wall is $\bar{a}$, the change in activation energy of the system is $E' = 2 \cos \theta . I_s . \bar{a}\, \delta l . \Delta H_i$. Hence, comparing with equation (8),

$$q = 2 \cos \theta . I_s . \bar{a} . \delta l.$$

If magnetization proceeds by movement of 180° boundary walls

$$q = 2I_s \,.\, \bar{a}\delta l \qquad \ldots(16)$$

As a measure of the order of magnitude of the volume $\bar{a}\delta l$, the mean value of q derived from measurements on an Alnico specimen ($H_c = 350$ oersted) has been substituted into (16) and $\bar{a}\delta l \doteqdot 10^{-17}$ cm^3, assuming a mean value of $I_s = 10^3$ gauss. In this case $\bar{a}\delta l$ is of the same order of magnitude as the volume of a cube of linear dimensions equal to the thickness of a boundary wall (about 200 Å).

From Figure 9, when the domain system acquires sufficient energy to carry the boundary wall over the potential-energy barrier at B, the wall will reach stable equilibrium at position C. The contribution to the intensity of magnetization after activation, $\bar{\imath}$, is equivalent to a re-orientation of the magnetization vector in the volume of the domain system included between the positions of the wall A and C. The volume of the material contributing to $\bar{\imath}$ is thus not necessarily related to the volume $\bar{a}\,.\,\delta l$, on this interpretation.

20

THE ASSESSMENT OF INHOMOGENEITY IN THIN STRIPS OF HIGH-PERMEABILITY ALLOYS

A. C. Lynch

(Post Office Engineering Research Station)

Abstract: The permeability of layers near the surface of a strip can be measured by using frequencies so high that the flux penetrates no further than the layers in question.

The layers on nine samples were of the order of 10 microns thick, and their mean permeability was of the order of 10 000. They cannot account for the observed loss at low frequencies, most of which is probably "residual loss".

1. INTRODUCTION

Measurements of thin strips of high-permeability nickel-iron alloys often suggest that the permeability is not uniform through the whole thickness of the strip; it tends to be low near the surfaces. If this is so, the alternating-current loss is greater, and the permeability at high frequencies is less, than those of a uniform strip. It is also well known that the permeability varies widely between one specimen and another, and this might perhaps be due to the presence of low-permeability layers on some specimens but not on others. This explanation, however, was already doubtful, and the present work confirms that even material having a high average permeability may have these surface layers.

Feldtkeller (1949a) interpreted the excess loss at low frequencies as additional eddy-current loss and used it as a measure of the inhomogeneity. This may sometimes be permissible. But as Epelboin (1951a) pointed out, this excess loss might also be caused by "magnetic viscosity". Halsey (1950) had assumed that both sources of loss were present, but it is not clear how he could distinguish one from the other. Hence we need some additional technique for showing whether the permeability is uniform. Two methods have been used. One is measurement of the permeability after the surface layer has been removed by either etching (Peterson and Wrathall, 1936) or electropolishing (Epelboin, 1951a), but the work on which the present paper is based is concerned mainly with strip of thickness 50 microns or less, which is difficult to etch or electropolish uniformly. The other method is the measurement of the permeability at very high frequencies, at which the magnetic flux is concentrated in the outer part of the strip (Feldtkeller, 1949a, pp. 85-102). The present paper gives a new method of analysis of the high-frequency data which is rougher than Feldtkeller's (but as good as the data justify), and some examples which suggest that Feldtkeller's model is not always satisfactory.

2. THEORY OF METHOD

Suppose the specimen, of total thickness a, to consist of material of permeability μ_1, with a layer at each surface having permeability μ_2 and thickness ma. (See Figure 1.)

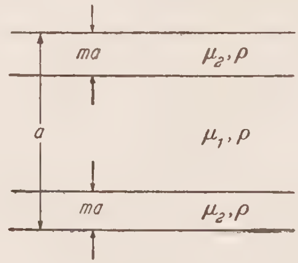

Figure 1. The model assumed for the calculation.

The resistivity of both layers is ρ*. Consider the frequency f_m such that the depth of penetration of flux is ma. The properties of the specimen at this frequency would be unaltered if the central part were removed and replaced by material of permeability μ_2, thus making a uniform strip. The properties of this uniform strip can be described by the usual equations, and for a given value of resistivity there is only one value of μ_2 which results in the observed inductance at the frequency f_m.

The specimen carries a winding, of which we measure the inductance L. Let L_0 be the inductance at low frequencies, L_m the parallel inductance at frequency f_m.

Then
$$\frac{L_m}{L_0} = 2m\frac{\mu_2}{\bar{\mu}} \qquad \ldots(1)$$

where $\bar{\mu}$, the mean permeability, $= 2m\mu_2 + (1 - 2m)\mu_1$.

Also, from the usual theory for a uniform strip,

$$\frac{L_m}{L_0'} = \frac{1}{\mu\sqrt{f_m/f_2}} \qquad \ldots(2)$$

where L_0' is the inductance at low frequencies of our fictitious uniform strip and f_2, its "characteristic frequency",† is $\rho/\mu_2 a^2$.

But
$$\frac{L_0'}{L_0} = \frac{\mu_2}{\bar{\mu}} \qquad \ldots(3)$$

Combining equations (1), (2) and (3),

$$L_m f_m = \frac{1}{2\pi^2{}_m} L_o f_o \qquad \ldots(4)$$

* Epelboin (1951b) suggests that the resistivity may also vary, but this effect is not likely to be large.
† This is greater than Feldtkeller's "Grenzfrequenz" by a factor π^2. (Note that his μ_A is in a system of rationalized units.)

If we have chosen a value of m, and wish to know the ratio $\mu_2/\bar{\mu}$ for a layer of this thickness, we can now plot (on log-log paper) a curve for L against f, and also the straight line of equation (4): their intersection gives L_m, and equation (1) then gives the required ratio. The value of μ_2 found in this way is, of course, an average for the layers; the permeability may not actually change abruptly from one layer to another.

This calculation can be repeated for various values of m. The process is limited only by the difficulty of measuring L at sufficiently high frequencies. Then when we have found the mean permeability between the surface and a depth x, and also that between the surface and a depth y, we can deduce the permeability of the layer between depths x and y.

An important difference between this treatment and Feldtkeller's is that it makes use of measurements at frequencies such that the flux penetration is limited to the layers in question. Admittedly these measurements are difficult. Feldtkeller's treatment uses frequencies between one-hundredth and one-tenth of these, and is permissible only if the particular model that he uses represents the distribution of permeability sufficiently closely.

3. EXPERIMENTAL RESULTS

The following results were obtained with material from nine different casts of Mumetal (approximately 76% Ni, 14% Fe, 5% Cu, 4% Mo), which was available in both 50 and 200-micron thicknesses. The specimens consisted of flat rings, punched from wide strip. They were annealed in hydrogen for 3 hours at 1050°C, and cooled at the natural rate of cooling of the furnace (of the order of 100°C per hour). Five such rings were stacked together, insulated by paper and protected by a polystyrene former. A 20-turn toroidal winding was applied, and its inductance and resistance measured at frequencies from 1 kc/s to 50 Mc/s.

The results were:—

Cast No.	Thickness, microns	Mean permeability, $\bar{\mu}$	Mean permeability of layers		
			from surface to 5 microns	from 5 to 25 microns	more than 25 microns from surface
1	200	21 500	4 000	14 500	24 000
	50	12 000	6 100	13 500	—
2	200	35 000	9 700	24 000	39 000
	50	27 000	15 000	30 000	—
3	200	24 500	8 500	21 500	25 500
	50	17 500	8 200	20 000	—
4	200	42 000	13 500	40 500	44 000
	50	32 500	13 500	37 000	—
5	200	16 500	7 500	16 000	17 000
	50	17 500	13 500	18 500	—

Continued on next page

Cast No.	Thickness microns	Mean permeability $\bar{\mu}$	Mean permeability of layers		
			from surface to 5 microns	from 5 to 25 microns	more than 25 microns from surface
6	200	29 000	9 500	26 500	31 500
	50	20 000	10 000	22 500	—
7	200	37 000	9 500	36 500	40 000
	50	16 500	8 000	18 500	—
8	200	44 000	15 000	37 500	47 000
	50	28 000	19 500	30 500	—
9	200	31 000	12 000	26 500	33 000
	50	16 000	7 200	18 000	—

Knowing from these figures how the permeability varies with depth, we can deduce (by the method given by Feldtkeller, 1949a, p. 84) the additional low-frequency loss introduced by inhomogeneity. We write "g" for the ratio of the loss in the inhomogeneous strip to the calculated loss in a uniform strip of the same mean permeability. This ratio g is Feldtkeller's η. We have to assume that the permeability at the surface is small; if this assumption is wrong the calculated value for the ratio g will be too high. For the 200-micron specimens we find:—

Cast No.	Feldtkeller's index k	g calculated	g observed
1	7	1·23	1·62
2	9	1·17	1·39
3	12	1·14	1·39
4	16	1·12	1·36
5	34	1·07	1·14
6	17	1·11	1·47
7	11	1·15	1·26
8	18	1·11	1·37
9	23	1·09	1·33

The differences between the last two columns may be the result of "magnetic viscosity", or, using the language of powder-cores, "residual loss".

The observed value of g is not quite constant with frequency and in the table it has been quoted for frequency $\rho/20\bar{\mu}a^2$, which is low enough for the parallel resistance to be practically unaffected by eddy-current screening. This variation with frequency is alone enough to show that there is some source of loss other than inhomogeneity.

4. CONCLUSIONS FROM THIS WORK

A typical high-permeability nickel-iron alloy has surface-layers of lower permeability than the rest of the material; but in the nine casts tried, of widely differing permeability, the layers are thinner (of the order of 10 microns) and their permeability is higher (of the order of 10 000) than some of the earlier workers had reported (Peterson and Wrathall, 1936; Feldtkeller, 1949a, p. 102). The present results more nearly resemble those of Epelboin (1951a), and the thickness of the layer agrees with that observed by x-ray methods by Wyart and Epelboin (1949). As suggested by Epelboin, the surface-layers seem to be generally similar on different thicknesses of material from any given cast, and of the same absolute (not relative) thickness.

Near the surface, but at a depth sufficient for measurements to be possible, the variation in permeability is not of the type which Feldtkeller discusses.

In seven of the nine casts, residual loss is more important at low frequencies than is extra eddy-current loss caused by inhomogeneity.

The Mumetal was supplied by the Telegraph Construction and Maintenance Co. Ltd.

All the measurements reported in this paper were carried out by Mr. P. C. Jones, and the information is now used by permission of the Engineer-in-Chief of the Post Office.

DISCUSSION

Mr. E. V. Walker:

In an attempt to discover the nature of low-permeability surface layers, we have examined the microstructure of a large number of samples of thin nickel-iron-molybdenum-copper strip.

We have found that on many of the samples examined there exists a surface layer of small crystals and non-metallic inclusions. The depth of the layer varies from one sample to another. Figure 2 is a photomicrograph of a thick surface layer on strip 380 microns thick.

We have measured the depth of the surface layers revealed in the microsections of six 200-micron samples* examined by Mr. Lynch.

We will call the permeabilities found for the 0-5, 5-25 and > 25 micron layers, μ_1, μ_2 and μ_3 respectively. We will assume that the strip is made up of a core of high uniform permeability (μ_3) on which exists a surface layer of uniform low permeability (μ_1) and that μ_2 is derived from two materials whose permeabilities are μ_1 and μ_3.

Consider the strip 200 microns thick: if x microns is the thickness of the material within the 5 to 25-micron layer whose permeability is μ_1, then the total thickness of the surface layer is given by the expression:—

$$20 \frac{(\mu_2 - \mu_3)}{\mu_1 - \mu_3} + 5$$

* Three of these, although included in the original version of the Paper, have been omitted from the present form of it.

The values obtained from this expression can now be compared with those resulting from direct measurement.

Samples	Depth of layer by direct measurement, microns	Depth of layer deduced from magnetic measurement, microns
1	13	15
2	7	9
3	15	15
4	15	10
5	6	11
6	9	9

Thus for four out of the six samples there is very fair agreement between the two sets of results and I suggest that the surface-layer effect is due to the lowering of permeability caused by the presence of small crystals and non-metallic inclusions.

As further support to this suggestion, we have examined the microstructure of a number of samples which Mr. Lynch's measurements have shown to be free from surface layers. Our observations confirm his.

Dr. H. H. Scholefield:

We are in accord with Mr. Walker's suggestion that non-metallic inclusions adjacent the surface are probably responsible for the "layers" inferred from magnetic measurements. We feel, however, that their presence is due to impurities in the atmosphere during heat-treatment (both intermediate during the course of rolling, and final for the development of magnetic characteristics). In these circumstances, attention should be directed not to greater care during the hot-rolling operation or subsequent descaling and pickling but to the use of pure atmospheres during intermediate and final heat treatment.

Prof. R. Feldtkeller:

Our experiences have shown that it is necessary to define the inhomogeneity factor in terms of the reciprocal of the complex impedance. The reciprocal of the complex impedance of the lamination under test is measured over a frequency range of a few c/s to a few kc/s, and the effect of eddy currents is eliminated by trial and error with a few tentatively assumed values of the inhomogeneity factor (g of the Paper). From the resulting curves, the one is chosen which agrees, in form and frequency scale, with the calculated curve, based on the assumption that the relaxation times follow a Gaussian distribution law. This gives the correct inhomogeneity factor. This criterion is very sensitive and has led, for 36% nickel-iron of various thicknesses, to inhomogeneity factors between 0·95 and 1·3. We have not yet been able to find inhomogeneity factors in the neighbourhood of 2 and certainly not above 2.

Mr. R. E. S. Walters:

Microscopic examination of nickel-iron strip can give information about the size and shape of crystals, the purity of crystal boundaries, and the character and distribution of non-metallic inclusions. Microstructure is revealed by metallographic polishing and etching.

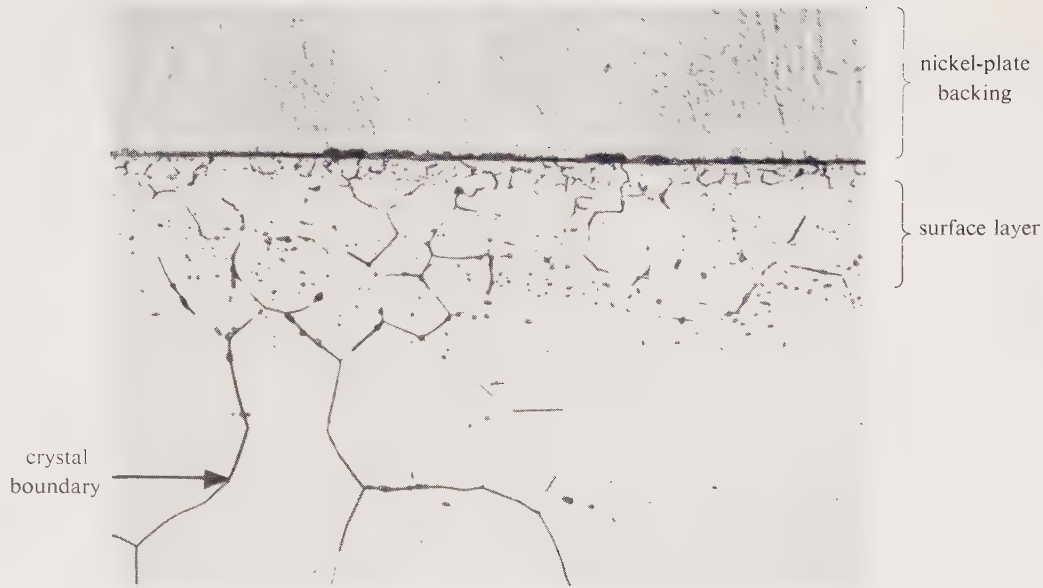

Figure 2. Microstructure of section through thickness of nickel-iron alloy strip; magnification, $\times$ 500.

For a complete picture of the microstructure of a strip, two types of section are required: (i) parallel to the rolling plane, (ii) normal to the rolling plane. The metallographic techniques used at the Post Office Research Station in the preparation of the two types of section are described below.

Sections parallel to the rolling plane can be polished either electrolytically or chemically. A suitable electrolytic method employs a bath of 60% sulphuric acid (by volume) at 30 to 60°C with a current density of about 0·5 A/cm^2; the cathode is stainless steel. A good metallographic surface is obtained in about one minute. Alternatively a chemical polishing mixture of the following composition will produce an equally good surface in about the same time:—

20 ml. glacial acetic acid
10 ml. nitric acid (sp.g. 1·42)
4 ml. hydrochloric acid (sp.g. 1·16).

The solution works at room temperature; it may be necessary to add a little hydrochloric acid from time to time if the solution is used for a long period.

Etching is usually necessary after either of the above treatments, and is carried out in a solution containing:—

90 ml. nitric acid (sp.g. 1·42)
10 ml. ortho phosphoric acid (spg. 1·75).

To about 10 ml. of this solution a few drops of hydrochloric acid are added just before the etching is to be performed. It is necessary to add further drops of hydrochloric acid if the solution is left for any length of time. The time of etching is about 15 seconds.

Sections normal to the rolling plane can be prepared only if special care is taken to preserve the outline. The best results are obtained by nickel-plating the strip before it is sectioned; this prevents disintegration and distortion of the edge during subsequent grinding and polishing.

Specimens are first cathodically cleaned to remove surface grease and dirt. This operation is most important as pickling cannot be carried out for fear of removing surface features. If the degreasing is not carefully done the adhesion of the plating is seriously impaired. The following cleaning bath has been found satisfactory:—

10% anhydrous sodium carbonate
2% sodium hydroxide
88% water.

It is used at 80 to 90°C with a loop of platinum wire as anode; current density is about 5 A/dm^2. Cleaning is continued until the surface of the specimen is completely wetted by water.

Plating is now done, using a conventional sulphate bath:—

Composition:	$\left.\begin{array}{l}240 \text{ gm } NiSO_4 . 7H_2O\\ 30 \text{ gm } H_3BO_3\\ 19 \text{ gm } KCl\end{array}\right\}$ per litre
Temperature:	40°C
Agitation:	Compressed air, bubbling over specimens
Current density:	1·5 to 2·0 A/dm.^{2}
pH:	2·0
Time:	20 hours

A nickel plate about 0·5 mm thick is deposited under these conditions.

After plating, specimens are cut on a guillotine to obtain the section required; they are then mounted in a phenolic resin with the plane of the strip vertical.

Grinding on emery papers is carried out in the usual way and is followed by polishing on the wheel with alumina on Selvyt, and the final polish is given by hand with gamma-alumina on Selvyt, the cloth being kept fairly wet.

Plated specimens cannot be etched by ordinary chemical methods owing to the protective electrochemical action of the nickel. Quite good results are obtained, however, by etching electrolytically in a 20% (by volume) sulphuric acid solution. The cathode is stainless steel, and an electrical supply of 3 V is required. Time of etching is about 15 seconds.

Figure 2 is an example of the microstructure that is revealed by the metallographic technique described above.

Dr. A. Fairweather:

It sometimes happens with 50-micron strip that metallurgical examination of a normal section including the surface does not reveal a layer whose existence has been suggested by electrical measurements. In such circumstances, the metallurgical problem might, perhaps, be eased by the use of a taper section, and of a section which includes the edge where the layer should be much thicker.

Mr. Lynch (in reply):

There can be no doubt that high values of g or σ/σ_a sometimes occur (Buckley et al., 1953; Parkin, 1953; Abgrall and Epelboin, 1952); possibly these values occur only in oriented materials or very thin strip. There is a wide variation possible for 50-micron strip (not oriented), for which I have found values of g ranging from 1·03 to 1·6. The point I wish to emphasize is that there may be more than one cause for a high value of g, and that therefore the permeability variation or "texture" cannot always be deduced from it.

21

SOME PROBLEMS OF OSCILLOGRAPHIC MEASUREMENT OF CHARACTERISTICS OF "RECTANGULAR"-LOOP MAGNETIC MATERIALS

G. R. Jackson, W. S. Melville and D. W. R. Sewell
(The British Thomson-Houston Company)

Abstract: The paper describes some developments in techniques for determining the a.c. dynamic characteristics of "rectangular"-loop magnetic materials. The special problems of the measurements are discussed and the proposed methods of overcoming them outlined. The paper is intended as a review for comment.

1. INTRODUCTION

Among the most significant results of material technology in recent years has been the translation of the desirable characteristics of single crystals of soft magnetic materials to the practical form of grain-oriented thin strip with magnetic characteristics which approach the ideal of the single crystal.

These developments have brought in their train the demand for more detailed information about the dynamic characteristics of the materials and have revealed new problems in measurement and presentation.

Many of the principles around which the art and science of magnetic material measurements have developed are rooted in the lore of the ballistic galvanometer and the a.c. bridge. These are admirable tools in their proper context and indeed for d.c. measurements the ballistic galvanometer in one form or another has not yet been superseded. On the other hand, it is open to question whether any kind of power-measuring device which depends for its operation on frequency-sensitive elements is likely to prove a reliable tool for a.c. loss measurements on non-linear materials. Even if the assumption is made that the fundamental B/H characteristic is free from non-linearity or hysteresis loss, for most practical materials the representation of the eddy-current contribution by equivalent resistive components in a bridge network is at best an over-simplification which obscures rather than reveals the nature of the phenomenon.

With the development of these special materials the problems of measurement have been thrown into even greater relief. The "rectangular"-loop characteristic imposes on the measuring circuits a range of frequency components which extends to tens of times the fundamental, and orthodox bridge or wattmeter measurements can yield no more than an approximation to the loss characteristics. One solution is to measure losses by calorimetric methods but these are tedious to apply and in some cases are even more successful than bridge methods in obscuring useful information.

2. APPLICATIONS

The need for more information is of particular significance if one bears in mind the kinds of uses to which these special materials are put. For example, in magnetic amplifiers, saturable reactors, pulsactors, pulse transformers and magnetic storage elements, the component designer is interested in much more than an estimate of the total loss which he can expect under various amplitudes of sinusoidal magnetization. He wants to know, or to be given sufficient information about the characteristics of the material to enable him to estimate, the shape and form of the dynamic total-loss loop for his particular kind of magnetization. In the applications which have been mentioned the shape of the loop is usually of greater significance than the average losses represented by its area; and while there is no real substitute for measurements carried out under the actual operating conditions there is nevertheless such a wide divergence between the kind of information which is available to the designer and that which he requires that it is desirable to explore what other methods of measurement and presentation are available.

3. DYNAMIC LOSS LOOPS

All the required information exists in its most fundamental form as a dynamic characteristic in which, for the particular kind of magnetization, flux-density is plotted against total magnetizing force in orthogonal co-ordinates. This is usually referred to as a B/H loop but is more accurately a dynamic characteristic which for stable conditions is a closed loop whose area is proportional to the total losses. From a family of such loops for various amplitudes of magnetizing force or flux change, and various polarizing fields, the complete behaviour of the material under the specified magnetization can be deduced to an adequate accuracy either graphically, or analytically by mathematical approximations.

4. SPECIFICATION OF TEST EQUIPMENT

The problem of how to obtain the necessary information can be considered under four headings.

(*a*) **The test sample.** The size of the test sample should be representative of practical cores for which the materials are likely to be used since "bulk" effects are significant in this kind of work. Analysis of applications suggests cores of up to at least 20 c.c. nett volume and 1 sq. cm cross-sectional area.

For speed and convenience in testing the number of copper turns should be a minimum and in any case less than twenty on each of the magnetizing and search windings. To ensure uniform magnetization the winding should be evenly distributed round the periphery of the sample and a minimum of about ten turns is desirable from this point of view. This implies that both the excitation and search coil voltages will increase with increasing frequency for a given sample size.

(*b*) **Display of results.** For the kind of information that is required, some

form of visual presentation is necessary. Ideally the characteristics would be presented as a permanent record to convenient scales and various electro-mechanical methods of doing this have been suggested. However, as will be shown, the required bandwidth of operation is far beyond the present capabilities of such systems.

A cathode-ray tube and an associated camera are the most practical devices available. Either electro-magnetic or electrostatic deflection may be used but the former is difficult to apply since it requires special deflection coils whose inductance and capacitance are significant at the high rates of change imposed by "rectangular"-loop measurements. In the case of electrostatic deflection, deflecting voltages of the order of 100 V are necessary, with an input capacitance of less than 10 pF per pair of plates. To minimize astigmatism and defocusing the deflecting voltages should be "push-pull", and since in many measurements it is desirable to work directly off the face of the tube, the screen should be flat and special care must be taken to ensure orthogonality of the plates and linearity of deflection. Power supplies to the cathode-ray tube must be stabilized since the deflection sensitivity is affected by the H.T. voltage on the tube.

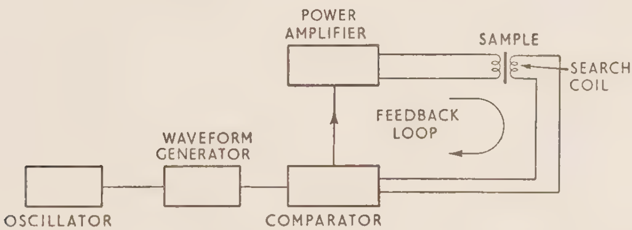

Figure 1. Method of magnetization with a defined voltage wave-form.

Shift voltage must be provided for both X and Y co-ordinates to allow the co-ordinates of individual points to be measured and so that complete loops may be replotted for accurate record and measurement. These arrangements eliminate errors due to astigmatism, non-linearity and deflection sensitivity changes, and with the relatively simple "rectangular"-loop forms are fairly quick and accurate to apply. The shift voltages must present a negligible load on the measuring circuits.

(*c*) **Source of magnetization.** In the new uses of magnetic materials the excitation is, in general, periodic but may differ very significantly from a sine wave, thereby affecting the shape of the dynamic characteristic. The method of magnetization which is described below is intended to provide the means for applying any desired form of magnetization as determined by the voltage induced in its search coil winding. The method can also be adapted to give a desired form of magnetizing current.

A schematic diagram of the proposed system for magnetization due to a defined voltage form is shown in Figure 1.

The desired form of voltage is set up by the oscillator and waveform-generator circuit, the output from which is amplified and applied to the magnetizing winding of the sample. The output from a search coil on the sample gives a true measure of the voltage corresponding to the induced flux, and is fed back and compared with the reference voltage; the comparator circuit modifies the input to the amplifier, to attain correspondence between input and output in the usual way.

The useful range of magnetization periodicities is limited by the minimum thickness in which "rectangular"-loop materials are available. The mean losses depend on the number of magnetization cycles and also on the rate of magnetization as affecting eddy currents. Examination of the problem suggests that the full available flux changes cannot be used above about 5000 magnetization cycles per second. A practical lower limit is 25 c/s.

It has been pointed out that practical considerations restrict the inductance of the sample within comparatively narrow limits and that as a consequence the source of magnetization must be capable of providing a wide range of output voltage depending on the frequency of magnetization.

The required range is thus about 200 : 1. Since the peak current is, to a first order, the same in all cases it is clearly necessary to match the amplifier to the impedance of the sample circuit. Practical considerations indicate that to obtain a loop in which the peak magnetizing force is, say, ten times the coercive force, the source should be capable of generating power corresponding to between 20 and 100 times the highest mean loss which has to be measured. For the size of sample suggested, the amplifier requires to have a mean rating of about 500 W.

The form of magnetizing voltage, in the circuits in which these special materials are used, usually includes a "unit function" change and therefore contains significant harmonic amplitudes of at least ten times the fundamental frequency. The amplifier must have a bandwidth of this order if it is to reproduce such waveforms faithfully. Thus the bandwidth must be from, say, 20 c/s to 50 000 c/s.

(*d*) **The measuring circuits.** The method of measurement is conventional in that H is measured by amplifying the voltage drop across a small non-inductive resistive shunt in series with the main magnetizing winding; B is measured by integrating the voltage across a search coil wound alongside the magnetizing winding; the integrator output is then amplified. The special problems in measuring these quantities for "rectangular"-loop materials arise from the high-frequency components contained in the H and B waveforms. Small errors in phase or amplitude result in severe distortion of the loop, and amplifiers with constant gain and zero phase-shift over a wide frequency range are required. The factors influencing their performance are described in the following paragraphs.

Maximum slope of *H* voltage. The equivalent circuit of the magnetization arrangement for sinusoidal magnetization is shown in Figure 2a and the waveforms are shown in Figure 2b: an explanatory simplified magnetization curve is shown in Figure 2c.

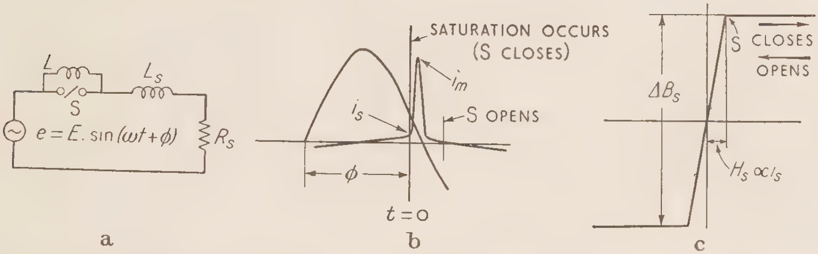

Figure 2a. Equivalent circuit of magnetization arrangement for sinusoidal magnetization.
Figure 2b. Waveforms in circuit of 2a.
Figure 2c. Simplified B/H curve.

Then neglecting the effects of saturation in the previous half-cycle and assuming $\omega L \gg (\omega L_s + R_s)$:—

$$i_s = \int_{-\phi}^{0} (E \sin \overline{\omega t + \phi}/2L)\, dt \qquad \ldots(1)$$

and

$$\Delta B_s = (2\, L i_s / NA) \,.\, 10^8 \qquad \ldots(2)$$

where NA is the turns-area product.

When S closes (i.e. saturation occurs) :—

$$i = (E/\psi L)\,(\sin \overline{\omega t + \phi - \theta} + e^{-\beta t} \sin \overline{\theta - \phi} + i_s e^{-\beta t}\ ) \qquad \ldots(3)$$

where

$$\tan \theta = \omega/\beta,\ \psi = (\omega^2 + \beta^2)^{-\frac{1}{2}},\ \beta = R_s/L_s,$$

and

$$i = k i_s \qquad \ldots(4)$$

where k is a factor (say 10). From these four equations E and ϕ may be found.

The maximum slope of current occurs at the instant of saturation, i.e. $t = 0$.

Then from equation 3:—

$$[di/dt]_{t0} = (E/L) \sin \phi - \beta i_s \qquad \ldots(5)$$

This can be evaluated and for the required shunt R_s the maximum slope of input voltage to the H amplifier can be determined, i.e.

$$[dv/dt]_{max} = [(E/L) \sin \phi - \beta i_s]\, R_s \qquad \ldots(6)$$

and the peak H voltage $= i_m R_s$.

***H*-Amplifier.** The *H*-amplifier consists of several identical push-pull stages, the gain of each being stabilized by negative feedback. For the arrangement used the minimum bandwidth required is given by $\Delta f = (100/2\pi) \times$ (slope of input voltage)/(peak input voltage).

For typical test conditions as described here, a bandwidth of at least 0·5 Mc/s is required and with 6F12-type valves a gain of about 4·5 per stage is obtained. Five directly-coupled stages of amplification are provided, this being the maximum number which it has been found possible to combine without serious effects due to valve noise.

***B*-integrator.** The integrator circuit is identical in arrangement with the *H*-amplifier except that the feedback resistor is replaced by a condenser. A time constant of integration of 1·2 sec. is achieved, giving an error of less than 1% at 50 c/s. The output from the integrator stage is amplified through several stages identical with those of the *H*-amplifier.

5. RESULTS AND CONCLUSIONS

The equipment has not yet been calibrated in detail, but measurements have been made which show that the amplifiers have a constant gain up to about 1 Mc/s. It is expected that this can be increased to 3 Mc/s. Dynamic characteristics into saturation of HCR, Mumetal and Permalloy F have been plotted from 50 c/s up to 2000 c/s without sign of " crossover". With these materials and sinusoidal magnetization less than 2% distortion of the source was observed. Further work remains to be done on the feedback system and waveform generator. A method of presenting superimposed photographic traces so as to build up families of loops has also to be investigated.

The Authors' thanks are due to the Directors of The British Thomson-Houston Company for permission to publish the paper and to several colleagues for helpful suggestions and discussions. In particular they are grateful to Mr. C. F. Wilkinson for his work on the B- and H- amplifiers.

22

X-RAY DIFFRACTION METHODS IN THE APPRAISAL OF NICKEL-IRON POWDER-CORES

N. C. Tombs

(Research Laboratories, The General Electric Co. Ltd.)

Abstract: Some ways in which x-ray diffraction techniques can be utilized in the appraisal of magnetic powder-cores are illustrated by reference to the preparation of cores of 80/20 nickel-iron alloy powder, made by a reduction process followed by ceramic insulation of the resulting powder.

Crystal size of the alloy is an example of a factor influencing the quality of powder-cores and difficult to assess except by x-ray methods.

The more extensive use of x-rays in the development and understanding of insulation processes would appear to be profitable.

1. INTRODUCTION

The use of the so-called powder-diffraction x-ray method in the investigation of phase diagrams of metal systems is well known, and the approach involved in the application of x-ray diffraction techniques to metals for powder-cores is in some respects similar. In phase diagram studies, however, the usual requirement is a knowledge of the phases existing at equilibrium in the metal system under known conditions. In the case of powder-core metals the aim is to obtain a material having certain characteristics, which can be recognized by the x-ray diffraction effect which they cause.

It will be convenient to consider the various applications of x-ray methods during the preparation of powder-cores of a particular metal, viz., 80/20 nickel-iron alloy.

2. EXAMINATION OF METAL-OXIDE RAW MATERIALS

Raw materials suitable for preparation of 80/20 nickel-iron alloy by a powder-reduction process are nickel oxide, NiO, and alpha-ferric-oxide, Fe_2O_3. The level of impurity in the oxides should be low, since otherwise the permeability of the finished powder-cores may be lowered considerably. This is apparent when it is remembered that a core made from metal of permeability several thousand has a permeability in the region of 100 when 2% by weight of ceramic insulation is incorporated. Moreover, a ceramic-like impurity in the raw material oxides does not seem to reduce the eddy-current losses in the finished core, so that it cannot be regarded as a substitute for a part of the normal ceramic insulation. On the other hand, such an impurity may degrade the alloy by promoting strain, and lead, for example, to increased hysteresis loss.

X-ray examination of the oxides, using the powder method, is thus valuable, since it can reveal the presence of impurities, and used in conjunction with chemical and spectrographic studies can indicate the suitability or otherwise of the oxides as raw materials for the alloy preparation. The powder method, using a rod-type specimen and a large-diameter camera (19 cm), is adopted.

3. PRELIMINARY MIXING OF RAW MATERIALS

Suitable high-purity oxides are mixed and ball-milled to ensure thorough and homogeneous mixing and to decrease the particle size. X-ray powder photographs can give useful information concerning the progress of this treatment, and are particularly valuable when experimental batches are being prepared.

In this application it is not the distribution of the X-ray reflections which is of interest, but the degree of diffuseness of the lines. Whereas at the commencement of milling the lines are sharp and well defined, as the particles become strained and reduced in size the lines become progressively broadened. Another source of diffuseness of X-ray reflections, to which reference will be made subsequently, is inhomogeneity of a crystalline phase, i.e. point-to-point variation in composition of the crystal lattice. As regards the origin of its effect on the diffraction of X-rays this condition can be regarded as similar to strain and small crystal size.

When diffuseness of reflections is encountered in an X-ray photograph it is essential to eliminate defects in technique as even a contributory cause. It is then usually possible to decide which of the three possible causes discussed above (namely, strain, small crystal size and inhomogeneity) is responsible from the context of the problem, or from an X-ray photograph taken after some further treatment of the material. Thus, with milled oxides, inhomogeneity can be ruled out, and annealing of the material for, say, 1 hour at 600°C, to relieve any strain, has little effect on the diffuseness of the reflections in a subsequent X-ray photograph. This diffuseness can thus be used as a measure of the crystal size of the oxides, which in turn indicates the effectiveness of the milling treatment. Using a 19-cm powder camera, diffuseness of reflections becomes apparent when the crystal size falls below about 0·2 microns. However, even without any knowledge of absolute crystal size it is possible to set some arbitrary standard of diffuseness for which the size permits successful results to be obtained in the subsequent stages of the processing.

4. REDUCTION OF MIXED OXIDES TO METAL

Treatment in hydrogen at 600°C is used to convert the thoroughly mixed oxides to nickel-iron alloy. Although inhomogeneity of this alloy phase is of little consequence since it is readily eliminated by subsequent processing,

Figure 1. x-ray powder photographs (19-cm camera, Co K radiation) of nickel-iron powder containing various small amounts of iron oxide, Fe_3O_4.

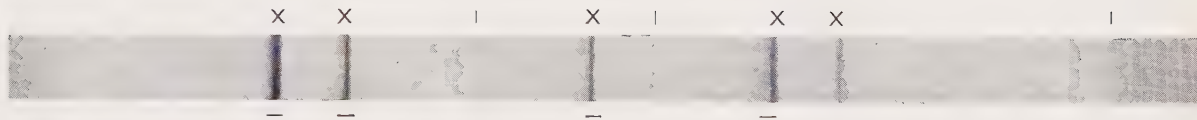

Figure 2. x-ray powder photograph of "reduction-stage" 80/20 nickel-iron alloy, showing additional phases. X, 80/20 nickel-iron ; |, near-iron ; —, iron-rich nickel-iron.

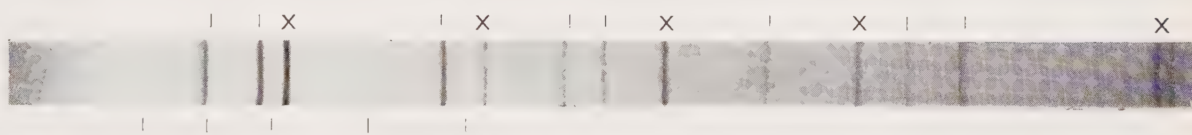

Figure 3. x-ray powder photograph of incompletely-reduced alpha-Fe_2O_3, showing Fe_3O_4 and FeO in addition to iron. (upper row) X, Fe ; |, FeO ; (lower row) |, Fe_3O_4.

it should contain no unreduced oxide. Such oxide might ultimately escape reduction altogether, or at least would lead to deposition of alloy on that formed initially.

X-ray powder photographs (such as Figures 1 and 2) provide a ready check on the phases present in the reduced material, and enable the optimum conditions of reduction, such as duration and hydrogen flow, to be determined experimentally. As in the mixing of the oxides, the aim is to secure a closely-controlled result from a particular stage of the processing, so that any unusual feature of the final product is more likely to be interpretable.

The occurrence of any metal phase of composition markedly different from that of the main face-centred-cubic 80/20 nickel-iron phase, e.g. an iron-rich body-centred-cubic phase, indicates that the mixing of the oxides was unsatisfactory.

In the preparation of iron powder from an iron oxide, usually ferric oxide, Fe_2O_3, the use of the X-ray examination after reduction is confined to the detection of oxide phases (Figure 3). There is a complication, however, in that reduced iron readily reoxidizes on cooling in wet hydrogen to give ferrosic oxide, Fe_3O_4. The presence of this oxide may therefore be due to this reoxidation process, rather than incomplete reduction of the original oxide.

5. HOMOGENIZATION OF ALLOY

If the initial stages of the process have been successful, the result will be a single alloy phase of the required overall composition near to 80/20 nickel-iron, but lacking in homogeneity. To render the alloy of uniform composition it is treated in hydrogen at a temperature higher than the 600°C used for the reduction. The upper limit to the temperature employed is set by the tendency of the material to sinter to a massive cake which cannot readily be converted to powder by crushing and milling. It is usually found undesirable to exceed about 950°C, and this temperature appears to suffice for homogenization of the alloy.

The progress of the homogenization can be followed by the increasing sharpness of the reflections in X-ray powder photographs of samples treated for successively longer periods and higher temperatures. If, however, the material has sintered to such an extent that cold-working is unavoidable in producing a suitable specimen powder, then an annealing treatment at 600°C in an evacuated hard-glass tube is necessary. Otherwise, the X-ray reflections may be rendered diffuse by strain in the alloy.

It is important to estimate the crystal size of the sintered material, since this sets an upper limit to the crystal size of the alloy powder obtained by breaking down the sintered mass. In general, it has been found that the hysteresis loss of insulated 80/20 nickel-iron alloy powder-cores is lowered by an increase in the crystal size of the alloy. If we accept the desirability

of increasing the crystal size of the final alloy powder, it will be apparent that the crystal size at the sinter stage should also be increased, since during the subsequent conversion to powder there will inevitably be some subdivision of crystals, and an increase in the number of crystals and decrease in their mean size. Further heat-treatments will not then be expected to lead to the same result as if the mean crystal size of the original sintered material had been larger. This has been borne out in practice, and an alloy of unusually small crystal size at the sinter stage always appears to yield insulated cores of inferior hysteresis loss, irrespective of any further sintering treatments to which the powder may have been subjected.

It was stated earlier that the x-ray powder method, using copper or cobalt $K\alpha$ radiation, can indicate the crystal size of a material, when this falls below about 0·2 microns, by reason of the increasing diffuseness of the x-ray reflections which occurs with crystal size decreased below this level. The method is not applicable, however, to the estimation of crystal size between about 1 and 100 microns, since over this range, with the rotating specimens usually employed, sharp lines are obtained on the photograph, provided that strain, and lack of homogeneity within a phase, are absent. For crystal sizes above about 100 microns, discontinuous "spotty" reflections are given by the powder method, but it is the 1- to 100-micron region which is of interest in the case of powder-core alloy.

For measurements in this 1- to 100-micron region of crystal size the back-reflection method is used (Figure 4). In this way, for the conditions of focus and collimation usually employed, the individual crystals yield discrete reflection spots for crystal sizes of about 1 micron upwards, and with increasing crystal size the size of the spots increases and their number per unit area of the film decreases. Suitable standards for comparison are obtained by taking similar back-reflection photographs of a powder, such as diamond dust (Figure 5), which consists of single-crystal particles of a size which has been determined by some other method, e.g. microscopically.

It is convenient to examine a freshly-broken surface of the sintered material, since modification of crystal size by cold work is thereby avoided, and the specimen is in a form suitable for mounting.

6. PREPARATION OF ANNEALED ALLOY POWDER

The sintered mass obtained as described above is converted to powder by crushing followed by milling. The mill may conveniently incorporate an air stream which carries off material as it reaches the desired particle size. The resulting powder may be given a second high-temperature treatment in hydrogen, e.g. at 950°C, although the amount of sintering experienced is usually less than in the first case and the subsequent milling does not need to be so severe.

The final powder is graded into particle-size fractions and annealed in

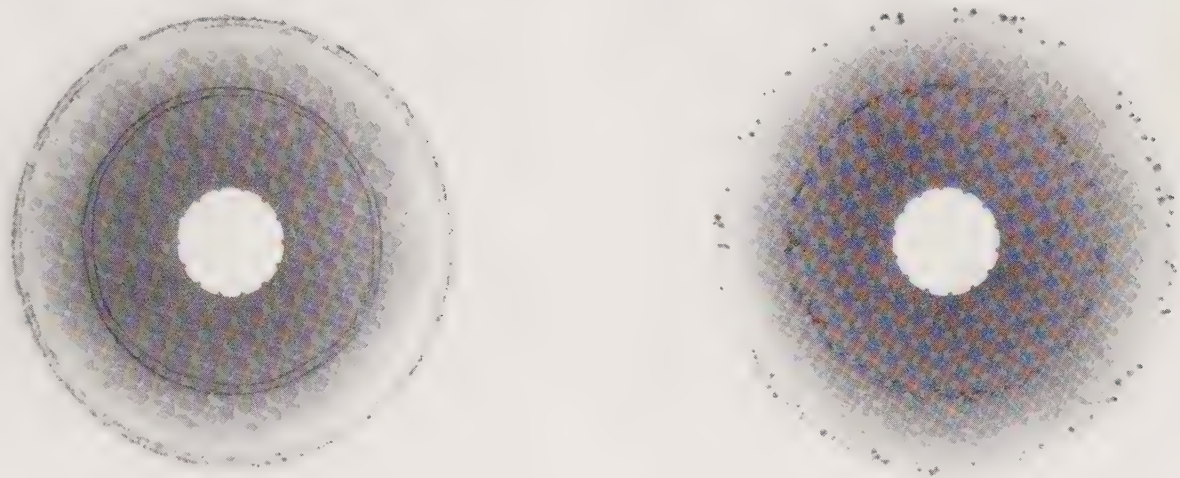

(*a*) (*b*)

Figure 4. x-ray back-reflection photographs of 80/20 nickel-iron alloy powders of mean ultimate crystal size (*a*) about 15 microns, (*b*) about 50 microns.

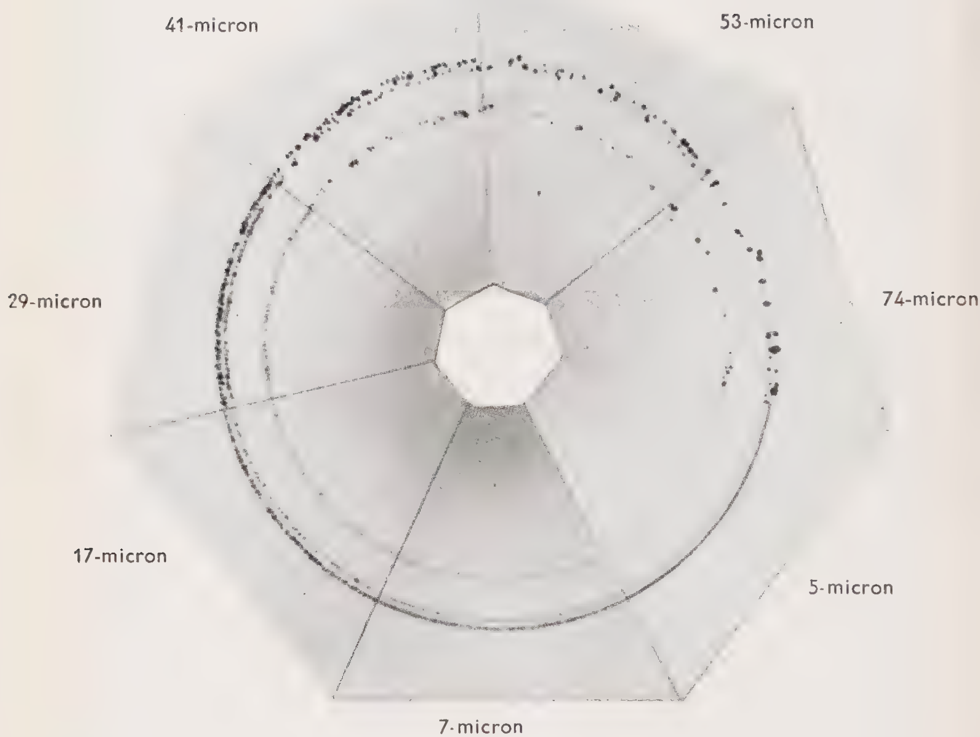

Figure 5. x-ray back reflections of graded diamond powders.

Figure 6. x-ray back-reflection photographs (Cu Kα radiation) of nickel-iron powder after heat-treatment at successively higher temperatures, showing relation between lattice distortion and resolution of reflections.

(a)
(b)
(c)

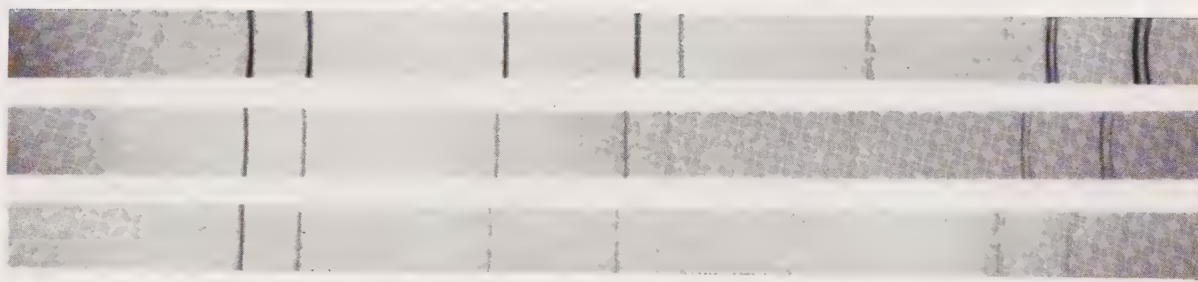

Figure 7. x-ray powder photographs of (*a*) nickel, (*b*) 80/20 nickel-iron alloy, (*c*) 50/50 nickel-iron alloy.

hydrogen at about 600°C. At this temperature negligible sintering occurs, so that further cold work of the powder is avoided. It is important to obtain strain-free powder at this stage because in subsequent compaction of the powder coated with ceramic insulation the work-hardened metal particles would fail to distort. The density of the resulting compact would therefore tend to be low, and the hard metal would readily break through the insulation.

X-ray powder photographs are used to determine the homogeneity and freedom from strain of the alloy, and to confirm the absence of any other phases (Figure 6). Back-reflection photographs are used to estimate the crystal size of the alloy which, of course, tends to increase with increasing particle size of the powder.

In addition to all the above information, the actual nickel/iron ratio of the alloy can be determined quite accurately from the X-ray powder photographs (Figure 7). A change of nickel/iron atomic ratio from 80/20 to 80·1/19·9 produces a decrease of about 0·0001 Å in the unit-cell size, whilst it is reasonable to expect an accuracy of better than 0·0005 Å in unit-cell measurements of this kind. The accuracy with which the composition can be deduced is thus comparable with that of a chemical determination, although it must be emphasized that the method assumes the absence of a third alloying element, and spectrographic confirmation of this may be desirable.

7. FABRICATION OF INSULATED CORES

The annealed alloy powder is mixed with small proportions of materials such as sodium silicate and clay, with the object of coating each particle with an electrically-insulating layer. The powder is subsequently pressed into the shapes required, e.g. toroids, at pressures up to about 100 tons/sq.in., and these compacts are then heat-treated at, say, 600°C in hydrogen in order to relieve strain introduced by the pressing operation. The detection of strain is accomplished by means of the back-reflection technique. The degree of sharpness of the spot-like X-ray reflections from a broken surface of the core affords a guide to the completeness of the annealing process. The powder method is unsuitable here, since cold working of the metal would be unavoidable in the preparation of a powder specimen.

The composition of the insulation and the way in which it is applied to the powder require careful control if the metal particles in the final core are to be well insulated from one another. There should be scope for application of X-ray methods to the development of insulation processes, but so far they seem to have been little exploited.

DISCUSSION

Mr. C. E. Richards:

Is the effect of oxide the promotion of strain, or does it merely prevent strain relief during the annealing cycle? There must in any case be plenty of strain in a ball-milled powder.

23

THE STRUCTURE OF CARBONYL IRON

A. Taylor

(The Mond Nickel Co. Ltd.)*

Abstract: Carbonyl-iron powder in the "as-prepared" or "E" condition consists of hard particles built up from concentric layers of body-centred cubic iron crystallites into spheroids having a mean diameter of 5 microns approximately. These crystallites are roughly 200 Å across and are subject to internal stresses of 130 tons/sq. in. or more. Face-centred cubic γ'-Fe_4N is present in the spheroids, while carbon to the extent of 0·6 per cent or more is there either in monolayers or as a highly dispersed carbide. By suitable high-temperature heat-treatment and quenching, the structure of the particles may be converted to tetragonal martensite. In the decarburized "C" condition the particles of powder consist of soft body-centred cubic ferrite. Compressing these powders into toroidal cores at a pressure of 96 tons/sq. in. gives rise to line-broadening effects in the x-ray diffraction spectra. Analysis shows that the line broadening is consistent with residual lattice stresses which may attain a value of 35 tons/sq. in. or more according to the amount of insulator employed. If crystal fragmentation occurs during the distortion of the decarburized spheroids under pressure, the size of the resulting crystallites must be appreciably larger than 1000 Å, since line-broadening due to crystallite size is negligible.

1. INTRODUCTION

The efficiency of inductors used in radio and telecommunications equipment may be considerably increased by filling the air-space with a suitable ferromagnetic material.

A good core material will have low losses and high effective permeability, the latter being a function of the intrinsic permeability of the iron and of the gaps introduced into the magnetic circuit by the insulation surrounding the particles of iron for the purpose of reducing eddy-current losses.

In radio-frequency work it is essential to reduce the eddy-current losses to a minimum while maintaining the permeability suitably high. E-type carbonyl-iron powder is ideally suited to this purpose since the particles are spherical and hard, thus ensuring a high packing density with a minimum of insulation, and a resistance to distortion which prevents rupture of the insulation during the pressing process. At frequencies below 100 kc/s where, as in telecommunications equipment, high permeability becomes more important, it is usual to employ a soft powder, in order to compress the maximum amount of ferromagnetic material into the core. Iron-nickel alloys of the permalloy composition and C-type powder prepared by the decarburization of E-type carbonyl iron are most frequently employed for this purpose.

Now with Horizons Inc., Cleveland, U.S.A.

Some typical constants of compressed iron-powder cores are as follows (the notation is that of Legg (1936)—see for example, p. 234 of this book) :—

		Grade ME	*Grade MC*
Effective permeability ...	μ	12 to 15	50 to 55
Eddy-current-loss coefficient	e	$<0{\cdot}2\times10^{-9}$	$2{\cdot}0\times10^{-9}$
Initial-loss coefficient ...	c	200×10^{-6}	200×10^{-6}
Hysteresis-loss coefficient	h	$8{\cdot}0\times10^{-6}$	12×10^{-6}

Although considerable quantities of E- and C-type powders are employed in electronic and telecommunications equipment generally, little is known about their physical and metallurgical characteristics. The production of carbonyl-iron powder and some of its properties and applications have been surveyed by Pfeil (1947). The powder is formed endothermically by the decomposition of iron pentacarbonyl $Fe(CO)_5$ at a temperature in the region of 250°C. The formation of iron is immediately followed by an exothermic secondary reaction $2\,CO = C + CO_2$ which takes place at the same temperature. This results in a cyclic cooling and heating of the iron particles as they form, and leads to the presence of carbon which is entrapped in the particles, and also to free carbon. The free carbon is reduced in quantity by carrying out the decomposition of the carbonyl in the presence of ammonia gas, but a consequence of this procedure is that the particles of iron powder also contain appreciable quantities of nitrogen. The iron particles commence as minute crystallites which immediately become covered with a thin layer of carbon, so that the subsequent layer of iron which is deposited cannot adopt the same crystallographic orientation as that of the iron lattice beneath. Thus, as a result of the many cyclic coolings and heatings, the iron particles grow in the form of spheres having a characteristic layered or "onion-skin" structure which can be clearly seen in the microstructure of the material. The particles have a mean diameter of 5 to 6 microns and contain about 0·6% carbon and 0·6% nitrogen. The powders are extremely hard (about 850 V.P.N.), similar to fully martensitic steel with a carbon content in excess of 0·5%.

Published X-ray diffraction patterns of a typical carbonyl iron, in the as-produced "E" condition, reveal broadened diffraction haloes which are an indication that the particles consist of submicroscopic crystallites or of crystallites in a highly stressed condition. These patterns are essentially those of a body-centred-cubic structure such as that possessed by ferrite,* and give no indication of the high degree of tetragonality which a fully martensitic steel with the same carbon and nitrogen content would reveal.

Rooksby (1942) considers an E-type powder to be a form of martensite and has shown that heating such a powder at 350°C results in a mixture of unstressed ferrite and cementite, Fe_3C. Jack (1951) has taken the same

* In the metallurgical sense of the word.

powder as used by Rooksby, and heat-treated portions of it for 40 days at 120°C, 8 days at 250°C and 24 days at 250°C. At these temperatures the ferrite reflexions gradually sharpened, the changes that occurred being exactly the same as those observed during the third stage of tempering of martensite. He showed that very thin platelets of cementite were precipitated and gave rise to X-ray reflections of which those from (hk0) planes were strong and sharp, whilst those from (hkl) planes, where l is large, were broad and diffuse or were absent, indicating that the plane of the cementite platelet was parallel to the (001) crystal plane of the ferrite lattice. Jack considers that the carbon in the original carbonyl iron must be in a state very different from that in the cementite into which it eventually transforms, and surmises that the very low temperature of formation of the carbonyl-iron powder precludes its existence as tetragonal martensite and that the existence of cubic martensite is most improbable. Without carrying out any line-broadness measurements, he ascribes the breadths of the lines to a combination of the effects of crystallite size and lattice strain. The carbon of carbonyl iron is considered to be present as a precipitate of hexagonal ϵ-iron carbide, possibly coherent and too finely dispersed to give any characteristic X-ray diffraction effects, and the condition of carbonyl iron is believed to be similar to that reached at the end of the second stage of the tempering of steel. In the absence of chemical analysis of the powder, particularly in regard to the nitrogen content, these conclusions of Jack must be considered as only tentative.

The present work describes an X-ray investigation of a variety of carbonyl-iron powders. The crystallite size and lattice stresses in E-type powders have been measured, and similar measurements were made on C-type powders after compression into toroidal cores.

Materials examined. A large number of experimental E-type powder specimens were studied by X-ray diffraction. Since the patterns were very similar to each other, only the typical specimens given in Table 1 will be described. X-ray data showing the effects of core formation on the crystallite size and lattice stresses in C-type powders are printed in Table 2, along with the chemical analyses of the samples.

Micrographic examination. The "onion-skin" nature of the carbonyl iron in the E condition is illustrated in the optical micrograph, Figure 1. Heat-treatment without decarburization destroys the layer structure, with associated precipitation of carbo-nitride, as shown in Figure 2. To reveal more detail in the structure of the layers a number of powders were examined with the aid of electron microscopy, using the well-known formvar replica technique. Typical electron micrographs taken at a magnification of 7000 are shown in Figures 3 and 4, which reveal a substructure within the individual layers. The units within the substructure are very probably individual crystallites of carbonyl iron.

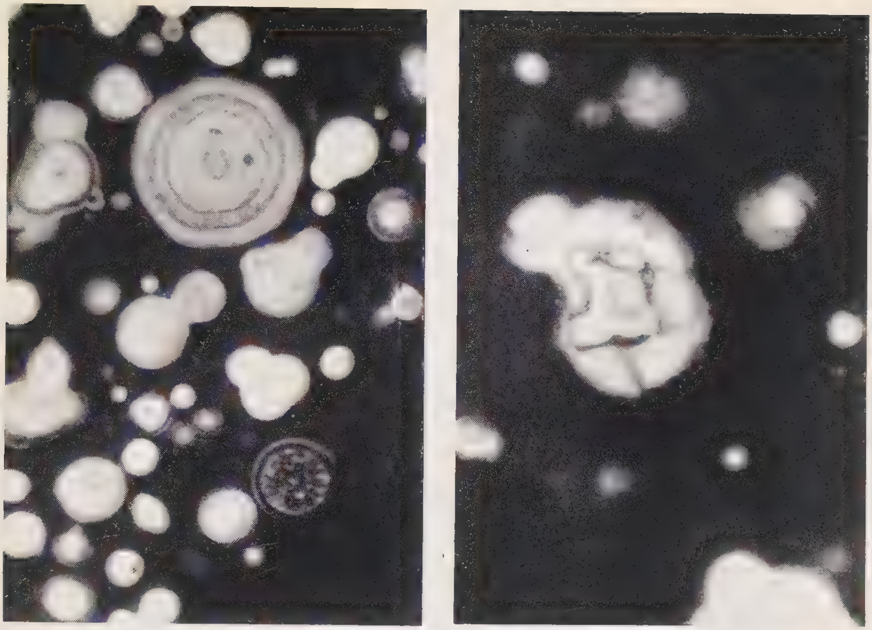

Figures 1 and 2. Optical micrographs of E-type powder. Magnification $\times$ 2000.
Figure 1, (left) as received ; Figure 2, (right) after annealing in vacuo at 70 °C.

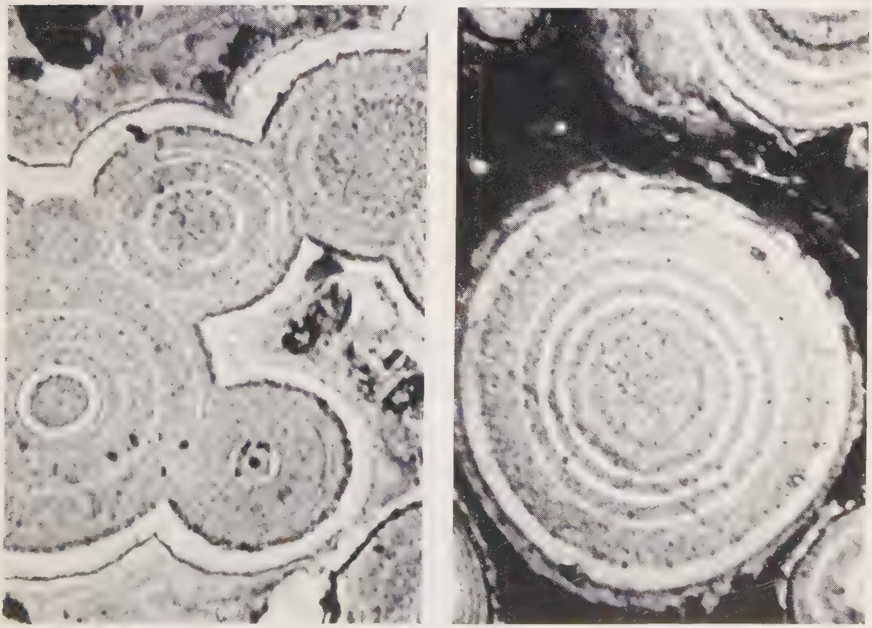

Figures 3 and 4. Electron micrographs of two E-type powders. Magnification $\times$7000.

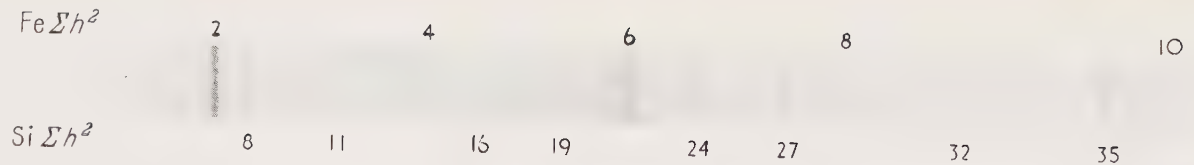

Figure 5. E-type powder.

Figure 6, C-type powder.

Figures 5 and 6. Debye-Scherrer patterns for carbonyl-iron powders with silicon calibration ; Co Kα radiation, 19-cm camera.

2. X-RAY DIFFRACTION PATTERNS

X-ray diffraction patterns were taken with filtered cobalt $K\alpha$ radiation, and in some cases with filtered iron $K\alpha$ radiation using a rotating-anode X-ray tube (Taylor, 1949). Most of the diffraction patterns were taken in a 19 cm-diameter Debye-Scherrer camera and in a flat-plate back-reflection camera.

For accurate line-breadth measurements it is essential to use a calibration material which gives extremely sharp spectra, in order to make a correction for specimen diameter and beam divergence. Silicon proves an ideal calibra-

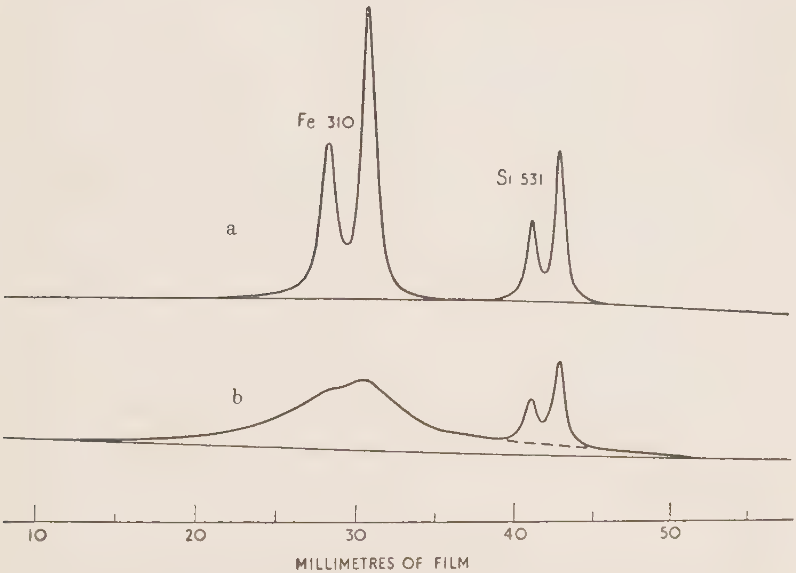

Figure 7. Microdensitometer trace for MC powder : (*a*) as decarburized ; (*b*) as core pressed at 96 tons/sq.in. with 0·8% binder.

tion material for use with iron-powder specimens since its brittle nature enables it to be ball-milled to an extremely fine powder without any appreciable broadening of its diffraction spectra. At the same time the large number of diffractions which it yields are sufficiently close to the iron lines without actually overlapping them, enabling accurate corrections to be applied to the line widths, while the low absorption coefficient of silicon, coupled with the high intensity of its spectra, results in powder-diffraction patterns of very high quality.

The samples of iron powder were mixed in roughly equal quantities with silicon powder having a particle size of approximately 10 microns and,

using dilute glue as a binder, cylindrical specimens $\frac{1}{2}$ mm in diameter were extruded through a glass capillary tube and allowed to dry.

To obtain the highest accuracy in line-breadth measurement in the lowest orders where broadening is least, all diffraction patterns for microdensitometry were taken in the 19-cm-diameter Debye-Scherrer camera. After exposure, a calibration step-wedge was printed on each film by means of a rotating sectored wheel (Taylor, 1945), and the film was photometered. using a manual instrument of high accuracy (Taylor, 1951). Figure 5 shows a typical diffraction pattern from an E-type powder mixed with silicon, while Figure 6 shows the same iron powder after it has been decarburized to the C condition.

Figure 7 shows a microdensitometer trace from the 310 reflexion of MC powder and the 531 reflexion from the silicon calibration pattern.

The line breadths, B_0, were computed by the Laue method, by dividing the area between the line contour and the background by the maximum height of the peak. These breadths were corrected for the angular separation of the $\alpha_1\alpha_2$ components of the radiation, using the method of Jones (1938), and the true angular broadening β was then obtained from the corrected breadths B by allowing for the instrument broadening. This was achieved by plotting a curve of doublet-corrected breadths for the silicon calibration lines against tan θ and interpolating the breadths b for crystals of effectively infinite size corresponding to the positions of the iron lines. The exact calculation of β from B and b depends on the theory of broadening employed. The broadening defined by the equation

$$\beta = [(B - b)\sqrt{B^2 - b^2}]^{\frac{1}{2}} \qquad \ldots(1)$$

is very convenient (Taylor, 1941), and approximates very closely to the experimental Jones curve which correlates β/B with b/B. This value of β is in millimetres and is converted into radian measure by dividing it by the radius of the camera.

If all the line broadening, β, is entirely due to the extreme smallness of the crystallites from which the iron particles are composed, their size may be computed from the simple Scherrer formula

$$\beta = (K\lambda/\epsilon) \sec \theta \qquad \ldots(2)$$

where K is the constant which is approximately 1·07, λ is the wavelength of the radiation in centimetres, θ the Bragg angle of reflexion and ϵ is the crystal dimension measured in a direction normal to the reflecting planes.

On the other hand, if all the line broadening is due to random lattice stresses which disturb the interplanar spacings, an approximate measure of the mean maximum stress T in dynes/cm² may be obtained using the equation (Megaw and Stokes, 1945) :—

$$T = (E_{hkl}\beta/4) \cot \theta \qquad \ldots(3)$$

where E_{hkl} is the modulus of elasticity for the lattice direction (hkl), β is the line broadening in radians and θ is the Bragg angle.

The appropriate value of E_{hkl} may be computed from a knowledge of the elastic constants of the material by means of the equation (Schmidt and Boas, 1950 ; Stokes and Wilson, 1944):—

$$1/E = s_{11} - 2\,[(s_{11} - s_{12}) - \tfrac{1}{2}s_{44}]\,H$$

where

$$s_{11} = 7{\cdot}57 \times 10^{-13}\ \text{cm}^2/\text{dyne}$$

$$s_{12} = -\,2{\cdot}82 \times 10^{-13}\ \text{cm}^2/\text{dyne}$$

$$s_{44} = 8{\cdot}62 \times 10^{-13}\ \text{cm}^2/\text{dyne}$$

and H represents the function $(h^2k^2 + k^2l^2 + l^2h^2)/(h^2 + k^2 + l^2)^2$.

It follows from equations (2) and (3) that if the line broadening is due solely to small crystallite size, the values of β against sec θ will plot as a straight line through the origin, while if the broadening is due entirely to lattice stresses, then $E\beta/4$ should plot against tan θ as a straight line through the origin. If, as may be the case, broadening effects due to a combination of crystallite size and lattice stress are present, the broadening may be represented by the additive equation

$$\beta = (K\lambda/\epsilon)\sec\theta + (4T/E)\tan\theta \qquad \ldots(4)$$

or

$$\beta/\sec\theta = K\lambda/\epsilon + (4T/E)\sin\theta \qquad \ldots(5)$$

and it follows that if $\beta/\sec\theta$ is plotted as a function of sin θ, a straight line should result whose intercept on the $\beta/\sec\theta$ ordinate yields the crystallite size and whose slope yields the value of $4T/E$ from which the lattice stress may be computed.

It was often of interest to know the lattice parameters of the powders. On account of the great diffuseness of the high-order reflections in the iron pattern, the angles at which the lines occurred were determined from the microdensitometer traces, using the silicon lines as reference points. The accuracy of the parameters obtained in this manner was probably of the order of one part in 10 000. Where E-type powder had been heat-treated so that diffraction patterns of ferrite with highly resolved high-order lines were obtained, the lattice parameters were derived by plotting the parameter values for each Bragg angle θ against the function $f(\theta) = \frac{1}{2}(\cos^2\theta/\theta + \cos^2\theta/\sin\theta)$ and extrapolating to $f(\theta) = 0$ in the manner described by Taylor and Sinclair (1945).

3. X-RAY RESULTS : E-TYPE POWDERS

Samples E1, E2 and E3 were x-rayed in the "E" condition and all gave the type of diffraction pattern shown in Figure 5. Owing to the great breadths of the diffraction haloes from the iron in the higher orders it was not possible

to make satisfactory densitometer traces beyond the 220 reflexion, and only values of β for the 110, 200, and 211 and 220 reflexions could be obtained. Plotting $E\beta/4$ versus tan θ and β versus sec θ showed that both lattice-stress and crystal-size broadening were operating, and in order to separate the two effects it was essential to plot $\beta/\sec\theta$ against sin θ. A typical plot for powder E1 is illustrated in Figure 8.

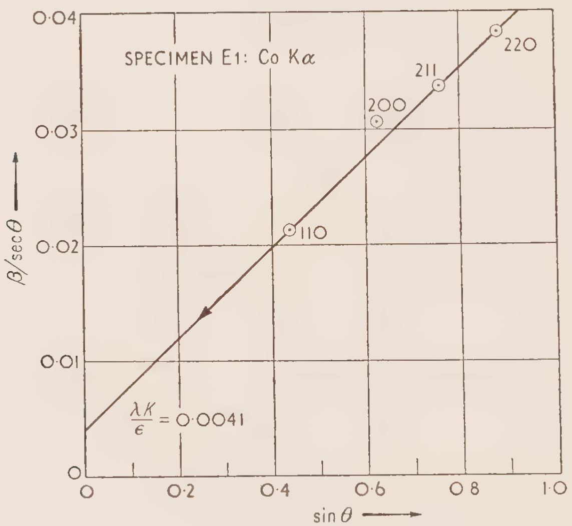

Figure 8. Plot of $\beta/\sec\theta$ against sin θ for powder E1.

Using equations (2) and (3), the following values of crystallite size and lattice stress were obtained for powders E1, E2 and E3:

Powder sample	%C	%N	Radiation	Crystal size, Å	Lattice stress, tons/sq.in.	Lattice parameter kx
E3	0·63	0·57	FeKα	203	96	$2{\cdot}863_2$
E2	0·64	0·55	CoKα	163	82	$2{\cdot}863_6$
E1	0·68	0·63	CoKα	467	133	$2{\cdot}863_6$

The values of crystallite size and lattice stress are probably correct to within $\pm$ 10% relative to each other. Using the positions of the silicon lines as fiducial marks in the microdensitometer traces, the angular positions of the broadened iron lines were determined and the lattice parameters of the specimens were computed, the values of which are given in the last column of the above table.

The X-ray results indicate that the spherical particles of E-type powders consist essentially of crystallites which are in a highly-stressed condition and which are a few hundred Ångstrom units in diameter. The precise values of the lattice stress and ultimate crystallite size are probably functions of the manner in which the powder is produced, and much further work would be required in order to correlate all the factors which influence them. It is of interest to note, however, that the crystallite size computed from the X-ray data is of the same order as the size of the crystallites observed in the electron micrographs.

If all the nitrogen and carbon, which total 1·2% by weight approximately, were in solution, as in a fully martensitic steel, it would be anticipated that the unit cell would exhibit a marked tetragonality which, according to the latest data published by Jack (1951a), would have an axial ratio of 1·02. This ratio would show itself by a marked splitting of the X-ray reflections, but since no trace of this could be seen, nor any corresponding asymmetry of the lines in the microdensitometer traces, it may be assumed that tetragonality is either very small or entirely absent.

Pfeil (1947) has mentioned the presence of extra, faint lines in the diffraction patterns of an E-type powder, corresponding to the presence of a face-centred-cubic austenite phase, and states that " while the presence of this phase might be due to the considerable nitrogen content of the powder, it lends support to the hypothesis that the particles form originally as austenite, despite the low temperature of formation (below 400°C) and subsequently break down to martensite on cooling to room temperature". Recent inspection of the diffraction pattern of E-type samples E1, E2 and E3 revealed the presence of similar lines, but closer checks showed that their spacing corresponded not with that of retained austenite, but with the larger spacing of γ'-Fe_4N. This was confirmed by direct comparison with a diffraction pattern taken from a sample of Fe_4N kindly supplied by Dr. Jack. Even if all the nitrogen were accounted for as Fe_4N, there would still be 0·6% of carbon available to go into solution in the ferrite lattice and give a martensite with a readily observable tetragonality, unless the cubic β-martensite postulated by Honda (Honda and Nishiyama, 1932) really can exist. Failing this, and ruling out the possibility of a transformation from a pre-existing austenitic phase to a bainite, or to martensite which is subsequently lightly tempered to the cubic form, on account of the low temperature involved in the decomposition of the carbonyl, it would seem that body-centred-cubic iron is formed directly in the decomposition and that the nitrogen is present in the form of a very highly dispersed nitrogen austenite, namely γ'-Fe_4N.

No sign of iron carbide is visible in the diffraction patterns of E-type powders. It is highly probable that the carbon is dispersed monatomically on the surfaces of the "onion-skins" and also to some extent over all the

actual surfaces of the individual iron crystallites. On account of the high energy such a large internal surface created by the interfaces between the crystallites would possess, and on account of the large stresses prevalent in the particles as a whole, conditions are ripe for a large degree of atomic mobility at very low temperatures. Heating E-type powders at 120°C is sufficient to aggregate the carbon in the form of Fe_3C, while the lines of the ferrite diffraction pattern sharpen to indicate crystal growth and relief of lattice stress.

In an attempt to ascertain the nature of the carbon in the spheroidal particles, about $\frac{1}{2}$ kg of powder was dissolved in dilute hydrochloric acid, in the hope of leaving a small carbon-rich residue which could be examined by X-ray diffraction. However, the diffraction pattern, which would have been capable of showing the broad diffraction haloes from carbon crystallites only 10 Å in diameter, showed no traces of free carbon. Thus it would seem that the carbon is dispersed in extremely small atomic groups over the large internal surface created by the boundaries of the crystallites within the iron spheroids, or alternatively it is in the form of monomolecular films of hexagonal ϵ-carbide which are too dispersed to give rise to X-ray diffraction effects after the manner postulated by Jack (1951). Tempering the particles, as carried out by Jack, leads to the formation of cementite and the process quite naturally follows the later stages of the tempering of martensite (Antia, Fletcher and Cohen, 1944). The carbon is not rejected from a martensite lattice, however, but merely migrates and, with the nitrogen, forms a carbide similar in structure to Fe_3C by a process of nucleation and growth.

It has often been stated that the hardness of martensite is associated with its tetragonality. Since the particles of carbonyl iron are essentially cubic in character it would seem that their extreme hardness is caused partly by their high internal stress and partly by the smallness of the crystallites which, surrounded by thin films of carbide and nitride, are prevented from distorting or slipping under load upon favoured lattice planes.

It will be noted that the lattice parameters of the three E-grade samples, $2{\cdot}863_2$, $2{\cdot}863_2$ and $2{\cdot}863_6$ kX, are quite markedly higher than that of pure iron, which has a cell edge of $2{\cdot}860_5$ kX (Bradley, Jay and Taylor, 1937).

It could be argued that some carbon and nitrogen are in solution and are so distributed among the vacant lattice sites that the structure remains essentially cubic. Considering the high rate of mobility of carbon and nitrogen in martensite at 250°C, which is the temperature reached by the iron particles in the course of their formation, this explanation would seem unlikely. An increase in the lattice parameter could be forced on the ferrite lattice, if within and at the boundaries of the minute crystallites there were coherent zones of hexagonal ϵ-iron carbide or cementite, since in these latter compounds the distances between the iron atoms must be somewhat larger than in free ferrite on account of the carbon and nitrogen which are in

interstitial solid solution. This type of argument has already been put forward by Wrazej (1946) to account for the high spacing, 2·866 kX, of the ferrite formed subsequent to the tempering of martensitic steels.

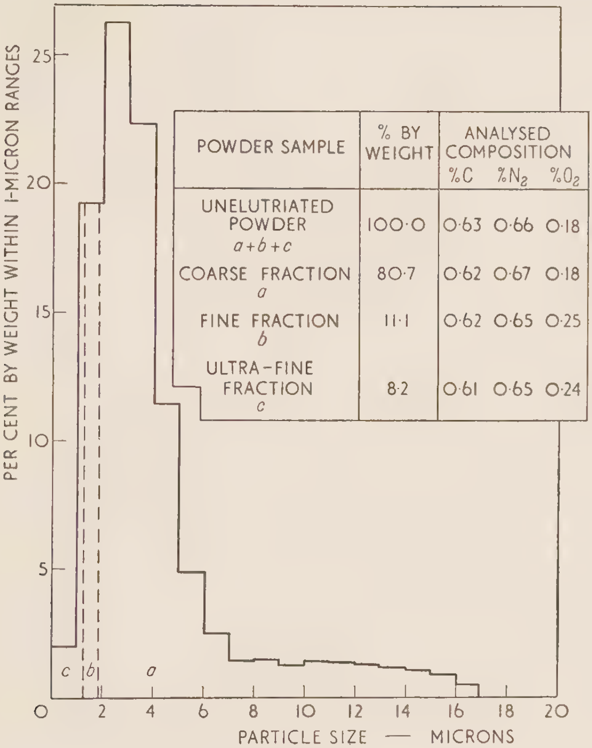

Figure 9. Histogram for sizes of typical E-type powder.

In the above discussion it has been assumed that all the particles, irrespective of size, in any single unblended batch of powder are chemically alike. Table 1 gives only the mean particle sizes of powders obtained by the Fisher air-permeability method (Gooden and Smith, 1940), but in reality there is a

Table 1. Analysis of E-type powders

Sample No.	Powder type	Particle size, microns	Analysis—Weight %		
			C	N_2	O_2
E1	E	5·5	0·63	0·57	0·29
E2	E	6·1	0·64	0·55	0·26
E3	E	6·0	0·68	0·63	0·24
Nitrogen-free	E	—	1·22	0·00	—

considerable statistical spread of sizes about this mean. The histogram in Figure 9 shows the particle-size distribution obtained by an optical-extinction sedimentation method (Rose and Lloyd, 1946) in a typical E-type powder. Since there was no *a priori* reason to assume that particles in the fine, medium and coarse size ranges are similar in composition, it was decided to separate these fractions in an air elutriator and subject them to chemical analysis. The results are indicated on the histogram and show that within the limits of experimental error the particles in each size fraction have substantially the same composition as the particles in any other fraction.

4. EFFECT OF QUENCHING E-TYPE POWDERS FROM ELEVATED TEMPERATURES

The X-ray results discussed in the previous sections seem to indicate that, irrespective of size, all the spheroids in any given batch of E-type powder consist essentially of body-centred-cubic ferrite crystallites having a very high internal stress and an overall size of a few hundred Ångstrom units. Because the carbon and nitrogen content of the powders is extremely high the absence of tetragonality is one of the surprising features of the powders, since in many respects they possess the characteristics of a typical martensite. It would be expected, therefore, that raising the temperature of the powders sufficiently would cause all the carbon and nitrogen to be absorbed interstitially in the lattice of face-centred-cubic austenite, and that subsequently quenching should yield tetragonal martensite.

In order to test this theory, samples of E3 and a nitrogen-free E-type powder were sealed into evacuated thin-walled silica tubes having an internal diameter of approximately 1/3 mm and a wall thickness less than 1/10 mm. The specimens were heated at 850°C and 1000°C respectively for about 20 minutes in a vertical furnace and then pushed out into a flask of liquid nitrogen, the whole operation taking only a fraction of a second. It was hoped by this means to obtain suitable X-ray specimens in the martensitic condition and with a minimum amount of untransformed austenite, on account of the low temperature of the quenching medium.

Sample E3, after quenching, gave the diffraction pattern of a typical martensite, showing a marked tetragonality and a line diffuseness consistent with a high degree of lattice stress. The nitrogen-free powder, however, gave quite a different result. Instead of a typical diffuse pattern of tetragonal martensite, with, possibly, a little retained austenite which had not broken down at the liquid-nitrogen temperature, the diffraction pattern was of body-centred-cubic ferrite containing a large percentage of Fe_3C. In addition, the diffraction lines were quite sharp, and the high-order lines 220, 310, were clearly resolved, thus indicating that the crystallite size had increased within the powder particles, and that the particles were substantially stress-free.

It is interesting to compare the behaviour of the powder with that of a

typical steel, in massive form, containing 0·57% carbon, 0·24% manganese (United States Steel Corporation, 1943). The "nose" of the S-curve for such a steel is at 450°C and the transformation from austenite to ferrite and cementite begins in less than a second. It is probable that the rate of quenching attained with the minute specimens of powder was much higher than could be achieved with the steel in massive form, and it would be anticipated that the transformation to ferrite-plus-cementite would be suppressed, and that the retained austenite would be subsequently converted to martensite, at the liquid-nitrogen temperature, by a diffusionless transformation. That this does not happen with the nitrogen-free powder is probably associated with the high ratio of surface area to crystal volume, which has increased the rate of nucleation so that the rate of quenching is insufficient to suppress the transformation from austenite to ferrite-plus-cementite.

It was thought that, although the rate of quenching in liquid nitrogen would be extremely rapid with such small X-ray specimens, there was still the possibility of the formation of a pocket of gas which would surround the specimens and retard the quenching rate. Accordingly it was decided to quench the specimens in iced brine, to avoid the formation of a gaseous film. The result of such a quench on a nitrogen-free specimen was the formation of tetragonal martensite, plus the retention of a large amount of untransformed austenite. Thus it was evident that the rate of quenching had been increased to such an extent that the nose of the S-curve was passed before any of the austenite could transform into a mixture of ferrite plus cementite.

It would seem that, in the absence of nitrogen, the carbon atoms in these small particles have very high mobility, and that in the course of the quench in liquid nitrogen the bulk of the crystallites become substantially carbon-free. However, this carbon does not escape from the lattice to form free graphite, but becomes confined to a region where it forms cementite. As shown by Jack (1951a), there is a very close relationship between the atomic packing in cementite and that of tetragonal martensite, and it may well be that the formation of cementite is merely an alternative way of entrapping the diffusing carbon interstitially in the lattice.

Although much more work is required to interpret these results completely, the above experiments do indicate that the structure of a normal E-type powder containing both carbon and nitrogen can be converted to that of a typical tetragonal martensite provided it is heat-treated like a steel and quenched from the austenitic condition. It would seem, then, that for powders in the as-produced condition all the evidence points to the particle being composed of concentric layers of highly-stressed sub-microscopic crystallites of pure iron, interspersed with almost monomolecular layers of Fe_4N and iron carbide or carbo-nitride. The extreme hardness of the particles is probably associated with the high internal stress and slip-interference between the crystallites. The X-ray observations of Jack on heat-treated

carbonyl iron, which indicated changes similar to those obtained in the third stage of martensite tempering, are quite consistent with the picture of the structure of carbonyl iron as described above, since the very high internal surface created by the crystallite boundaries and the very high internal stress would lead to an unduly high free energy, and this in turn would be expected to result in the rapid formation of cementite platelets during tempering.

5. X-RAY EXAMINATION OF C-TYPE POWDERS

E-type powder is converted into the soft easily deformable C-type, for use in high-permeability cores, by decarburizing and denitriding in hydrogen. When the decarburized powder is removed from the furnace it is found to be in the form of a lightly sintered briquette which, in commercial practice, is milled until broken down into its individual particles. This process introduces a measure of line-broadening in the diffraction pattern which, being due to random residual stresses which modify the lattice parameter from point to point in the deformed crystals, follows a tan θ law.

If, after the annealing treatment, the crystal size is still small enough to give line-broadening effects, the value of the broadening will follow a sec θ law. In marginal cases, where the amount of broadening is very little and only measurable with any real accuracy in the highest-order reflection, 310 with Co Kα radiation, it is almost impossible to ascertain the cause of broadening, since in the high orders sec θ and tan θ are almost equal, while in the low orders, where they are very different, the errors in computing the small degree of broadening are very great. It is therefore of very great importance, in examining a powder prior to pressing into a compact, to avoid ball-milling the sintered cake so as not to introduce stress-broadening.

A number of typical x-ray results for C-type powders is given in Table 2, along with details of chemical analysis, particle size and heat-treatment data.

Table 2. Deformation characteristics of C-type powders

Sample	Condition	Fisher size, microns	Analysis %C	Analysis %N_2	Crystal size, Å	Residual lattice stress, tons /sq.in.
C1	As received and decarburized	6·0	0·012	0·016	955 or	5·1
	After 60 hrs. at 375°C + 3 hrs. at 400°C	—	—		1600 before pressing	0
	Pressed 96 tons/sq.in. without insulation	—	—		> 1000 after pressing	45
	Pressed 96 tons/sq.in. with 0·8 % binder	—	—		> 1000 after pressing	34
C2	Pressed 96 tons/sq.in., 0·8 % binder	5·39	0·055	—	> 1000	35·9

In the as-received condition, sample C1 showed a small degree of line broadening, which is primarily due to the combined effects of crystal size and ball-milling. Since a satisfactory determination of the line broadening could be done only for the single 310 reflection, Table 2 lists 955 Å and 5·1 tons/sq. in. as alternative possibilities. The main emphasis should probably be placed on the stress determination, on account of the ball-milling process. Annealing the powder for 60 hours at 375°C, plus 3 hours at 400°C, sharpened the end-doublets, and since the anneal, in this case, was not followed by ball-milling, the small degree of residual line-broadening could be attributed to a crystallite size of approximately 1600 Å. Owing to the possibility of recrystallization processes within the particles during the heat-treatment, it may well be that the computed size does not truly represent the dimensions of the original lightly stressed and now fully recovered crystallites, but rather the dimensions of newly-formed grains. A considerable amount of work, probably requiring the aid of electron microscopy, would be required to settle this point conclusively.

When standard cores are made of C-type powder with 0·8% of insulating binder, the pressure employed has a marked influence on the diffraction patterns. A series of back-reflexion patterns taken from cores pressed at 5, 50 and 100 tons/sq.in. showed a progressive broadening of the 310 reflexion. Probably on account of the friction between the powder and the walls of the die during the pressing operation, there was a tendency for the exterior cylindrical surface of the specimen to receive rather more cold-work than the interior, and this was revealed by a greater broadening in the 310 reflexion. It would be of very great interest to study this aspect of core formation still further and obtain the distribution of stresses and crystallite sizes across the section of a core, especially as the precise mode of distribution is likely to affect its electromagnetic characteristics.

It would be expected that the amount of insulating binder employed in the making of a core would influence, to an appreciable extent, the degree of cold work and crystal fragmentation within the individual particles.

Although it has been possible to carry out only a limited number of experiments, it has been conclusively demonstrated that the presence of a binder effects a marked reduction in the degree of line broadening. Figure 10a shows the diffraction pattern of a C-type powder after annealing for 2 hours at 1050°C. The extremely sharp end-doublets indicate that the particles of powder consist of stress-free crystallites which are appreciably larger than 1000 Å. Forming such a powder into a toroidal core at a pressure of 96 tons/sq.in. in the standard way using 0·8% insulating binder, yielded the diffraction pattern with broadened high-order reflexions shown in Figure 10b. On the other hand, making a core under the same conditions, but with the complete absence of insulation, resulted in the diffraction pattern of Figure 10c in which the high-order reflections are considerably

broader than in the previous case. An analysis of the microdensitometer traces over the full range of Bragg angles led to the surprising and very important result that in each case the broadening was attributable entirely to the effects of internal stresses, and any crystal fragmentation which occurred in the deformation of the particles still yielded crystallites appreciably larger than 1000 Å. The internal stress in the uninsulated powder particles was 45 tons/sq.in., while that in the insulated particles was only 34 tons/sq.in. It would seem that during the pressing of a core, the particles of powder not only deform directly under the pressure, but that they also slide past each other, and part of the residual stresses are brought about by shear. The insulator in a normal core would act as a lubricant, which would permit a certain degree of local sliding at the points of contact, and this would tend to result in a lower residual internal stress.

It is of interest to note that line-breadth measurements made on the Debye-Scherrer patterns of a whole series of compacted C-type powders give essentially the same result, namely, that the broadening is due to residual stresses in the crystal lattice. Thus, on the basis of the detailed analysis made on the complete spectrum recorded in the 19-cm-diameter camera, the progressive broadening of the single reflection 310 in the back-reflection patterns may now be interpreted as being due entirely to the progressive increase in residual lattice stress as the forming pressure was raised from 5 to 100 tons/sq.in.

6. CONCLUSIONS

The hard particles of E-type iron powder prepared by the decomposition of iron pentacarbonyl are spherical and contain approximately 0·6% C and 0·6% N_2 by weight. The X-ray diffraction patterns indicate that some, if not all, of the nitrogen is in the form of face-centred cubic γ'-Fe_4N. Carbon has not been detected in the diffraction patterns and it is probable that this element forms coherent zones or monolayers of hexagonal ϵ-carbide or orthorhombic Fe_3C. The "onion-skin" structure of the spheroids consists essentially of concentric layers of body-centred-cubic iron crystallites which are approximately 200 Å across, and which are subject to internal stresses which attain a level of 130 tons/sq.in. or more. Crystallites on the same scale of these are readily detected in electron micrographs of the iron spheroids.

Since the crystallites are essentially body-centred-cubic ferrite, the amount of carbon and nitrogen in solid-solution must be extremely small. The rapid formation of carbides and the growth of undistorted iron crystallites, which have been reported at the relatively low temperature of 120°C, are probably due to the high rates of diffusion along the grain boundaries occasioned by the high free energy which results from the combination of lattice stresses and large internal surface. Thus the formation of cementite during low-temperature annealing need not be associated with the breakdown of

Figure 10. Typical diffraction patterns for MC powder ; Co Kα radiation, 19-cm camera. (*a*) annealed for 2 hours at 1050°C ; (*b*) annealed, then pressed into cores at 96 tons/sq.in. with 0·8% binder. Powder mixed with silicon ; (*c*) as *b*, but without insulation.

tetragonal martensite by the diffusion of carbon through the lattice as occurs in solid steel specimens. Particles of E-type powder may, however, be converted to a tetragonal martensite by quenching at a sufficiently fast rate from elevated temperatures.

By measuring a sufficiently large number of spectra in the Debye-Scherrer patterns from compressed cores made from C-type powders, it has been established that the principal cause of line-broadening is residual stress and not crystal fragmentation. These stresses are sensitive to the amount of insulating material employed in making the cores and also to the forming pressure. With no binder and a forming pressure of 96 tons/sq.in. the residual stresses were of the order of 45 tons/sq.in., while when using the standard quantity, 0·8%, the stresses fell to 34 tons/sq.in.

The author wishes to thank the Mond Nickel Co. Ltd. for permission to publish this paper. He also wishes to thank the British Non-Ferrous Research Association for preparing the electron micrographs shown in this paper and Mr. C. V. Smith for assisting in the taking of X-ray diffraction patterns.

DISCUSSION

Mr. F. F. Roberts:

My remarks on another Paper (p. 243) are also relevant here. I should like to add that the general appearance in electron micrographs of nearly equal thicknesses for what are presumably the pure iron and the intermediate shells of the "onion-skin" structure may arise naturally from the breakdown, due to etching or otherwise in the preparation of the sections, of the highly strained innermost and outermost layers of each pure iron shell.

24

EXPERIMENTAL INVESTIGATIONS ON NICKEL-MOLYBDENUM-IRON ALLOYS WITH EXTREMELY HIGH INITIAL PERMEABILITY

Fritz Assmus

(Vacuumschmelze A.-G., Hanau-am-Main)

Abstract: This paper deals first of all with a reproduction of the alloy Supermalloy, which is at the present time the "softest" magnetic material. It is then shown that such properties can be obtained, not only with the previously known composition, but also with a whole series of others. Some anomalies, in particular a rise of electrical resistivity, occur during the heat-treatment intended to produce the highest permeability. The activation energy of the underlying effect is obtained from the time and temperature laws of the resistance changes.

1. INTRODUCTION

Three stages stand out in the development of high-permeability materials: first the discovery of the original binary alloy Permalloy by Arnold and Elmen (1923) and its further development to materials with more constituents which were known by the trade names Permalloy C, Mo-Permalloy, Mumetal, etc. Then later came the discovery by Neumann (1934), as a result of systematic investigation of nickel-iron-copper alloys with and without the addition of molybdenum, of alloys with considerably higher permeability. Of these the alloy M 1040 was for a long time the magnetically softest material. Finally, there is the discovery of Supermalloy by Boothby and Bozorth (1947). Figure 1 shows the permeabilities of the commercial alloys already mentioned and of an alloy corresponding to Supermalloy.

Parallel with this rise of permeability went a reduction of coercive force, the three stages being characterized by approximate values of 0·07, 0·02, 0·003 oersted respectively. As a result of this development, the magnetic hysteresis, at least for open magnetic circuits, has been so much reduced that it is practically negligible.

The first part of this paper gives some results for the alloy Ultraperm 10 (Assmus and Pfeifer, 1951), which corresponds to Supermalloy. Then it is shown that similar effects can also be obtained with other alloys (Assmus and Pfeifer, 1953). Finally, effects are discussed which are tied up with the special heat treatment necessary to obtain extreme magnetic softness.

2. SUPERMALLOY AND SIMILAR ALLOYS

The last of the three stages of development described above is of particular interest here. It consisted of the discovery by Bozorth and Boothby of a peculiar annealing effect. Previously, from the earliest work of Arnold and

Elmen on binary Permalloy, it was thought that high permeability could only be obtained by rapid cooling after the final heat treatment and that the addition of further elements could, at most, result in a reduction of the sensitivity to the rate of cooling. On the other hand, Boothby and Bozorth found, surprisingly, a considerable rise of permeability as a result of an accurately controlled additional heat treatment in the temperature range between 400 and 500°C which had previously been regarded as dangerous. This additional heat treatment followed an annealing process at a higher temperature. We reproduced these results without particular difficulties, provided all the precautions were taken which are usually necessary in the manufacture of magnetically soft materials. The upper curve of Figure 1 shows permeability values obtained in this way, and Figure 2 shows the considerable improvement obtained by the further annealing process.

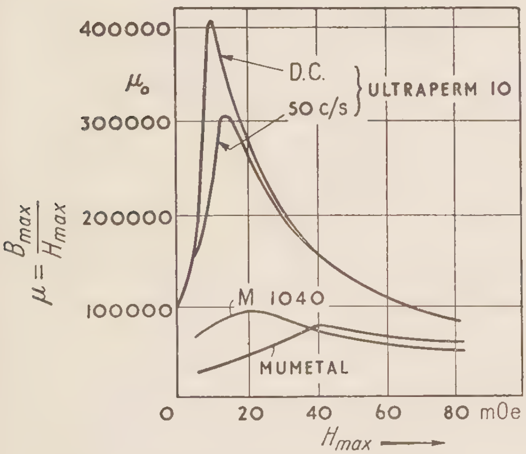

Figure 1. Development of high-permeability alloys.

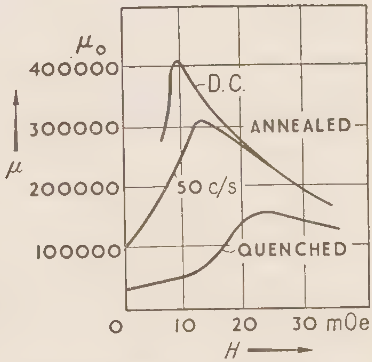

Figure 2. Effect of annealing on Ultraperm 10.

These curves of Figures 1 and 2 were obtained on tape cores with a tape thickness of 0·05 mm. Figure 3 shows similar curves for two other thicknesses. It is seen that, for d.c. measurements, about the same permeability is obtained for all thicknesses; the latter thus has no appreciable effect on permeability over this range of thickness. With a.c. measurements, on the other hand, with a thickness of 0·05 mm and a test frequency of only 50 c/s, there is a considerable reduction of the maximum permeability as a result of eddy currents; this effect is naturally more marked for the thicker tapes. So, for the realization of high permeabilities for alternating field applications, very thin laminations are required even at 50 c/s. Measurements up to higher frequencies are shown in Figure 4; they are at low field strengths such as those of particular interest for transformers. Figure 4 shows families

of curves of complex permeability plotted for constant frequency and varying field strength or for varying frequency and constant field strength. The ordinate is the "series inductance permeability" μ_{LR} as introduced by

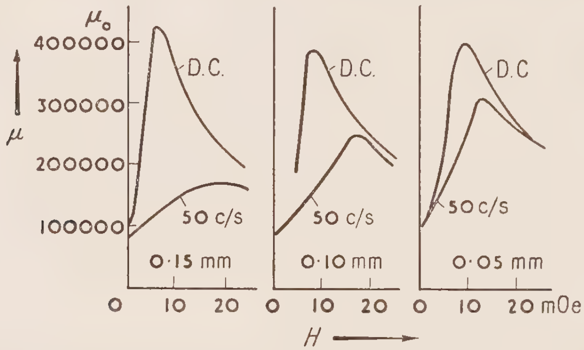

Figure 3. Effect of eddy currents in Ultraperm 10 (50-c/s measurements with Ferrometer).

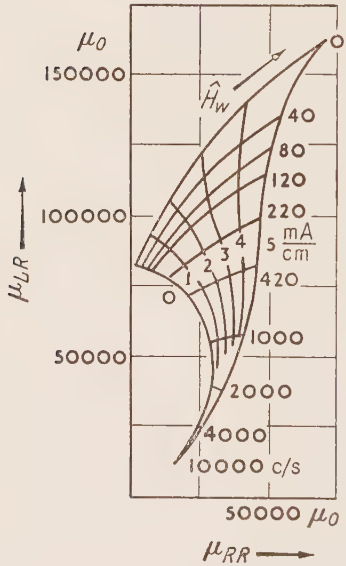

Figure 4. Complex permeability of Ultraperm 10 for tape of thickness 0·05 mm.

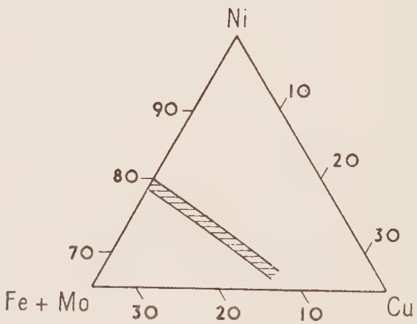

Figure 5. Zone of extremely high permeability after annealing.

Feldtkeller (1949a), i.e. the component of the complex permeability which determines the inductance; the abscissa is the "series resistance permeability" μ_{RR} (Feldtkeller, 1949a), which determines the loss resistance.

From these families of curves, we can obtain the permeability and loss angle for various frequencies and field strengths. For example, at 1000 c/s and 4 mA/cm, the following values are obtained: μ_{LR} about 56 000 and μ_{RR} about 40 000. This gives the tangent of the loss angle as about 0·7.

3. COPPER-BEARING ALLOYS OF HIGH PERMEABILITY

The extremely high-permeability values of Boothby and Bozorth were obtained, as far as is known, exclusively on a particular ternary nickel-molybdenum-iron alloy which contained about 79% nickel, 5% molybdenum, 0·5% manganese and traces of the usual impurities.

Similar Patent Specifications confined themselves to alloys within a narrow range around the above composition, suggesting that this order of permeability was not thought possible for any other alloys. Such a single occurrence of extreme permeability would be physically acceptable, since according to the present view (Boothby and Bozorth, 1947; Bozorth, 1951) these high permeabilities require a particularly favourable combination of certain magnetic crystal constants, such as the anisotropy constant and magnetostriction. Furthermore, disturbances, such as, for example, internal stresses and inclusions, must be sufficiently small. It thus appears possible at first sight that only with the composition corresponding to Supermalloy is it possible to obtain the set of conditions which must be satisfied in order to obtain initial permeabilities of the order of 100 000.

Surprisingly, however, our investigations have shown that many alloys respond in a similar way to an additional low-temperature annealing process, and thereby attain permeabilities which equal that of Supermalloy. Among these alloys particular mention should be made of those with an addition of copper. Our investigations (Assmus and Pfeifer, 1953) on alloys of the nickel-iron-copper-molybdenum system showed that the alloys with permeabilities like those of Supermalloy lie within a narrow zone of the triple system nickel-copper-(iron + molybdenum) starting with Supermalloy and running in towards the interior of the system (Figure 5).

It is noteworthy that, among the alloys in this zone, there are also some to be found which have already been known for a long time and are of considerable practical use; for example, the alloys Mumetal and M 1040. They are representatives of the first two stages in the development of magnetically soft materials. If, however, we can produce them with properties belonging to the third stage of development, we can state that the improvement in this third stage is not because of the particular composition, but because of a special treatment, although this treatment can only produce extremely high permeabilities in particular ranges of alloys.

As examples of the zone shown in Figure 5, permeability curves of the above-mentioned alloys, with and without additional annealing, are shown in Figure 6. Comparison with the materials similar to Supermalloy (Figures

1 to 3) show that the initial permeabilities are fully as high and the maximum permeabilities nearly as high as those of the latter. Amongst the above alloys, those which have been quoted as examples are not just particularly good exceptions; in fact roughly the same properties are obtainable over the whole zone. The annealing conditions and optimum molybdenum content vary over the zone, however, according to a definite law.

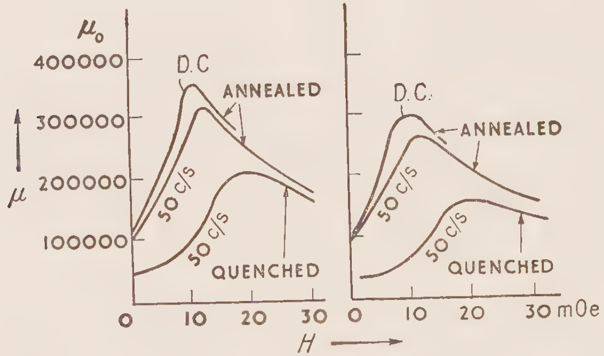

Figure 6. Effect of annealing on Mumetal and on M 1040.

4. EFFECTS OF ANNEALING

The alloys described thus attain their extremely high permeability only after an additional heat-treatment at a relatively low temperature, following annealing at a higher temperature. One naturally asks what structural changes are brought about by the heat-treatment. No clear answer has yet been found.

It has long been known that, for binary nickel-iron Permalloy, annealing between about 400 and 500°C causes a severe reduction of permeability (Arnold and Elmen, 1923) and a lowering of electrical resistivity (Dahl, 1936). It is known that both effects depend on the formation of an Ni_3Fe superlattice (Becker and Döring, 1939). We have already appreciated from the foregoing paragraphs that the permeability of Supermalloy shows the opposite effect; we have also found the opposite behaviour for the resistivity (Assmus and Pfeifer, 1951). Since it appeared possible that this contrary effect might be bound up with varying impurity contents of the alloys, we carried out some investigations on binary nickel-iron Permalloy under the same conditions as for Supermalloy.

The result is compared in Figure 7 with the earlier measurements by Elmen. It is seen that the newly-tested material showed almost exactly the same fall of permeability during annealing as that previously found, and that a fall of resistance occurred as well. Elmen's results are thus well confirmed. The

different behaviour of the alloys with more constituents is therefore not a result of different methods of melting, annealing, etc.

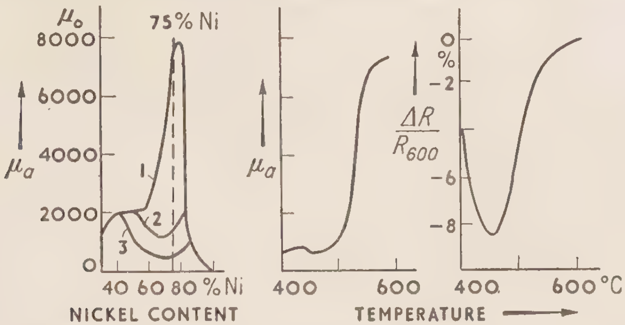

Figure 7. Initial permeability and resistivity (after annealing) of nickel-iron alloys.

Figure 8 shows how the initial permeability and resistance of alloys like Supermalloy vary with additional annealing. For permeability, we see a clearly defined maximum within a narrow temperature range. The electrical

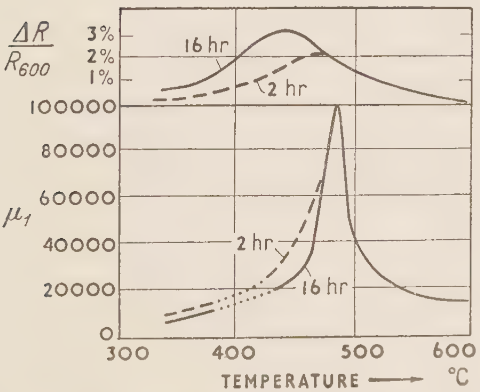

Figure 8. Initial permeability and resistivity (after annealing) of Ultraperm 10.

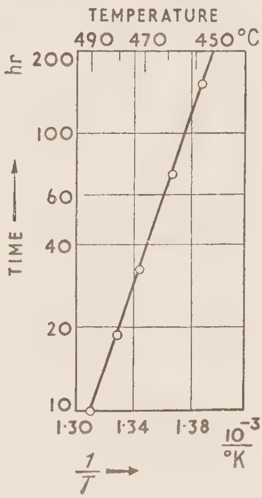

Figure 9. Half-value time of the resistivity change in annealing of Ultraperm 10.

resistance of the alloy at room temperature shows a small but noticeable rise, starting at high annealing temperatures. At low temperatures there seems to be again a decrease of electrical resistance; this is because the annealing time was not sufficient for the final value to be attained.

The copper-bearing alloys, mentioned in section 3, show a similar behaviour of initial permeability and cold resistance as a result of annealing (Assmus and Pfeifer, 1953), so that the results of measurements will be omitted here.

Valuable information about the process which goes on during annealing can be obtained from a study of the rate of this change of the resistance. It is found that, for Supermalloy, the variation with time t follows an exponential law of the form e^{-at} and is independent of the previous thermal history. The constant a varies with temperature T according to a law of the form $e^{-c/T}$. The "half-value time" of a resistance change thus appears as an exponential function of the inverse temperature. Figure 9 shows how well the measurements fit this law.

This law of the form $e^{-c/T}$, for the factor which determines the speed of the resistance change, suggests that a thermal activation is necessary for the appropriate structural change to take place. The magnitude of the activation energy is obtained from the measurements as about 70 000 cal/Mol for the alloy investigated. This value is within the order of magnitude of activation energies for the diffusion of many atoms in metallic lattices.

In general, the resistance effects observed with alloys of the Supermalloy type are very much like those which have been found for a whole series of solid-solution systems (Thomas, 1951), of which only nickel-chromium need be mentioned. There are so far no clear ideas about the phenomena which produce these anomalies.

Apart from these resistance changes, measurements made by Josso (1950), on the changes of length which occur during annealing, are important in explaining the effects under discussion. He investigated binary nickel-iron alloys and also those with added constituents such as copper, molybdenum or chromium. All alloys showed similar changes of length during annealing at temperatures in the regions of superlattice formation or destruction. The addition of copper caused a reduction in the magnitude of this effect but did not change its basic character.

Josso concluded from this result that a superlattice was formed in the complex alloys just as in the binary ones. The results of resistance measurements mentioned above are contrary to this since conditions such as those in Ni_3Fe should give a fall in resistance whereas a rise was actually found. The fundamental process thus appears to be more complicated than the normal formation of a superlattice, even if it is not indeed of a different type altogether.

The measurements for Figure 4 were kindly carried out in Prof. Feldtkeller's Institute.

25

THE PROPERTIES AND POTENTIALITIES OF COLD-REDUCED NICKEL-IRON

W. F. Randall and H. H. Scholefield

(Telegraph Construction and Maintenance Co. Ltd.)

Abstract: The paper deals with the effect of progressive cold reduction on the structure and magnetic properties of nickel-irons of the 50/50 and 80/20 types. The effect of heat treatment on these cold-reduced materials over the temperature range 500 to 1100°C is then considered and the implications of the various factors for the development of magnetic properties are discussed.

1. INTRODUCTION

With a few obvious exceptions, nickel-iron alloys containing more than 30% of nickel react similarly to similar conditions. Owing to lack of full experimental data, inferences and theories here introduced are based on information derived either from the 50/50 or 80/20 nickel-iron alloys.

It is proposed to deal first with the effect of progressive cold reduction on the magnetic properties and characteristics of nickel-irons and secondly with the effect of subsequent heat-treatment on these properties. The implications of these factors are discussed in the third section.

2. THE EFFECT OF PROGRESSIVE COLD REDUCTION ON NICKEL-IRON ALLOYS

The first effect of cold working appears to be the adaptation of the crystals to the applied stress by twinning. The limit of twinning accommodating the cold working has been passed at 50% reduction, at which stage grain distortion and slip bands have made their appearance. At 66% reduction, the grains have been broken up to a large extent although it would appear that strain has been taken up mainly by a matrix of grains of definite orientation while others are apparently undisturbed. At 85% reduction, this process has progressed much further, the idiomorphic grains are not so evident and any which persist have been broken down to a much smaller size. At higher reductions, up to 95%, crystal-grain structure is completely obliterated, giving place to a more or less uniformly striated appearance (Figure 1).

A back-reflection x-ray photograph (Figure 2) shows, in the original hot-rolled and annealed sample, large grains with marked residual strain. The large grains are associated with high-temperature heat-treatment, but it is noteworthy that this residual strain persists. It seems to be associated with the small degree of cold work induced towards the end of the hot-working operation when the temperature of the material has fallen to a level

where it is capable of retaining plastic strain and does not undergo spontaneous recrystallization. As is shown later, it is extremely difficult to remove small strains even at high temperatures. In a similar photograph after only 10% reduction, a continuous diffused ring shows that grain break-up has commenced. Some grains still persist, as indicated by the presence of discrete spots, but the greater number of spots per unit area of the ring shows that the average size of the crystals has been reduced. After 25% reduction, the x-ray photographs show almost complete break-up of the grains with few discrete spots persisting although the micrographs show a high proportion of idiomorphic grains. At 50% reduction, a minimum crystallite size, as indicated by line breadth, has been reached. From 50% reduction onwards, the gradual breaking up of this ring points to increasing orientation, this being pronounced at 80% reduction. Specific examination of the development of preferred orientation, using a silver target, gives no evidence of such an effect up to 50% reduction. Further working produces it in an increasing degree until at 95% reduction the 111 axis of all crystallites lies within 5° of the direction at right angles to the rolling direction in the rolling plane. No signs of spontaneous recrystallization are found even in the most heavily cold-worked samples. Parameter measurements, made perpendicularly to the rolling plane, show a gradual decrease reaching 0·2% at 50% cold work. This is apparently the maximum compression that the lattice can permanently tolerate as measurements of this dimension at greater reductions show irregular behaviour, which can be due to overstrain adjustments.

Figure 3 shows the variation in hardness with increasing reduction. The cold-rolled samples show a steady rise in hardness from 220 V.P.N. at 10% reduction to a maximum of 340 V.P.N. at 80% reduction. Increasing the cold work beyond this point shows a fall to 300 V.P.N. at 97% reduction.

The magnetic properties of series such as are described above are such that the initial stage where B is proportional to H, hardly discernible in annealed material, increases in extent with cold working. It reaches a maximum at approximately 70% reduction after which it remains sensibly constant. At a field strength above 4 oersteds, the induction progressively diminishes with reduction to a minimum, the position of which seems to be determined by the grain size of the original material. Increased reduction results in increased induction until at 95% it has attained approximately two-thirds that of the annealed material (Figure 4).

While the variations in the normal induction curve due to the reductions of 10 to 90% are quite small, a large effect is produced by reductions beyond 90%. The difference is emphasized if the reduction at this stage is carried out in a larger number of passes.

Maximum permeability varies in much the same way as induction at 4 oersteds but initial permeability progressively diminishes with increasing cold work.

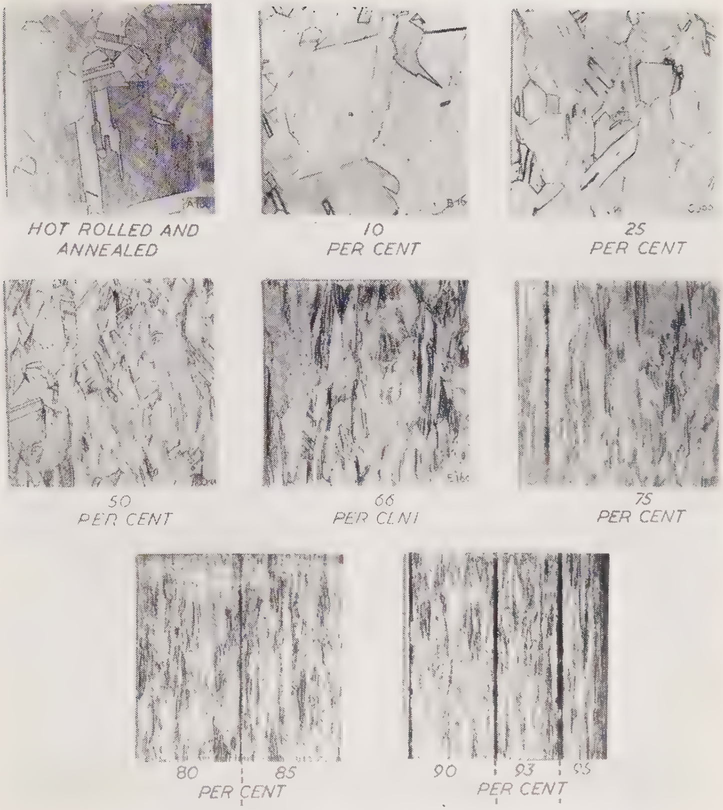

Figure 1. Series of micrographs showing the effect of progressive cold reduction on Mumetal.

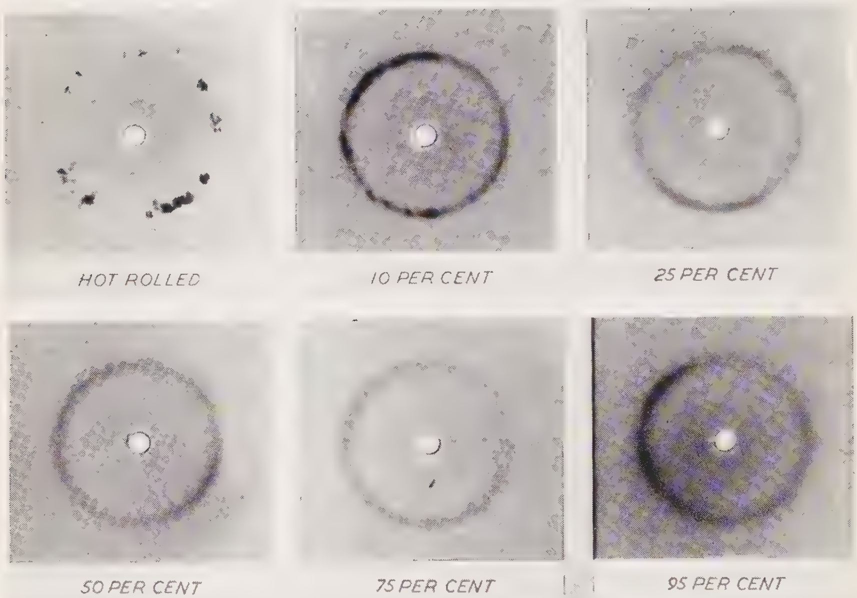

Figure 2. Series of x-ray back-reflection photographs showing the effect of progressive cold reduction on Mumetal.

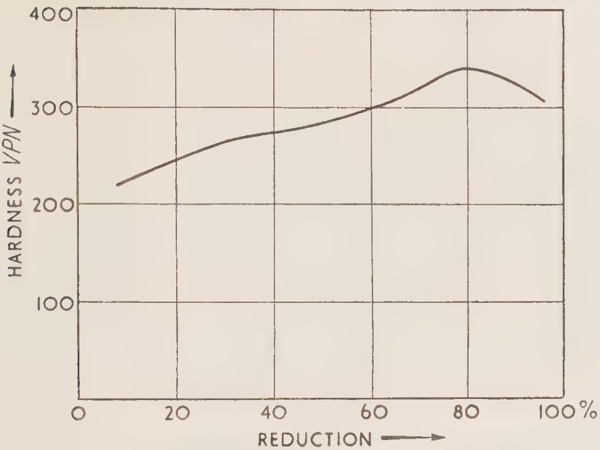

Figure 3. Change of hardness with progressive cold reduction.

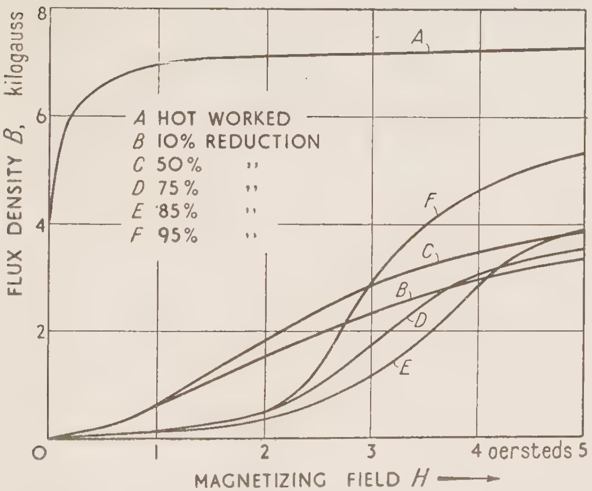

Figure 4. Change of normal-induction curves with progressive cold reduction.

The phenomena described above have been put to practical use in the isoperms. In this alloy a high degree of reduction applied to properly heat-treated material develops very low hysteresis.

Extended linearity in the initial stages of magnetization and the lowest induction at 4 oersteds are associated with complete fragmentation of the

Figure 6 shows normal-induction curves for lightly-reduced Mumetal after heat-treatment at various temperatures from 500 to 1100°C, and Figures 7 and 8 similar sets of curves for the alloy subjected to intermediate and heavy reductions.

The maximum permeability of lightly-reduced material increases slowly with increasing temperature of heat-treatment up to 800 or 900°C. At 900°C it jumps rapidly to a high value and the rate of growth is maintained at still higher temperatures. With intermediate reductions, the same general development is followed, but the temperature of sudden increase is lowered to 700 or 800°C. With extreme reductions above 90%, the high maxima of up to 250 000 which may be attained with less cold work are never achieved even after annealing at 1100°C.

Maximum permeabilities

Temperature, °C	Light reductions	Intermediate reductions	Heavy reductions
500	5 000	3 500	7 000
600	6 000	9 000	30 000
700	9 000	35 000	40 000
800	25 000	75 000	60 000
900	85 000	110 000	65 000
1 000	150 000	160 000	—
1 100	200 000	250 000	110 000

The permeability at relatively low field strengths attains its greatest values for intermediate reductions and is not substantially increased by heat-treatment above 900°C. It has been found that hysteresis loss and coercivity in heavily-reduced material are much greater after annealing than those of more lightly worked material heat-treated at the same temperature.

Correlation of magnetic properties with structural differences indicates that the poorer magnetic quality obtained with light reductions is associated with residual strain which persists even after heat-treatment at high temperatures. The falling-off at high reductions is probably associated with smaller grain size and the development of preferred orientation in which the preferred axis does not coincide with a direction of easy magnetization for the alloy. The magnetic characteristics for material subjected to heavy reductions were necessarily determined on specimens which were thin and the "skin" effect already mentioned would consequently have a pronounced effect.

The discussion so far has referred, in the main, to an alloy of the 80/20 type. The 50/50 alloy undergoes similar structural changes but the orientation developed after heat-treatment is such that the direction of easy magnetization coincides with the preferred axis. In this respect, therefore, the 50/50

alloy differs from the 80/20. The structural changes and their effect on magnetic characteristics have already been examined by other investigators and discussed in detail (Schmid and Thomas, 1950; Scholefield, 1949; Crede and Martin, 1949). An interesting feature of this alloy which still requires

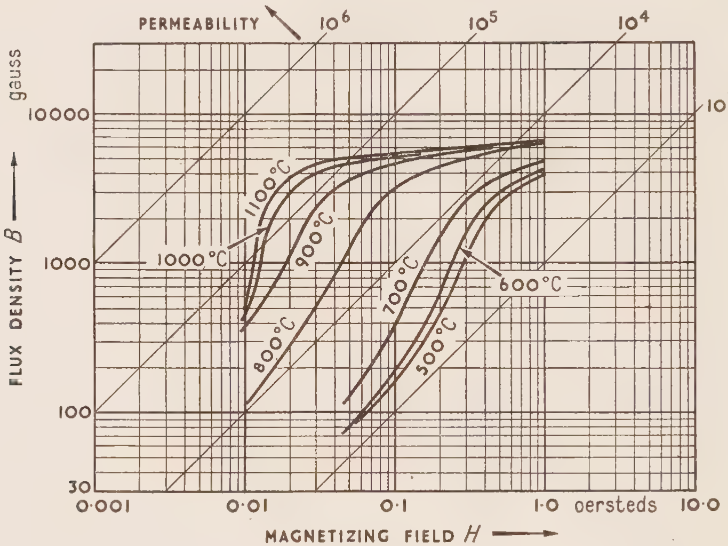

Figure 6

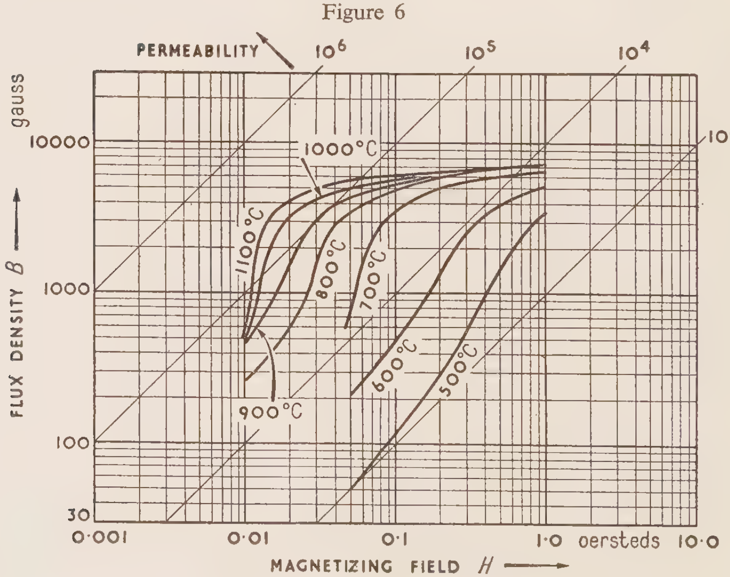

Figure 7

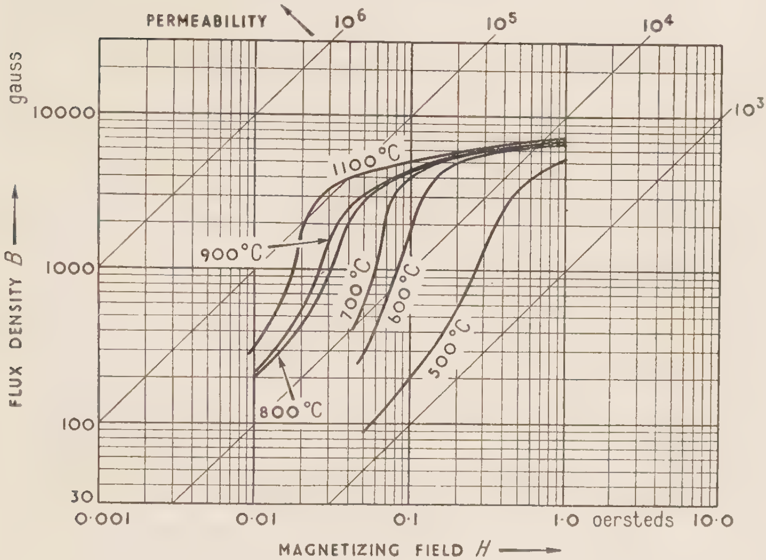

Figure 8

Figures 6, 7 and 8. Normal-induction curves for Mumetal after heat-treatment at various temperatures.

Figure 6, after 10% reduction ; Figure 7, after 66% reduction ; Figure 8, after 96% reduction.

full explanation is the decrease in initial permeability associated with orientation of the crystals and domains instanced in the table (Randall and Scholefield, 1950) for 50/50 nickel-iron.

	μ_a (measured at $H = 0{\cdot}001$ oersteds)
Random grain and domain orientation	3 000 to 6 000
Grain-oriented (partial domain-orientation)	1 000 to 1 500
Grain-oriented and domain-oriented	< 900

It would appear that when the domains are oriented in the direction of the applied field, there is some phenomenon which delays their response to it until it reaches a certain threshold value when they assume this direction *en bloc*. This results in the characteristic normal-induction curve of this class of materials.

5. POTENTIALITIES

It is clear that exactitude of composition and heat-treatment which achieves homogeneous structural conditions give rise to extremely high permeabilities which, in the zero-magnetostriction range, may be infinite. This has been

demonstrated by the work carried out on Supermalloy at the Bell Telephone Laboratories. In general, impurities or adventitiously occurring bodies—whether gaseous or solid, soluble (substitutional or interstitial) or insoluble—have a detrimental effect on the potential magnetic properties of the binary nickel-iron matrix. This appears to be due to local stresses set up in the crystal or lattice structure of the material. They can act in a secondary manner by disturbing crystal orientation and affecting grain size by acting as crystal nuclei. Their removal always results in improved permeability. The advances which might result from refined metallurgical methods in production of ingots and by high-temperature gas reactions in the course of production have not yet been fully exploited.

Schumacher (1950), for example, points out that the presence of less than 0·1% MgO in 80/15/5 nickel-iron-molybdenum alloy can so far affect the establishment of optimum structural conditions as to reduce the maximum permeability to one-tenth and the initial permeability to one-third. Also the efficiency of pure hydrogen treatment has been demonstrated, and the efficacy of this increases as the impurities present in the hydrogen atmosphere decrease. The effect of high temperatures in increasing the speed of reactions is also a significant factor in achieving removal of impurities.

From the above it is apparent that permeability is related to structural condition. One interference most difficult to control is the adventitious impurities. Some work has been done in this field. Melting has been carried out under reduced pressures in an endeavour to reduce the interfering inclusions mentioned above.

Some structural changes, such, for example, as are caused by domain movement, are not easily discernible by micro-examination or X-ray analysis, but it has been shown that they can be controlled to some extent by heat-treatment in magnetic fields with enormous effects on magnetic characteristics, particularly the maximum permeability, which may increase tenfold. Initial permeability may suffer diminution. A full knowledge of the effects of field strength, alternating or direct current, range of temperatures over which the field is applied, etc., is not available, and more work is necessary in this field. Potential developments must be applied with caution as secondary effects such as increased a.c. losses and possible instability have been observed.

The two aspects considered above are interdependent. Magnetic annealing is more efficacious on pure than on impure material, and Schumacher suggests that this is due to the restriction imposed by dispersed impurities on domain movement. Such experiments which have been made have not taken account of strain centres due to the inevitable impurities contained in commercial materials. When, however, pure materials and optimum magnetic annealing conditions are brought together, it may be that our present conceptions of the effects will have to be revised.

26

SOME CHEMICAL AND PHYSICAL PROPERTIES OF IRON POWDERS AND THEIR EFFECTS ON THE MAGNETIC PROPERTIES

C. E. Richards

(Post Office Engineering Research Station)

Abstract: A study has been made of some of the chemical and physical properties of iron powders to see if these could be related to their magnetic properties. A reasonably quantitative relationship has been established and it has been shown that:

(*a*) both hysteresis and eddy-current losses increase with particle size;

(*b*) the measured eddy-current losses are somewhat higher than can be accounted for theoretically;

(*c*) a possible reason for this is "frequency-dependent residual loss";

(*d*) improved powders for use at high (radio) frequencies, say > 5 Mc/s, are less likely to result from the use of alloys having higher resistivities than from comminution either actual or effective (as in E-type carbonyl iron).

1. INTRODUCTION

As part of a study of methods for improving the performance of magnetic powder-cores an investigation was made into the characteristics of "carbonyl iron" which are associated with its superiority for high-frequency inductors. It was, of course, well known that some grades of carbonyl iron are outstanding for this use, but there was no very clear idea why this should be. It was important to find this out before trying to develop improved materials.

There is some confusion in the literature about "carbonyl iron" and the term may refer to one of the many grades of powder (usually unspecified), to a sintered or cast block made from the powder or to a rolled sheet made from a sintered block or casting. In this paper specific types of powder only are considered. Reference will, however, be made to the properties of electrolytic iron and to carbonyl nickel-iron powders also.

Carbonyl iron powder is made by volatilizing iron pentacarbonyl (a liquid at ordinary temperatures) into a hot chamber known as a "decomposer", where it breaks down according to the reaction

$$Fe(CO)_5 \rightleftharpoons Fe + 5\,CO$$

At low temperatures the reaction goes from right to left and at higher temperatures left to right. An important side reaction which may occur is

$$2\,CO \rightleftharpoons CO_2 + C$$

It is usual to dilute the gases in the decomposer with nitrogen; ammonia gas also may be added and, if so, appears in the iron powder as up to 0·6%

16

combined nitrogen. The powder "as deposited" contains also up to about 0·8% carbon.

This complicated system in which an iron particle is born in the presence of $Fe(CO)_5$, CO, CO_2 and NH_3, all of which may participate in the reactions, is responsible for the series of powders known as "carbonyl iron". The various qualities which are of interest in telecommunications engineering are distinguished by code letters.

For convenience Table 1 gives actual grades and sources of carbonyl irons.

Table 1

Type of powder	German	American	British
Finest for highest frequency	—	SF	MF
Fine for highest frequency	H	TH	ME
Normal for high frequency	E and EN	E	ME
Soft for carrier frequency	C	C	MC
Special for low frequency and inductance tuning	—	L	MP

E-type powders are characterized by an "onion-skin" structure which tends to disappear when the impurities (carbon and nitrogen) are removed by annealing in hydrogen to give C-type powders.

All cores considered in this paper were made with 1% insulant and 3% synthetic-resin binder by weight, and they were pressed at 20 tons/sq.in.

In estimating magnetic losses Legg's analysis of the losses in a wound core (Legg, 1936) has been used.

$$R_m/L_m = \mu h \hat{B} f + \mu c f + \mu e f^2$$

in which R_m and L_m = resistance and inductance due to the core;

μ = initial permeability;

h, c and e = hysteresis, residual and eddy-current loss coefficients;

f = frequency (c/s);

$\hat{B}$ = peak flux density (gauss).

2. EFFECT OF PARTICLE SIZE ON MAGNETIC LOSSES

Richards *et al.* (1950) gave some figures which indicate a dependence of hysteresis loss on particle size but the evidence is not conclusive. Experiments have now been made with iron powders of different sizes and types whose differences in size were attained in different ways.

Measurement of particle size. Some difficulty was experienced in measuring the effective sizes of many of the powders. Carbonyl irons were fairly

simple—being approximately spherical they gave consistent results on both the Fisher "Sub-Sieve-Sizer" (Gooden and Smith, 1940) and by direct microscopic measurement—but the Fisher instrument was found to give incorrect results on the electrolytic powders, particularly the larger sizes, and finally a curve was constructed from microscopic measurements and actual counts of weighed samples of powders. From this it was possible to estimate the equivalent diameter of any powder from microscope measurements. It was found that direct microscope measurements were satisfactory up to about 15 to 20 microns, but that above this the particles tended to lie flat on a slide and the size estimate became far too high. This irregularity of shape makes eddy-current calculations less reliable as the particle sizes become bigger.

Preparation of graded powders. Graded powders were made in the following ways:—

(*a*) A sample of American electrolytic iron powder was separated by sifting and sedimentation into four fractions of mean (r.m.s.) particle size 82, 66, 22 and 12 microns.

Table 2

Material	Particle size (microns)	Permeability	Magnetic loss coefficients		
			$h \cdot 10^6$	$c \cdot 10^6$	$e \cdot 10^9$
(*a*) Electrolytic (sifted)	82	31	360	1400	41
	66	32	300	1400	26
	22	29	260	1300	14
	12	23	230	1100	4·5
(*b*) Electrolytic (pebble mill)	18	12	239	1800	9·5
	15	11	232	2100	8·3
	16	10	190	2300	6·2
	14	10	195	2300	4·1
	12	10	173	2400	2·9
(*c*) C-type powder	7·0	17	90	1100	3·9
	4·6	12	44	700	0·8
	3·0	10	32	800	0·3
(*d*) E-type powder	4·0	8·4	11	200	0·2
	3·5	8·1	7·4	not measured	
	3·1	7·5	6·7		
	2·8	6·9	5·8		
	2·2	7·0	4		
	1·7	6·8	4		

(*b*) Another sample of electrolytic iron of different origin (British) was pulverized in a pebble mill for varying times, samples being taken at different stages; these had estimated particle sizes 18, 15, 16, 14 and 12 microns.

(*c*) Samples of carbonyl irons of MP, ME and MF grades all from the same source were decarburized by a long heat-treatment in hydrogen at 400°C giving substantially carbon-free powders of 7·0, 4·6 and 3·0 microns.

(*d*) A single sample of E-type (ME grade) carbonyl iron was pulverized in a pebble mill as (*b*) and powders of 4·0, 3·5, 3·1, 2·8 and 1·7 microns were collected.

Measurements of graded powders. Powders of series (*a*) and (*b*) were annealed at 400°C in hydrogen for 24 hours before making into cores. All these powders were made into ring cores and examined magnetically; the results are in Table 2.

The correspondence between particle size and both eddy-current and hysteresis losses is marked. Assuming other factors to remain constant, eddy-current loss coefficients should vary as

$$\frac{(\text{diameter of particle})^2}{\text{resistivity}}$$

In Figure 1 eddy-current coefficients are plotted against (diameter of particle)^2 and hysteresis coefficients against particle diameter. From these curves we can deduce the following empirical relationships.

For E-type carbonyl iron

$$e.10^9 = 0{\cdot}015\, d^2 \qquad \ldots(1)$$

$$h.10^6 = 1{\cdot}75\, d \qquad \ldots(2)$$

For C-type iron and electrolytic iron

$$e.10^9 = 0{\cdot}03\, d^2 \text{ or } 0{\cdot}045\, d^2 \qquad \ldots(3)$$

$$h.10^6 = 13\, d \qquad \ldots(4)$$

where *d*, the diameter, is in microns.

It is probable that the better value in equation (3) for soft iron powder is $0{\cdot}045\, d^2$ obtained by using the curve through the points for C-type carbonyl only. With electrolytic and other powders which have been broken down from bulk material by attrition mills there is an unknown shape factor which shows up increasingly with the larger-sized particles. For example the 82-micron particles mentioned in Table 2, on microscopic measurement, proved to be over 200 microns so that their average thickness must have been of the order of 10 microns only. Although therefore the combined curve shows the essential similarity of the materials it is probably less correct fundamentally than the short one.

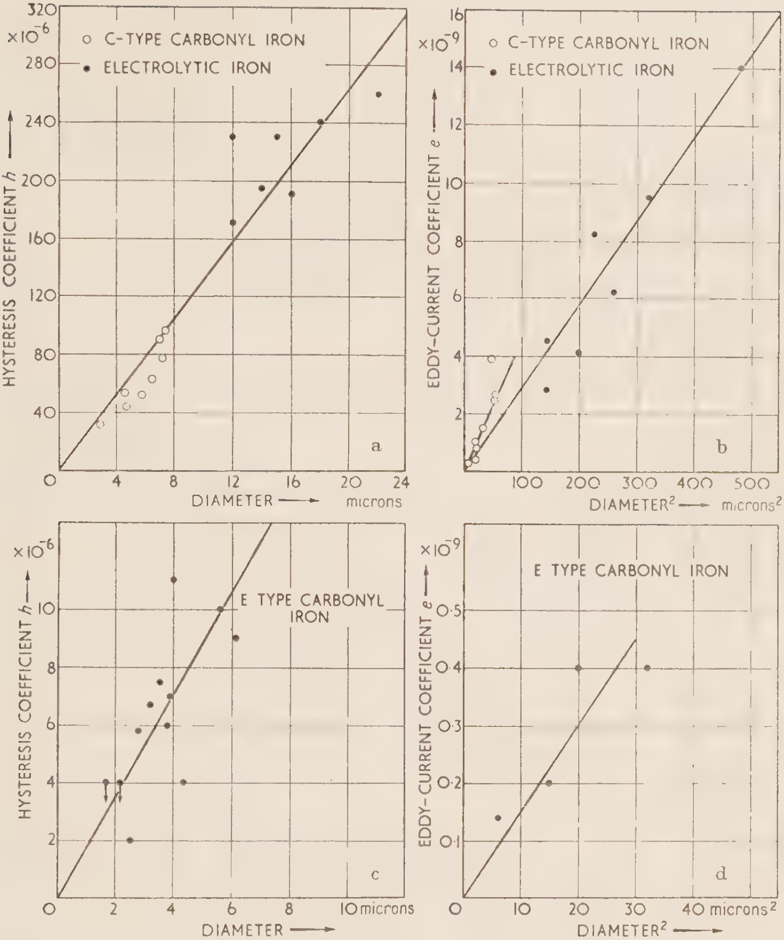

Figure 1. Variation with particle size of hysteresis and eddy-current coefficients.

Now, if we know the size and resistivity of the iron particles in a core the eddy-current loss coefficient can be calculated :

$$e = \frac{2\pi^3 d^2}{5\rho\gamma^{1/3}} \qquad \ldots(5)$$

where d = diameter of particles,

ρ = resistivity,

γ = packing factor.

Considering 5-micron particles we get the following values for e by calculation and empirical formula.

Table 3

Material	Calculated $e \cdot 10^9$ from equation (5)	Observed $e \cdot 10^9$ interpolated from equations (1) and (3)
E-type carbonyl	0·17	0·38
C-type carbonyl and electrolytic	0·34	1·1

In the above calculations ρ was taken as 10 microhm-cm for C-type and electrolytic powder and 20 for E-type powder. The reason for this difference is explained below (section 5).

The discrepancy between calculated and measured eddy-current losses may be in some measure due to a proportion of the particles not being effectively insulated though this seems unlikely as the results are the same for a number of insulating media. It is possible that we have here to consider the existence of a frequency-dependent residual loss of the type described by Richter (1937).

3. EFFECT OF CARBON ON MAGNETIC LOSSES

Both carbon and nitrogen can be removed from E-type carbonyl iron by prolonged heating in hydrogen at about 400°C and a series of partly decarburized irons was prepared and their magnetic properties determine d These are given in Table 4.

Table 4

Carbon, %	Permeability	Magnetic loss coefficients		
		$h \cdot 10^6$	$c \cdot 10^6$	$e \cdot 10^9$
0·62	11·1	42	700	1·1
0·57	11·2	44	700	1·0
0·45	11·6	54	800	1·0
0·35	11·6	55	800	1·2
0·18	12·9	62	800	1·4
0·08	13·4	68	900	1·8
0·07	13·2	72	900	1·7

It is clear that removal of carbon results in a progressive increase in permeability and also in all losses.

4. EFFECT OF NITROGEN ON MAGNETIC LOSSES

The nitrogen can be removed from E-type carbonyl iron without substantially changing the carbon content or interfering with the "onion-skin" structure. The following table contains magnetic data for four such powders which were denitrided in slightly different ways.

Table 5

Powder	Permeability	Magnetic loss coefficients		
		$h \,.\, 10^6$	$c \,.\, 10^6$	$e \,.\, 10^9$
Original E-grade ..	10·8	6	200	0·2
Denitrided	10·0 to 10·5	10 to 12	500 to 1000	$<$ 0·3

5. DISCUSSION OF THE EFFECT OF VARIOUS TREATMENTS ON THE MAGNETIC LOSSES

The measurements under discussion were made on magnetic powder in bulk, so some of the effects may be related either to differences between homogeneous powders or to differences between mixtures. Every effort was made to see that each powder was homogeneous but the possibility of some not being so must not be overlooked.

Eddy-current loss. Within the range of particle sizes which have been examined there is a general rule that eddy-current loss $\propto$ diameter^2 for any one material. There are, however, differences between materials and difference from theory which cannot be dismissed as experimental error.

The powders used form two families and one explanation of their differences has been based on their different liabilities to plastic flow causing different amounts of insulant breakdown.

This explanation does not seem good for the following reasons :—

(*a*) A great many measurements on all types of powder with many kinds of insulant have shown that the eddy-current loss coefficient is substantially independent of core-making pressure until the insulant breaks down completely at high pressure.

(*b*) Experiments in which the insulant was omitted but the binder retained showed a dependence of eddy-current loss coefficient on core-making pressure.

Table 6 gives typical measurements.

Table 6

Material	Treatment and pressure	Permeability	Eddy-current loss coefficient $e \,.\, 10^9$
E-type (ME grade)	Insulant and binder; 20 tons/sq.in.	11·1	0·3
,,	,, ,, 90 ,, ,,	14·7	0·3
C-type (MC grade)	,, ,, 20 ,, ,,	15·9	2·4
,,	,, ,, 60 ,, ,,	21·1	1·9
,,	Binder only .. 30 ,, ,,	14·2	7·8
,,	,, ,, .. 50 ,, ,,	18·1	12

The influence of carbon on the behaviour of E- and C-type carbonyls was considered. The eddy-current loss figures in Table 4, plotted against carbon content, fall on a smooth curve and can be extrapolated to zero carbon content. Yensen (1924) gives the resistivity of pure iron as 9·6 microhm-cm at 20°C and the increase in resistivity per 1% of added carbon as:—

0 to 0·02% : 82·5 microhm-cm;
0·02% to 0·85% : 4·5 microhm-cm.

The product of eddy-current loss coefficient and resistivity should be constant. Table 7 sets out calculated $e.\rho$ products for the materials quoted in Table 4, and for some others with widely differing values of ρ.

Table 7

Composition of powder	$e \cdot 10^9$	ρ, calculated	$e \cdot \rho \cdot 10^9$
Pure iron	2·3	9·6	22
0·07% carbon	1·7	11·4	19
0·08% ,, ...	1·8	11·5	20
0·18% ,, ...	1·4	11·9	17
0·35% ,, ...	1·2	12·7	15
0·45% ,, ...	1·0	13·1	13
0·57% ,, ...	1·0	13·7	14
0·62% ,, ...	1·1	13·9	15
Ni/Fe 50/50	0·3	45	15
Ni/Fe 60/40	0·7	37	26*
Ni/Fe 86/14	1·1	17	19
E-type carbonyl	0·3	21·4†	6

* This powder had a rather larger particle size than the others, 6 microns against the usual 5.
† Correction of + 7 microhm-cm for nitrogen in accordance with Norbury (1920). Yensen gives no figure.

For clarity it should perhaps be stated that the decarburized irons are all substantially free from nitrogen (see sections 3 and 4) and that the nickel-irons are necessarily C-type, having been heat treated to develop the alloy structure.

It will be seen that the eddy-current loss of E-type carbonyl iron is of a different order from that of the other powders, and on the basis used for calculation we must assign an effective resistivity of about 60 to bring it into line.

A more reasonable explanation would be that the effective particle size is not the one measured. If we allow a resistivity of 10 for C-type carbonyl and 20 for E-type, it is only necessary to postulate an effective diameter of 4 microns for E-type against a measured diameter of 5 microns for both types to account for the differences in eddy-current loss. An inspection of any photomicrograph of E-type carbonyl iron will show that a fair proportion

of the larger particles are agglomerates in which the effective size for the circulation of eddy currents is half or less of the actual particle diameter. This argument, of course, assumes that the shell structure in E-type carbonyl presents an effective barrier to currents flowing across laminations but none to those along them.

Hysteresis loss. It is clear that the general rules covering the hysteresis losses in E-type carbonyl irons and others are similar but the order is different. Size for size the losses in C-type carbonyl iron and electrolytic iron are about eight times those in E-type carbonyl. Since decreasing the carbon content by normal decarburization techniques *increases* hysteresis loss, it can be inferred that the carbon is not held in the usual form as in a steel. Since also comminution in all cases reduces hysteresis loss, it is reasonable to ask whether, in fact, the only difference between the grades is the broken structure of E-type iron due to "onion-skinning" which progressively degenerates as the carbon is removed. Removal of nitrogen does increase hysteresis loss slightly, but not nearly to the same extent as removal of carbon.

If we regard E-type carbonyl iron as consisting of particles each made up of a series of concentric shells, whether partially insulated from each other or not, we have a uniform structure in which the decay of these shells by decarburization should have no effect on the eddy-current loss, no matter how much it affected the hysteresis loss. If, however, we imagine that some of the shells are not complete and may enclose part of a layer only, and if we remember that many of the larger particles of E-type powder are multiple small particles having two or more centres, we have the structure described above in which removal of the "onion-skin" structure should lead to increased eddy currents. The disappearance of these boundaries between layers will also make the existence of larger magnetic domains possible, so that domain walls will have more room to move.

It has been shown by Stewart (1951) that part at least of the hysteresis loss is due to eddy currents set up by the movement of domain walls; it is now suggested that in fine particles of the type here discussed, hysteresis loss is dependent on the distances through which domain walls can move in the different sizes and types of particles, and should therefore qualitatively (for any one type of powder) depend on effective particle size.

6. CONCLUSIONS

The object of this work was twofold; there was the desire to know more about the influences controlling the performance of iron powder, and there was the need for a pointer to help in the future development of improved powders. It has been shown that, basically, all iron powders behave in much the same way, so far as hysteresis and eddy-current losses are concerned. The superiority of E-type carbonyl iron over all others for use at high frequencies lies more in its effective subdivision into particles which

behave as though they were smaller than actual measurement proves them, than in any intrinsic metallurgical superiority. When carbon is removed from the metal the main effect is to increase the distances through which eddy currents can flow and domain walls move. There seems no reason why electrolytic iron powder should differ in behaviour from C-type carbonyl provided the particle size is made comparable. (Some difficulty exists in measuring the effective particle size of irregular powders such as electrolytic iron.)

Should it become necessary to improve on E-type carbonyl iron for use at high frequencies it is unlikely that the use of alloys such as 50/50 nickel-iron of higher resistivity than pure iron will enable lower-loss powders to be made, because the nickel-iron alloy powders are structurally homogeneous and comparable rather with C-type carbonyl irons. Comminution, either actual or effective, seems a more useful way.

With regard to eddy-current loss, theory predicts only about half the loss which is measured. In a matter of this sort this might be taken as a reasonable degree of agreement, but there are two further possibilities. (1) Snoek (1947, p. 74) has stated that although the use of a residual-loss coefficient independent of frequency may be justified for powder and laminated cores, the residual losses of ferrites are "anything but independent of frequency". It may be that a factor of this nature is involved, though the present work makes this look unlikely. (2) Alternatively, a better assessment of particle size might bring the two sets of figures closer together.

The effect of nitrogen in E-type powders is of secondary importance only, though its removal does increase losses slightly.

The measurements reported here were made by members of the Materials Division of the Post Office Engineering Research Branch, and the information is now used by permission of the Engineer-in-Chief of the Post Office.

DISCUSSION

Mr. A. C. Lynch:

The loss caused by eddy currents must be inversely proportional to the resistivity; so measurements at two temperatures will show whether the observed loss can be due to eddy currents, provided that other sources of loss remain substantially constant. The broken lines in Figure A show the results of such measurements on a C-type carbonyl iron, at temperatures such that the resistivities of iron are in the ratio of 9 : 1. Both lines are fairly straight, and by extrapolating them to zero frequency we find the value conventionally quoted for "residual loss". (It is subject to criticisms such as those of Feldtkeller (1953a) and Polder (1953).) The residual loss at —180°C is about twice that at 20°C.

From each measured loss we can subtract the calculated eddy-current loss for particles of known size (7 microns*) and resistivity (10 microhm-cm.). We thus obtain the full lines in Figure A, which are nearly parallel. Unless this is accidental, there must be a source of loss which is independent of resistivity and temperature, but which varies with frequency in the same way as eddy-current loss. Roberts (1950) has suggested a possible cause for a loss of this type.

* Unfortunately the eddy-current loss is very sensitive to the size, which is not very precisely known. But no other size makes the results easier to explain.

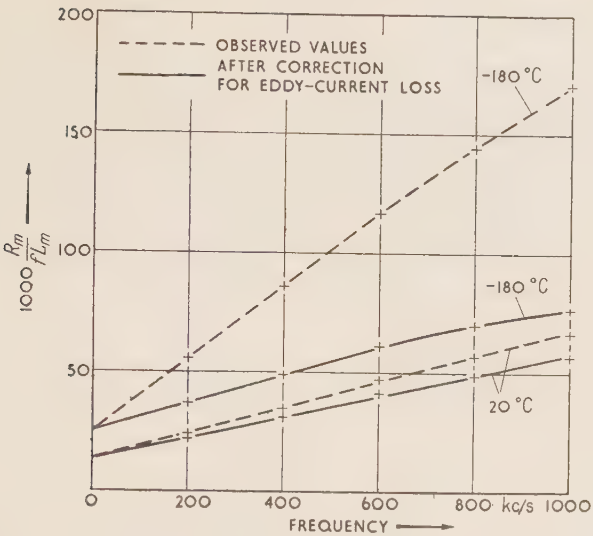

Figure A. Losses at two temperatures in C-type carbonyl-iron powder.

Mr. F. F. Roberts:

The possible explanation, to which Mr. Lynch refers, of the "extra" eddy-current loss is simply that this type of loss-versus-frequency behaviour arises as the low-frequency "tail" of a relaxation or damped resonance phenomenon associated with a loss maximum at a considerably higher frequency. The reality of loss mechanisms due to other than eddy currents is demonstrated by the behaviour of ferrites in the 1 to 100 Mc/s frequency range and by the great breadth of the induced precession resonance in the ferromagnetic metals and alloys at microwave frequencies; Bloembergen's (1950) results suggest that the latter resonance breadth does not decrease appreciably with temperature below room temperature in the case of nickel or Supermalloy, and a similar near-constancy for iron would, if confirmed, appear to be consistent with Mr. Lynch's finding of near-parallelism for his curves after correction for eddy currents.

Referring now to Mr. Richard's paper, I should like to suggest some features which may be expected on physical grounds in the "onion-skin" structure of carbonyl-E particles. Electron micrographs indicate that each shell in these structures has a thickness of about 100 iron-crystal unit cells. Now it is impossible to construct a perfect spherical layer, even one unit cell in thickness, using cubic unit cells as building blocks: there must be dislocations, distributed randomly over the surface of the layer, or more probably grouped in some particular pattern of lines dividing the layer into a number of areas relatively free of dislocations but probably still in a state of strain. Likewise it is impossible to build up a thick spherical shell by adding on successive layers one unit cell in thickness, without either introducing dislocations between layers or else strains within layers. It is suggested that the attainment of a limiting strain determines the actual number of layers in a shell. It is further suggested that the dislocations within layers and between shells are stabilized by carbon or nitrogen atoms or both, the number of dislocation sites available (assuming a

simple pattern of line and surface dislocations) agreeing in order of magnitude with the maximum C-plus-N content actually found.

Magnetically, the dislocation-free areas of each shell would tend to be single "domains" magnetized along one of the preferred crystalline cube-edge directions parallel to the surface of the shell, and the lines of dislocations would substantially fix the "walls" between these "domains". Thus magnetization of such a particle will take place essentially by rotational processes within each "domain" and consequently no hysteresis is to be expected while magnetocrystalline anisotropy enhanced by the large strains present will necessitate a large external field to cause approach to saturation. The regions referred to as "domains" in this context will be less sharply defined than in large crystals of more normal structure, owing to the comparable magnitudes of the shell thickness and the usually estimated domain wall thickness for iron.

Electrically, the line and surface dislocations will increase the resistance of eddy-current paths in a direct manner, while some further increase may be expected from the approach of the shell thickness to the mean free path of electrons in the iron.

Mr. A. E. De Barr:

There seems to be some misunderstanding about the properties to be expected of powder cores if they include particles which are single domains. Aggregates of such particles will have a large coercive force when magnetized to medium or high induction but, for small alternating magnetization as usually encountered in communication work, the magnetization processes will be reversible, and will not therefore involve hysteresis. Under these conditions the true permeability of the material will be small but this effect may not be noticeable in powder-cores. After heat-treatment which results in the formation of larger particles, the material would be expected to have a smaller coercive force but a larger hysteresis loss for small alternating magnetization, since irreversible magnetization processes are now involved. Thus the results reported by Mr. Richards are not incompatible with the hypothesis that, in part of the material at least, single domain particles are involved.

Dr. A. Fairweather:

Measurements of the magnetic behaviours of powder aggregates are made for a variety of purposes; and for all of them it is unfortunate that the magnetic properties of an aggregate are insensitive to changes in those of the powder material. The main use of such tests is, perhaps, to provide comparative data for different materials: the kind of data required then determines the experimental procedure to be employed.

Thus a core-designer may have standardized a particular production process and may wish to know which of several powders should be used for a specified purpose. Accordingly, a comparison is made of the magnetic behaviours of cores having the same proportions of powder, insulant and binder, and fabricated at the same pressure. The desired information is obtained, but the results do not provide a measure of the magnetic properties only of the powders. The results depend also upon the absolute and relative mechanical properties of powder, insulant and binder. Hard and soft powders compress to different extents: the thickness of the insulating film between adjacent particles depends upon the relative hardnesses of the constituents, and upon the surface roughness of the particles. A comparison of the magnetic properties (as distinct from the core-making properties) of powders is best done, perhaps, with aggregates pressed to the same volume and,

preferably, pressed as little as possible. This latter requirement greatly increases the difficulties of measurement.

In considering the area of contact between particles, it is important to distinguish between non-metallic contact, with an intervening film of insulant or binder, and metallic contact which occurs when the film is penetrated. A soft powder may give a large area of non-metallic contact, and little likelihood of film penetration. A hard powder may give a small area either of metallic contact, or of non-metallic contact with an intervening film severely reduced in thickness. Thus, somewhat paradoxically perhaps, the greater the particle deformation, the less the likelihood of film breakdown. And, similarly, the softer the film, the greater the dependence of eddy loss upon pressure. These considerations are not inconsistent with the results given in the Paper.

Mr. S. E. Buckley:

It has not been found by all investigators that the hysteresis loss coefficient is proportional to the particle size of iron powders. For example, on some electrolytic iron powders (Speed and Elmen, 1921; Legg and Given, 1940), the following values are quoted:—

Powder Type	Particle size	Core permeability	Hysteresis Loss coefficient h
Grade B	80 mesh (approx. 60 microns)	35	49.10^{-6}
„ C	200 „ („ 25 „)	26	81.10^{-6}

In this example the two grades are thought to have been sieved from the same basic product; it will be noted that the cores compressed from the smaller particles have a higher hysteresis loss coefficient than those produced from larger particles. It is interesting to note that these coefficients are much lower than those quoted for electrolytic iron powders in Table 3 of the Paper.

Further, in work carried out in France (Steinitz, 1948), on cores pressed from special iron powders of very small particle size, permanent magnet properties were obtained, thus indicating that the hysteresis loss coefficient of these very small iron particles is very high.

Dr. Fairweather mentions the possible effect of metallic contacts between particles in influencing eddy-current losses in cores. We have found that when uninsulated Carbonyl E iron powder is pressed at 100 tons/sq.in., the particles do not bond together at all, whereas Carbonyl C iron powder under the same conditions compresses into a solid core. This may have some bearing on the observed result that the eddy-current losses of insulated Carbonyl E cores are so much lower than those of insulated Carbonyl C cores.

Dr. V. G. Welsby:

In the design of directional filters for telephone repeaters the choice of the core materials for the coils may be dictated by hysteresis rather than Q, with the result that cores used may have a much lower permeability than that which would give the optimum Q at the frequency concerned. These low effective permeabilities may be obtained by using "gapped" cores of various types, attended by increasing screening difficulties as the gap ratio is increased. The alternative is to use a toroidal core and to "dilute" the core material to the desired extent by the inclusion of non-magnetic material to form a powder-core. Since the low permeability in this case is required only from the point of view of hysteresis there is no

necessity for the core particles to be as small as they normally would for a low-permeability core intended for use at higher frequencies. I suggest that the core manufacturers might consider the need for toroidal powder-cores having permeabilities of, say, 3 or 4 and relatively large particle sizes, in an attempt to avoid the disadvantages shown by Table 1 of my paper (Welsby, 1953).

Mr. Richards (in reply):

The iron particles discussed in the paper are, in the main, larger than those which are known to become magnetically hard. We had reasoned, however, on the lines suggested by Dr. Wohlfarth (p. 13), that permanent magnet effects might begin to appear gradually as the particle size was reduced. The experimental fact is that the smaller the particle the lower the hysteresis loss—over the particle size range considered. Not only was this so at very low inductions, but tests made in medium to high fields have confirmed the tendency. The powder compacts used are similar in density to those of powder permanent magnets, so similar amounts of interaction are probable.

Heat treatment, which softened the powder and removed carbon and nitrogen, always resulted in increased hysteresis loss and, in higher fields, increased coercivity. This heat-treatment resulted in a negligible amount of particle growth and would not, of itself, be expected to influence the hysteresis loss.

Electron micrographs of E-type carbonyl iron, besides showing the "onion-skin" structure, also seem to show that the shells are not all concentric; some enclose only a small volume of metal. Owing to the difficulty of making these micrographs one should be wary about drawing too definite conclusions about structures. Many particles are, however, agglomerates and have more than one set of shells.

The difficulty of building spherical structures from cubic bricks is clear but the relative sizes of the bricks and the structures concerned is so different that no difficulty is seen in building structures which to the eye, and even the microscope, appear spherical—though in fact only approximately so—and are quite solid.

Unless the intrinsic permeability of the outer shells in E-type material is improbably high they could not act as an effective screen at the frequencies concerned.

The use of the solid core technique has the limitations suggested by Dr. Fairweather, but I do not think their effect is great. The method has the merit of assessing material under working conditions and although changes occurring during loading are a legitimate study they were not the factors we had in mind. We had hoped to eliminate insulation troubles by keeping the technique constant and pressures low. Experiments specifically to see whether insulation breakdown was occurring showed that this was not so.

The trend of the figures given in the paper differs from those quoted by Mr. Buckley, and I know of no complete reason for this. It is, however, difficult to draw conclusions because Legg and Given's figures seem to refer to blended powders consisting in part of unannealed and part of annealed powder; the binder content of cores made from the two grades was also different, the finer grade being more extended than the coarser. This generally increases hysteresis loss. The same difficulties exist when comparing the magnitudes of the hysteresis-loss coefficients; annealing affects the figures and the temperature of annealing is important. Speed and Elmen, although saying that they anneal some of their powder, give no details.

27

50/50 CARBONYL NICKEL-IRON POWDERS

C. E. Richards and D. C. Shotton

(Post Office Engineering Research Station)

Abstract: A study has been made of the behaviour of 50/50 carbonyl nickel-iron powder. As supplied, the material consisted of two phases, iron with a little nickel and nickel with a little iron. Low-temperature heat treatment converts this into a homogeneous alloy powder with which magnetic cores can be made. These combine to some extent the properties of E-type and C-type carbonyl irons in that cores having the permeability of C-type iron cores, but losses more nearly those of E-type iron, can be made.

1. INTRODUCTION

Nickel-iron alloy powders have been used in communications engineering for many years and have generally been made by melting the constituents in a high-frequency furnace, followed by rolling and pulverizing the metal or by sintering followed by pulverizing. Powders prepared in this way consist of particles of assorted shapes and those from the second method may be micro-porous. The carbonyl process would appear to offer some advantages since the alloys produced are in the form of dense spherical particles.

Both nickel and iron give carbonyls which are liquid at ordinary temperatures and which, when heated, decompose giving the metal. By passing the mixed vapours into a hot decomposer, apparently homogeneous nickel-iron powders of any composition can be produced. It has been found, however, that although the powders seem to be chemically homogeneous they are not fully alloyed and need heat-treatment to develop the alloy structure.

This paper describes experimental work in a sample of 50/50 carbonyl nickel-iron powder made by the Mond Nickel Co. Ltd. The powder has been examined by magnetic methods and X-ray diffraction.

2. PREPARATION OF THE POWDERS

All heat-treatment was done in an atmosphere of pure dry hydrogen. Preliminary work showed that heat treating the raw powder above 400°C. gave tough, intractable sinter cakes ; the powder was therefore insulated with 1% magnesium oxide (as Cream of Magnesia B.P.) and dried before commencing heat-treatment. After annealing, the magnesia was removed by boiling in dilute acid. The resultant powders were examined by X-rays and cores were made for magnetic analysis. For core-making the powders were insulated with 0·9% SiO_2 by hydrolysis of silicon ester, and 4% phenolic binder was added. All pressing was at 20 tons/sq. in.

3. PROPERTIES OF THE POWDERS

Heat treatments were given at temperatures from 280 to 1050°C. All treatments but the highest were for 20 hours; the 1050°C run was only 7 hours.

Figure 1. Effect of annealing temperature on properties of carbonyl nickel-iron powders. Top to bottom: permeability ; hysteresis loss coefficient ; residual loss coefficient ; eddy-current loss coefficient ; particle diameter.

In spite of the magnesia insulation some small-scale sintering did take place and was shown up by particle size measurements.

The results are plotted in Figure 1 (the bottom curve), where it will be seen that there was a steady rise in particle size as the temperature of heat-treatment increased. These measurements were made by the air permeability method (Gooden and Smith, 1940) using the proprietary equipment known as the "Fisher sub-sieve-sizer". Attempts to confirm these measurements by microscopic examination broke down because the agglomerates formed during sintering existed as long strings or as clusters, and no reliable measurements could be made. It was, however, established that the original particles were spherical and that in forming agglomerates they were only joined together at relatively small areas. No solid lumps were found. It is probable that the size measured by the air permeability method is a fair estimate of the mean diameter and makes allowance for the areas of contact between spheres.

(*a*) **Permeability.** The top curve of Figure 1 shows that permeability is mainly a function of particle size. Previous work of a similar nature on C-type carbonyl-iron powders of 3 to 7 microns diameter showed a relationship between a (diameter in microns) and μ (permeability)

$$\frac{d\mu}{da} = 1{\cdot}7 \qquad \ldots(1)$$

whereas for this series of nickel-irons

$$\frac{d\mu}{da} = 5 \qquad \ldots(2)$$

Making allowance for the effect of increase in diameter

$$\mu_t = \mu_0 + 0{\cdot}01T \qquad \ldots(3)$$

when μ_t = corrected permeability of nickel-iron powder after heat-treatment at a given temperature

μ_0 = corrected permeability of nickel-iron powder when just converted to alloy

T = temperature, °C, above that necessary for alloy formation.

The temperature necessary for alloy formation is shown more accurately by loss measurements than by permeability (see (*c*) and (*d*) below).

(*b*) **Eddy-current loss.** The curves do not reflect any change in loss coefficients due to metallurgical changes during heat-treatment except in the lowest range. From the data available for all temperatures above the lowest alloying point (about 360°C) there is a steady increase in eddy-current loss coefficient with temperature. Considered as a function of particle size the relationship is

$$10^9 \frac{de}{da} = 0{\cdot}026a \qquad \ldots(4)$$

compared with the figure $0{\cdot}09a$ obtained for C-type carbonyl iron (Richards, 1953). Since, however, the resistivity of 50/50 nickel-iron is about four times that of pure iron the slopes of the curves agree reasonably well, and indicate that no fundamental change takes place in the resistivity of the metal between 360 and 980°C.

It must be emphasized that the lowest figures quoted are so near the limit of measurement that they can only be regarded as indications of the general trend.

In Figure 1 two high figures for eddy-current loss coefficient have been ignored. This is justifiable because it is quite possible to make a core having a large eddy-current loss from powder which is intrinsically low-loss, but it is not possible to make a core having low eddy-current loss from a high-loss powder. The low-loss points are therefore probably the more accurate.

(*c*) **Hysteresis loss.** Above about 360°C changes in hysteresis loss coefficient follow similar lines to those of eddy-current loss. Changes evidently occur up to 300 or 400°C but above that temperature the metal exhibits almost constant properties, increase in hysteresis coefficient being probably attributable in the main to particle size.

$$\frac{dh}{da} = 22 \text{ (against 15 for C-type carbonyl iron (Richards, 1953))}.$$

(*d*) **Residual loss.** Previous work—mainly on iron powders—has produced no evidence that, within the particle size limits now under consideration, residual loss depends on particle size. The present work shows that the original unannealed powder starts with a very high residual loss which falls rapidly with increasing temperature of heat-treatment up to 500 or 600°C, after which it remains constant. This behaviour differs sharply from that of E-type carbonyl iron which, as deposited, has a very low residual loss. Heat-treatment of iron powder increases this loss to a figure similar to that of the 50/50 nickel-iron powder.

4. X-RAY EXAMINATION

The original powder consists of a body-centred (α) phase and a face-centred (γ) phase. The iron (α) phase gives very diffuse reflections, but appears to be alloyed with a few units per cent of nickel. The nickel (γ) phase gives a somewhat sharper pattern and appears to contain a little over 10% alloyed iron. The diffuse nature of the pattern can be caused by the presence of a continuous range of different alloy compositions (either in single particles or in the powder as a whole) and by the presence of strain or small crystallites in the particle. Reflections from the annealed samples are much sharper. In powders treated above 540°C, unrotated samples give spotty reflections; this is generally accepted as indicating the presence of crystallites larger than 10 microns, though in most of these powders particles over 10 microns are not likely to exist.

Interdiffusion occurs quite readily on heating. In the sample treated at 280°C, the constituents of the original powder are accompanied by a second nickel-rich phase containing 40 to 45% iron and after 20 hours at 360°C about 95% of the alloying is complete. The lattice parameter of the main constituent remains substantially constant above 500°C. Nevertheless, there is a small and diminishing indication of the α phase up to the highest temperatures investigated. This may be due to the presence of a few detached grains of iron which would be isolated by the magnesia-coating during heat-treatment. These iron particles might be formed by some irregularity in the decomposition of the gaseous carbonyls, or arise from accidental contamination of the original nickel-iron powder. The lattice parameter of the 1050°C sample was estimated to be 3·5787 kx, corresponding to 50% iron and no evidence of heterogeneity was found. In the samples heat-treated at 360° to 540°C a few faint extra lines were observed and identified as due to Fe_3O_4. Comparison with a synthetic mixture suggested that the amount present was of the order of 1%.

5. DISCUSSION

Both magnetic and X-ray data indicate that changes due to alloy formation take place up to about 500°C. Above that temperature the material has constant properties except for variations due to slight sintering which causes an increase in the mean particle size.

The basic powder, which has the familiar "onion-skin" structure, seems to consist of particles which are, generally speaking, chemically identical; each particle is, however, a heterogeneous mass. The X-ray data show that the original powder consists of two phases, an iron phase slightly contaminated with nickel, and a nickel phase containing a little over 10% iron. These two phases must exist in each particle because heating an insulated powder at 500°C gives a substantially uniform 50/50 nickel-iron alloy and it is inconceivable that the metals should diffuse through the magnesia insulant.

Alloying apparently takes place quite readily, and is evident at 280°C; at 360°C it is almost complete. This makes it seem possible that during decomposition of the mixed carbonyls, nickel and iron are thrown down not together but alternately, so that each particle consists of exceedingly small elements of nickel interspersed with similar elements of iron. At the temperature in the decomposer, alloying would start at once, but the particles would not remain hot long enough for the process to be completed. There is some doubt about the metallurgical significance of the trace of iron which persists in the powder after heat-treatment. It may be due to the powder having been made in a pilot plant previously used for iron-powder preparation or even to handling in two laboratories which were engaged on iron-powder work. Magnetically it is probably insignificant.

The trace of iron oxide found in samples which were heat-treated below 540°C may be more important. The magnetic measurements have shown that these samples also have high residual-loss coefficients, and although this may be due to some metallurgical phenomenon in the powder, there is evidence from other experiments that the presence of quite small amounts of oxide can cause a remarkable increase in residual loss.

6. TECHNICAL SIGNIFICANCE OF THE RESULTS

The experimental work was done to see whether any field existed in which 50/50 carbonyl nickel-iron powder was appreciably superior to iron powders. The data so far obtained refer only to cores made at low pressures and must be supplemented by further work at higher pressures. Perhaps the simplest way to present a comparison is by a table, and the following one compares the properties of E- and C-type carbonyl irons with 50/50 nickel iron, all cores having been made in the same way.

Powder	Type	Grade	Particle size, microns	Heat-treatment	Permea-bility	Magnetic loss coefficients		
						$h \times 10^6$	$c \times 10^6$	$e \times 10^9$
Carbonyl iron	E	ME	5·0	None	10·8	4·5	200	0·2
,, ,,	E	MF	3·0	None	9·0	<2	<100	<0·2
,, ,,	C	C	7·4	None	16	100	700	2·5
,, ,,	C	MC	5·8	None	14·5	36	1 000	0·7
50/50 nickel iron	—	—	5·4	at 600°C	15	30	500	0·4

Thus for the lowest losses, E-type carbonyl iron is the best material, but should it be necessary to make cores with higher permeabilities than are normally attainable with E-type powders, 50/50 nickel-iron will give lower losses than C-type carbonyl iron.

7. CONCLUSIONS

This work has shown that carbonyl nickel-iron powder (50/50) as deposited, consists of a mixture of two phases, a nickel-contaminated iron and an iron-contaminated nickel. Diffusion alloying starts at very low temperatures (below 280°C) and above about 500°C is complete in 20 hours. The powders offer possibilities in the manufacture of cores having losses almost as low as those of E-type carbonyl irons, but with permeabilities approximately the same as for C-type carbonyl irons. Further work at higher core-making pressures is needed.

Metallurgically the most important point is that it seems unnecessary to exceed 500 to 600°C in order to complete the alloying of the powder. Alloying, in fact, proceeds quite rapidly at much lower temperatures.

The measurements were made by members of the Materials Division of the Post Office Engineering Research Station and the information is now used by permission of the Engineer-in-Chief.

28

FACTORS INFLUENCING THE MEASURED VALUE OF HYSTERESIS LOSS OF POWDER-CORES

P. R. Bardell

(Research Laboratories of The General Electric Co., Ltd.)

Abstract: The influence on hysteresis loss of powder-cores by variation of a number of factors is described. The factors are flux-density, magnetic history, degree of annealing, nature of insulant, particle-size, and internal discontinuities in particles. The influence of each factor is considerable, implying that the flux-density (or coil current for a given coil) must be specified when quoting hysteresis loss and that careful control during manufacture can result in considerable reduction of hysteresis loss.

For cores comprising single-crystal particles of Ni-Fe alloy materials the loss appears to be less for larger particles; this is the reverse of the findings of other workers for carbonyl and electrolytic iron powders, in which the particles are multi-crystalline.

1. INTRODUCTION

The magnetic properties of powder-cores bear little relation to those of the parent metal. For example, the barriers of non-magnetic insulant result in decreased permeability; the residual stresses in the crystal lattices and the discontinuities of flux within and between particles result in increased hysteresis loss. This paper gives quantitative results which emerged during development work.

Before discussing the experimental results it is necessary to define the units employed.

Permeability, μ, is calculated from the inductance of a single-layer coil wound on a ring-shaped specimen; the measurement is made at a frequency of 1 kc/s, with a coil current of 5 mA. The permeability is expressed relative to that of free space. Hysteresis loss is measured in terms of the effective resistance of a 10 mH winding on the core, the standard conditions being currents of 4 and 8 mA, and frequencies of 4, 8 and 16 kc/s.

The hysteresis coefficient h' is defined by the equation

$$h' = \frac{\delta R}{Lf'\delta/l}$$

where δR = change in effective resistance (in ohms) due to a change in current of δI amperes;

L = inductance of coil, wound on a toroidal specimen, in henrys;

f' = frequency, kc/s;

l = mean length of magnetic path, cm, $= 4\pi$ cm for tests described here.

The Legg hysteresis coefficient, a or h, is related to h' by the equation

$$h = \frac{h'}{1775 \,.\, \mu^2}$$

where μ = permeability of core (relative to permeability of free space)

2. SCOPE

(*a*) **Flux-density.** For powder cores it has been found that the relation between coil resistance and coil current at audio frequencies is linear for only very low flux-densities (below about 5 gauss). The departure from linearity is different for different materials, e.g. the ratio of h' at 3·5 gauss to h' at 75 gauss is approximately 1·6 for 80/20 nickel-iron alloy powder and 2·5 for 2/81/17 molybdenum-nickel-iron material.

It is of interest to note that Kornetzki (1943) has drawn attention to similar departures from linearity of the curve of coil resistance against coil current. He has deduced from considerations of the "shearing" or lateral displacement of the hysteresis loop due to the presence of air-gaps in the specimen that the higher the permeability of the particles, the greater should be the departure from linearity of the resistance/current curve. The above data would appear to be consistent with this since the permeability of the molybdenum-nickel-iron alloy is considerably greater than that of the nickel-iron alloy.

(*b*) **Magnetic history of core.** Certain test specifications require that the inductance of a coil wound on a powder-core shall be remeasured after passage for 5 seconds of a direct current of about 200 times the value of alternating current used for normal tests. The change in inductance with modern materials does not exceed $\pm 1\%$, but the change in hysteresis coefficient is often considerably greater. In early work on 80/20 Ni-Fe cores an increase of 100% was reported. A.c. demagnetization failed to restore the original value of h', but this was achieved by reheating the core above the Curie point.

The effects of magnetic shock appear to be greatest for iron cores, less for nickel-iron, and least for alloys of nickel-iron and a third element.

(*c*) **Influence of degree of annealing.** Powder-cores are formed by applying pressures of up to 100 tons/sq.in. The metals employed are very strain-sensitive, as regards magnetic permeability and hysteresis. Examination of crystal lattice distortion by X-ray techniques shows that the residual stress set up during pressing is removed by heat-treatment at temperatures in excess of 580°C, and it is interesting to note that it is necessary to anneal the cores at temperatures in the neighbourhood of 600°C to obtain optimum

magnetic properties. Actually the preferred temperature from the magnetic point of view is about 50°C above the stress-relief temperature, as indicated by x-ray examination, and it is possible that magnetic measurement provides a more sensitive method of detecting internal changes in the material.

Values of permeability and hysteresis loss for cores made of an 80/20 nickel-iron alloy with a refractory insulant are as follows:—

Heat-treatment temperature, °C	Permeability, μ	Hysteresis coefficient, h'
As pressed	31	60
575	93	23·5
600	96	19·5
625	97·5	18·0
650	98·5	18·0
675	99	19·5

The improvement in hysteresis loss is more marked than appears at first sight, since the hysteresis coefficient depends on permeability and should be higher for higher values of permeability.

The rate of heating-up and duration of the annealing process do not appear to be very critical so long as a period of 5 minutes at temperature is exceeded, but varying the rate of cooling has an interesting effect on the susceptibility of the cores to magnetic shock. In the following table the values of permeability and hysteresis loss are given for cores of an experimental 80/20 nickel-iron alloy, heated at 625°C for 30 minutes and then cooled at different rates. The percentage increases in these values after passing a direct current of 2A for 5 seconds through the 10-mH test winding are also given. This magnetizing current represents a flux-density in the core of about 5000 gauss as compared with the test value of about 20 gauss.

Cooling rate* (°C/min.) from heat-treatment temperature of 625°C	Permeability μ	Hysteresis coefficient h'	Percentage increase in μ and h' after passing 2A through coil	
			in μ	in h'
2·0	85·5	17	2·4	105
5·0	89	20	1·7	90
7·0	88·5	20	1·3	105
28	88·5	22	0·7	90
45	89·5	23	0·6	80
66	91·5	23	0·15	70
87	92	25	0·15	50

* Assessed from the time required to cool from 600°C to 500°C.

(*d*) **Influence of the nature of insulant.** Special materials and processing have been developed to enable cores to be heat-treated at about 600°C without breaking down the very thin walls of insulant which separate the metal particles. For some years a chemical method of oxidation was employed. It is probable that chemical attack of the metal impaired the hysteresis loss, but the effect was obscured by the inability of this form of insulation to withstand a temperature above 520°C, so that some residual strain was left in the metal. In the development of a more refractory type of insulation, one difficulty was common to each material tried, namely that dimensional changes occurred which affected not only the covering power of the insulation, but also the hysteresis loss of the heat-treated core. The latter is presumably due to residual strain, although its presence was not detected by X-ray methods. One example of the influence of the nature of the insulant is illustrated by the behaviour of an insulation mixture which included some kaolin. As is well known, on heating up to 600°C, kaolin loses about 13% of combined water. Consequently, in one set of experiments the mixture of metal powder and insulant was heat-treated at 600°C before being pressed. The difference in the properties of such cores from those made from un-heat-treated powder was well marked as is shown by the following data:—

Insulated powder heat-treated	$\mu = 11, h' = 3{\cdot}5$
Insulated powder not heat-treated	$\mu = 20, h' = 25$

Both sets of cores were heat-treated at 600°C.

In another set of experiments in which a very hard material was used for one of the insulating ingredients the hysteresis loss of the resulting cores was much higher than normal. It appears therefore that the effects of the stresses applied to the metal powder by the contraction or by the hardness of the insulant are not completely removed by the heat-treatment.

(*e*) **Influence of particle-size of the metal powder.** Experiments to determine the influence of particle-size on magnetic properties are rather difficult to arrange, particularly if the particles are of irregular shape. In the case of unannealed carbonyl-iron powder having spherical particles, it appears to be well established that the use of smaller particles gives rise to lower hysteresis loss, but the reverse often holds good for alloy powders. On theoretical grounds one would suppose that the fewer the diversions of flux in the core the better would be the hysteresis loss, and one has to take into account any irregularities there may be within a particle as well as the gaps between particles. It has been found that the more nearly the crystal size approaches the particle size the better is the hysteresis loss and in these circumstances, the use of larger particles reduces the hysteresis loss.

The magnitude of the effect is shown by the following data for cores of 14 permeability from coarse and fine fractions of alloy powders, having a crystal-size approaching the size of the particles.

Powder batch No.	Hysteresis factor h', for cores of 14 permeability	
	Coarse fraction (15 microns to 100 microns)	Fine fraction (under 15 microns)
1	1·7	2·3
2	2·0	2·8
3	2·0	2·9

(*f*) **Influence of discontinuities within particles.** Imperfections inside the metal particles can be produced by the presence of cavities and by chemical impurities.

It was possible during experimental work to produce particles having a considerable number of internal cavities. The particles could be consolidated by ball-milling, and it is interesting to note that the porous particles gave cores having high hysteresis loss, and that the loss of cores pressed from the powder after several hours' milling was considerably lower. Both powder and cores were annealed before use.

90-permeability core pressed from porous particles : $h' = 79$
90-permeability core pressed from milled particles : $h' = 53$

A detailed study of the effect of chemical impurities in the metal has not been made, but in some very early development of alloy powder made by a powder-reduction process, a small quantity of residual oxide was left in the particles. It was found that the hysteresis loss of resin-bonded cores was directly proportional to oxygen content (up to about 1·5% O_2) and that the increase in hysteresis loss corresponding to an increase in oxygen content of 1% was approximately 40%.

3. CONCLUSION

The purpose of this paper has been to discuss some test data indicating the extent to which various factors influence hysteresis loss in a powder-core. It is by paying close attention to such details that it has been possible to reduce the size of cores for a given performance to a very marked extent. The limit of size-reduction has probably been reached since any further reduction would make it very difficult to wind a satisfactory coil on the core. Even so, it is still true to say that the hysteresis coefficient of a powder-core is considerably greater than that of the parent metal, and therefore one must conclude that further reductions in hysteresis loss should be technically possible.

The author wishes to thank the Director of the Research Laboratories of The General Electric Co. Ltd. for permission to publish this paper.

DISCUSSION

Mr. S. E. Buckley:

We also have found that in cores compressed from insulated nickel-iron powders (and

nickel-iron-molybdenum powders) the hysteresis-loss coefficient is greater in cores composed of fine particles than in those composed of coarse particles. The hysteresis-loss coefficient is also found to be higher as lower permeability cores are produced from a given powder by increased dilution (Legg and Given, 1940).

It should be appreciated that the hysteresis-loss coefficient is dependent on the complete cycle of mechanical treatment given to the magnetic material. For example, if the particles are very severely deformed during pressing, then the temperature of recrystallization is lowered more than if the deformation is slight. On subsequent heat-treatment of the pressed cores, a lower hysteresis-loss coefficient is often obtained in the core which initially had the more severe mechanical treatment.

Mr. C. E. Richards:

It is stated that the effect of magnetic shock is greater with some materials than others. Can this be related in any way to their saturation magnetostrictions? The three examples quoted make this seem possible. If the effect is due to magnetostrictive strains, could these be severe enough to require the metal to be heated to the recrystallizing temperature rather than the Curie point? Information on iron cores which recrystallize well below the Curie point may supply the answer.

It should not be overlooked that ball-milling, besides consolidating a powder, also comminutes it, and although the experiments in section 2(*e*) of the paper showed that fine powders had a higher hysteresis loss than coarse ones, the reverse is so in section 2(*f*).

Mr. Bardell (in reply):

I would stress the importance of Mr. Buckley's remark that the hysteresis-loss coefficient is dependent upon the complete cycle of mechanical treatment given to the magnetic material. It is this fact which makes it very difficult to devise a series of controlled experiments to ensure that in drawing conclusions from practical data one has taken into account all the significant variables. It is, therefore, reassuring to have Mr. Buckley's confirmation that with insulated nickel-iron powders, the hysteresis-loss coefficient is greater in cores composed of fine particles than in those composed of coarse particles. Mr. Richards makes the comment that in section 2(*f*) of my paper, it would appear that the reverse may be true. Actually, in the experiments to which reference is made in that paragraph, there was little difference in the particle size of the milled and unmilled particles. I agree, however, that cores composed of particles each containing a large number of very small crystals will behave differently from those in which the particles consist substantially of single crystals.

Regarding Mr. Richards's suggestion that the effects of magnetic shock may be related in some way to the saturation magnetostriction of the material, whilst I agree that this possibility must not be overlooked, there is some experimental evidence to indicate that magnetostrictive strains do not play a major part. For example, examination by X-ray diffraction techniques does not reveal any noticeable change in the condition of the material after a heavy magnetic surge has been applied. Also the permeability after application of the surge is often somewhat higher than before; if there were any major strain-effect this would almost certainly be reflected in a lowering of the permeability.

29

SOME PROPERTIES AND APPLICATIONS OF SILICON-IRON

J. McFarlane and N. F. Mole

(G.K.N. Research Laboratories)

Abstract: The paper reviews the important properties of both non-oriented and oriented silicon-iron alloys, and their application to the magnetic circuits of transformers and other equipment.

Some fabrication considerations are discussed.

1. INTRODUCTION

Modern civilization depends to a very large extent on the existence of the electrical industry and the availability of electric power. These, in turn, depend on the phenomenon of ferromagnetism, which is found only in three elements, iron, nickel and cobalt. These elements, and their many alloys, provide magnetic materials having a wide range of properties.

In power applications of magnetic materials the most desirable properties are high saturation-induction, to allow the greatest possible output for a given frame size; high permeability to reduce magnetizing currents to a minimum; and low hysteresis and eddy-current losses to limit heat dissipation and improve efficiency. The material moreover must have mechanical properties which allow of fabrication. When large quantities of the material are used, the cost is an all-important factor.

Of the ferromagnetic elements, iron is the most plentiful and the cheapest. When alloyed with considerable quantities of nickel, very high permeability and low losses are achieved, but the saturation-induction is reduced, and the cost is high.

When alloyed with silicon, the magnetic properties of iron are improved in certain respects, and it is this material which provides the most economic solution to most power-engineering problems.

The annual production of silicon-iron sheet material has risen to about 150 000 tons. The bulk of this material is used in electrical machines and transformers. It is interesting to note that the British Electricity Authority has a total alternator capacity of over 14 million kVA, and that this is supported by high voltage and distribution transformers having a total capacity of at least 50 million kVA. All these, together with much of the apparatus which consumes the electrical power, employ silicon-iron materials.

2. PROPERTIES OF SILICON-IRON ALLOYS

The earliest electrical machines and transformers employed Swedish iron as the core material. The work of Hadfield (1904) and others at the beginning

of the present century, showed that the addition of silicon to iron had a fourfold advantage. It raised the permeability, reduced the hysteresis loss, reduced the eddy-current loss by increasing the resistivity, and eliminated "ageing", i.e. deterioration of magnetic properties when subjected to temperature of about 100°C over long periods.

Subsequent work in the United States by Yensen, Cioffi and others (Bozorth, 1951) showed that very pure iron has a much higher permeability and lower hysteresis loss than any of the silicon-iron alloys. With total impurities less than 0·05%, initial and maximum permeabilities of 10 000 and 2 000 000 respectively, were recorded. It was shown, however, that very small amounts of impurities, particularly oxygen, carbon and sulphur, have a very severe effect on the magnetic properties, and the permeabilities quoted above are reduced perhaps 40 times in commercial iron, while the hysteresis loss is increased about 20 times.

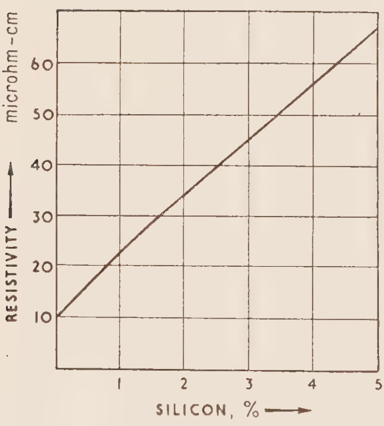

Figure 1. Variation of resistivity with silicon content in silicon-iron.

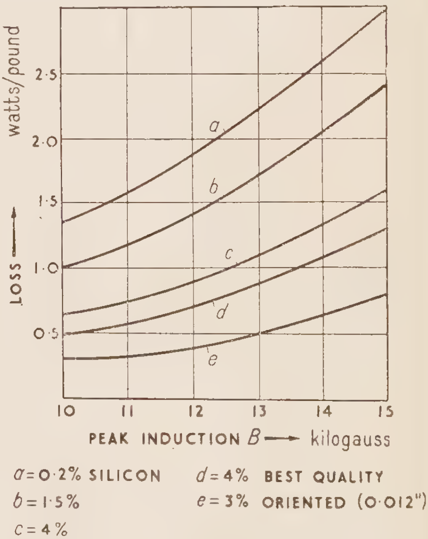

Figure 2. Variation of loss with induction in various grades of silicon-iron (thickness 0·014 in. except for curve e); frequency 50c/s.

The addition of silicon does not improve the magnetic properties of iron. By acting as a deoxidizer, and by precipitating other elements, it allows the inherent properties of iron to be approached, and to be retained throughout manufacture, fabrication and use. Silicon is advantageous in one other respect: it increases the resistivity very considerably, and hence reduces eddy-current losses, which are inversely proportional to resistivity. Figure 1 shows this effect.

The effect of silicon on losses of 0·014-in. sheet is shown in Figure 2. The losses decrease as the silicon content is increased up to 4%. The "4% Best Quality" material is further improved by virtue of less total impurity and

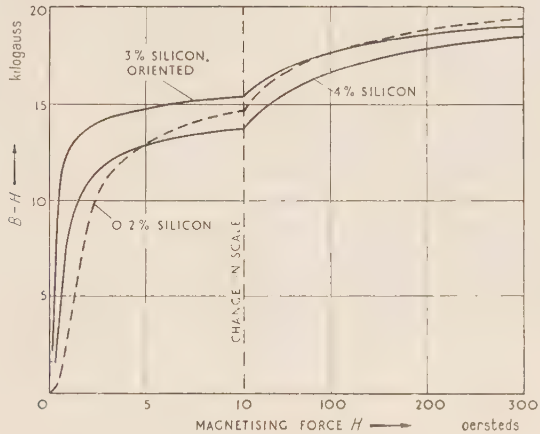

Figure 3. Induction curves for various grades of silicon-iron.

better annealing treatment. 4% or 4½% silicon content is not exceeded because the sheet becomes so brittle that it cannot be punched or sheared.

Figure 3 demonstrates the effect of silicon on the B/H curve. At inductions

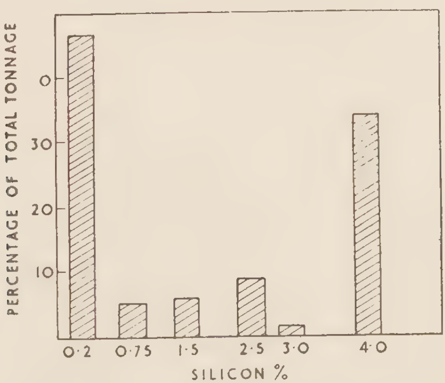

Figure 4. Relative outputs of various grades of hot-rolled silicon-iron.

below the knee of the curve, the permeability is increased by the addition of silicon.

At high inductions silicon has the detrimental effect of reducing the saturation-induction. It acts as a diluent, and causes the saturation-induction to drop in proportion to the atomic percentage of silicon.

The relative outputs of various grades of sheet material are plotted in Figure 4, which shows peaks at each end of the silicon range. The lowest silicon grade is most widely used, partly because it is cheapest, and partly because it has the highest saturation-induction. The highest-silicon grade is widely used in those applications in which improved magnetic quality justifies the higher cost, which is about 50% more than for 0·2% silicon sheet.

The eddy-current loss is proportional to $B^2f^2t^2/\rho$, where B is the induction, f the frequency, t the thickness and ρ the resistivity. Although reduction in thickness reduces the eddy losses, it increases both the sheet manufacturing costs and the assembly costs. The low-silicon grades are rarely rolled thinner than 0·018 in., while the 4% silicon material is almost entirely 0·014-in. thick. This results, at 50 c/s, in eddy-current losses of the order of 10 to 20% of the total loss. When the material is required for use at higher frequencies, it may be rolled to 0·007-in. gauge. Thinner material cannot readily be manufactured by the hot-rolling technique.

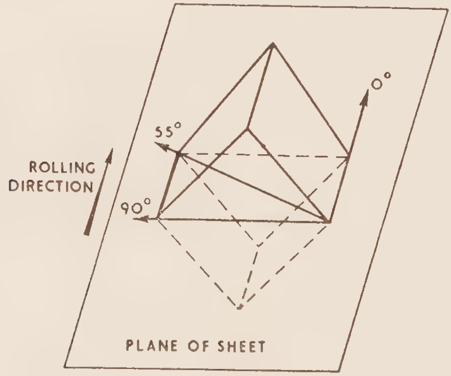

Figure 5. Preferred crystal alignment in oriented silicon-iron.

Oriented materials. The crystal structure of iron forms a body-centred cubic lattice which is most easily magnetized along the cube edge. A technique has been developed by Goss (1934), involving cold rolling and high-temperature annealing, which causes the crystals to have the preferred orientation shown in Figure 5. This material has greatly increased permeability and reduced losses (see Figures 3 and 2) when magnetized in the rolling direction, although little is gained as compared with randomly-oriented material when it is magnetized in other directions (Figure 6). A silicon content of about 3% is not exceeded because of rolling difficulties.

3. APPLICATIONS TO MACHINES AND TRANSFORMERS

The bulk of silicon-iron sheet production is used in the manufacture of rotating machines and power transformers. Broadly speaking, the lower-

silicon grades are used in small machines where high saturation-induction is of greatest importance; medium-silicon grades are used in larger machines, where reduction of losses assumes greater importance, and the highest-silicon grades are used for power transformers, where low losses are essential. Further improvement in this direction has been achieved by the use of oriented strip, which has also been used in the segments of large a.c. machines (Apperson and Fontaine, 1951).

Space does not permit of detailed considerations of these applications here.

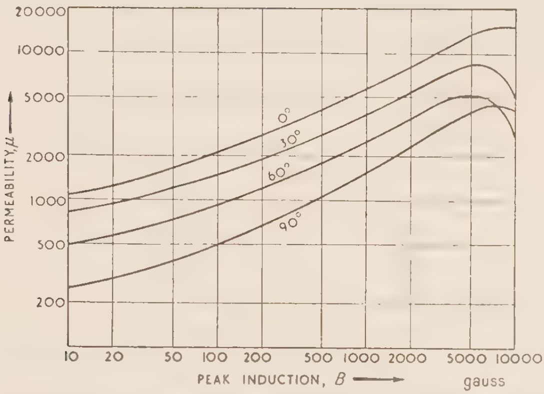

Figure 6. Modulus of complex permeability for magnetization in various directions in oriented 3% silicon-iron. Frequency, 50 c/s.

4. INSTRUMENT TRANSFORMERS

The essential requirement in a precision current transformer is that the magnetizing current should be a very small fraction of the load current. The high-permeability nickel-iron alloys are most suitable when high precision is required, but 4% silicon-iron operating at inductions of the order of 100 to 1000 gauss, is extensively used when high precision is not important. Oriented material, wound in spiral cores, is being used to an increasing extent, and gives better performance than the hot-rolled material. In this case spiral cores are not disadvantageous, since they replace ring stampings.

In voltage transformers, the core material requirement is less stringent, and it is permissible to have magnetizing currents of the same order as the load current. $3\frac{1}{2}$ or 4% silicon-iron, operated at 7 to 9 kilogauss, is generally used, and is replaced by nickel-irons only when the burden is small and when the highest precision is required.

5. MISCELLANEOUS USES

Although machines and power transformers consume most of the tonnage of silicon-irons, these materials are used in a large number of applications,

such as watt-hour meters, audio-frequency transformers, voltage-stabilizing transformers, television deflector-coil yokes, relays, contactors, and electromagnets. Two other applications are discussed below.

Chokes and inductors. In rectifier circuits, where polarized chokes are widely used as smoothing elements, high incremental permeability is desirable, and 4% silicon material is commonly used. If large polarizing fields are used, higher incremental permeability may be obtained from low-silicon grades.

Unpolarized chokes with air gaps are used in several fields, of which fluorescent lighting chokes are typical. In this case, where cost is a prime factor, thicker laminations of low-silicon content are used.

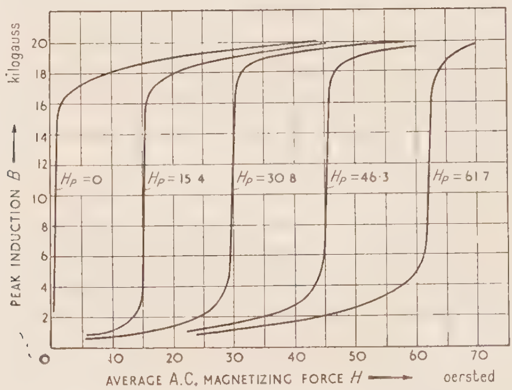

Figure 7. Characteristics of series-connected magnetic amplifier with oriented silicon-iron core.

Magnetic amplifiers. The most desirable properties of core materials for magnetic amplifiers are high permeability in the unsaturated region and a sharp knee on the magnetization curve.

Although nickel-iron alloys have most favourable properties in this respect, oriented silicon-iron is acceptable. Its high saturation-induction and low cost commend its use in cases where appreciable power output is required. Typical characteristics are shown in Figure 7.

6. FABRICATION CONSIDERATIONS

The production of laminations raises problems of working to close dimensional tolerances, with the added problem of obtaining the optimum magnetic properties from the finished lamination. It has already been noted in section 2 that the low-silicon grades are less brittle. A further factor in their favour is their lower shear strength, shown in Figure 8, which increases with silicon

content. Thus, bigger presses are needed for higher grades of material, and die life is decreased.

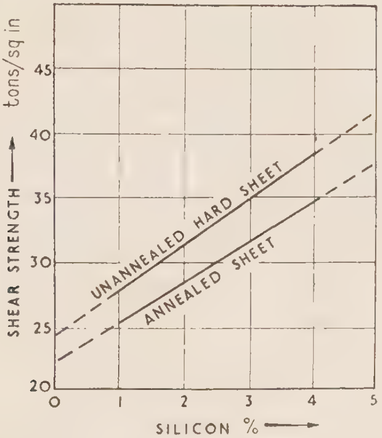

Figure 8. Punching stress for hot-rolled silicon-iron sheet.

Effects of stress. Although sheet material is annealed after rolling to relieve internal stresses, subsequent operations of punching, shearing or bending can introduce stresses which have the harmful effects of increasing hysteresis losses and reducing permeability. Shearing and punching may be regarded as destroying the magnetic properties of the material for a distance of the order of 0·030 to 0·120 in. from the cut edge. Thus the effective cross-section of the material is reduced and the flux-density is increased. The amount of material damaged depends on the thickness of the sheet and the condition of the shear blade or punch and die. The effects of shearing are most pronounced on narrow sections, such as the limbs of small laminations or the teeth on machine stampings. In large transformer laminations, the effect is negligible. These effects can be minimized by employing sharp shears, and by reducing die tolerances to a minimum. The designer can assist by keeping the periphery of the sheared edge to a minimum. Further annealing treatment can be used to remove shearing and punching strains, if the additional expense is justified by the improvement in performance.

Oriented materials are much more sensitive to the effects of strain than non-oriented materials. Moreover, strain may be introduced by the bending which occurs in forming wound cores, and it becomes essential to anneal the material in its final form.

Insulation. Some form of insulation is required to reduce eddy-current flow between laminations. Several types commonly applied to silicon-iron are listed below:—

Oxide coatings. A layer of oxide which is formed during the annealing process has insulating properties which are sufficient for some applications, particularly for the smallest laminations.

Clay compounds. These are cheap and easily applied by spraying on one side only, and are widely used. They tend to be hygroscopic and do not protect the laminations from rusting.

Organic varnishes. These are also widely used. The varnish, which is rolled on to both sides, has comparable insulating properties to the clay compounds, and protects the sheet from rusting.

Phosphate coatings. Coatings of this type, which involve a chemical treatment, can be produced which do not deteriorate at strain-relieving temperatures. This is an important property when wound cores of oriented silicon-iron are used, since an insulating coating cannot be applied after annealing in the final form.

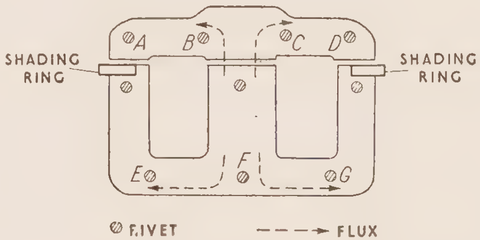

Figure 9. Faulty design of contactor core.

Burrs and burr grinding. Burrs which appear on cut edges may create short circuits across the interlaminar insulation. Good shearing will produce negligible burr, but, due to the clearance necessary between punch and die, there is more tendency to cause burr by stamping. This can be controlled by good toolmaking and by regrinding the tools when necessary.

Burr grinding may be carried out in certain cases, but the operation can set up stresses which require further annealing treatment for their removal.

Bolts and rivets. Small cores are frequently bolted or riveted together with no insulation between the bolts and the core. Short-circuit paths can easily be created by the bolts or rivets, and may cause appreciable eddy-current losses unless the bolts are carefully placed so that the minimum amount of flux links these paths. The contactor core illustrated in Figure 9 has several short-circuit paths (e.g. between rivets B and C, E and F, F and G). The total loss was made up as follows:—

Iron loss, 12%

Loss in shading rings, 27%

Copper loss in windings, 20%

Loss due to rivets, 41%

This last amount could be saved by insulating the rivets.

7. CONCLUSIONS

The design of many devices incorporating silicon-iron is of such a complex nature that it is often necessary to resort to empirical methods, frequently based on past experience. Nevertheless, the optimum utilization of these materials in magnetic circuits can best be achieved by a full understanding not only of the magnetic properties, but also of fabrication considerations, and it has been the purpose of this paper to draw attention to some of the relevant factors.

30

A LAMINATED FLAKE-IRON POWDER MATERIAL FOR USE AT AUDIO AND ULTRASONIC FREQUENCIES

G. Campbell and F. J. Wood

(The Plessey Company, Ltd.)

Abstract: A material consisting of flakes of iron pressed into a solid block, although originally intended for use at 50 c/s, has been found useful at frequencies up to 10 kc/s. Its permeability is of the order of 500 and the loss is of the order of 30 watts/pound at 1 kG, 10 kc/s. It is strong and can be machined.

1. INTRODUCTION

Laminated flake-iron powder material was developed as a substitute for conventional transformer laminations which were in short supply. The usual type of radio-frequency powder-core was unsuitable due to its low permeability and high cost.

The first objective was the production of E-shaped cores for the ballast chokes used in fluorescent lighting units. When cores consisting of transformer laminations were used, they had to be assembled with a gap to control the voltage/current characteristic of the choke. It was found that cores made from iron-powder flakes approximately 25 microns thick, suitably insulated, and arranged in layers to correspond with the magnetic flux path, had the necessary amount of internal air gaps to permit the cores to operate with butted faces. The permeability of the material was adequate and although the power losses at 50 c/s were rather higher than those of the grade of silicon-iron laminations then available, and the temperature rise of the choke was consequently greater, a satisfactory design of coil and core was developed for this application.

About the time this result was obtained, the development of television receivers introduced a number of inductive components which operated at frequencies at and above 10 kc/s. Blocks of the flake-iron material were found to have permeability and loss properties suitable for cores of these components. Since then the material has been used largely for this purpose. The chief reason for its success in this frequency range is that the laminar structure of the cores is composed of flake-iron particles only 25 microns thick, and consequently the eddy-current loss is low. For applications at still higher frequencies cores made from flakes 15 to 20 microns thick have also been used.

The material has magnetic properties at mains, audio and radio frequencies which make it suitable for certain applications in these frequency bands.

For the material to be used efficiently at power frequencies, however, a higher permeability and lower magnetic losses, of which the predominant portion is hysteresis loss, are necessary.

In the account which follows, the material in its present form is described, the method of manufacture outlined and the properties and applications discussed.

2. DESCRIPTION OF THE MATERIAL

The cores are made by pressing iron-powder flakes into blocks, which are either to size or for subsequent machining to the required dimensions. Due to the shape and the layering of the iron-powder flakes in the die before the core is pressed, there is a high degree of lamination in the block, and the cores are so designed that in use the direction of magnetic flux, as far as possible, is parallel to the laminations. This is illustrated by the photomicrograph in Figure 1a which shows the laminar structure of a core pressed from flakes about 25 microns thick.

The amount of insulator and binder in the block shown in Figure 1a is only $\frac{3}{4}\%$ by weight and the core has a density of 7·0 gm/c.c. This figure compares well with the density 7·9 gm/c.c. of solid iron. A still higher core density can be obtained by increasing the pressing pressure. Other grades of the material are made with higher percentages of insulators and binders for applications requiring cores with lower eddy-current losses. Cores from these grades, of course, have a lower density and consequently a lower permeability, but they are stronger and easier to machine.

For each frequency and operating field there is a certain percentage of insulator and binder which will give the core with the best combination of permeability and loss characteristics. Once the amount of insulator has been decided, the aim is to produce a block of the highest possible density with the lowest pressing pressure from the flake powder, insulator and binder mixture. The maximum degree of lamination is necessary, air gaps between flakes are kept as small as possible and the amount of flake distortion and work hardening on pressing are reduced to a minimum.

3. METHODS OF MANUFACTURE

(*a*) *Raw materials*

The chemical composition of the original iron powder is important and impurities such as carbon, sulphur and phosphorus are kept to a low value. Compositions of typical commercially-available iron powders after reduction in hydrogen at 700°C are :—

	C	Mn	Si	S	P
Electrolytic iron powder	0·027%	0·017%	0·011%	0·023%	0·007%
Swedish sponge iron powder ..	0·084%	0·023%	0·211%	0·022%	0·009%

The particle shape and size of the powder is controlled so that good quality flakes are obtained. The best flakes are regular in shape, smooth, and have a suitable diameter-to-thickness ratio.

(*b*) *Flake manufacture*

The flakes are made by cold rolling the iron powder in one or two passes with or without intermediate annealing, in a high-speed rolling mill. The rolls are mounted horizontally and the powder is fed vertically into the "nip".

(*c*) *Annealing*

The rolled flakes are considerably work-hardened and it is necessary to anneal them to develop the best magnetic properties. This is done by mixing the flakes with an inert inorganic powder material such as alumina and annealing at 950° to 1000°C in hydrogen. The inert material prevents the flakes from sintering, and it is removed later by sieving.

(*d*) *Addition of insulators, binders and lubricants*

The insulators and binders are added to the annealed flakes, the quantities added being dependent on the grade of material required and ranging upwards from a minimum of $\frac{3}{4}\%$ by weight.

The flakes may be insulated by phosphating, silicating or oxidizing, and the binder may be a thermosetting resin or thermoplastic material. The importance of a smooth flake surface is at once evident, as the requisite degree of insulation can then be obtained with the thinnest possible layer of insulator.

In most grades the binder can also act as the insulating medium. This method is used especially when a high permeability is required and maximum density is the aim. The addition of $\frac{3}{4}\%$ by weight of binder gives the necessary strength, and a certain degree of insulation is also imparted to the flakes by this amount of binder.

(*e*) *Pressing*

The filling of the die with the flakes is probably the most critical operation of the process.

The simplest method is the most effective, and good layering of flakes takes place if they are allowed to fall freely into the die cavity. The die must be filled uniformly as there is no sideways flow of this type of powder on pressing, and bad die-filling cannot be rectified by the subsequent pressing operation. Figure 1b shows a photomicrograph of a badly laminated block; cores with this structure have inferior magnetic properties.

Usually the blocks are cold pressed on automatic tabletting presses. Pressures are comparatively low and vary according to the shape, strength and magnetic properties required in the finished core. This low pressing pressure enables cores 10 to 20 square inches in area to be made.

(a)

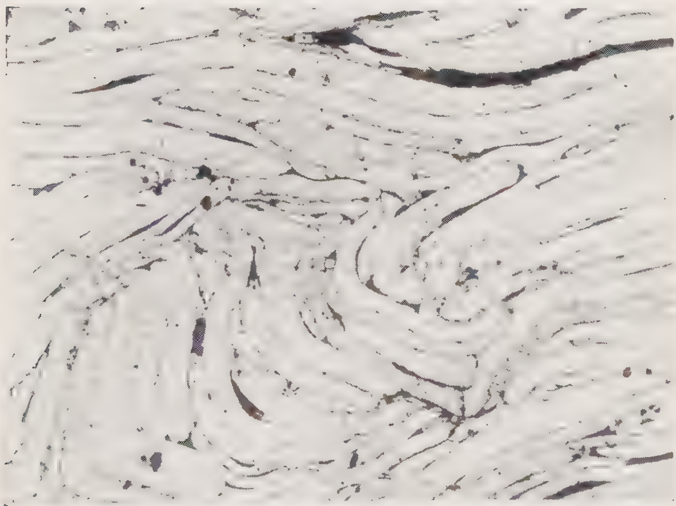

(b)

Figure 1. Structure of the flake-iron powder material; magnification, $\times$ 100.
(a) good structure ; (b) bad structure.

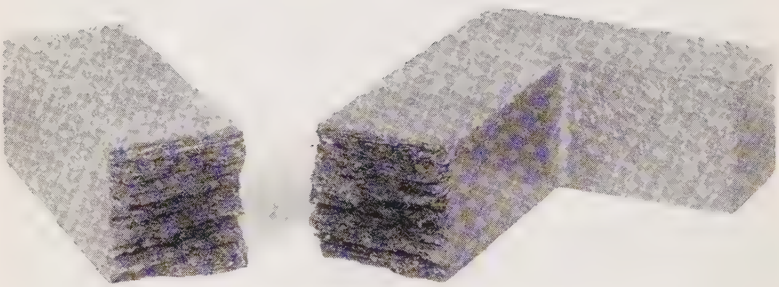

Figure 2. Fracture of a flake-iron powder-core.

The compression ratio of the flakes is approximately 4 to 1, and the core thickness is usually limited to about $1\frac{1}{4}$ inches to obtain uniform density throughout the block. Thicker blocks can be made, however, by sticking two or more blocks together with a suitable cement so that the laminations in adjacent blocks are parallel. By this method any practical thickness can be built up, and the resultant block can be machined satisfactorily.

(*f*) *Finishing operations*

If a thermosetting resin has been used as a binder the blocks are cured to polymerize the resin. Any machining or finishing operations are then carried out. Finally the blocks are checked for mechanical and magnetic properties. As a result, cores are sent to the assembly lines as "inspected" components.

4. PROPERTIES

(*a*) *Grades of material*

As already indicated there are various grades of material depending on the insulator and binder content of the blocks, the pressing pressure, and the type of iron flake used. Three chief grades designated 3, 4 and 5 have been adopted as standards for the present, and they contain different amounts of insulator and binder, Grade 3 having the lowest amount and Grade 5 the highest.

An extra letter (e.g. Grade 5D) identifies secondary variations within these grades resulting from varying the pressing pressure and type of iron flakes used.

In the description of properties which follows, the chief grades only are discussed.

(*b*) *Mechanical properties*

Strength. The cured blocks are quite strong and typical modulus-of-rupture figures are as follows :—

Grade 3: 20 000 lb./sq.in.
Grade 4: 25 000 lb./sq.in.
Grade 5: 30 000 lb./sq.in.

In addition to the effect of the binder, the strength is due partly to the interlocking of flakes in the material. This is illustrated in Figure 1a and also in Figure 2 which shows the type of fracture obtained when a core is broken. It is possible to place together the fractured pieces of the core so that the join is almost invisible. A highly efficient joint is formed as the magnetic permeability of the jointed core is only about 5 to 10% lower than that of the original.

Dimensions of cores. As already indicated, cores with an area of 10 to 20 square inches, depending on the grade of material, and of any reasonable thickness, can be produced.

Cores made with press tools can be held to reasonably close tolerances. Typical values are as follows:—

Diameter: 0·005 in. tolerance
Thickness: 0·010 in. tolerance.

Cores can, if necessary, be ground or sized to precise dimensions.

Machinability. The material machines similarly to cast iron and it can be turned, ground, drilled and bored by methods which are standard for cast iron. If a complicated section has to be made, however, it is best to support the material otherwise "flaking" results. This property of relatively

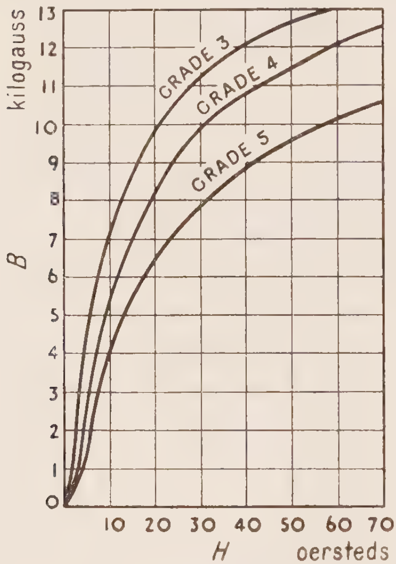

Figure 3. Typical B/H curves for flake-iron powder material.

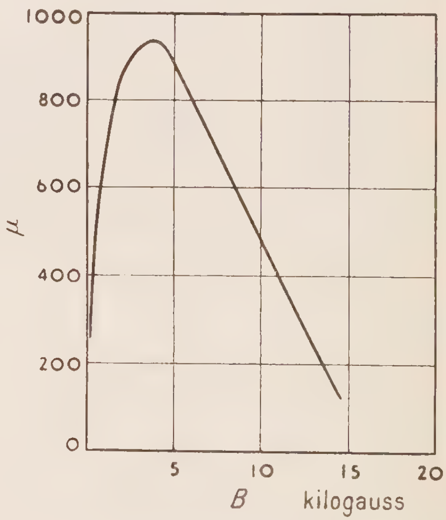

Figure 4. Variation of d.c. permeability with induction B in Grade 3 material.

easy machining enables sample cores to be made from blocks of the material without first producing expensive press tools.

It is possible to screw and tap the material and, in addition, self-tapping screws can be driven into drilled holes in cores. This provides a convenient method of mounting components. Due to the structure of the material the clamping used to reduce objectionable "hum" is unnecessary.

The machinability of the material improves as the binder content increases. Core blocks made from thin flakes also show improved machining properties. Even with standard Grade 3 material, however, machining by production methods is possible. A typical example of this is the production of a cylindrical core 0·934 in. $\pm$ 0·001 in. diameter from a pressed block

1·06 in. square, of Grade 3 material. This core, which is used in a magneto, replaced wedge-shaped laminations which were arranged radially into a cylindrical form.

(*c*) *Magnetic and electrical properties.*

Specific resistance. The control of eddy currents can be considered as resulting from modifications in the specific resistance of the blocks. The

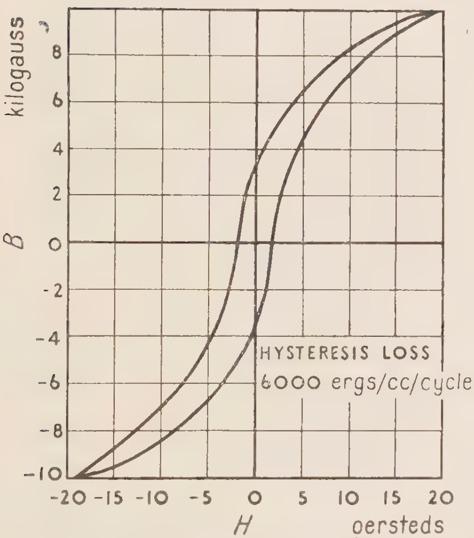

Figure 5. Typical hysteresis loop for Grade 3 material.

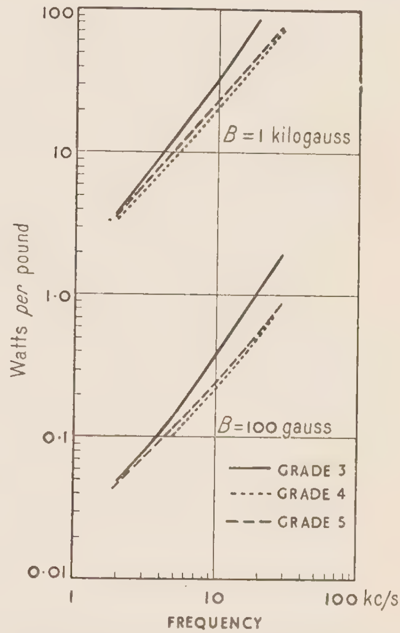

Figure 6. High-frequency losses in flake-iron powder material.

variation in the amount of insulator and binder causes alterations in specific resistance illustrated by the following examples:—

	Grade 3	*Grade* 4*D*	*Grade* 5
Plane of laminations (ohm-cm) . .	0·002	0·01	0·02
Perpendicular to laminations (ohm-cm)	0·12	0·27	0·60

D.C. and a.c. (50 c/s) properties. The general quality level of the material and differences between grades are shown in the figures below. In addition the B/H curves for Grades 3, 4 and 5 are illustrated in Figure 3, the μ/B curve for Grade 3 in Figure 4 and a B/H cycle for Grade 3 in Figure 5.

	Grade 3	*Grade* 4	*Grade* 5
D.C. initial permeability (100 gauss) ..	250	220	170
D.C. effective permeability (10 kilogauss) ..	500	300	180
D.C. maximum permeability	950	560	470
Total a.c. loss in watts/lb. at 10 kilogauss, 50 c/s	2·6	2·8	3·0
Coercive force (oersteds)	1·8	2·0	2·1
Saturation flux density (kilogauss)	15·5	14·0	13·0

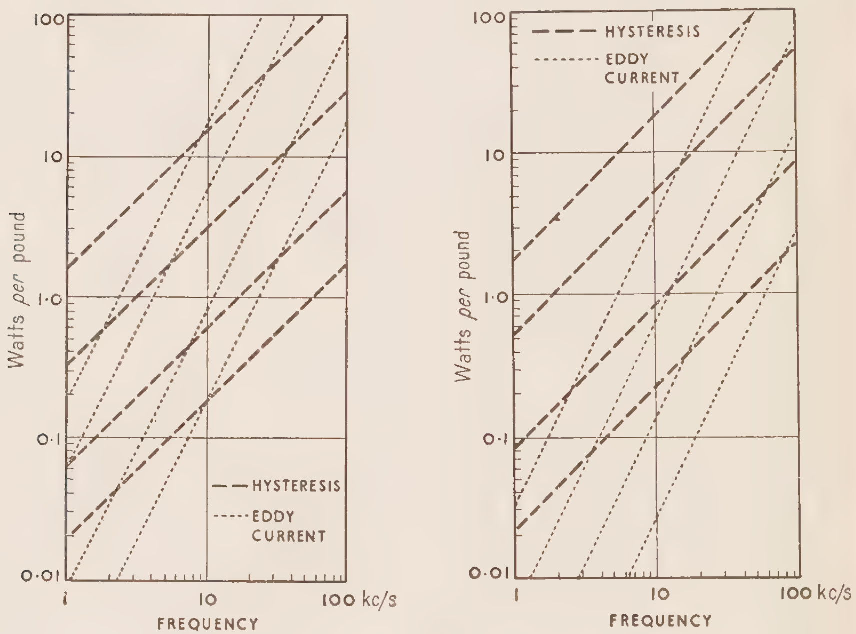

Figures 7 and 8. Separation of high-frequency losses: Figure 7, Grade 3; Figure 8, Grade 5.

High-frequency properties. For a given flux density the hysteresis loss in a core is proportional to the frequency of a.c. applied, while the eddy-current loss is proportional to the square of the frequency. Thus, as the frequency is increased the effect of eddy currents becomes more important, both as a contribution to the total energy loss in the core and in reducing the effective permeability of the core.

The properties of the various grades of material at high audio and ultrasonic frequencies and with fairly high values of flux density are shown in Figures 6, 7, 8 and 9. The loss factors tabulated below summarize the data of these curves:—

Flux density, gauss	Grade 3		Grade 4		Grade 5	
	Hysteresis mW/kc	Eddy current mW/(kc)^2	Hysteresis mW/kc	Eddy current mW/(kc)^2	Hysteresis mW/kc	Eddy current mW/(kc)^2
100	6	0·6	6	0·11	7	0·08
200	20	3·0	22	0·55	26	0·38
500	100	20	130	2·6	160	2·0
1000	500	60	500	14·0	550	> 10

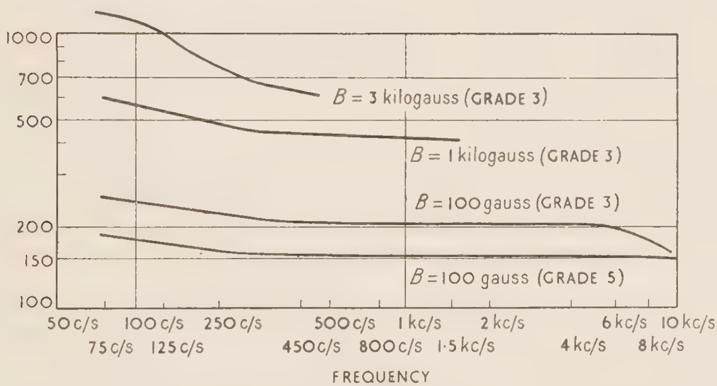

Figure 9. Variation of permeability with frequency.

5. APPLICATIONS

(a) General

Television receivers contain a number of components which operate at a frequency of 10 kc/s and generate harmonics of a high order up to several Mc/s. They are all associated with the line-scanning time-base of the receiver. Of these components, some are transformers and chokes and at the above frequencies the eddy-current loss in cores of conventional laminations becomes appreciable while radio-frequency type powder-cores have such a low permeability that they are unsuitable where high inductance or efficiency is required. The laminated flake-iron cores, on the other hand, have a permeability comparable with that of laminations at these frequencies and much lower eddy-current losses. These properties make the material, usually in Grades 4A or 5D, suitable for use in the components which are described below.

In addition to components for television receivers, some other applications are described.

(b) Television receiver components

Squegging transformers. In television receivers which employ a squegging oscillator and a separate amplifier valve to produce the appropriate output to the scan coils, it has been found convenient to use this type of core not only for the squegging transformers of the line-frequency oscillator, but also for the 50 c/s frame oscillator.

Line and E.H.T. transformers. Nearly all modern television receivers generate their E.H.T. supply from the fly-back pulse of the line-scanning oscillator. This involves a special transformer which fulfils several functions. It gives a positive feedback to the grid of the oscillator valve, matches the oscillator output impedance to the impedance of the scan coils, acts as a step-up transformer for the very short high-voltage pulse associated with the fly-back stroke of the time-base current, and supplies the heater current for a small rectifier valve which enables a steady voltage of about 7 to 20 kV, depending on the type of receiver, to be obtained from the high-voltage pulse.

Considerable development has been carried out on this type of component and several designs have been used in the last few years based on laminated flake-iron cores. The latest design is capable of supplying the E.H.T. voltage and scanning power required by the new wide-angle television tubes from a high-tension line of only 190 V.

Scan coils. It is usually found desirable to place a magnetic yoke round the outside of the scanning coils of any television tube and various types of cores have been used including iron wire, Mumetal sheet, ferrites and laminations of transformer steel. Good results can be obtained on the normal type of television tube with a pair of C-shaped laminated flake-iron cores closed round the scan coils. For wide-angle tubes a more complex core, which has several slots to accommodate the windings in an otherwise bulky pair of C-shaped cores, is more convenient. Small changes in the orientation of the slots in the core enable identical coils to be used in conjunction with tubes of different face curvature and still give rectangular rasters.

Width controls. In all television receivers some means is required of adjusting the amplitude and waveform of the scan-currents by means of width (or height) controls and linearity controls respectively. The most economical methods of making these adjustments in the case of the line-frequency circuits is by means of small chokes of variable impedance. Initially, iron powder-cores were satisfactory for this application, but by using flake-iron cores of the same dimensions and the same coils an improvement of 50% in maximum inductance is obtained.

(c) Other applications

Radio interference suppressors. Considerable investigation has been carried out with a view to using this material in mains-interference suppressor chokes.

Since the permeability of the Grade 5 material is appreciable up to 10 Mc/s it operates very effectively throughout the range of normal broadcast frequencies. The "lossy" nature of the material at these frequencies causes the inductors to have very low Q values and hence to be very non-selective. In this application this is an advantage over the more expensive cores of higher efficiency. The fact that a high polarizing field is permissible without saturating the core is another factor in its favour for use in suppressor units where a large 50 c/s current may be flowing.

A series of units using Grade 5 material has been produced ranging from high-power types to very small units for use in electric irons and a special type is in use for suppressing the interference on the long and medium wavebands produced by the line-scanning oscillators of television receivers.

Audio-frequency output transformers. The flake-iron type of core can be used for audio-frequency transformers in broadcast receivers; in particular cores of this type are used for loudspeaker output transformers. For this application Grade 3 is the most suitable type as it has the highest low-frequency permeability and satisfactory losses up to 15 kc/s. With these cores, however, the bass response and efficiency obtained with conventional laminations can only be attained by using correcting circuits to boost the output below about 400 c/s.

The laminated flake-iron powder material is known as "Caslam". It was developed in the laboratories of the Plessey Company Limited, Towcester, Northants, by a group working on soft magnetic materials. Thanks are due to the Directors of the Plessey Company for permission to publish the results.

31

THE PULSE CHARACTERISTICS OF FERRITE MAGNETIC MATERIALS

A. Langley Morris

(Telecommunication Research Establishment)

Abstract: This paper describes the investigations under pulse conditions of British and American commercial ferrite cores. Certain grades of the material were found to be suitable for pulse-transformer applications, but for magnetron drives a d.c. bias would be advisable so as to make full use of the material.

1. INTRODUCTION

The ferrite materials have been developed for high-frequency applications, so should be suitable for circuit components for microsecond pulses. They thus constitute alternative materials to thin laminations of the well-known iron alloys, and probably will be cheaper. The component known as a pulse transformer is frequently used in electronic circuits, and there are two distinct types—those used for low power levels, and those for power purposes, such as for magnetron drives, where a high flux swing is essential.

Certain grades of ferrite appear quite suitable for low-power applications where the conditions are similar to those met in the design of radio-frequency transformers. This paper, however, is more concerned with the power application, for the pulse measurements were made at high flux densities.

Most of the commercial ferrite materials are complex, and it is likely that no two manufacturers' products will be identical in characteristic or in composition. A wide range is made by both British and American manufacturers, but the pulse-transformer designer may be somewhat uncertain which grade to use since there are no published data concerning the behaviour of ferrite cores under pulse conditions. Some guidance is possible, based on experience with ordinary strip materials; for pulse permeabilities between 400 and 1000 are usual with 0·004 and 0·002-in. laminations with a pulse-flux-density range between 5000 and 10 000 gauss. Now the saturation of ferrite materials is usually about 4000 gauss, while their initial permeabilities extend from quite low values to around 1500. It could be expected that they would have pulse permeabilities somewhat in accordance with the initial values and therefore could be used for pulse transformers, although their low saturation is a disadvantage for power applications.

The pulses required by a magnetron are unidirectional, and it is usually necessary to provide the transformer cores with some means of demagnetization between pulses; an air-gap is usual. If, however, a current bias is used,

demagnetization is achieved with the added advantage of an improved pulse permeability and a pulse flux density theoretically equal to twice the saturation value of the material. Such a bias may be obtained by pre-pulsing the core or by means of a d.c. winding. Most of the measurements described in this report relate to biased cores; American and British cores were investigated.

2. APPARATUS

The test-pulse length was approximately 1 microsecond and the repetition frequency 50 c/s. A pulse-voltage range of approximately 700 to 3500 V was available. The permeability and flux density were derived from the pulse B/H loop displayed on a cathode-ray tube. The equipment cannot be considered as a precision device, but for pulse-transformer design data an approximate value of the permeability suffices.

3. INVESTIGATIONS ON AMERICAN CORES

Table 1

Material	1	2	3	4	5
Curie temperature °C ..	260	165	160	160	150
Saturation flux density, gauss	1900	3100	3800	3200	3400
Maximum permeability ..	183	1030	1710	3300	4300
Resistivity, ohm-cm. ..	2×10^5	3×10^7	4×10^5	$1{\cdot}5 \times 10^8$	1×10^4
Initial permeability at 1 Mc/s	95	410	750	410	850

Table 1 shows some of the characteristics of the American materials as quoted by the manufacturer. All the grades have a very high resistivity and the initial permeability at 1 Mc/s for two grades is just below 1000. Most of the cores tested were toroidal, but measurements were made on two butted rectangular cores. The composition of these American ferrites was not known, but they were probably manganese-nickel-zinc ferrites.

(*a*) **Pulse permeability without d.c. bias (ungapped cores).** The cores were toroidal, having an inside diameter of $1\frac{1}{2}$ in. and $\frac{1}{4}$ in. square section. The results of the tests are shown in Table 2.

Table 2

Grade	Permeability, μ, at flux densities (gauss): 880	1150	1280	1480	1500
1	75	—	—	—	38
2	—	—	—	—	172
3	—	—	—	—	497
4	—	465	375	347	347
5	—	—	—	—	260

It may be noticed that at moderate levels of flux density the permeability is well below the initial figure quoted in Table 1.

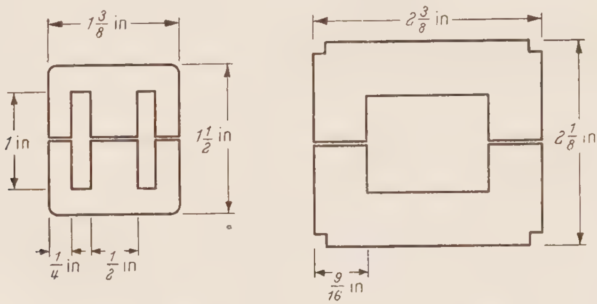

Figure 1. Shapes of gapped cores used in experiments.

(*b*) **Pulse permeability without d.c. bias (gapped cores).** The two types of cores investigated are shown in Figure 1. Each core consists of two sections butted together. The cores were tightly clamped so that there was virtually no air-gap. Table 3 shows the measured results.

Table 3

Grade	Permeability, μ, at flux densities (gauss) :			
	1400	1500	2000	4480
3	850	—	510	48
4	—	450	—	—

The figures for Grade 3 are an improvement on those in Table 2, but the figure for Grade 4 was rather disappointing. To see whether a small gap would give improved results, a piece of paper 0·0025-in. thick was placed between the butting surfaces of the core, and Table 4 shows that the permeability was considerably improved, attaining a value greater than the initial permeability quoted by the maker.

Table 4

	Permeability, μ, at flux densities (gauss) :		
	1410	1710	2020
Grade 4, 0·0025-in. gaps	652	550	186

Nevertheless, a flux density much in excess of half the saturation figure was not possible without a considerable loss in permeability and, therefore,

for magnetron pulse transformers they could hardly compete with strip materials unless d.c. bias excitation is used.

(*c*) **Pulse permeability with d.c. bias (ungapped cores).** The toroidal cores were provided with bias windings of 3 to 5 turns, connected via pulse-stopping air-cored chokes to a d.c. supply. For each pulse voltage the bias current was adjusted to give the maximum pulse permeability.

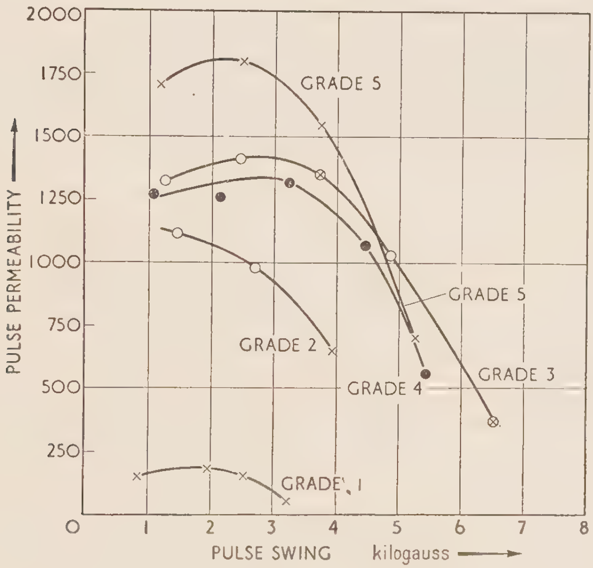

Figure 2. 1-microsecond pulse permeability of American ferrite cores, with d.c. bias winding.

The results of these measurements are shown in Figure 2. As would be expected from Table 1, Grade 5 had the highest permeability, and Grade 1 the lowest. Grade 3 had the greatest flux-density range. Of the five grades, 3 and 5 are the most suitable for pulse transformers—Grade 3 for power purposes, and Grade 5 where high inductance is needed. Figure 3 shows the relation between the pulse flux density and the d.c. bias value in oersteds. The curves are approximate since the bias current was not very critical.

(*d*) **Pulse permeability with d.c. bias (gapped cores).** The results in section 3(*b*) indicate that ferrite cores can be butted together, with practically no air gap at the joints. It should, therefore, be possible to use d.c. bias without too great an expenditure in d.c. excitation on the gap.

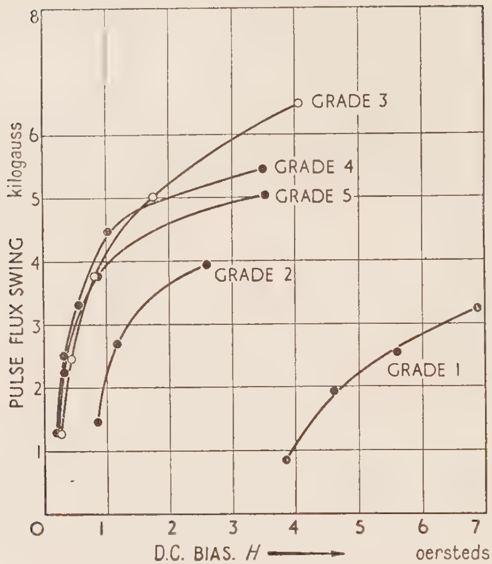

Figure 3. Variation of pulse flux-swing with d.c. bias, for American ferrite cores.

Measurements of the two cores shown in Figure 1 are given in Table 5.

Table 5

Flux density, gauss ..	1540	1590	2940	3520	4420	5300	6150
D.C. bias, oersted ..	0·15	0·19	0·43	0·46	1·0	1·41	3·0
Permeability: Grade 3	1280	—	1340	—	1130	—	800
Grade 4	—	1040	—	1060	—	713	—

These results show that a d.c. bias can be used with advantage on butt-jointed cores. Such cores enable preformed windings to be used—a decided advantage over toroidal cores. It would, of course, be essential to ensure that the joints were well-fitting and the core clamping rigid under all conditions of use.

4. TEST RESULTS ON BRITISH FERRITE CORES

Five grades were available for test, each consisting of a small toroidal ring approximately $\frac{1}{8}$ sq. in. in cross section and $1\frac{1}{2}$ in. outside diameter. Some characteristics quoted by the maker are shown in Table 6.

Table 6

Material	6	7	8	9	10
Curie temperature, °C	180	170	190	155	250
Maximum flux density at 20°C, gauss ..	3400	3800	3400	3500	3400
Maximum permeability	—	2500	2000	2500	—
Resistivity, ohm-cm	100	50	50	100	10^5
Initial permeability	850	—	1200	1500	200

It may be noticed that four of the grades have a low resistivity and one sample has a high resistivity comparable with that of the American materials. The low-resistivity cores were all manganese-zinc ferrites, and the high-resistivity core was thought to be a nickel-zinc ferrite.

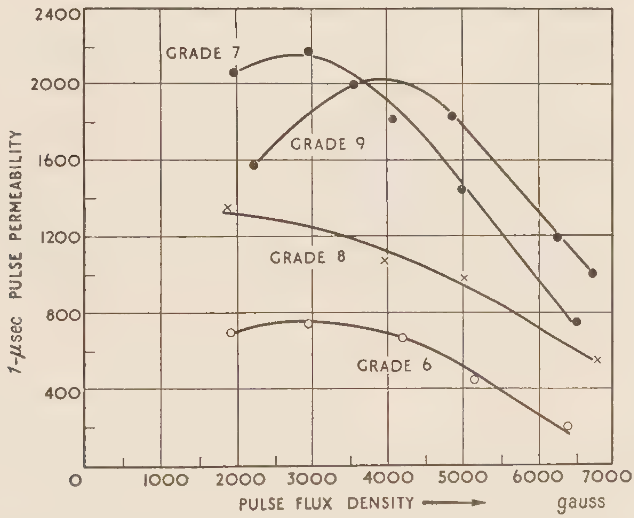

Figure 4. 1-microsecond pulse permeability of British ferrite cores, with d.c. bias winding.

The pulse-permeability measurements were confined to those with d.c. bias, and the results are shown in Figure 4. It is clear that these cores could be used for pulse transformers operating at 5500 gauss, and two of the grades have a permeability in excess of 1000. These figures are somewhat higher than those possible with the American cores and may be due to the fact that they are of the low-resistivity type. The British high-resistivity material (sample 10) has rather too low a permeability to be satisfactory for pulse transformers, and consequently, the bias excitations were recorded

for only the low-resistivity cores and are shown in Figure 5. Figure 5 confirms the findings of Figure 4 that Grades 7 and 9 are the best.

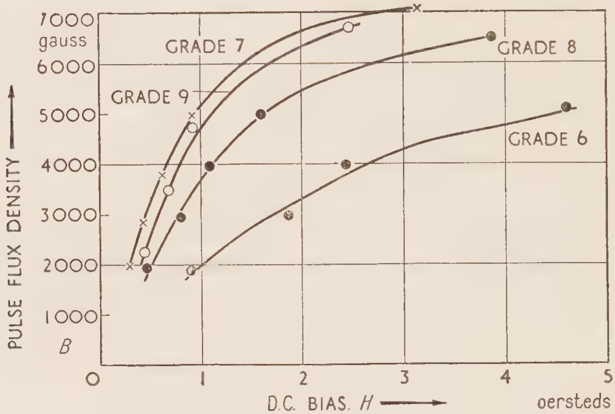

Figure 5. Variation of pulse flux-swing with d.c. bias, for British ferrite cores.

The pulse permeability of the high-resistivity grade, when pulsed without any bias excitation, underwent a permanent change. This behaviour was not noticed with any of the low-resistivity grades, where it was looked for, and did not appear to occur with any of the American grades. The test results are shown in Table 7.

Table 7

	Before saturation	After saturation
Pulse flux density	650	640
Pulse permeability	350	181

The permeability could be recovered by reversing the pulse windings or by the application of a d.c. bias. Such a property may have special applications, for example, in storage devices.

5. OBSERVATIONS

Since all the experimental evidence in this paper relates to 1-microsecond pulses, the figures should hold good for longer pulse lengths, but may fall off at pulse lengths around 0·1 microseconds ; this may be more likely with the low-resistivity materials.

Attempts were made on another piece of gear to see if any difference could be noticed between the high-resistivity and the low-resistivity materials at

pulse lengths down to $\frac{1}{4}$ microsecond. The pulse permeability for both seemed to be lower than the 1-microsecond figures, but there was nothing to show any superiority of the high-resistivity materials. The measurements were confined to tests on toroidal cores without d.c. excitation. It is likely that only where the 1-microsecond pulse permeability is reasonably high would any difference be noticeable, and cores having a larger section than the present samples would be required to bring any effect into prominence. It is known that dimensional effects exist with manganese-zinc-ferrite low-resistivity cores, and that at 1 Mc/s they are troublesome with a core-section in excess of $\frac{1}{2}$-in. square. It has also been stated that the nickel-zinc ferrites are considerably less prone to dimensional effects, but measurements on much larger sections than employed for this work would be needed to clear these points.

The results in this paper show that ferrite cores with completely closed magnetic circuits are not satisfactory for pulse purposes unless the flux density is small; then the pulse permeability approaches the initial permeability figures. Obviously for applications where the input power is small, material having a high initial permeability should be chosen. When the pulse flux density is sufficiently high to preclude the use of completely closed magnetic circuits, a gapped core is feasible, and Table 3 shows that pulse permeabilities in excess of the initial permeabilities are possible. The operating flux density should be about half the saturation figure.

For magnetron pulse transformers, it would appear necessary to make use of d.c. bias, for then flux densities between 4500 and 5500 would be possible, and permeabilities in excess of 1000 would be obtained. It is, however, doubtful whether ferrite cores would be used for pulse lengths of 1 microsecond and above, for the normal strip magnetic materials, even without a d.c. bias, would be preferable.

On the evidence in the paper the low-resistivity materials have both a higher pulse flux density and a higher permeability than those of high resistivity.

Acknowledgment is made to the Chief Scientist, Ministry of Supply, for permission to deliver this paper. Crown copyright is reserved. Reproduced by permission of the Controller of H.M. Stationery Office.

DISCUSSION

Dr. H. P. J. Wijn:

Mr. Langley Morris has found that the pulse permeability of ferrites depends on the pulse length, especially when ferrites with a high permeability are used. A possible explanation of this effect can be the frequency dependence of the magnetization curve found for ferrites with a high initial permeability (see e.g. Wijn, 1953, Figure 2). The relaxation frequency of the irreversible Bloch-wall displacements is found to be of the order of several hundred kc/s, which corresponds to the pulse time lengths used by Mr. Langley Morris.

32

SOME PULSE TESTS ON MAGNETIC SPECIMENS HAVING RECTANGULAR HYSTERESIS LOOPS

P. F. Dorey

(King's College, London*)

Abstract: Small cores of materials having rectangular hysteresis loops are used for storage purposes in binary digital computors. The results of a simple circuit theory for such a core, based on a solution to the diffusion equation for an idealized B/H loop, are given. The theoretical treatment enables an estimate to be made of the time and energy required to extract information from a core, and the limiting conditions for successful information transfer can be obtained. Some pulse tests to verify the theoretical analysis are described. It is shown that only qualitative agreement with the theoretical treatment is obtained, but if the constants of the equivalent rectangular loop are determined experimentally the accuracy of prediction can be improved.

1. INTRODUCTION

One of the applications of magnetic materials having "rectangular" hysteresis loops is that of storage of binary digital information (An Wang and Way Dong Woo, 1950; An Wang, 1951). In such storage devices, small clock-spring-type cores, consisting of a few turns of thin tape, are employed, the binary digits "1" and "0" being represented by one or other of the remanent points of the hysteresis loop. A number of cores are interconnected by windings to form a line, and binary information is supplied at the line input by means of polarizing current pulses applied to a winding on the first core in the line. This information can be passed to the second core by applying a "shifting" pulse of current to the first core. The resulting change of flux in this core produces an output pulse which can be used to polarize the second core, causing it to assume the same magnetic state as that previously held by the first. In this manner, the information supplied at the input can be propagated down the line by the application of suitable current pulses to the windings of selected cores.

At present very little published information is available about the performance of such cores under conditions of pulse excitation, and this paper describes tests based on a simple non-linear solution of the equation of magnetic diffusion valid for B/H relationships of the step-function or rectangular form. This form of solution enables the effects of a limited number of linear circuit parameters to be treated, and a simple circuit theory can be developed for such an idealized core when used in combination with other circuit elements or other cores. In particular this treatment enables a prediction to be made of the energy required to extract information from a

* Now with Elliott Brothers Ltd.

core, and the time that such a process requires. It also permits the limiting conditions for complete flux, or information, transfer between cores to be obtained.

2. THEORETICAL RESPONSE OF THE IDEALIZED CORE WHEN SUBJECTED TO RECTANGULAR PULSES

In this treatment the flux-retarding mechanism is assumed to be wholly that of eddy currents flowing within the core. Making certain assumptions, the equation to be satisfied is that of magnetic diffusion, viz. :—

$$\partial^2 H/\partial x^2 = K\, \partial B/\partial t \qquad \ldots(1)$$

where H = field acting at a depth x inside the specimen;
B = induction at a depth x inside the specimen;
K = a constant = $4\pi/10^9\rho$ in "engineering" units;
ρ = resistivity of the material.

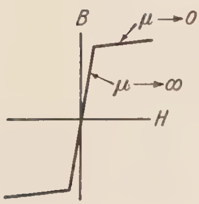

Figure 1. Idealized B/H curve.

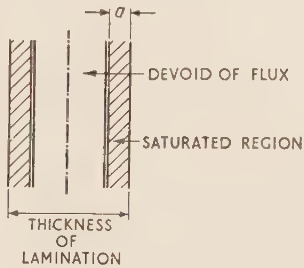

Figure 2. Two regions in lamination having B/H curve as in Figure 1.

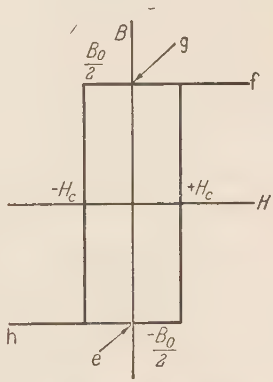

Figure 3. Step-function type of B/H curve.

A simple form of solution to this equation when the B/H curve may be represented, to a fair degree of approximation, by that shown in Figure 1, has been suggested by Ganz (1946). It is approximately true to regard a core lamination of such a material as divided, at any instant of time, into two regions, an inner region devoid of flux, and an outer region of depth a which is saturated (Figure 2). This state of affairs exists until the saturated region extends to the centre of the lamination, when the whole lamination is saturated. This form of solution appears to be rigorously true for a B/H relationship which is of step-function form (Figure 3), and solutions can be obtained for a variety of boundary conditions. The solutions have the simplest form when the width of the B/H loop, $2H_c$, is indefinitely small, and this will be considered first.

Consider a toroidal core in the form of a thin-walled hollow cylinder of

height b, wall thickness d, and of mean diameter D, where both D and b are very much greater than d. Let the core have a B/H loop of the form shown in Figure 3, H_c *being indefinitely small* and assume the core to have been previously magnetized to the point e. Assume that a field $H(t)$, which is some function of time, is applied to the core by a uniform magnetizing winding of N turns, and in such a direction as to tend to change the magnetization in the core to some point f (Figure 3).

Then if a is the penetration depth of the saturated regions into the thickness of the cylinder wall at a time t after applying the field, it can be shown, by solving (1) for the step-function B/H relationship, that

$$a^2 = 2/KB_0 \int_0^t H(t)\,dt, \quad a \nless 0 \qquad \ldots(2)$$

Similarly, if a voltage $E(t)$ is applied to the magnetizing winding, the penetration depth can be shown to be

$$a = 10^8/(2B_0bN) \int_0^t E(t)\,dt, \quad a \nless 0 \qquad \ldots(3)$$

Three boundary conditions are of interest for rectangular pulse shapes. They are:—

(i) A voltage of the form $Eh(t)$ (where $h(t)$ is the Heaviside step function) applied to the magnetizing winding, the total circuit resistance being zero.

(ii) A current of the form $Ih(t)$ forced through the magnetizing winding.

(iii) A case intermediate between these two—i.e., a voltage of the form $Eh(t)$ applied to the magnetizing winding via a resistance of value R, comparable with the impedance of the magnetizing winding.

Solving the penetration equations (2) and (3) for boundary condition (i) above yields the result that both the total flux in the core and the surface field increase linearly with time, and the appearance to the external circuit is that of a *linear* inductance, although the core is at all times partly saturated. The magnitude of this apparent linear inductance is given by the core dimensions in the usual manner, with the permeability μ defined by the ratio B_0/H_r, where H_r is the value the surface field attains at the instant of saturation. All the energy supplied, however, is dissipated in eddy currents; there is no stored magnetic energy since $\int HdB$ is zero. When the magnitudes of E and I in boundary conditions (i) and (ii) above are such that the surface fields at the instant of saturation are the same, then a simple relationship exists between the energies and times required to saturate the core under these extreme conditions, viz. : the flux-penetration or saturation time for a step-field is one-half that for step-voltage conditions, and the energy required to saturate the core in the former case is twice that required in the latter. (The penetration or saturation time is the time required for the saturated regions to reach the centre of the core, i.e. the time at which $a = \frac{1}{2}d$.)

Finite width of the B/H loop may be treated by introducing into the initial conditions a current I_c sufficient to supply the field H_c. Figure 4 shows the various quantities of interest for such an idealized core both for zero and

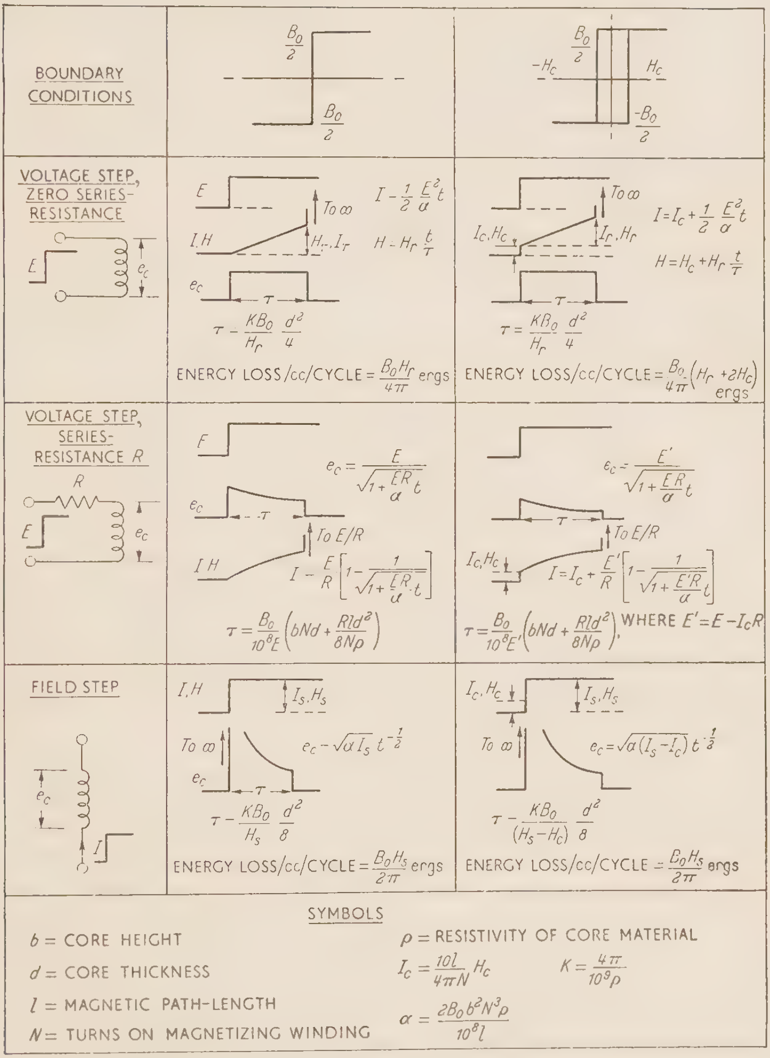

Figure 4. Responses of idealized cores to rectangular pulses.

finite values of H_c. In this Figure and throughout the paper the special case of a toroidal core is considered. The treatment may be extended to core

structures having n spiral turns in the core by replacing the core height b wherever it appears by nb.

In what follows the response of a core, under conditions approximating one of the three boundary conditions, is compared with the theoretical response shown in column 3 of Figure 4. It might be expected that the field H_c would correspond to the d.c. coercive field. The initial current steps I_c shown in the Figure would then be those required to supply the coercive field and the hysteresis loss, and currents in excess of this value may be regarded as supplying the eddy-current loss. But the following tests show that the value of the initial current step may be observed, or inferred, to be many times that required to supply the d.c. coercive field.

3. FORM OF THE TESTS AND TEST SPECIMENS

The tests were conducted on HCR specimens formed into single-turn toroidal cores having a welded lap joint, the overlap being about 0·2 in. The cores were thus in the form of thin-walled hollow cylinders, the cylinder height and diameter being 0·5 in. and 0·75 in. respectively, and the wall thickness being that of the tape used. The cores were enclosed in thin-walled plastic cases, resting in a narrow slot and free from mechanical constraint. A 160-turn search coil was wound directly on to the case and two field windings, each of 110 turns, were wound on top of the search coil. All windings were insulated from each other and were uniformly wound.

The test pulse was applied to the specimen by means of one of the field windings. The duration of this pulse is sufficient to ensure a change of magnetic state of the material from, say, e to f (Figure 3). On removal of this pulse, the core material returns to g. The material is then returned to the starting point, e, by applying a "reset" pulse to the other field winding of amplitude and duration sufficient to ensure all the core material reaching h before the pulse is removed.

The significant quantities are the time required for the magnetization of the material to change from the point e to the point f, and the manner in which the voltage induced in the search coil and the magnetizing current vary during this time. The voltage and current waveforms were displayed on an oscillograph, together with a timing wave. Photographs of them were projected on to squared paper, the waveforms drawn in, and scaled axes added to enable comparison with the theoretical wave forms to be made.

The tests were carried out at pulse repetition frequencies between 200 and 2000 c/s, using a pulse generator employing type 807 valves in the output stages. The step-field boundary condition was simulated by exciting the cores with square pulses of current obtained from the anode circuit of the valves, and the step-voltage-via-series-resistance boundary condition was approximated by using the output valves as cathode followers. The method of satisfying boundary condition (i) is described in section 4(c).

The output impedance of the pulse generator is in all cases finite and non-linear. Fortunately, it is possible in most cases either to correct for this, or to show the errors introduced to be negligibly small. The rise time of the current supplied by the pulse generator was of the order of 0·2 μsec. When exciting a core connected in the anode circuit of the output valves, however, it is not possible to enforce this rate of current rise on the core, due to the winding and circuit capacitances, and it is necessary to correct for this rise time at the shorter pulse lengths. Under these conditions the applied field is a good approximation to an exponential rise which may be treated by equation (2).

4. TEST RESULTS

(*a*) **Field step.** Figure 5 shows a typical oscillogram obtained from a 0·002-in. specimen for a large-amplitude field step, together with a theoretical voltage curve of the form const $\times\ t^{-\frac{1}{2}}$. It will be observed that the voltage produced by the core does not fall to zero when the saturated regions reach the centre

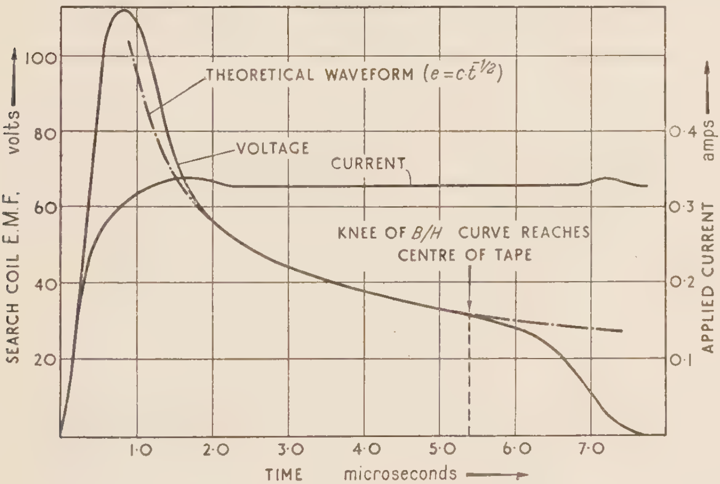

Figure 5. Response to a step-field: 0·002-in. specimen.

of the core, due to the finite slope of the B/H curve above the "knee". The general shape of the pulse "tail" can be predicted by theory, but the point where it commences is difficult to determine, as the knee on the specimens tested was not sharply defined. For results requiring an accurate determination of this point (e.g. as in (*d*)), the recorded waveform was replotted on log-log paper. The portion corresponding to the propagation of the saturated regions then appears as a straight line, and departure from it at the pulse

tail is easier to observe. The necessity to correct for the finite rise time of the applied field at large step-fields, when the saturation time is small, is also apparent. In Figure 6 are shown curves of total saturation time plotted against the amplitude of the step-field for 0·001-in. and 0·002-in. specimens. The total saturation time includes the pulse tail and the current rise time. When these factors are allowed for, the experimental quantities are still greater than the theoretical values.

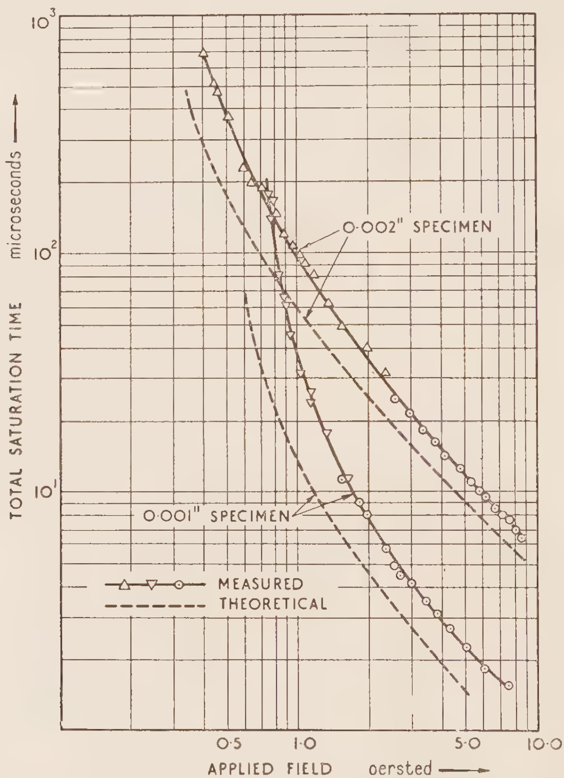

Figure 6. Saturation time against field: step-function surface-field conditions.

(*b*) **Voltage step applied through a resistance.** A typical oscillogram obtained from a 0·002-in. specimen is shown in Figure 7. The measured saturation time is again greater than the theoretical, and in this case the surface field appeared to be somewhat greater than that predicted by theory. Theoretical curves have been plotted to fit the experimental oscillogram as well as possible, and this suggests an effective value of H_c of 1·9 oersted which is considerably larger than the d.c. coercive field.

(*c*) **Voltage step applied through zero series-resistance.** This case may be investigated experimentally either by applying to the magnetizing winding a step-voltage via zero series-resistance, and observing the current drawn by the core, or by supplying the expected current wave-form to the winding from a high-impedance source, and observing the voltage across the search

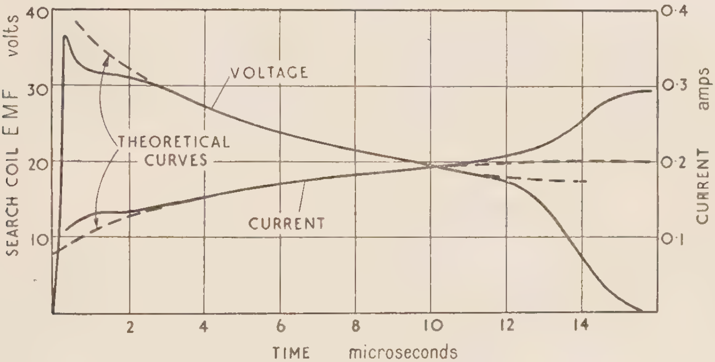

Figure 7. Response to a step voltage applied through a series resistance: 0·002-in. specimen.

coil, which should then take the form of a voltage step. As the zero circuit-resistance requirement is difficult to satisfy practically, the second method of test was adopted, and the core was excited with a current having an initial step followed by a linear rise, obtained from the anode circuit of the pulse-generator output valves. The amplitude of the step and the rate of rise of the current were adjusted in an attempt to produce a voltage step across the search coil. Some search-coil voltage oscillograms are shown in Figure 8

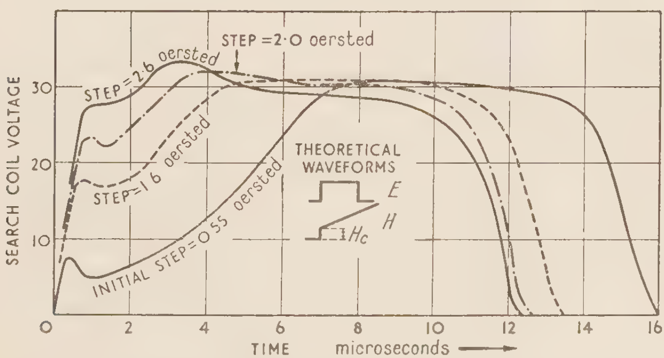

Figure 8. Stages in the production of a "square" voltage pulse: 0·002-in. specimen.

for a 0·002-in. specimen. For these the rate of rise of current was kept approximately constant, and the amplitude of the initial step was varied from about two to ten times the d.c. coercive field. For the low-amplitude initial-step case, the voltage wave-form is characterized by an initial slow rise of voltage. This can be largely compensated for by increasing the amplitude of the initial step above the theoretical value.

(*d*) **"Separation of the losses" in the step-field test.** The results of the foregoing tests suggested a method of dealing with the excess saturation times observed under conditions of step-field. The saturation time, when corrected for current-rise time and pulse tail, should be characteristic of the material thickness and magnetic constants. For an idealized loop of finite width it is given by

$$\tau = KB \,.\, d^2/8\,(H_s - H_c) \qquad \ldots(4)$$

where H_s is the amplitude of the step-field. Consequently, plotting H_s against $1/\tau$ should yield a straight line cutting the H axis at H_c. This is shown in Figure 9 where both $1/\tau$ defined as above, and $1/(\tau + \text{pulse tail})$ have been plotted. Over a large part of the range the curves are linear, the intercept on the H axis being 0·65 oersted, but at large values of τ the curve departs from a straight line and deflects towards the d.c. value of H_c.

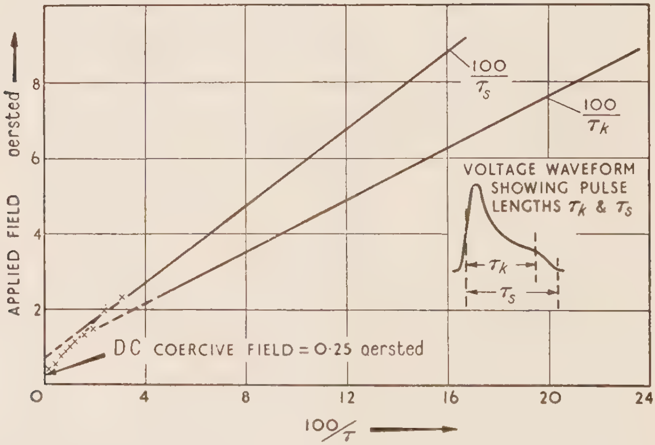

Figure 9. Separation of losses observed in a step-field test: 0·002-in. specimen.

5. DISCUSSION OF RESULTS

The tests described above have been applied to a number of specimens, and the waveforms shown in Figures 5, 7 and 8 are typical of all 0·002-in.

specimens tested. The agreement obtained between the shape of the theoretical and recorded waveforms, neglecting the discrepancy in the magnitude of H_c, is in general only obtained with large step-voltages and fields, the agreement becoming poorer as the amplitude of the disturbance applied to the core is reduced. In particular, for low values of step-field, the search coil voltage exhibits a rise time which is associated with the material and not with the external circuit, the time of rise increasing as the amplitude of the step-field is reduced until, with step-fields of three or four times the d.c. coercive field, it occupies about half the total saturation time, and the pulse shape becomes "Gaussian". An effect of this nature is also noticeable in Figure 8 for low-amplitude initial steps. The effects of shunt capacitances and finite circuit impedances have been considered, and the degree of approximation involved in regarding the B/H curve as a step-function has been investigated by numerical solutions. While these factors do modify the results, they cannot give rise to the form or magnitude of the discrepancies observed. The magnitude of H_c suggested by the "best fit" curves of Figure 7 is much greater than that obtained for the step-field test by separating the losses. The results of the former test have yet to be completely analysed, and it is not possible at this stage to state to what this is due. A similarly large value of H_c may be inferred from the curves of Figure 8. The good agreement between the theoretical and recorded waveforms in Figure 5 suggests that inhomogeneity within the specimen is not serious. The uncertainty of the core behaviour for small values of time, which is observable in all cores under all conditions of test, may suggest surface layer effects. Although this explanation is inconsistent with some of the observed discrepancies, it may cause part of the difference in the values of H_c obtained by the different methods.

The greater part of the discrepancies observed in these tests can possibly best be explained by postulating some additional mechanism retarding changes of induction, such for example, as has been discussed by Stewart (1950). The curve of Figure 9 is similar to one obtained by Stewart for alternating induction (i.e. a curve of total loss/frequency), the similarity being greater when it is remembered that for a rectangular B/H loop, applied field is proportional to energy loss/cycle, and that the abscissa has the dimensions of 1/time. For the practical application of these results it will be assumed that all the discrepancies observed are due to a time lag between B and H, and that such an effect can be represented by an increased effective H_c, assumed constant for the duration of the pulse. An extension of the theoretical treatment to a case of particular interest in the design of storage systems employing these cores will now be considered.

6. APPLICATION OF THE TEST RESULTS TO THE PROBLEM OF FLUX TRANSFER BETWEEN CORES

One of the problems in the design of storage systems using these cores is

that of obtaining the conditions for complete transfer of flux from one core to another when a pulse is applied to the first. This problem is non-linear, but a simple solution is possible by an extension of the penetration theory to the case of two cores.

Core 1 is at rest at the point g, Figure 3, and core 2 is at rest at point e. On the application of a pulse to core 1, the flux in core 1 changes from g to h. The voltage available from a search coil wound on core 1 is appliied to the magnetizing winding of core 2 via a series resistance R_s, and during the time that the flux in core 1 changes from g to h, that in core 2 must be caused to change from e to f. It is required ideally that the two cores shall saturate fully at the same instant, since if core 1 saturates before core 2, flux transfer between the two cores is incomplete, and if core 2 saturates

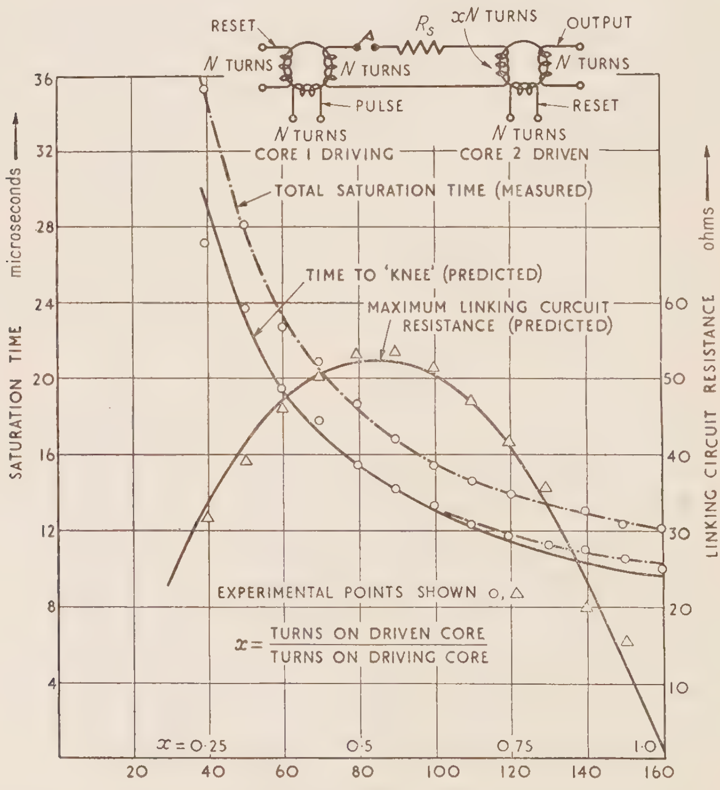

Figure 10. Conditions for complete flux-transfer (measured and calculated values): 0·002-in. specimen, step of 8·5 A-turns/cm. applied to core 1.

first, the resistance R_s loads the search coil of core 1. In a practical application it may be necessary to restrict the choice of the magnitude of R_s for other reasons, but this will not be considered here.

If the ratio (turns on magnetizing winding of core 2)/(turns on search coil of core 1) be x, all other windings having N turns (Figure 10), then for a field step H applied to core 1, H_c being zero, it may be shown that

$$x = \tfrac{1}{2}\left(1 \pm \sqrt{1 - 2Pd}\right) \qquad \ldots(5)$$

$$\tau' = (KB_0 d^2/8H)\,[(x+1)/x] \qquad \ldots(6)$$

where

$$P = KR_s\, 10^9 l/16\pi N^2 b \qquad \ldots(7)$$

and τ' is the saturation time for the pair of cores.

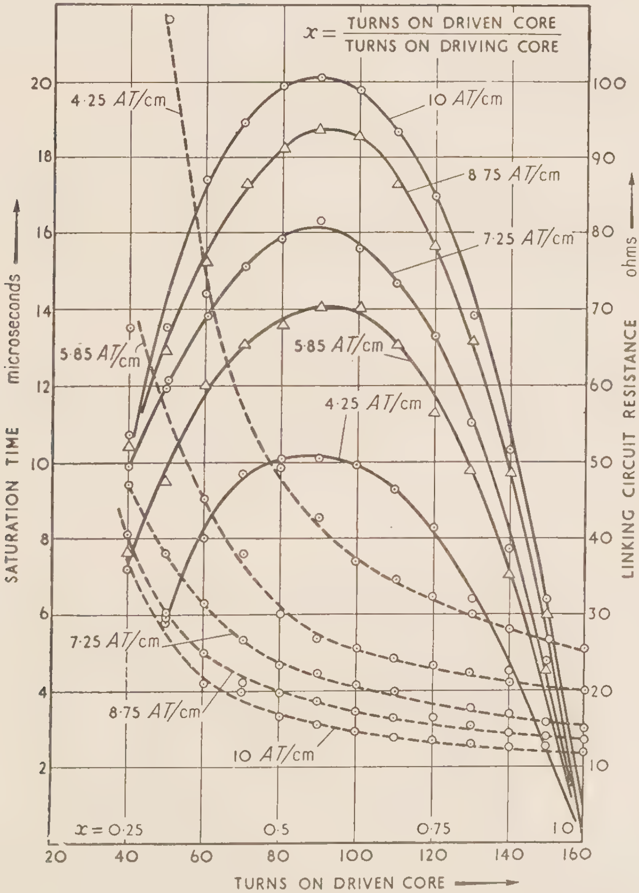

Figure 11. Measured conditions for complete flux-transfer: 0·001-in. specimens, various step fields applied to core 1.

In this case it will be seen that the maximum permissible value of R_s occurs when $x = \frac{1}{2}$ and is given by

$$R_s = 8\pi N^2 b / K 10^9 l d \qquad \ldots(8)$$

The saturation time for a pair of cores is twice that for one core excited with the same step-field when x has the value unity, and increases progressively as x is reduced.

When H_c is finite and such that $H_c = kH$, these equations become

$$x = [1/2(1-k)]\,[1 \pm \sqrt{1 - 2\,(Pd + 2k)\,(1-k)}] \qquad \ldots(9)$$

$$\tau' = (KB_0 d^2/8H)\,[(x+1)/(x - \overline{kx+1})] \qquad (10)$$

The effect of finite H_c is to reduce the maximum permissible value of R_s and to shift the x value for maximum R_s towards the $x = 1$ point, and also to increase the values of τ' given by equation (6).

In Figures 10 and 11, measured values of R_s and τ' are shown for specimens of 0·002-in. and 0·001-in. thickness. These were obtained for pairs of cores wound uniformly with 3 windings each of 160 turns, the magnetizing windings of each driven or second core being tapped every 10 turns. In practice, rectifier elements have to be used to isolate each pair of cores in a line during the flux-transfer process. In this test the function of these rectifiers was performed by a relay contact, enabling a wholly linear component to be used for R_s. The experimental results have the same form as that predicted by theory, and if the core constants are determined experimentally by separating the losses as in Figure 9, and using the values of H_c and $KB_0d^2/8$ so obtained, the accuracy of prediction can be quite high for large step-fields. Predicted curves obtained from equations (9) and (10) in this manner are shown in Figure 10 for the 0·002-in. specimens. When shunt rectifiers are used, the optimum transfer conditions are a little different from those given above.

7. CONCLUSIONS

The purpose of this work was to provide a greater understanding of some factors influencing the design of binary digital storage systems employing cores having rectangular hysteresis loops. With existing theories of operation it is not possible to predict the time or energy required to saturate a core, or to obtain the limiting conditions for flux transfer. In this paper an attempt has been made to add to existing knowledge by introducing a circuit theory based on eddy currents flowing within the core. The treatment is necessarily highly idealized and is only approximately true, since eddy currents do not completely express the mechanism by which changes of induction take place in the core. In spite of the imperfections of the theoretical approach, the treatment is capable of indicating the form of the result when cores are used in combination with other elements. The practical

application of such elements requires, in general, an approximation to step-field excitation, and for such a case the prediction can be improved by determining the constants of the equivalent rectangular loop experimentally. The theoretical treatment forms a suitable basis for a first design, and for this purpose Figures 6, 10 and 11 are probably the most useful.

The work was carried out in the Department of Electrical Engineering, King's College, London, and the author wishes to express his gratitude to Professor J. Greig for his advice and encouragement, and to Professor G. Temple for his helpful suggestions. Acknowledgment is also due to The Telegraph Construction and Maintenance Co. who supplied the cores, to the University of London for a Scholarship, and to the Ministry of Education for a grant which made this work possible.

DISCUSSION

Mr. F. F. Roberts:

During the reversal of magnetization in rectangular-loop material, individual domain walls probably extend over large areas and there are only a small number, perhaps only one or two, of such walls present in the thickness of the strip. Under these conditions the diffusion law of equation (1) will be a poor approximation. A better description would seem to be one in terms of the propagation of a single eddy-current-braked domain wall from each surface into the mid-plane of the strip. It seems possible that an applied step-field just exceeding the static coercive force could fail to initiate domain-wall propagation from one surface of the strip, in which case the total saturation time would be doubled and the voltage halved. In the case where the strip is not entirely saturated in the reverse direction before the application of the step-field in the forward direction, a true diffusion process would take place before the field effectively reached the nearest domain wall from the surface. Neither this diffusion, however, nor domain-wall inertia effects appear capable of explaining directly the slow build-up shown in Figure 3 for small step-fields.

Mr. A. E. De Barr:

Mr. Roberts's remarks raise the interesting question of the relation between the purely electromagnetic solution, which, in effect, assumes that the material is homogeneous and isotropic, and the solution for a material which is known to have a domain structure. The electromagnetic equations imply that the changes of magnetization are constrained to take place by the propagation of a domain wall from each surface into the mid-plane of the strip at just snch a rate that the eddy currents induced reduce the applied field to the value H_c at the domain boundary. This solution gives, therefore, a lower limit to the time required to complete the flux change. In large applied fields, when the applied field and the eddy-current fields are the most important factors, the time required to reverse the magnetization in an actual material might be expected to be given by the solution to the diffusion equation, whatever the domain structure of the material might be. With smaller applied fields, internal fields due to inhomogeneities in the material will become comparable with the other fields and will have to be taken into account. Under these circumstances the limiting time of propagation given by the purely electromagnetic solution will be exceeded, since the changes of magnetization are not taking place in the most straightforward manner but are influenced by the internal domain structure of the material. Such

internal fields would be expected to be of the order of H_c so that, in small applied fields, they might control the time required for penetration.

Micro-eddy currents associated with the domain wall itself might be expected to be significant at very high rates of change of flux.

Mr. Dorey (in reply):

Although the diffusion equation has been used as a basis for these tests, it is not a linear type of diffusion that takes place. The particular solution to the equation for the B/H relationship assumed in the paper takes the form of an induction "step" of height B_0 moving in from each surface of the strip, the field in this outside region being reduced linearly from the external value, acting at the surface, to H_c at the foot of the "step". As indicated by Mr. De Barr, this form of solution can be regarded as a form of domain-wall propagation from each surface of the strip, with the proviso that in this treatment the only braking effect considered is that of macro-eddy currents, flowing behind the wall. Figures 5 and 6 suggest that for the thicker specimens, the purely macro solution is a large part of the total effect which cannot be ignored. The treatment breaks down because it assumes that the induction at the step can change instantaneously from $-\frac{1}{2}B_0$ to $+\frac{1}{2}B_0$, and the results can be interpreted as indicating that this condition is only approached when moderately high values of step-field are applied to the cores. For step-fields a few times H_c, and for the thinner materials, I share Mr. Roberts's view that a better theoretical treatment should be sought. In this region explanations of the behaviour of the core on the lines of the propagation of a domain wall from each or one surface probably represent an oversimplification of the mechanism of magnetization. The diffusion process referred to by Mr. Roberts, when the strip is not entirely saturated, would presumably involve only inductions of the same order of magnitude as the applied field. It would be thought that these effects could be neglected in comparison with those dependent on inductions of several kilogauss. Incomplete saturation in either direction was eliminated by choosing the repetition frequency and pulse length of the applied field to be sufficient to completely saturate.

Mr. De Barr's remarks on the effects of inhomogeneities in the material are of interest. The rate of build-up of voltage observed for low step-fields appears to be markedly temperature-dependent, and this may support the view that impurities are responsible.

33

MAGNETIC CORES FOR INSTRUMENT TRANSDUCTORS

A. E. De Barr and E. H. Frost-Smith

[Elliott Bros. (London) Ltd.]

Abstract: A core material for transductors should have (among other things) high permeability, sharp saturation and good linearity. A proposed figure-of-merit takes these three properties into account, and is shown to assess the available materials reasonably. Certain combinations of materials can be predicted to be better than any one alone, and this has been checked by experiment.

1. INTRODUCTION

Although the development of magnetic materials in the last few years has greatly increased the scope of devices using them, the ideal magnetic material has not yet been produced, and further improvements in the performance of equipment using magnetic cores depend to a large extent upon overcoming the limitations imposed by existing materials. There is also the need for economy, particularly in the use of nickel which is both expensive and scarce.

General requirements for magnetic cores for transductors, and indeed for many other applications, may be summarized as follows:—

(i) high permeability;

(ii) linearity of the B/H curve between the origin and the "knee", and a sharp "knee" in the curve;

(iii) high saturation flux-density;

(iv) low hysteresis and eddy-current losses;

(v) low cost.

The best silicon-iron alloys, although relatively cheap and having a high saturation flux-density, have also lower permeabilities and a less linear B/H curve than the high-permeability nickel-iron alloys. There is little doubt that, eventually, greatly improved alloys will be produced; in the meantime, however, it has been thought worth while to investigate the possibilities of obtaining improved performance by combining, into one core, materials of different properties, in proportions chosen to give an inexpensive core with overall characteristics suitable for the particular application.

This paper is concerned particularly with the development of cores for transductors and contains also some considerations on the assessment of the suitability of a core material for this application. It is, however, believed that similar principles can be applied to the construction of cores for other purposes.

2. CORE REQUIREMENTS

A transductor (Lamm, 1943) may be regarded as a direct-current amplifier whereby the power supplied by a low-impedance source is controlled by a continuously variable reactance in series with the load (Frost-Smith, 1949). Variations of signal current in the polarizing windings on the core cause corresponding changes in the reactance of the windings carrying the load current which is thereby varied in the same way.

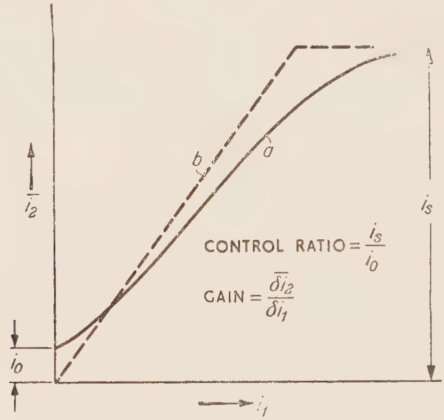

Figure 1. Control-current characteristic for a simple transductor : *a*, actual ; *b*, ideal.

The general shape of input-current/output-current characteristics obtained is shown in Figure 1 (curve *a*). Ideally a characteristic like that at *b* is required. Referring to these characteristics it will be clear that

(i) the control ratio (i_s/i_o) should be large;

(ii) the characteristic should have a high slope;

(iii) the characteristic should be linear up to saturation;

(iv) where large powers are to be handled a large saturation current i_s, and therefore a high saturation flux-density in the core, is desirable.

In order to correlate these requirements with the properties of the core, it is convenient to refer to a family of curves in which the mean supply voltage to the transductor $\bar{E}_2$ is plotted against the mean rectified current $\bar{i}_2$, for zero load impedance and for various values of signal or control current i_1. Such a family of curves is shown in Figure 2*a* and from these the performance of the transductor when supplying a resistive load R_L may be predicted. The load line XY is drawn with slope $-R_L$ and the transductor operates between the limits X and Y. At any point on the load line, $\bar{V}_T$ represents the mean transductor voltage and $\bar{V}_R = \bar{i}_2 R_L$ represents the mean voltage across the load.

The curve in Figure 2a for which $i_1 = 0$ is the a.c. magnetization characteristic for the core. Curves for other values of i_1 are similar, but are displaced

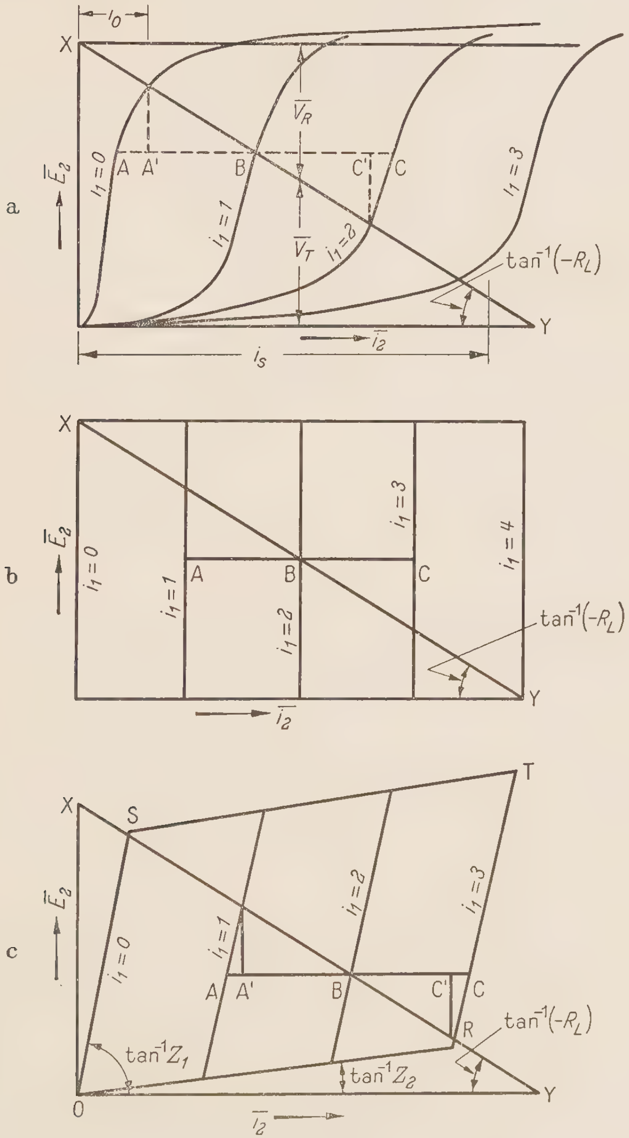

Figure 2. A.C. magnetization characteristics: a, actual; b, ideal; c, allowing for finite permeability and winding losses.

towards higher values of $\bar{\imath}_2$ by amounts proportional to i_1. It may be seen that

(i) i_0, which affects the control ratio, is determined by the slope of the a.c. magnetization curve;

(ii) the current gain $\delta\bar{\imath}_2/\delta i_1$ is given by $A'B$;

(iii) for linearity $A'B = BC'$, etc.

It will be shown in a paper to be published later that, when the transductor is operating under self-excitation conditions, linearity in the magnetization characteristic becomes considerably more important. Many materials, particularly those in which the coercive force is not small, have a low initial permeability, and this means that the permeability varies over the unsaturated portion of the magnetization curve. This gives rise to non-linearity in self-excited transductors.

These considerations indicate that the ideal magnetization curve would be as shown in Figure 2*b*. Here $i_0 = 0$, $AB = BC$, and the maximum possible current gain is given by AB. In practice modifications must be made to take account of

(i) the finite permeability and energy losses which together reduce the initial slope of the magnetization curve to, say, Z_1;

(ii) winding resistance and inductance giving a final slope of, say, Z_2.

$$Z_1 \doteqdot 1/\sqrt{1/k\mu^2 + 1/R^2} \qquad \ldots(1)$$

where μ is the permeability of the unsaturated core, assumed constant, R is an equivalent parallel resistance representing losses and k is a constant for a given transductor operating at a given frequency. Further, from Figure 2*c*

$$\delta i_1/\delta i_2 = A'B = AB/(1 + R_L\sqrt{1/k\mu^2 + 1/R^2}) \qquad \ldots(2)$$

and when μ and R are infinitely great $A'B = AB$.

Although a core with the characteristic shown in Figure 2*c* will give a smaller current gain than one for which Figure 2*b* applies, the permeability is constant and therefore the amplifier is still linear.

The most useful improvement in magnetic cores would result from the production of a core in which the transition from the high permeability region to the saturated region occurs as abruptly as possible, high permeability itself being a secondary consideration. At the same time the energy losses should be as small as possible so that variations in R do not affect the linearity.

3. A FIGURE-OF-MERIT FOR CORE MATERIALS FOR TRANSDUCTORS

Actual materials have B/H characteristics which deviate from the ideal shown in Figure 2*c* and it is useful to have some criterion by which their

suitability for this particular purpose may be assessed. It has long been recognized that a sharp "knee" in the characteristic is desirable, and it has been suggested that the sharpness of the knee should be used as a measure of the suitability of a material for use in magnetic amplifiers. Sharpness, however, is not easy to define, and moreover, as pointed out in section 2, it is not the only factor to be considered. Borg (1949) has suggested an alternative figure-of-merit, but this also does not take into account some of the important features of the characteristic.

The figure-of-merit should assess

(*a*) the sharpness of the knee of the B/H curve;

(*b*) the linearity of the B/H curve between the origin and the knee;

(*c*) the steepness of the B/H curve between the origin and the knee.

In general, the saturation flux-density of the material should be included, but in the type of transductor particularly considered here, high power-handling capacity is not an important requirement, and a high saturation induction is considered to be less important than a suitably shaped magnetization characteristic. For this reason the proposed figure-of-merit does not include saturation flux-density.

Sharpness. For our present purpose the knee of the magnetization curve may be said to begin at the point of maximum permeability ($H = H\mu_{max} = H_1$ say). The transition from the high-permeability region into the approach to saturation may be considered to be complete when the slope of the magnetization curve has fallen to, say, 1% of the maximum permeability attained ($H = H_2$ say). The sharpness of the knee may be defined as the difference between these two values of magnetizing field, i.e. $H_2 - H_1$, a quantity which would be zero in the ideal magnetic material.

Non-linearity. The initial permeability μ_a is almost invariably less than the maximum permeability μ_{max} and non-linearity may be measured as the percentage change of slope of the B/H curve between the origin and the point of maximum permeability, i.e. $100\,(\mu_{max}/\mu_a - 1)$, and should ideally be zero.

The sharpness and non-linearity factors together assess the shape of the magnetization curve and their product may be used as a measure of shape for our present purpose.

Steepness. A convenient measure of steepness is $1/\mu_{max}$. This quantity, like the other factors defined above, should ideally be zero.

Reference to Table 1 shows that in the readily available materials the shape factor $100(H_2 - H_1)\,(\mu_{max}/\mu_a - 1)$ and the scale factor $1/\mu_{max}$ both vary over the same sort of range, i.e. about 100 : 1, and it would seem therefore that their product would be a suitable criterion of a core material

for magnetic amplifiers, equal weight thus being given to shape and to scale of the magnetization curve. The proposed figure-of-merit is

$$\log_{10}\left(\frac{\mu_{max}\,\mu_a . 10^{-2}}{(H_2 - H_1)\,(\mu_{max} - \mu_a)}\right)$$

where H_2 and H_1 are measured in oersteds and μ_{max} and μ_a are the relative maximum and initial permeabilities of the material.

Indirectly, this figure-of-merit includes the effects of hysteresis loss too, since a large hysteresis loss is associated with a large coercive force which in turn implies a large ratio of μ_{max}/μ_a. The effects of eddy currents could be taken into account by including the resistivity of the material in the figure-of-merit if desired.

Since $H_2 - H_1 \fallingdotseq H_2$ for most materials and $(\mu_{max}/\mu_a - 1) \fallingdotseq \mu_{max}/\mu_a$, an approximation to the figure-of-merit, useful for easy comparison of different materials, is $\log_{10}(\mu_a \times 10^{-2}/H_2)$.

Values of this figure-of-merit for a selection of magnetic materials are given in Table 1. The data are taken from manufacturers' publications (extrapolated where necessary), or from measured results on actual samples.

A figure-of-merit which takes account of all the relevant core properties would be of great assistance in the design of magnetic amplifiers although in the final assessment geometrical factors such as core length and area will be involved. The proposed figure-of-merit is suggested as a first step in this direction but is not necessarily in the best form; other ways of combining the quantities making it up may be worth consideration.

4. THE COMPOSITE MAGNETIC CIRCUIT

Magnetic cores of the kind in which we are interested are usually magnetized by means of a current in a coil linking the magnetic circuit. Interest is then centred not so much on the relation between B and H as on that between the total magnetic flux in the core, Φ, and the applied magnetomotive force (m.m.f.) or ampere-turns. The ratio of these quantities is, of course, the total reluctance of the magnetic circuit.

In the most general case we have a core made up of a number n of sections 1, 2, 3, etc., in series, each section containing a number s of parallel components a, b, c, etc. Then if l_1, A_{1a} and μ_{1a} are the length, cross-sectional area and permeability respectively of the component $1a$,

$$\frac{\Phi}{\text{m.m.f.}} = \frac{1}{\Sigma_n(l_1/\Sigma_s A_a \mu_a)} \tag{4}$$

Parallel combinations of different magnetic materials have been used to obtain improved characteristics for cores of current transformers (Halacsy, 1951) and series combinations have been used in "peaking" transformers.

Table 1.—Figure-of-merit for various materials

Material	μ_{max}	H_1, oersted	μ_a	$\frac{\mu_{max}}{\mu_a} - 1$	H_2, oersted	$H_2 - H_1$	$\frac{\mu_{max} \times 10^{-2}}{(H_2 - H_1)(\mu_{max}/\mu_a - 1)} = \gamma$	$\log_{10} \gamma$
Supermalloy ..	445 000	0·009	90 000	3·9	0·15	0·14	$8{\cdot}1 \times 10^3$	3·9
Mumetal ..	90 000	0·04	30 000	2·0	0·70	0·66	$6{\cdot}8 \times 10^2$	3·9
Deltamax ..	150 000	0·1	1 000	150	0·50	0·40	$2{\cdot}5 \times 10$	1·4
Crystalloy ..	17 500	0·4	2 000	7·8	3·6	3·2	6·9	0·8
Radiometal ..	22 000	0·3	2 200	9·0	4·0	3·7	6·6	0·8
H.C.R.	60 000	0·2	1 000	59	1·8	1·6	6·3	0·8
Super Stalloy..	9 500	0·6	1 500	5·3	10	9·4	1·9	0·3

By suitably choosing the areas and lengths of different magnetic materials, improved magnetic-amplifier characteristics can also be obtained.

Consider a core consisting of a bridge section of material 1, the magnetic circuit being completed by a yoke consisting of materials 2*a*, 2*b*, 2*c*, etc., in parallel. Then equation (4) becomes

$$\frac{\Phi}{\text{m.m.f.}} = \frac{A_1\mu_1/l}{\alpha + (1-\alpha)(A_1\mu_1/\Sigma A_2\mu_2)} \qquad \text{...(5)}$$

where l is the total length of the magnetic circuit and α is the fraction of that length occupied by material 1. If the reluctance of the yoke can be made negligible at all values of Φ, then

$$\Phi/\text{m.m.f.} \risingdotseq A_1\mu_1/\alpha l \qquad \text{...(6)}$$

Thus the reluctance of the core is less by a factor α than for a core of uniform cross section consisting entirely of material 1. The effective initial and maximum permeabilities are increased by a factor $1/\alpha$ whilst the polarizing field at which the slope of the B/H curve is 1% of μ_{max} is reduced to α times its previous value. The new figure-of-merit is then

$$\log_{10}\left\{\frac{\mu_{max}\,\mu_a\,.\,10^{-2}}{(H_2-H_1)(\mu_{max}-\mu_a)\alpha^2}\right\},$$

H_2 and μ_a referring to the magnetization curve for material 1 which should, of course, be a material particularly suitable for magnetic-amplifier cores, e.g. a high-permeability nickel-iron.

One method of reducing the reluctance of the yoke would be to make the whole core of material 1, but to increase the cross-sectional area of the yoke portion. This is equivalent to constricting the core over a short length, as has been proposed for "peaking" transformers (Kiltie, 1932) and magnetic amplifiers (Latimer and Macdonald, 1950) in order to provide an easily saturable section. A similar effect may be achieved by making the yoke material 2*a* in the less expensive grain-oriented silicon-iron.

If the ratio of the cross-sectional areas of the bridge and yoke is correctly chosen, then when the bridge is becoming saturated the flux-density in the yoke can correspond to the point of maximum permeability, thus increasing the sharpness of the knee of the composite core.

A disadvantage of silicon-iron for this purpose is its low initial permeability. This means that although the knee of the composite core is sharper than for the uniform core, its effective initial permeability is low unless an excessively large yoke is used. This defect may be remedied by placing in parallel with the silicon-iron yoke a small amount of a material 2*b* with a high initial permeability. Then, referring to equation (5), initially $A_{2b}\,\mu_{2b}$ is large so that $A_1\mu_1/\Sigma A_2/\mu_2$ is small and

$$\Phi/\text{m.m.f.} \risingdotseq A_1\mu_1/1 \qquad \text{...(7)}$$

At higher flux-densities $A_{2b}\ \mu_{2b}$ and $A_{2a}\ \mu_{2a}$ are both large, so that the same effect is achieved, whilst when the bridge approaches saturation, although $A_{2b}\ \mu_{2b}$ is small, $A_{2a}\ \mu_{2b}$ reaches its maximum value, and equation (7) again holds.

Such a composite core is somewhat larger and heavier than a core of the same length consisting of a uniform section of nickel-iron but, in addition to being cheaper and using less nickel, results in an improved magnetic-amplifier characteristic. The actual performance achieved depends upon the size of the yoke used, but the figure-of-merit may, in the limit, be increased by log $1/\alpha^2$. α will usually be about 0·25. It will be shown below that a useful improvement in magnetic-amplifier characteristics is possible without the use of an excessive amount of material.

5. EXPERIMENTAL RESULTS

(*a*) **Magnetization curves.** Experimental verification of the ideas of the previous section is provided by the magnetization curves, obtained by a ballistic method, shown in Figure 3. The curves shown refer to:—

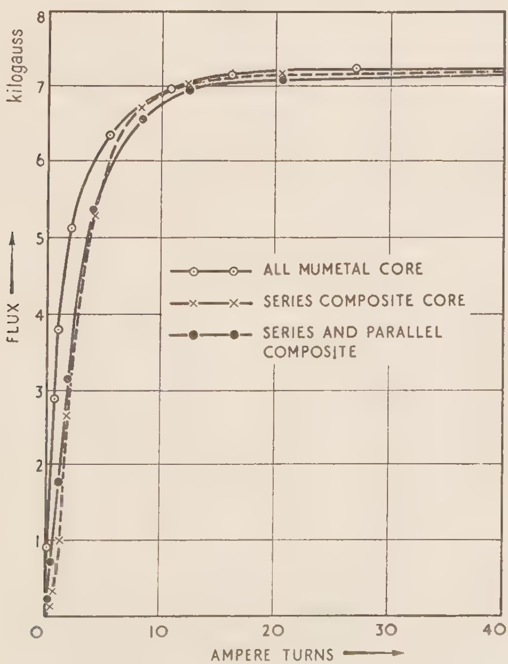

Figure 3. d.c. magnetization curves.

(1) A Mumetal core of uniform cross-sectional area.

(2) A core in which 27% of the magnetic circuit is Mumetal of the same cross-sectional area as in (1), the circuit being completed by a Crystalloy yoke of 2·15 times the cross-section of the Mumetal. The Crystalloy was used in the form of U-shaped laminations chosen to minimize the effect of the flux in the base of the U not being in the easy direction of magnetization.

(3) A core as in (2), in which 10% of the Crystalloy is replaced by Mumetal.

Core (2) shows a sharper knee than core (1), but a reduced slope and greater non-linearity near the origin. In core (3) the increased initial permeability of the yoke results in a more linear characteristic at the expense of a slightly less-sharp knee. Although the effective maximum permeability is less in core (3) than in core (1), this effect is compensated by the greatly improved linearity.

(*b*) **Transductor characteristics.** The results described here are preliminary only, included to give some idea of the characteristics which may be expected from magnetic amplifiers using composite cores.

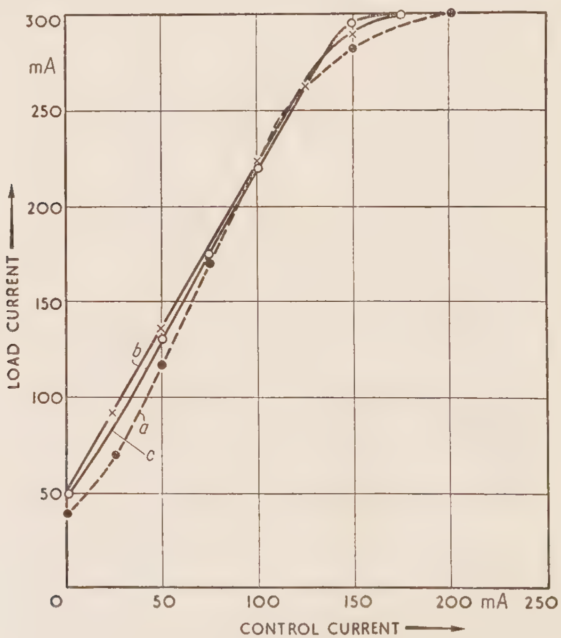

Figure 4. Control-current characteristics without self-excitation: *a*, all-Mumetal core; *b*, series composite core; *c*, series and parallel composite core.

The tests were carried out using small transductors excited at 500 c/s. The three types of core used were very similar to those described in (*a*) above.

(1) All Mumetal, uniform cross-section.

(2) 25% Mumetal: Crystalloy yoke of area 2·15 times that of the Mumetal.

(3) As (2) with 10% of the Crystalloy replaced by Mumetal.

Control-current characteristics for the three cores are shown in Figure 4, these curves relating to transductors operating with zero self-excitation. The greatly increased linearity of the curves for the composite core, at the expense of a reduced gain, is clearly evident.

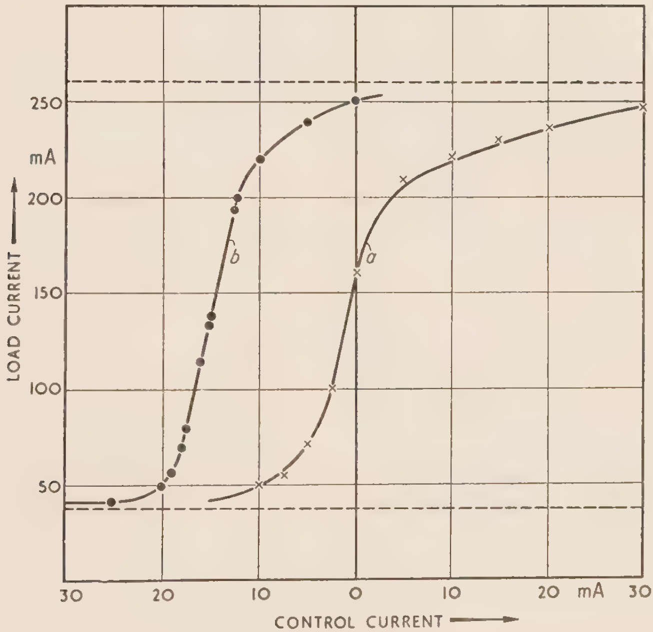

Figure 5. Control-current characteristics for self-excited core: *a*, all-Mumetal core; *b*, series and parallel composite core.

Figure 5 shows curves for cases (1) and (3) operating with self-excitation. The current gain in each case is increased by a factor of about 13, and the curves show quite clearly the superiority of the composite core as far as linearity is concerned.

6. CONCLUSIONS

A simple "figure-of-merit" has been suggested which is shown to express quite well the relative suitability of a number of typical magnetic materials for transductors. This "figure-of-merit" also gives an indication of the improvement in transductor characteristics to be expected by the use of a composite magnetic core in which different materials are combined in a

suitable way. Magnetization curves for some experimental composite cores confirm the results predicted by a simple analysis of the magnetic circuit.

The principles involved have been applied to the construction of experimental magnetic amplifiers, and preliminary results indicate that composite cores should form a useful addition to existing techniques. The results obtained are preliminary only, and do not represent the final improvement that can be obtained. Further work is in progress.

34

SOME A.C. MEASUREMENTS ON A MATERIAL HAVING A RECTANGULAR HYSTERESIS LOOP

S. E. Buckley, G. A. Jackson and A. G. F. Thomas
(Standard Telephones and Cables Ltd.)

Abstract: Measurements made of the a.c. core losses of a domain-oriented material, which has a rectangular hysteresis loop, show that they are higher than would be expected from the d.c. magnetic characteristics and other properties of the material. When an analysis is made of the core-loss coefficients at low values of applied field, it is found that the eddy-current loss is much greater than would be expected, while the hysteresis-loss coefficient increases with increasing frequency. The divergence of measured results from calculated values becomes greater as the hysteresis loop is made more rectangular. The same effect has been found also in some grain-oriented materials which have rectangular hysteresis loops.

The high losses are believed to be related to the observed effect that it is extremely difficult, if not impossible, to demagnetize materials of this class completely.

1. INTRODUCTION

The two principal methods by which a rectangular hysteresis loop may be obtained in some materials are Grain Orientation and Domain Orientation. In the former method, the degree of cold working of the metal during rolling is closely controlled, while in the latter method, a magnetic field is applied to the sample during part of the cycles of heat-treatment. Grain Orientation, which is most usually applied to materials of the 50-50 nickel-iron type was first developed in Germany (Both, 1947). Domain Orientation, which can be produced in materials having a relatively high Curie point, high magneto-striction, and no phase transformation below 500°C, has been described by Bozorth and Dillinger (1935).

There have been unpublished reports that the a.c. characteristics, particularly core losses, measured on rectangular loop materials, do not agree with what might be expected from the d.c. characteristics and other properties of the materials. In this paper some a.c. characteristics have been recorded on a domain-oriented 65% nickel-iron.

2. TEST SAMPLES

The test samples were wound from strip 0·5 inch wide and 0·002 inch thick into toroidal cores of external diameter 1·2 inches, and internal diameter 1·0 inch. The cores were given a preliminary anneal in pure dry hydrogen at 1100°C, followed by a further heat-treatment in hydrogen during which a

magnetic field was applied between 600°C and 400°C. To avoid mechanical strain on the test cores, they were placed in an annular box and the windings applied over it.

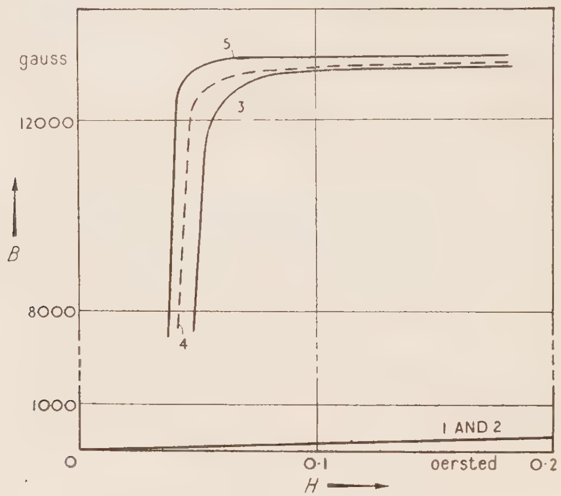

Figure 1. B/H curves (d.c. tests).

3. METHODS OF MEASUREMENT

D.C. measurements. B/H curves and hysteresis loops were measured by the usual ballistic galvanometer methods.

A.C. test. B_{max} v. H_{RMS}. In these tests the magnetizing current was measured by means of an a.c. milliammeter; the applied field strength H_{RMS}

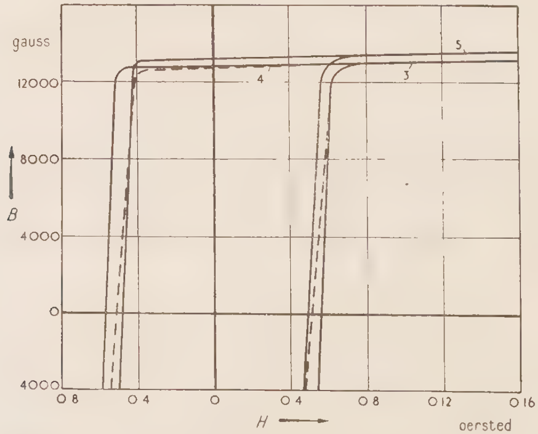

Figure 2. Hysteresis loops for samples heat-treated with magnetic field.

was calculated from the value of the current, the dimensions of the core and the number of turns. The flux density B_{max} was calculated from the voltage measured across a second winding assuming a form factor of 1·11. Measurements were made at 50 c/s and 400 c/s.

A.C. core loss tests. A direct comparison bridge consisting of 10-ohm ratio arms, an air-cored inductometer, a non-inductive resistance box and two screened transformers, was used. B_{max} was calculated (see Appendix) from the impedance measured and H_{RMS} from the current flowing through the test winding. The test frequencies were again 50 c/s and 400 c/s.

A.C. hysteresis loss and eddy-current loss coefficients. The same bridge was used. The flux density was restricted to below 100 gauss, but frequencies up to 1800 c/s were used. The general method was that described by Legg, 1936.

4. RESULTS OF MEASUREMENTS

D.C. measurements. B/H curves and hysteresis loops for samples heat-treated with and without a magnetic field are shown in Figures 1, 2 and 3.

Sample 1 was annealed at 1100°C only; sample 2 was annealed at 1100°C, followed by heat-treatment from 600°C without a magnetic field; Samples 3, 4 and 5 show the various degrees of rectangular loop properties obtained by heat-treatment in a magnetic field.

Table 1 (p. 319) summarizes these results.

A.C. measurements. Curves for B_{max} v H_{RMS} at 50 c/s and 400 c/s are shown in Figure 4. Curves of core loss against B_{max} at 50 c/s and 400 c/s are shown in Figures 5 and 6 respectively. Measurements of a.c. hysteresis loss coefficient are recorded in Figures 7 and 8, and the results are summarized in Table 2.

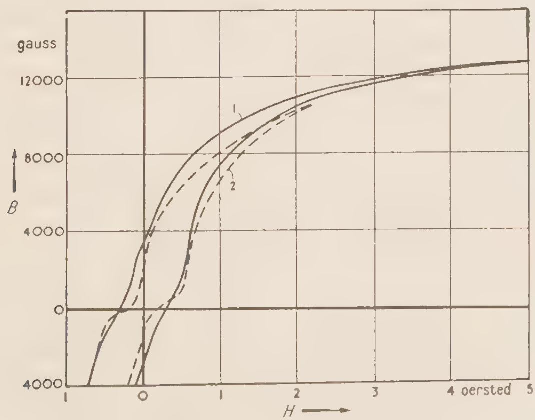

Figure 3. Hysteresis loops for samples heat-treated without magnetic field.

5. DISCUSSION OF RESULTS AND CONCLUSIONS

As a check that high eddy-current losses were not due to a failure of insulation between the turns of tape in a core, Sample 5 was subsequently re-heat-treated in hydrogen at 1100°C without the application of a magnetic field.

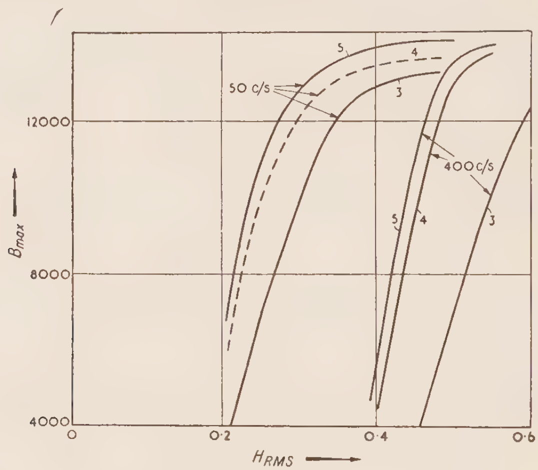

Figure 4. B_{max} against H_{RMS} (50 c/s and 400 c/s tests).

The eddy-current loss then measured was comparable with that of Sample 1. Also, a check was made of the accuracy of the test circuit by measuring the eddy-current and hysteresis loss coefficients of a core wound from a normal high-permeability nickel-iron alloy; the results obtained were of the same order as those predicted by calculation.

During measurement it was found that to obtain some degree of consistency of results, special care had to be given to demagnetization. It is

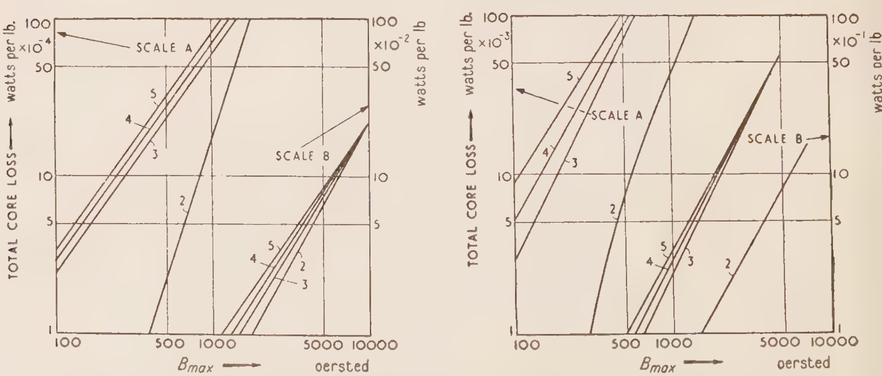

Figures 5 and 6. Total core losses at 50 c/s (Figure 5) and 400 c/s (Figure 6).

doubtful if complete demagnetization of rectangular-loop samples is possible (Bozorth and Dillinger, 1935). Reversals of d.c. field at the rate of 6 times per second were applied from $H = 20$ down to the field strength at which the measurement was to be made.

The B/H curves for a.c. are found to be sheared over towards the H axis as is usual for high-permeability materials, and the degree of shearing is considerable as a result of the high values of permeability concerned.

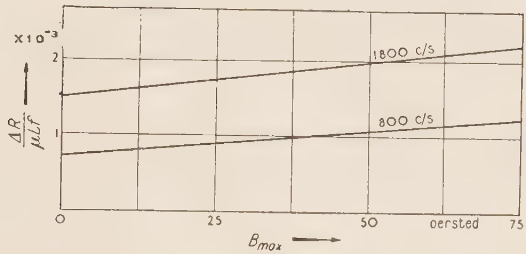

Figure 7. Determination of hysteresis loss coefficient: Sample 1.

The a.c. core losses at low flux densities (see Table 2) are higher than would be expected from calculations based on the Rayleigh conception of small hysteresis loops bounded by two parabolae. The eddy-current coefficient for samples heat-treated in a magnetic field is many times greater than would be expected from calculation, and the more rectangular the loop the higher

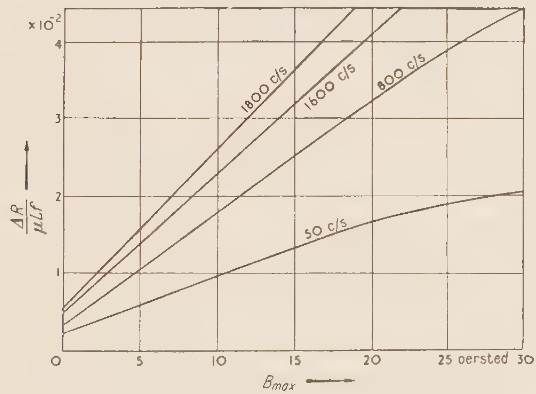

Figure 8. Determination of hysteresis loss coefficient: Sample 5.

the loss coefficient, while for samples not so treated it is in better agreement with the calculated value. The hysteresis coefficient of the former samples appears to increase as the frequency is increased, while the coefficient for the latter samples is more constant. It may be that these effects result from the inability to demagnetize the samples completely, which leads to the measurements being unavoidably made on polarized samples.

As an illustration of the difficulty of demagnetizing, a hysteresis loop at a frequency of 1000 c/s was observed by oscillograph on Sample 5. The loop was pointed above the H axis and rounded below it, thus indicating the presence of even harmonics. A d.c. field was then superimposed. Momentarily, the loop became symmetrical, consisting of two parabolae. However, asymmetry soon re-appeared but in the opposite sense from that of the earlier loop, as the second loop was rounded above the H axis and pointed below it.

The authors wish to thank Standard Telephones & Cables Ltd. for permission to publish this paper. The material described is known as Permalloy F.

APPENDIX

According to McLachlan (1936), the flux density should be calculated from the inductance corresponding to a parallel circuit L_p and R_p, not the series circuit L_s and R_s.

$$\text{Thus} \quad B_{max} = \frac{\sqrt{2}\, I\, L_s \,.\, 10^8}{NA \sin\theta}$$

where B_{max} is the maximum flux density,
I is the current in amperes,
L_s is the inductance in henries,
N is the number of turns carrying I,
A is the cross-section of the core,
θ is $\tan^{-1}(\omega L_s/R_s)$.

$$\text{But} \quad \sin\theta = \frac{\omega L_s}{\sqrt{\omega^2 L_s^2 + R_s^2}}$$

$$\text{therefore} \quad B_{max} = \frac{I\sqrt{\omega^2 L_s^2 + R_s^2} \,.\, 10^8}{\sqrt{2}\pi NAf}$$

It is interesting to note that since $I\sqrt{\omega^2 L_s^2 + R_s^2}$ is equal to E, the voltage which would be measured across the series circuit,

$$B_{max} = \frac{E \,.\, 10^8}{\sqrt{2}\pi NAf}$$

This expression is similar to that normally used to determine the relationship between B_{max} and E, assuming a form factor of 1·11, except that the voltage E is measured across the impedance and is not that corresponding to the reactive component alone.

Table 1. D.C. characteristics

D.C. properties	Sample No. 1	Sample No. 2	Sample No. 3	Sample No. 4	Sample No. 5
Maximum permeability, μ_{max}	6800	6600	207 500	233 000	262 000
Magnetizing force for μ_{max}, Oe	1·0	1·0	0·06	0·05	0·04
Maximum flux density, gauss	14 000	14 000	14 000	14 000	14 000
Coercive force, Oe, for $B = 13\,000$ gauss	0·3	0·175	0·056	0·051	0·048
Remanence, gauss, for $B = 13\,000$ gauss	3 160	1 700	12 800	12 700	13 000
Hysteresis loss, ergs/c.c./cycle, for $B = 13\,000$ gauss	985	790	240	213	209

Table 2. Hysteresis loss coefficients

Sample No.	Frequency c/s	Coefficient h
1	800	$0{\cdot}78 \times 10^{-6}$
	1800	$0{\cdot}95 \times 10^{-6}$
5	50	$0{\cdot}73 \times 10^{-3}$
	800	$1{\cdot}46 \times 10^{-3}$
	1600	$1{\cdot}80 \times 10^{-3}$
	1800	$2{\cdot}06 \times 10^{-3}$

Table 3. Eddy-current loss coefficients

Sample No.	e
1	$7{\cdot}7 \times 10^{-8}$
2	$9{\cdot}0 \times 10^{-8}$
3	$36{\cdot}0 \times 10^{-8}$
4	$70{\cdot}0 \times 10^{-8}$
5	$180{\cdot}0 \times 10^{-8}$

Calculated value: $3{\cdot}9 \times 10^{-8}$

DISCUSSION

Mr. B. G. Parkin:

The authors report large discrepancies between the measured and calculated values of eddy-current loss in domain-oriented material. We have observed this effect (although not on the same scale) in some other types of material as well.

Polder (1953) refers to Williams, Shockley and Kittel (1950) in which it is suggested that the eddy-current loss in a material having a domain-and-wall structure is higher than in a uniform one.

The argument may be summarized as follows. The reversal of a given amount of flux, whatever its distribution, causes the same induced voltage, E, to act round any given path. The total eddy-current loss is proportional to ΣE^2, but ΣE^2 is less when there are many small columns of flux, instead of a few large ones. In other words, the loss will be higher the less uniform the flux distribution. In a domain-and-wall structure the flux distribution is very non-uniform, for the permeability of the domain is unity while that of the volume swept out by the wall must be very high, in order to account for the observed values of permeability.

A slight extension of this argument would lead us to the conclusion that an increase in the domain size causes increased eddy-current loss, and we may therefore expect to find high values of g (the ratio of observed to calculated eddy-current loss) in materials that have large domains.

The words "large" and "small" mean, presumably, in comparison with the thickness of the material. The possible domain size is increased by grain growth, crystal orientation, or domain orientation, and we give below the results of tests, at 1 kc/s, on samples of each of these types.

(*a*) *Grain growth.* Samples of a Mumetal-type alloy were annealed at various temperatures. The grain size increased progressively with increase in temperature. The permeability values have been included to show that samples with similar permeability may have very different losses.

Temperature of anneal, °C	Grain size, microns	g	Initial permeability
1050	10	1·09	22 600
1150	15	1·12	25 600
1250	50	1·33	35 700
1350	85	1·67	35 200

However, this effect was found to be very much less marked in another material (an alloy of the Supermalloy type).

Temperature of anneal, °C	Grain size	g
1300	About ½ inch	1·23

(*b*) *Crystal orientation.* Two samples of grain-oriented 50/50 nickel-iron alloy gave g values of 2·4 and 3·1 respectively. A sample of similar alloy, not grain-oriented, had $g = 1{\cdot}7$.

(*c*) *Domain orientation.* Two samples of 65/35 nickel-iron alloy were tested. Both samples had been annealed in the normal way at about 1100°C, but sample 1 had been given a magnetic anneal in addition.

Sample	g
1	2·20
2	1·18

These specimens are the samples quoted by Fairweather (1953).

Mr. Buckley (in reply):

On Permalloy-F, the value of g measured on a sample which had not been domain-oriented was less than 2, whereas on oriented samples, by measurements below flux densities of 100 gauss and at frequencies up to 1800 c/s, the values obtained for g were much higher.

A Permalloy-C core (0·002 inch thick material) was measured at the same time in order to check the test circuit and this gave a value of $g = 1{\cdot}2$, which appears to agree with Mr. Parkin's results on Mumetal.

Under our conditions of test we measured unexpectedly high values of loss which were proportional to the square of the flux density and to the square of the frequency, and hence we described this loss as eddy-current loss.

35

THE MAGNETOSTRICTION OF FERRITES

P. Popper

(Material Research Laboratory, Mullard Limited)

Abstract: The saturation magnetostriction of different ferrites is compared with that of nickel. It is shown, however, that the magnetostriction at saturation alone is not a sufficient criterion of the suitability of a magnetostrictive material for various applications. The reversible magnetostriction and saturation magnetostriction are related to the reversible permeability and saturation polarization, respectively. From these considerations one may derive the general behaviour of the reversible magnetostriction as a function of the polarizing field. The complete magnetostriction equations are given and the properties of a ring vibrating in a radial mode and its equivalent electrical circuit are discussed. The a.c. magnetic field may be applied in a direction perpendicular to the d.c. field (Wiedemann effect) and it is practicable to excite ferrite vibrators in this way in a shear mode. Nickel-zinc ferrites of high zinc content can be used in the shape of rings, rods or tubes as electro-mechanical filters and transducers (receivers). The paper gives the properties of nickel-zinc ferrites and also some data of a permanent-magnet material which can be used to provide the polarizing field.

1. INTRODUCTION

Applications of magnetostriction have been limited in the past to ultrasonic transducers below 30 kc/s because of the eddy-current loss which requires assemblies to be made up of very thin laminations. Pierce (1928) has studied the application of magnetostrictive transducers to stabilize the frequency of oscillators; but in this as well as in filters it was found that the mechanical Q and the temperature stability were not high enough.

Most ferrites have a very high resistivity and eddy-current losses are consequently negligible. It is therefore of considerable interest to examine here the magnetostrictive properties of ferrites.

2. THE JOULE MAGNETOSTRICTION

The change in length which occurs in the direction of an applied magnetic field is called the longitudinal or Joule magnetostriction. A material which expands in the direction of the applied field is said to have a positive magnetostriction, one which contracts has a negative magnetostriction.

(*a*) **The saturation magnetostriction.** The saturation magnetostriction of all single cubic ferrites of spinel structure (i.e. compounds of the type $MO . Fe_2O_3$, where M stands for a bivalent metal) is negative with the sole exception of magnetite, $FeO . Fe_2O_3$. Table 1 gives the saturation magneto-striction for various ferrites and also for nickel.

Table 1

Material		Saturation magnetostriction $(\Delta l/l)_s$
		$\times 10^{-6}$
$FeO \cdot Fe_2O_3$		+ 40
$NiO \cdot Fe_2O_3$		− 27
$MnO \cdot Fe_2O_3$		− 2
$(Mn, Zn)O \cdot Fe_2O_3$		− 0·5
$(Ni, Zn) \cdot O. Fe_2O_3$ (in order of increasing nickel content)	Grade A	− 4
	„ B	− 7
	„ C	− 15
	„ D	− 18
	„ E	− 22
Nickel		− 45
$BaO \cdot 6\,Fe_2O_3$		− 5 approx.

The table includes a recently-developed permanent magnetic material (Went, Gorter, Rathenau, and van Oosterhout, 1952) which has a remarkably high coercive force. It is a barium ferrite, $BaO \cdot 6\,Fe_2O_3$; its structure is not of the spinel-type but belongs to the class of magneto-plumbites. Its resistivity is very high and it can therefore be used in high-frequency applications where

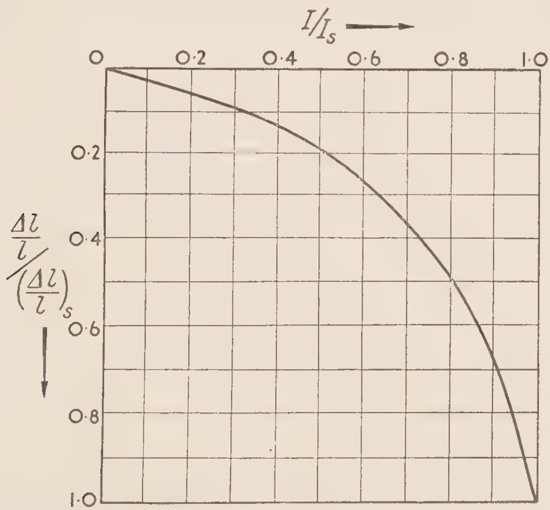

Figure 1. Longitudinal magnetostrictive strain as a function of magnetization in nickel-zinc ferrite.

the eddy-current losses in metal magnets may be objectionable. Other properties of these materials are given in Table 3 at the end of this paper. Data for MgZn and CoZn ferrites are given by Diethelm (1951).

Magnetostriction is closely related to the magnetization I since both are due to change of state of the domains. It is therefore possible to represent the magnetostriction as a function of magnetization by a single plot of $(\Delta l/l)/(\Delta l/l)_s$ as a function of I/I_s (Figure 1). From this curve and the B/H curve one can derive the relation between $\Delta l/l$ and H or $\Delta l/l$ and B.

(*b*) **The reversible magnetostriction.** In many magnetostrictive applications the material is subjected to only small flux-density variations. The static curve for $\Delta l/l$ against H or B is not of great importance in these cases; what is required is the reversible magnetostriction coefficient $(1/l)\ (\Delta l/\Delta H)$ or $(1/l)\ (\Delta l/\Delta B)$ as a function of H or B respectively.

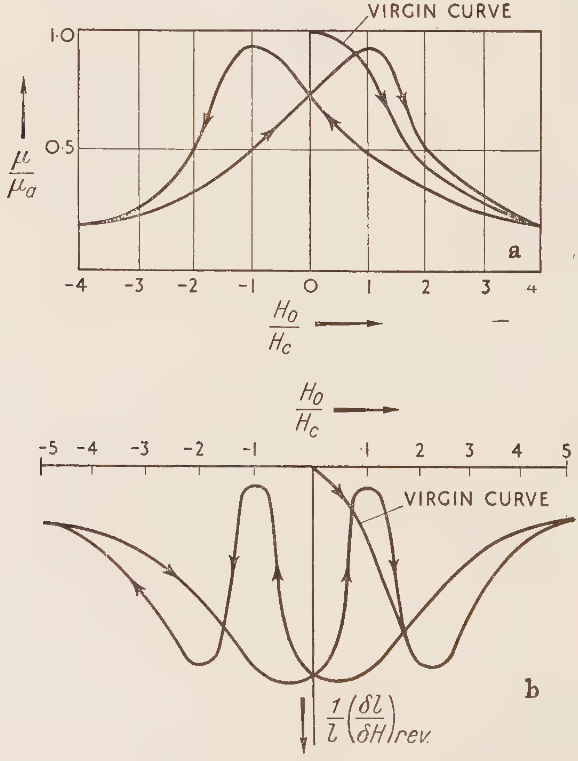

Figure 2. *a*, reversible permeability; and *b*, reversible magnetostrictive strain; as functions of magnetizing force in nickel-zinc ferrite.

The analogy between the reversible magnetostriction coefficient and the reversible permeability is in fact very close so that one can deduce—at least qualitatively—the field dependence of the reversible magnetostriction coefficient $(1/l)\ (\Delta l/\Delta H)$ by considering the field dependence of the reversible

permeability (Figure 2a). Here again one can cover the whole variety of nickel-zinc ferrites in a single graph, by plotting μ/μ_a against H_0/H_c where μ_a is the initial permeability, H_0 is the static polarizing field and H_c the coercive force.

The reversible magnetostriction coefficient $(1/l)(\Delta l/\Delta H)$ as a function of H_0/H_c is shown in Figure 2b. This curve, which differs from that shown in Figure 2a, has two characteristics of interest: (*a*) the initial reversible magnetostriction coefficient for the completely demagnetized material is zero; (*b*) at the coercive force points ($H_0 = H_c$) the reversible magnetostriction coefficient is again nearly zero.

Both facts are easily explained when one realizes that the magnetostrictive effect is independent of the direction of the magnetic field. In the demagnetized state and therefore also in the points $H_0 = H_c$ no vibration of the fundamental frequency can be excited but excitation of a vibration of twice the frequency of that of the exciting field is possible. The reversible magnetostriction coefficient at saturation is zero and a maximum is found near the half saturation point ($I = \frac{1}{2}I_s$, i.e. where H_0 is of the order $2H_c$ and near the remanence point).

The longitudinal or Joule magnetostriction can most conveniently be studied on ring samples (Butterworth and Smith, 1931) which avoid demagnetization effects. Alternatively, one can use spheroidal samples which are uniformly magnetized and have a calculable demagnetization. Beck *et al.* (1951) have recently investigated the magnetostriction of nickel and nickel-iron on very small prolate spheroids but their preparation is difficult in practice. Ring specimens have the further advantage that no additional polarizing field is required. They can be brought to a state of highest magnetostriction activity by applying for a short time a large d.c. field. After removal of the d.c. field the rings operate at the remanence point.

(*c*) **The magnetostriction equation.** The magnetostrictive activity has in the past been defined in many different ways depending on whether stress or strain has been related to induction B, magnetization I or field H.

Pierce (1928), one of the earliest investigators of magnetostriction, quotes two separate effects:

Law I, Joule effect : $\sigma = aB$

Law II, inverse Joule or Villary effect : $B = a'\epsilon$

These equations are not complete. Law I implies zero strain ($\epsilon = 0$, sample clamped), Law II implies $H = 0$. It can be shown by thermodynamics that under these assumptions a and a' are related to each other. A single constant is therefore sufficient and it is now usual to define the magnetostriction constant λ by $\lambda = -(\partial\sigma/\partial B)_\varepsilon$. The minus sign conforms to the old conventions, e.g. a clamped sample of positive magnetostriction will be under compression. The complete set of relations between the

quantities B, H, σ and ϵ can be written in many different ways (Beck *et al*, 1951). The following set of equations has been used by Sussmann and Ehrlich (1950):—

$$d\sigma = (\partial\sigma/\partial B)_\varepsilon dB + (\partial\sigma/\partial\epsilon)_B d\epsilon$$

$$dH = (\partial H/\partial B)_\varepsilon dB + (\partial H/\partial\epsilon)_B d\epsilon$$

Substituting from the thermodynamic equation

$$4\pi(\partial\sigma/\partial B)_\varepsilon = (\partial H/\partial\epsilon)_B$$

this becomes $\quad d\sigma = -\lambda dB + E d\epsilon$

and $\quad dH = dB/\mu - 4\pi\lambda d\epsilon$

where $\mu = (\partial B/\partial H)_\varepsilon$, the reversible permeability as determined on a clamped sample.

$E = (\partial\sigma/\partial\epsilon)_B$ is Young's modulus as measured at constant induction (e.g. half saturation); $E' = (\partial\sigma/\partial\epsilon)_H$ can be evaluated from the magnetostrictive equations by putting $dH = 0$ and substituting dB in the first equation. Thus $E' = (\partial\sigma/\partial\epsilon)_H = (1 - k^2)E$ where $k = \sqrt{4\pi\lambda^2\mu/E}$; k is called the electromechanical coupling coefficient.

k^2 represents the ratio of converted stored energy (e.g. $\frac{1}{2}E\epsilon^2$) to input stored energy (e.g. $(1/4\pi)\,(B^2/2\mu)$) for the case of no losses and no radiation.

Young's modulus changes with magnetization and this is often called the ΔE-effect (Bozorth, 1951).

The magnetostriction coefficients of section 2(*b*), $(1/l)\,(\Delta l/\Delta H)$ and $(1/l)\,(\Delta l/\Delta B)$, should now be rewritten as $(\partial\epsilon/\partial H)_\sigma$ and $(\partial\epsilon/\partial B)_\sigma$ respectively.

Using the general magnetostriction equations it is easily shown by putting $d\sigma = 0$ that $(\partial\epsilon/\partial H)_\sigma = (1/4\pi)\,(\partial B/\partial\sigma)_H = \Lambda/4\pi$ (see also section 4(*b*)) and $(\partial\epsilon/\partial B)_\sigma = \lambda/E$.

(*d*) **The equivalent electric circuit of vibrators.** Pierce and Butterworth have shown that a magnetostrictive vibrator behaves near its mechanical resonance frequency, f_r, as a circuit consisting of two impedances Z_c and Z_m in parallel. Z_c represents the impedance of the core alone neglecting its vibrations, i.e. at very high frequency or clamped. Z_m is the contribution due to the mechanical vibration and can be represented by a series resonance circuit L_m, C_m, R_m (see Figure 3a). Z_m is called the motional impedance and $f_r = 1/2\pi\sqrt{L_m C_m}$ is the resonance frequency of the vibrator.

For a ring specimen $f_r = (1/2\pi r)\sqrt{E/\rho}$ where r is the mean radius in cm and ρ the density; for rods or tubes $f_r = (1/2l)\sqrt{E'/\rho}$ where l is the length of the rods or tubes.

Whenever eddy-current losses are negligible, as in ferrites, a different equivalent circuit is advantageous (v.d. Burgt, 1952; Sixtus, 1951). This is based on the inverse instead of the direct analogy between mechanical and

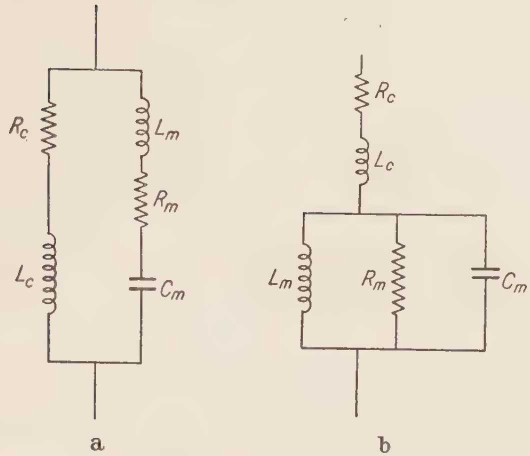

Figure 3. Equivalent circuits of magnetostriction vibrator.

electrical quantities which in general is the better way of describing electromechanical transducers of the electrodynamic or magnetostrictive type (Mason, 1942). The circuit consists of Z_c and Z_m in series. Z_m is in this case a parallel resonance circuit L_m, C_m, R_m, as shown in Figure 3b. The values of L_m, C_m, R_m are of course not the same as for the series resonance circuit. Z_c and Z_m have the same meaning as above and Z_c has to be measured at high frequencies or on a clamped specimen.

The components L_m, R_m, C_m can be found by bridge measurements at different frequencies near the resonance frequency. A more convenient way used by van der Burgt (1953) is to determine the absolute value of the impedance $|Z|$ by feeding the vibrator with a constant current of variable frequency and measuring the voltage across it. The frequency characteristic of $|Z|$ near f_r is shown in Figure 4. $Q_m = R_m/\omega_o L_m$ can be found in the usual way by determining the band width Δf at the $|Z|_{max}/\sqrt{2}$-level.

The mechanical quality Q_m which is due to internal losses and radiation is then $f_r/\Delta f$. Care must be taken in this measurement to avoid damping due to the winding.

The dip in Figure 4 occurs at the series resonance of Z_c and Z_m at the anti-resonance frequency f_a, where

$$f_a = (1/2\pi)\sqrt{(L_c + L_m)/L_c L_m C_m} \doteqdot f_r(1 + \tfrac{1}{2}L_m/L_c).$$

From the meaning of k^2 it is clear that $k^2 = L_m/L_c$ since this is the ratio of the converted stored energy to input stored energy. The electromechanical coupling coefficient can therefore be evaluated from the resonance and anti-resonance frequencies: $k = \sqrt{2(f_a/f_r - 1)}$.

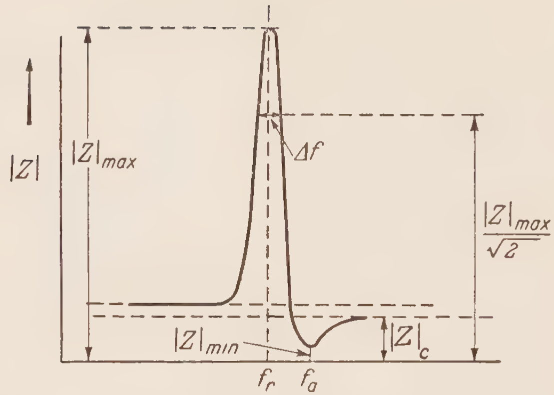

Figure 4. Impedance of magnetostriction vibrator as a function of frequency.

From L_c, $\tan \delta_c$, f_r, f_a and Δf one can evaluate all components of the equivalent circuit shown in Figures 3a and 3b and from $k^2 = 4\pi\lambda^2\mu/E$ the magnetostriction constant λ can be found.

It is instructive to investigate in what way the ratio $|Z|_{max}/|Z|_c$ depends on the material properties.

From the equivalent circuit one can see that it is equal to $|R_m + Z_c|/|Z_c|$ or approximately $Q_m\omega_o L_m/\omega L_c$ or $Q_m k^2$.

3. THE WIEDEMANN MAGNETOSTRICTION

The Wiedemann effect is the twist that occurs upon magnetization of a rod carrying a current. It can be interpreted in terms of the Joule effect by considering the helical magnetic field which results from the field of magnetization in an axial direction and the circumferential field due to the current.

(*a*) **The reversible torsional magnetostriction.** When plotting the twist which results from a small a.c. field against the polarizing d.c. field one might expect a graph similar to that shown in Figure 2b. Figure 5 shows, however, that the reversal of the polarizing field also reverses the direction of twist (Pidgeon, 1919).

(*b*) **Torsional vibrators.** Torsional vibrators made of non-magnetic metals have been described by Roberts and Burns (1949). These vibrators were excited by a nickel-plated layer or ferrite driving parts. Torsional vibrators using ferrite rings and tubes have for the first time been realized by v.d. Burgt (1952), who also worked out their theory fully. The properties referring to torsional vibrators denoted by the subscript " t " are also included in Table 3.

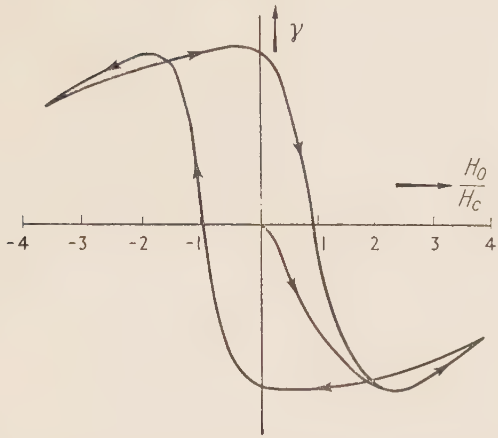

Figure 5. Shear strain as a function of magnetizing force (ΔH constant, ΔH perpendicular to H_o).

These vibrators are clamped by three needles in the nodal plane of the shear at $\frac{1}{2}l$ or $\frac{1}{2}h$ respectively as Figure 6 shows. The height governs the resonant frequency of the torsional ring vibrators and it is thus possible to obtain very much higher frequencies by using rings. λ_t can be derived from the electromechanical coupling coefficient k_t. The relation between k_t and the resonance frequencies is, however, slightly altered in the shear mode:—

$$k_t = \sqrt{(2\pi^2/8)\,(f_a/f_o - 1)}$$

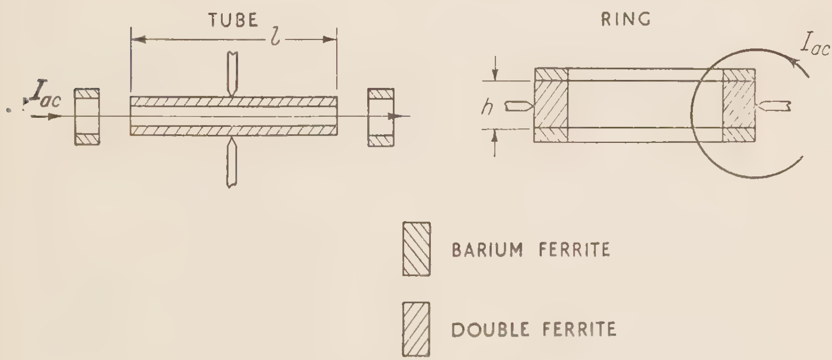

Figure 6. Torsional vibrators. For the tube, $f_r = \frac{1}{2l}\sqrt{\frac{G'}{\rho}}$; for the ring, $f_r = \frac{1}{2h}\sqrt{\frac{G'}{\rho}}$

4. APPLICATIONS

(*a*) **Filters and frequency stabilizers.** It has already become obvious in section 2(*d*) that both Q_m and k should be large and that $Q_m k^2$ is an important characteristic for applications in filters and stable-frequency oscillators.

Another important requirement is, of course, good frequency stability with temperature. $\phi = (1/f_r)(\partial f_r/\partial T)$ is the temperature coefficient of frequency.

From the relation $f_r = (1/2\pi_r)\sqrt{E/\rho}$ it can easily be shown that $\phi = \frac{1}{2}(\alpha + \eta)$ where $\alpha = (1/l)(\partial l/\partial T)$ is the thermal coefficient of expansion and $\eta = (1/E)(\partial E/\partial T)$ the thermal coefficient of Young's modulus.

Similarly for the torsional mode $\phi_t = \frac{1}{2}(\alpha + \eta_t)$ where $\eta_t = (1/G)(\partial G/\partial T)$ and G is the modulus of rigidity.

The thermal expansion coefficient α of ferrites is about 12/million/°C. The temperature stability of frequency is therefore mostly dependent on η or η_t respectively which is usually greater than α. A temperature coefficient of about 20/million/°C has been found for a nickel-zinc ferrite with large zinc content.

Although it is more complicated to investigate the material properties on rods, Diethelm (1951) has shown that these can be used in the construction of a band-pass filter centred at 80 kc/s with a band width of 3·5 kc/s.

(*b*) **Electromechanical transducers.** The coupling coefficient and the saturation polarization are important properties for transmitters. As both these quantities are low in ferrites one would not expect these materials to be particularly suitable for this application. The maximum power which can be transmitted is also likely to be severely limited by their low crushing strength.

For use in receivers high-μ materials are, however, required (Sussman and Ehrlich, 1950). The sensitivity of a receiver may be said to be the open-circuit voltage induced in a single turn per unit stress or $\Lambda = (\partial B/\partial \sigma)_H \fallingdotseq k^2\lambda$.

Table 2 gives values of $\Lambda = k^2/\lambda$.

Table 2

Material		Λ $\frac{\text{gauss}}{\text{dynes/cm}^2}$
		$\times 10^{-6}$
Nickel-zinc ferrite ..	A	− 3·4
	B	− 2·1
	C	− 2·0
Nickel		− 1·5
Permendur		+ 3·6
Hiperco		+ 3·7

Thus the ferrite may have twice the sensitivity of nickel and be nearly as good as the iron-cobalt alloys.

Table 3.—Properties of ferrites

Material Grade { Dutch code / British code	Manganese-zinc ferrite IIIB A1	Nickel-zinc ferrite IVA B1	 IVB B2	 IVC B3	 IVD B4	 IVE B5	Barium ferrite
Initial permeability, μ_a ..	1000	650	250	85	45	17	1·65
Loss (tan δ) at 100 kc/s ..	0·011	0·014	0·015	0·010	0·007	0·006	—
Loss (tan δ) at 1·5 Mc/s..	0·5	0·1	0·024	0·017	0·007	0·006	—
Limiting frequency, Mc/s (tan $\delta = 0{\cdot}1$)	0·5	1·5	5·5	16	29	60	—
Saturation flux-density, $4\pi I_s$, gauss	4650	3670	4170	4030	3550	2460	—
Remanence, B_r, gauss ..	1250	1700	2400	2300	1800	1100	2000
Coercive force ($_IH_c$), oersted	0·3	0·4	1·4	4·0	7·0	14	2500
Curie point T_c, °C ..	190	200	290	410	490	595	450
Density, ρ, gm/c.c. ..	4·9	4·9	4·5	4·2	4·1	4·0	4·6
Temp. coeff. of μ_a, $(1/\mu_a^2)(\partial\mu_a/\partial T)$, in 10^{-6}	+ 3	+ 9	+ 13	+ 20	+ 27	+ 40	—
Resistivity (d.c.) ohm-cm	50	} about 10^6					35×10^6
(at 100 kc/s) ohm-cm	40						
Young's modulus, E, in 10^{12} dynes/cm²	1·64	1·42	1·13	1·06	0·95	0·89	1·45
Mechanical quality, Q_m	3300	4000	3300	2860	2660	1575	3000
Reversible μ (at remanence)	1180	430	170	70	35	11	1·25
Electromechanical coupling coefficient k	0·0015	0·055	0·049	0·067	0·049	0·049	very small
Magnetostriction constant λ, dynes/gauss/cm²	16	890	1 140	2 350	2 300	4 100	,, ,,
Q_mk^2	0·007	12	8	13	11	6·5	,, ,,
Rigidity modulus, G, in 10^{12} dynes/cm²	0·614	0·540	0·427	0·417	0·37	0·36	0·58
Mechanical quality Q_t ..	5400	5400	5500	4900	4300	8600	3000
Reversible μ	750	480	250	96	56	11·5	—
Electromechanical coupling coefficient k_t	0·00099	0·055	0·030	0·050	0·095	0·078	very small
Magnetostriction constant, λ_t, dynes/gauss/cm²	72	520	350	570	2200	4100	,, ,,

5. CONCLUSIONS

The nickel-zinc ferrites, particularly those with low Curie point, are suitable

for use in magnetostrictive applications such as filters and ultrasonic receivers.

The author wishes to acknowledge the help of many of his colleagues, in particular that of Mr. C. M. v.d. Burgt, with whom he had many helpful discussions and who supplied much of the data contained in this paper. He also wishes to thank Dr. J. A. M. van Moll and the Directors of Mullard Limited for permission to publish it. The materials described are known commercially as Ferroxcube and Ferroxdure.

REFERENCES AND INDEX OF NAMES

Referred to on p.

ABADIE, P., and EPELBOIN, I., 1948, Comptes rendus, 226, p. 1707 .. .. 135, 138
ABGRALL, C., 1951, Diplôme d'Études supérieurs, Paris 141, 143
ABGRALL, C., and EPELBOIN, I., 1952, Comptes rendus, 234, p. 1265 .. 141, 143, 190
AN WANG, 1951, Proc. Inst. Radio Engrs., 39, p. 183 286
AN WANG and WAY DONG WOO, 1950, J. Applied Physics, 21, p. 49 286
ANTIA, D. P., FLETCHER, S.G., and COHEN, M., 1944, Trans. Amer. Soc. Metals, 32, p. 290 210
APPERSON, J. W., and FONTAINE, C. B., 1951, Trans. Amer. Inst. Elec. Engrs., 70, Part 1, p. 836 263
ARNOLD, H. D., and ELMEN, G. W., 1923, J. Franklin Inst., 195, p. 621 .. 218, 222
ASSMUS, F., 1953 : " Experimental investigations on nickel-iron-molybdenum alloys with extremely high initial permeability," this book, p. 218
ASSMUS, F., and PFEIFER, F., 1951, Z. Metallkunde, 42, p. 294 .. .. 218, 222
——, 1953, Metall, 7, p. 189 .. .. 218, 221, 224

BARBIER, J. C., 1950, Comptes rendus, 230, p. 1040 131
——, 1953, " The thermal-agitation after-effect ", this book, p. 130 .. 89, 176, 180, 181
BARDELL, P. R., 1953, " Factors influencing the measured value of hysteresis loss of powder-cores ", this book, p. 253 ; also discussion, p. 171.
——, see also RICHARDS, C. E. 234
BATE, G., SCHOFIELD, D., and SUCKSMITH, W., 1953, " Coercivities in dilute ferromagnetic alloys ", this book, p. 9 13
BATES, L. F., DAVIES, A. V., and HARPER, D. J., 1953, " A calorimetric method of finding the total loss in ferromagnetic specimens subjected to an alternating magnetic field", this book, p. 153.
BAUR, F., see EINSELE, T. 129
BECK, F. J., KOUVELITES, J. S., and MCKEEHAN, L. W., 1951, Phys. Rev. 84, p. 957 .. .. 325, 326
BECKER, R., 1932, Physik. Z. 33, p. 905 3
——, 1938a, Z. Tech. Physik, 19, p. 542 81
——, 1938b, Physik. Z., 39, p. 856 15
——, 1939, Ann. Phys. Leipzig, 36, p. 340 .. .. 3, 15
——, 1951, J. de Physique, 12, p. 332 .. .. 15, 52, 90, 169
BECKER, R., and DÖRING, W., 1939, " Ferromagnetismus " (Springer, Berlin) .. 222
BELJERS, H. G., 1949, Physica, 14, p. 629 82
BELJERS, H. G., and SNOEK, J. L., 1949, Philips Tech. Rev., 11, p. 317 52
BENNETT, W. R., see KALB, R. M. 37, 40
BITTER, F., and KAUFMANN, A. R., 1939, Phys. Rev., 56, p. 1044 9
BITTER, F., KAUFMANN, A. R., STARR, C., and PAN, S. T., 1941, Phys. Rev., 60, p. 134 9
BLOEMBERGEN, N., 1950, Phys. Rev., 78, p. 572 243
BOAS, W., see SCHMIDT, E. 207
BOOTHBY, O. L., and BOZORTH, R. M., 1947, J. Applied Physics, 18, p. 173. 218, 221
BORG, L. F., 1949, Proc. Inst. Elect. Engrs., 96, Part II, p. 316 305

Referred to on p.

KING, L. V., 1933, Phil. Mag., 15, p. 201 .. .. 161, 163, 167
KITTEL, C., 1946, Phys. Rev., 70, p. 281.. 81
——, 1949, Rev. Mod. Physics, 21, p. 541 .. .. 6, 43, 78
——, 1951, J. de Physique, 12, p. 291 .. .. 15, 80, 82, 90, 94
——, see also WILLIAMS, H. J. 78, 320
KORNETZKI, M., 1943, Elekt. Nachr. Techn., 20, p. 10... 254
——, 1953, discussion, this book, p. 82.
KOUVELITES, J. S., see BECK, F. J. 325, 326
KRONIG, R., 1948, Nature, 162, p. 528 94

LAMM, U., 1943, " The Transductor " (Esselte, Stockholm) 302
LANDAU, L., and LIFSHITZ, E., 1935, Phys. Zt. Sowj., 8, p. 153 80
LANGEVIN, A., 1951, J. de Physique, 12, p. 476 138
LATIMER, K. E., 1936, Electrical Communication, 14, p. 275 .. .. .. 39, 40, 41
——, 1953, " Non-linearity in magnetic core materials at low field strengths ", this book, p. 38.
LATIMER, K. E., and MACDONALD, H. B., 1950, Proc. Inst. Elect. Engrs., 97, Part II, p. 257 .. .. 69, 308
LAWTON, H., and STEWART, K. H., 1950, Proc. Phys. Soc., 63A, p. 848 20
LEGG, V. E., 1936, Bell System Tech. J., 15, p. 39 .. .. 77, 145, 152, 203, 234
LEGG, V. E., and GIVEN, F. J., 1940, Trans. Amer. Inst. Elec. Engrs., 59, p. 865 245, 246, 258
LIFSHITZ, E., see LANDAU, L. 80
LLIBOUTRY, L., 1950, Comptes rendus, 230, p. 1042 133
LLOYD, H. B., see ROSE, H. E. 211
LYNCH, A. C., 1953, " The assessment of inhomogeneity in thin strips of high-permeability alloys ", this book, p. 183 ; also discussions, pp. 159 and 242.
——, see also RICHARDS, C. E. 234

MACDONALD, H. B., see LATIMER, K. E. 69, 308
MCFARLANE, J., and MOLE, N. F., 1953, " Some properties and applications of silicon-iron ", this book, p. 259.
MACGREGOR-MORRIS, J. T., and GRISDALE, G. L., 1939, Phil. Mag. 28, p. 34 .. 159
MCKEEHAN, L. W., see BECK, F. J. 325, 326
MCLACHLAN, N. W., 1916, J. Inst. Elect. Engrs., 54, p. 480 145
——, 1936, Electrician, 117, p. 249 16
MAEDA, S., 1950a, J. Phys. Soc. Japan, 5, p. 538 105
——, 1950b, J. Phys. Soc. Japan, 6, p. 60 105
MARAIS, A., see EPELBOIN, I. 138, 139, 140
MARTIN, J. P., see CREDE, J. H. 231
MARTIN, W. H., see FONDILLER, W. 37
MASON, W. P., 1942, " Electromechanical transducers and wave filters " (Van Nostrand, New York) 327
MATTHIAS, B. T., see GALT, J. K. 63, 80, 81, 94
MEGAW, H. D., and STOKES, A. R., 1945, J. Inst. Metals, 71, p. 279 206
MELVILLE, W. S., see JACKSON, G. R.
MILLERSHIP, R., and WEBSTER, F. V., 1950, Proc. Phys. Soc., 63B, p. 783 18
MOLE, N. F., see MCFARLANE, J.

Referred to on p.

MORRIS, A. LANGLEY, 1953, " The pulse characteristics of ferrite magnetic materials", this book, p. 278.

NÉEL, L., 1946, Ann. Univ. Grenoble, 22, p. 299 .. .. 3, 4, 143
——, 1947, Comptes rendus, 224, p. 1488 9
——, 1950, J. de Physique, 11, p. 49 .. .. 90, 93, 130
——, 1951, J. de Physique, 12, p. 339 .. .. 88, 105, 130, 137, 143, 172
——, 1952, Ann. Inst. Fourier, Grenoble, 3, p. 301 318
——, 1953, " The influence of subdivision into elementary domains on the high frequency permeability of ferromagnetic conducting bodies ", this book, p. 15.
NEUMANN, H., 1934, Arch. für tech. Messen, Z 913-5, T 168 218
NICKS, P. F., see WELCH, A. J. E. 51, 81, 88
NISHIYAMA, Z., see HONDA, K. 209
NORBURY, A. L. 1920, J. Iron and Steel Inst., 101, p. 627 240

OOSTERHOUT, G. W. VAN, see WENT, J. J. 323

PAN, S. T., see BITTER, F. 9
PARKIN, B. G., discussion, this book, p. 319 190
PETERSON, E., 1928, Bell System Tech. J., 7, p. 762 .. .. .. 38, 39, 40, 41, 61
PETERSON, E., and WRATHALL, L. R., 1935, U.S., Patent No. 1,998,840 145
——, 1936, Proc. Inst. Radio Engrs., 24, p. 275.. .. .. .. 78, 145, 183, 187
PFEIFER, F., see ASSMUS, F. 218, 221, 222, 224
PFEIL, L. B., 1947, Iron and Steel Inst. Symposium on Powder Metallurgy, p. 47 203, 209
PIDGEON, H. A., 1919, Phys. Rev., 13, p. 209 328
PIERCE, G.E., 1928, Proc. Amer. Acad. Arts and Sci., 63, p.1 .. .. .. 322, 325
PISTOULET, B., 1952, Ann. des Télécommunications 136
POLDER, D., 1950, Proc. Inst. Elect. Engrs., 97, Part II, p. 246 .. .. 52, 77, 81
——, 1951, J. de Physique, 12, p. 337 81
——, 1953, " Physical aspects of losses in soft magnetic materials ", this book, p. 74 .. .. 54, 88, 242, 320
POLDER, D., and SMIT, J., 1953, Rev. Mod. Physics, 25, p. 89 81
POLIVANOV, K., 1948, Bull. Acad. Sci. U.S.S.R., 12, p. 98 .. .. .. 136, 139
POPPER, P., 1952, " The magnetostriction of ferrites ", this book, p. 322
PREISACH, F., 1935, Z. Phys., 94, p. 277 .. .. 43, 117, 130, 145

RADO, G. T., WRIGHT, R. W., and EMERSON, W. H., 1950, Phys. Rev., 80, p. 273 51, 80, 81, 88
RANDALL, W. F., and SCHOLEFIELD, H. H., 1950, Proc. Inst. Elect. Engrs., 97, Part II, p. 133 231
——, 1952, " The properties and potentialities of cold-reduced nickel-iron ", this book, p. 225.
RATHENAU, G. W., see WENT, J. J. 323
RAYLEIGH, LORD, 1887, Phil. Mag., 23, p. 225 .. .. 39, 97
REED, M., 1937, J. Inst. Elect. Engrs., 80, p. 567 .. .. 145, 152
REMEIKA, J. P., see GALT, J. K. 63, 80, 81, 94
RICHARDS, C. E., 1953, " Some chemical and physical properties of iron powders and their effects on the magnetic properties ", this book, p. 233 ; also discussions on pp. 106, 129, 201 and 258 .. .. 13, 250

Referred to on p.

RICHARDS, C. E., BUCKLEY, S. E., BARDELL, P. R., and LYNCH, A. C., 1950, Proc. Inst. Elect. Engrs., 97, Part II, p. 236 234

RICHARDS, C. E., and SHOTTON, D. C., 1953, " 50/50 carbonyl nickel-iron powders ", this book, p. 247.

RICHER, G. C., 1947, Nature, 160, p. 256 19

——, 1953, " The cardinal magnitudes of technical magnetization ", this book, p. 19

RICHTER, G., 1937, Ann. Physik, 29, p. 605 .. .. 97, 126, 145, 238

——, 1938, Ann. Physik, 32, p. 683 .. .. 109, 145

ROBERTS, F. F., 1950, Proc. Inst. Elect. Engrs., 97, Part II, p. 269 242

——, 1951, J. de Physique, 12, p. 301 51

——, 1953a, " A screening-factor technique for permeability determination and some experimental results ", this book, p. 161 94

——, 1953b, " Ferromagnetic resonances, hysteresis and residual losses in ferrites and metals ", this book, p. 90 ; also discussion, pp. 48, 63, 217, 243 and 299

——, see also WELCH, A. J. E. 51, 81, 88

ROBERTS, W. B., and BURNS, L. L., 1949, R.C.A. Rev., 10, p. 348 328

ROOKSBY, H. P., 1942, Cantor Lectures, Royal Society of Arts 203

ROSE, H. E., and LLOYD, H. B., 1946, J. Soc. Chem. Ind., 65, pp. 52 and 65 211

ROSTON, B., 1948, Wireless Engr., 25, p. 221 162

SCHELKUNOFF, S. A., 1934, Bell System Tech. J., 13, p. 532 .. .. .. 161, 163

SCHMID, E., and THOMAS, H., 1950, Z. Metallkunde, 41, p. 45 231

SCHMIDT, E., and BOAS, W., 1950, " Plasticity of crystals " (F. A. Hughes) 207

SCHOFIELD, D., see BATE, G. 13

SCHOLEFIELD, H. H., 1949, J. Sci. Instruments, 26, p. 207 231

——, 1953, discussion, this book, p. 188.

——, see also RANDALL, W. F. 231

SCHULZE, H., 1938, Wiss. veröff. Siemens-Werk., 17, No. 2, p. 39 .. 97, 110, 123, 129

SCHUMACHER, E. E., 1950, Trans. Amer. Inst. Min. and Met. Eng., 188, p. 1097 .. 232

SCOTT, K. L., 1930, Proc. Inst. Radio Engrs., 18, p. 1750 145

SCOWEN, F., 1947, " An introduction to electric wave filters " (Chapman and Hall, London) 71

SEWELL, D. W. R., see JACKSON, G. R.

SHOCKLEY, W., see WILLIAMS, H. J. 78, 320

SHOTTON, D. C., see RICHARDS, C. E.

SHURMER, H, V., see GREIG, J.

SINCLAIR, H., see TAYLOR, A. 207

SIXTUS, H., 1951, Frequenz, 5, p. 335 326

SKIDMORE, I. C., see TEBBLE, R. S. 22

SMIT, J., see POLDER, D. 81

SMITH, C. M., see GOODEN, E. L. 211, 235, 249

SMITH, F. D., see BUTTERWORTH, S. 325

SMITH, P. B., see STREET, R. 176, 178, 180

SNOEK, J. L., 1938, Physica, 5, p. 663 98

——, 1939, Physica, 6, p. 161 .. .. 79, 99

——, 1941, Physica, 8, p. 711 79

——, 1942, Physica, 9, p. 862 79

——, 1947, " New developments in ferromagnetic materials " (Elsevier, Amsterdam) 42, 52, 79, 108, 172, 242

Referred to on p.

SNOEK, J. L., 1948, Physica, 14, p. 207 .. .. 51, 53, 80
——, 1950, Physica, 16, p. 336 99
——, see also BELJERS, H. G. 52
SPEED, B., and ELMEN, G. W., 1921, J. Amer. Inst. Elect. Engrs. (now Electrical Engineering), 40, p. 1321 .. .. 245, 246
STARR, C., see BITTER, F. 9
STEINITZ, R., 1948, Powder Metallurgy Bull., 3, p. 124 245
STENECK, W. G., see BROCKMAN, F. G. 76
STEWART, K. H., 1950, Proc. Inst. Elect. Engrs., 97, Part II, p. 121 .. .. 78, 295
——, 1951, J. de Physique, 12, p. 325 241
——, see also LAWTON, H. 20
STOKES, A. R., and WILSON, A. J. C., 1944, Proc. Phys. Soc., 56, p. 174 207
STOKES, A. R., see also MEGAW, H. D. 206
STONER, E. C., and WOHLFARTH, E. P., 1948, Phil. Trans. Roy. Soc., 240, p. 599 .. 9, 14
STRATTON, 1941, " Electromagnetic theory " (McGraw-Hill, New York), pp. 490-524 162
STREET, R., and WOOLLEY, J. C., 1949a, Proc. Phys. Soc., 62A, p. 562 105, 131, 172, 173
——, 1949b, Proc. Phys. Soc., 62A, p. 743 .. .. 105, 131
——, 1950, Proc. Phys. Soc., 63B, p. 509 .. .. 173, 174
——, 1953, " Irreversible magnetic-viscosity effects ", this book, p. 172 88
STREET, R., WOOLLEY, J. C., and SMITH, P. B., 1952, Proc. Phys. Soc., 65B, p. 679 176, 178, 180
SUCKSMITH, W., 1952, British Electrical and Allied Industries Res. Assn. Report No. N/T/61 10
——, see also BATE, G. 13
SUSSMANN, H., and EHRLICH, S. L., 1950, J. Acoustic Soc. Amer., 22, p. 499 326, 330

TAYLOR, A., 1941, Phil. Mag., 31, p. 339 206
——, 1945, " An introduction to x-ray crystallography " (Chapman and Hall, London) 206
——, 1949, J. Sci. Instruments, 26, p. 225 205
——, 1951, J. Sci. Instruments, 28, p. 200 206
——, 1953, " The structure of carbonyl iron ", this book, p. 202 105
——, see also BRADLEY, A. J. 210
TAYLOR, A., and SINCLAIR, H., 1945, Proc. Phys. Soc., 57, p. 126 207
TEBBLE, R. S., SKIDMORE, I. C., and CORNER, W. D., 1950, Proc. Phys. Soc., 63A, p. 739 22
THOMAS, A. G. F., see BUCKLEY, S. E. 190
THOMAS, H., 1951, Z. Physik, 129, p. 219 224
——, see also SCHMID, E. 231
TOBUSCH, H., 1908, Ann. Physik, 26, p. 439 97
TOMBS, N. C., 1953, " x-ray diffraction methods in the appraisal of nickel-iron powder-cores ", this book, p. 197.

U.S. STEEL CORPORATION, 1943, " Atlas of isothermal transformation diagrams ", p. 29 212

VAN VLECK, J. H., 1951, Physica, 17, p. 234 .. .. 90, 93
WALKER, E. V., 1953, discussion, p. 187.

Referred to on p.

WALTERS, R. E. S., 1953, discussion, p. 188.
WAY DONG WOO, see AN WANG 286
WEBB, C. E., and FORD, L. H., 1934, J. Inst. Elect. Engrs., 75, p. 787 .. .. 102, 105, 159
WEBSTER, F. V., see MILLERSHIP, R. 18
WEIL, L., 1950, Comptes rendus, 231, p. 829 14
——, 1951, J. de Physique, 12, p. 437 .. .. 9, 13, 138
WELCH, A. J. E., NICKS, P. F., FAIRWEATHER, A., and ROBERTS, F. F., 1950, Phys. Rev., 77, p. 403 .. .. 51, 81, 88
WELSBY, V. G., 1950, "The theory and design of inductance coils" (Macdonald, London) 68
——, 1953, "Hysteresis intermodulation in directional filters", this book, p. 64; also discussion, p. 245.
WENT, J. J., and GORTER, E. W., 1951, Philips Tech. Rev., 13, p. 181 52
WENT, J. J., RATHENAU, G. W., GORTER, E. W., and OOSTERHOUT, G. W. VAN, 1952, Philips Tech. Rev., 13, p. 194 323
WENT, J. J., and WIJN, H. P. J., 1951, Phys. Rev., 82, p. 269 .. .. .. 80, 81, 94
WENT, J. J., see also WIJN, H. P. J. 41, 42, 43, 55, 57, 75, 81
WIEBERDINK, A., 1948, Nature, 162, p. 527 94
——, 1951, Physica, 17, p. 333 94
WIJN, H. P. J., 1953, "Frequency dependence of magnetization processes in ferrites and its relation to the distortion caused by ferrite cores", this book, p. 51; also discussion on pp. 95, 119 and 285 .. .. 42, 48, 95, 285
——, see also WENT, J. J. 80, 81, 94
WIJN, H. P. J., and WENT, J. J., 1951, Physica, 17, p. 976 .. 41, 42, 43, 55, 57, 75, 81
WILDE, H., 1949, Frequenz, 3, p. 309 .. .. 110, 123
——, see also FELDTKELLER, R. 117
WILDE, H., and BOSSE, G., 1948, Frequenz, 2, p. 214 126
WILLIAMS, H. J., 1947, Phys. Rev., 71, p. 646 4
WILLIAMS, H. J., SHOCKLEY, W., and KITTEL, C., 1950, Phys. Rev., 80, p. 1090 78, 320
WILSON, A. J. C., 1946, Proc. Phys. Soc., 58, p. 21 153
——, see also STOKES, A. R. 207
WOHLFARTH, E. P., 1953, discussion, this book, pp. 8 and 13 246
——, see also STONER, E. C. 9, 14
WOLMAN, W., 1924, Z. techn. Physik, 10, p. 595 121
WOOD, F. J., see CAMPBELL, G.
WOOLLEY, J. C., see STREET, R. 88, 105, 131, 172, 173, 174, 176, 178, 180
WRATHALL, L. R., see PETERSON, E. 78, 145, 183, 187
WRAZEJ, W. J., 1946, J. Iron and Steel Inst., 154, p. 147 211
WRIGHT, R. W., see RADO, G. T. 51, 80, 81, 88
WYART, J., and EPELBOIN, I., 1949, Comptes rendus, 229, p. 301 .. .. 139, 187

YENSEN, T. O., 1924, J. Amer. Inst. Elec. Engrs. (now Electrical Engineering), 43, p. 145 240

ZENER, C., 1937, Phys. Rev., 52, p. 230 .. .. 79, 88
——, 1938, Phys. Rev., 53, p. 90 79